NTNU
Kunnskap for en bedre verden

Thermal insulating concrete

A state of the art review

Morten Hoff

Bachelor i ingeniørfag - bygg
Innlevert: mai 2018
Veileder: Mohammad Hajmohammadian Baghban

Norges teknisk-naturvitenskapelige universitet
Institutt for vareproduksjon og byggteknikk

NTNU
Institutt for vareproduksjon
og byggteknikk

Dissertation title: Thermal insulating concrete; a state of the art review	Date: May, 30th. 2018 Number of pages: [sider]			
	Master thesis		Bachelor dissertation	X
Name: Morten Hoff				
Supervisor: Mohammad Hajmohammadian Baghban				
Any external professional contacts / supervisors: None				

Summary:

Purpose

The purpose is to research the following topic: “Thermal insulating concrete; a state of the art review.” The topic is rather composed and complicated. Concrete is the most commonly used construction material worldwide and concrete have a lot of advantages in the building construction industry. The physical strength is very good, but the thermal conductivity has traditionally been relatively high, and that result in huge CO2 emissions.

Method

The only method for this study has been a literature study. There has recently been conducted numerous studies on this subject, and the biggest challenge has been to find the best and most relevant studies. The topic is rather composed and complicated and the topic has only been loosely reviewed by the author earlier. The author is only on bachelor level and most of the literature available and which has been reviewed is written on doctorate level. Consequently, the learning curve have been tremendous. The intention was to start out with a wide range of search words, and brows the abstracts to get a fast overview. Unfortunately, I learned a little late that I probably should have concentrated on the latest articles earlier. Fortunately, the English language which is my second language, had been practiced extensively earlier.

Result and conclusion

There has been a huge development in the area in the last decade. R & D has introduced new additives in the building industry. Within some of these fields, a lot of basic research is still being performed. There seems to be an enormous worldwide commitment on energy savings and sustainability. All results are summarized in Appendix 1. Apparently, development is greatest within aerogel, while improvement is more modest in concrete mixtures.

Keywords:

Aerogel buildings	Heat insulating materials concrete
Compressive strength	Thermal conductivity
Foam concrete	Thermal insulating concrete

(sign.)

Abstrakt (norsk)

Hensikt

Hensikten er å undersøke følgende tema: "Termisk isolerende betong; en gjennomgang av de siste innen feltet." Emnet er ganske sammensatt og komplisert. Betong er det mest brukte byggematerialet over hele verden, og betong har mange fordeler innen byggebransjen. Den fysiske styrken er veldig god, men termisk ledningsevne har tradisjonelt vært relativt høy, og det resulterer i store CO2-utslipp.

Metode

Den eneste metoden for denne studien har vært en litteraturstudie. Det har nylig vært utført en rekke studier om dette emnet, og den største utfordringen har vært å finne de beste og mest relevante studiene. Emnet er ganske sammensatt og komplisert, og emnet har bare blitt løst gjennomgått av forfatteren tidligere. Forfatteren er kun på bachelorgrad, og det meste av litteraturen er tilgjengelig, og som har blitt gjennomgått, er skrevet på doktorgradsnivå. Følgelig har læringskurven vært enorm. Hensikten var å starte med et bredt spekter av søkeord, og så og se på abstraktene for å få et raskt overblikk. Dessverre erfarte jeg litt sent at jeg sannsynligvis burde ha konsentrert seg om de siste artiklene tidligere. Oppgaven er skrevet på engelsk som ikke er morsmålet mitt, hadde blitt praktisert mye tidligere.

Resulat og konklusion

Det har vært en stor utvikling i området i det siste tiåret. FoU har innført nye tilsetningsstoffer i byggebransjen. Innenfor noen av disse feltene utføres en del grunnforskning fortsatt. Det ser ut til å være en enorm verdensomspennende satsing på energibesparelser og bærekraft. Dessverre ser det fremdeles ut til at kombinasjonen av betong og isolasjonsmaterialene fortsatt fungerer bedre adskilt enn sammenblandet. Det er fortsatt en del som mangler på at man kan benytte løsningene for selvbærende isolerende yttervegger.

Abstract (English)

Purpose

The purpose is to research the following topic: “Thermal insulating concrete; a state of the art review.” The topic is rather composed and complicated. Concrete is the most commonly used construction material worldwide and concrete have a lot of advantages in the building construction industry. The physical strength is very good, but the thermal conductivity has traditionally been relatively high, and that result in huge CO_2 emissions.

Method

The only method for this study has been a literature study. There has recently been conducted numerous studies on this subject, and the biggest challenge has been to find the best and most relevant studies. The topic is rather composed and complicated and the topic has only been loosely reviewed by the author earlier. The author is only on bachelor level and most of the literature available and which has been reviewed is written on doctorate level. Consequently, the learning curve have been tremendous. The intention was to start out with a wide range of search words, and brows the abstracts to get a fast overview. Unfortunately, I learned a little late that I probably should have concentrated on the latest articles earlier. Fortunately, the English language which is my second language, had been practiced extensively earlier.

Result and conclusion

There has been a huge development in the area in the last decade. R & D has introduced new additives in the building industry. Within some of these fields, a lot of basic research is still being performed.

There seems to be an enormous worldwide commitment on energy savings and sustainability. All results are summarized in Appendix 1. Apparently, development is greatest within aerogel, while improvement is more modest in concrete mixtures.

Preface

This bachelor dissertation terminates the author's bachelor's degree program of Civil and Environmental Engineering at NTNU, with specialization in construction technology. The work has been administrated by the section of Materials Technology.

This is conducted through the part time program, so the author has been in full job during the entire time frame.

The dissertation was written during the first 20 weeks of the spring semester 2018, with some minor preparations during the last weeks of autumn semester of 2017. Unfortunately, the author had to conduct a shoulder surgery immediately after Easter, so this had slowed down the work for approximately 3 weeks.

This literature study comprises articles at the highest scientific level available. Consequently, there is a certain professional mismatch between the bachelor level and the level of the crawled articles. The learning curve after meticulously reviewing numerous articles have been steep and the knowledge is now much higher than when this work started out.

The contents of the dissertation presented is close to 99% other people's work. The studied articles are also condensed written articles which should be read in full to get the complete picture of the matter. It has therefore been a difficult choice how much to refer or quote from the mentioned work. It has also been concluded that it would take unacceptably much longer to recount this in the author's own words in a foreign language without reducing quality.

A multitude of studied articles and even multiple more abstracts are not referred. Updated recent searches have resulted in newer articles being prioritized. Attempts have been made to include a good representative selection of recent articles in the subject with emphasis on the most relevant content, although this would probably have been done better if the work had started at the current level of comprehension. The newest articles are based on numerous older groundbreaking articles, but a lot of the newer articles represent more "state of the art" results.

With an imminent danger of leaving out some excellent work, the author hopes that this dissertation will provide a useful introduction to a very complex subject.

Unfortunately, there have been some problems with the NTNU-Harvard English Copy in Endnote. There have been two occasions where it has been unstable, and not working as it should. This problem was solved once by going back to a previous back up file, but the last time happened just before the delivery date. Manual update was then the only solution.

Table of Contents

List of Figures

Acronyms and Abbreviations

AABC - Advanced Aerogel-Based Composite (Joly *et al.*, 2017)

AAC - aerated autoclaved concrete (Wang *et al.*, 2018)

ACC - autoclaved cellular concrete

AAM - alkali activated materials

AIC - aerogel-incorporated concrete (Wu *et al.*, 2015)

AIM - aerogel-incorporated mortar (Ng *et al.*, 2015)

ASAAC - alkali-activated slag-based AAC

CBC - Chemically Bonded Ceramics

CNT - Carbon nanotubes (Ng *et al.*, 2015)

CBPC - Chemically Bonded Phosphate Ceramics

FC - Foam concrete (Samson, Phelipot-Mardele and Lanos, 2017)

GGBS - ground granulated blast furnace slags (Tsioulou, Ayegbusi and Lampropoulos, 2017)

HPAC - High Performance Aerogel Concrete (Welsch and Schnellenbach-Held, 2017)

LAC - Lightweight aggregate concrete (Samson, Phelipot-Mardele and Lanos, 2017)

LA - Lightweight aggregate (Samson, Phelipot-Mardele and Lanos, 2017)

LC - Lightweight concrete (Samson, Phelipot-Mardele and Lanos, 2017)

LFC - Lightweight Foamed Concrete

LOI - loss on ignition

MPC - Magnesium phosphate cement (Xu, Ma and Li, 2015)

MKPC - Magnesium potassium phosphate cement (Xu, Ma and Li, 2015)

NAAC - non-aerated autoclaved concrete (Wang *et al.*, 2018)

NIM - Nano improved materials (Gangassaeter *et al.*, 2017)

ODPR - Oil-base drilling cuttings pyrolysis residues (Wang *et al.*, 2018)

ONAAC - ODPR non-autoclaved aerated concrete (Wang *et al.*, 2018)

OPC - Ordinary Portland cement (Wu *et al.*, 2015)

PEDS - a poly-ethoxy-disiloxane sol derived from TEOS)-based gel (Koebel *et al.*, 2016)

POREC - polyester-reinforced concrete composites (Simek and Uygunolu, 2018)

SCM - supplementary cementitious materials

TEOS - tetra-ethyl- ortho-silicate (Koebel *et al.*, 2016)

TMOS - tetra-methyl-ortho-silicate (Koebel *et al.*, 2016)

TI-LWC - thermal insulating lightweight concrete (Ali *et al.*, 2018)

UHPC - ultrahigh performance concrete (Ng *et al.*, 2015)

ULCCs - Ultra-lightweight cement composites (Wu *et al.*, 2015)

VIP - Vacuum insolasjon panels (Gangassaeter *et al.*, 2017)

1 Introduction

1.1 Motivation

This bachelor dissertation terminates the author's bachelor's degree program of Civil and Environmental Engineering at NTNU, with specialization in construction technology. The work has been administrated by the section of Materials Technology.

Concrete is the world's most used material in the building industry. Concrete has many excellent features that make it very favorable. Traditionally, it consisted of three constituents, which are Portland cement, water and stone deposits in varied sizes. Concrete also has very many different applications, where the desired properties can be widely different. This has especially resulted in more specialized cement types or products in recent decades.

One of the biggest disadvantages of concrete is that the Portland cement has been energy consuming to produce. Particularly in recent years, focus has significantly been made on energy efficiency and access to scarce raw materials.

Another weakness of concrete has been relatively poor insulation ability when used for space insulation to improve ever-increasing demands on human comfort. This will result in unnecessarily excessive costs for heating and cooling through the building life cycle.

It has also become a worldwide focus on CO_2 emissions. The underlying cause is the exponential increase in the world population and increased living standards and thereby increasing raw material consumption and increased CO_2 emissions.

Concrete has also been improved and developed in many different ways based on motives such as economy, environment and resource shortage. There is a significant pervasive research effort in the area. Cement replacements, fillers and structural change additives are tested and introduced in countless amounts.

Consequently, the material engineering structure has become very complex and complicated. The main focus of this study is, therefore, to give examples of new developments in concrete

and concrete substitutes, as well as attempting to compile results for two of the most significant properties such as thermal conductivity and compressive strength. These results are reported in Appendix 1.

Some of the literature studied are still at the basic research stage, but there are also several innovative ideas that can be put into production relatively soon. The application is worldwide and applies to world metropolitan-, urban- as well as rural-areas. The basis for material decision can therefore be fundamentally different and product selection accordingly.

The world's increasing consumption has also led to a huge trash issue. Accordingly, numerous studies have been made to find use of this as acceptable additive materials in concrete applications in the building industry.

All of the written material reviewed has been produced by the leading materials technology experts. Nevertheless, it would not hurt to take a little further overview.

Concrete and concrete substitutes with good insulation are therefore primarily suitable for building exterior walls and roofs, and some degree to flooring. There are already products in the LECA segment and prefabricated wall and roof elements segment with core of pure insulation material. Another option is to insulate more in situ poured concrete either outside or inside, whichever is most appropriate. There are also commercially insulation systems on the market that together with concrete will provide complete insulated walls.

In comparison with glass facades, concrete has the disadvantage that it is not transparent or emits light. Especially in centers of world metropolitan areas where land prices, space utilization and attractiveness can be the crucial element of lease rate, price and ultimately expectation of economic earnings, the choice of facade can be crucial. Basic tests for carrying out projects are that they must be politically, environmentally, technically and economically feasible.

Property managers have traditionally been concerned with rapid economic gain and have often used short-term perspectives. In recent years it has become more common to assess profitability over a more realistic life cycle. Depreciation rules has also traditionally been short, and simple, easy to use evaluation methods have likely resulted in brief time frames.

There has been a formidable quality improvement for buildings in the post-WWII period, and construction and especially loadbearing structures will be able to function for at least 100 years. There has also been a clear shift in the flexibility of the buildings, i.e. that the same building, or at least that the supporting structures can be used for multiple purposes. This make it easy to convert the buildings into other purposes.

1.2 Metodologi, literature search.

The method consisted of conducting an insightful literature search. The first thing that had to be done was choosing good keywords and related restrictions. It was therefore important to learn how to use search and literature reference tools. This proved to be extremely important. Somewhat unexpected and inexplicable, the literature references came out with the wrong format. The rescue was to return to the last backup of the report, and then to copy in the parts that was added to the previous backup.

For the best overview, it was necessary to review the article's summary with the purpose of sorting out studies that were appropriate and not. The search is conducted using the Comendex database on www.engineeringvillage.com. The search results were then systemized and categorized using Excel spreadsheet. Excels Scatter graphs was finally used for better visualization.

It was then attempted to get a good overview of the relevant substance in order to make a good outline for the report. Quality evaluations were regularly carried out with suggestions for improvements. This resulted in greater emphasis on the latest articles. Older reviewed articles were therefore omitted, partly due to lack of time.

1.3 Limitations

In order to keep the scope manageable for a single person, only scientific articles are searched. In order to improve this work even more articles should be included. Since this is a state of the art study, the main focus has been on articles that report the latest and best results, and consequently less focus on studies reporting mediocre results.

There are conducted several studies based on using waste of all categories. Even dough this do represent positive contributions to the environment, it is only mentioned rather modestly in this report.

There is also a lot of relevant and good substance on the supplier's web pages, but this has unfortunately been necessary to omit due to the lack of time.

In high-rise buildings, it is hardly appropriate to replace the traditional concrete of today for use in foundations, columns and floors. Since construction costs have gradually become higher, semi-solid and more bulky building materials will impound expensive rental areas. The overall environmental aspect also includes a high degree of transport and it involves environmental gains by concentrating building construction near the city centers with good and efficient transport solutions. This contributes to increasing land prices and thereby also additional expanding prices per square meters in buildings. Globally, we will still see increased population in large cities driven by environmental motives.

Here, there may be critical questions about the extent to which solutions will be found that, through a life cycle analysis, are able to compete with many improved solutions that have come within building materials and especially insulation products over the last few years.

Here are also improvements in heating solutions from solar and thermal solutions, such as thermal heat pumps with refrigeration, solar collectors, etc. Ovners will quickly reclaim the use of better and more suitable solutions for increased construction costs, at lower annual operating costs.

A major change in the concrete industry is also required especially in the more developed parts of the world. Today, there are very limited additives offered by the concrete suppliers at least in our country. It is also necessary to influence decision-makers like architects and consultation in order to change their choice of desired appearance of building facades. More and more buildings are being built as close as possible to central areas and towns. The important thing for the ovners is that they build what they have the greatest confidence can be rented out at highest prices. Within city centers and in the world metropolis, you can see entire facades in glass. Much depends on the well-being and visibility. As you know, it is impossible to look through concrete.

It is obvious that much of the available literature is developed by people in materials engineering, and it is striking how little is affecting concerns effective building methods, economy and profitability. However, this study is from a pure materials engineering point of view and the matters listed in this chapter will not be evaluated further in this assignment.

2 Industry Background

In the following are some quotes of industry background from referenced studies:

“During the last 30 years, lightweight concretes (LCs) have been developed in order to decrease the volume of load-bearing components, reduce the consumption of raw materials and obtain better thermal properties than those of conventional concrete. Several production processes can be employed. Lightweight aggregates can be used to decrease the density (lightweight aggregate concrete) or gas can be introduced by various methods (foam concrete (FC)). A wide range of properties can be achieved depending on several parameters (production process, binder choice, water/cement mass ratio, porous structure, admixture or surfactant content etc.).” (Samson, Phelipot-Mardele and Lanos, 2017)

“The building sector accounts for approximately 40% of the European energy demand. Space heating and cooling correspond to roughly 60% of the total energy consumed in buildings (Ozel, 2011; Zheng et al., 2010). Although several successive energy regulations have led to improvements in the properties of insulation materials, heat transfer through building envelopes remains the principal factor influencing the amount of energy consumed to cool/heat buildings. Innovative insulation solutions are thus required.” (Samson, Phelipot-Mardele and Lanos, 2017)

“The building sector is considered one of the most promising ways to be able to halt greenhouse gas emissions in the atmosphere [43]. From this point of view, a reduction of the energy consumption of buildings' HVAC systems is required to curtail CO2 output. It can be done with minimal effort by performing thermal insulation but it requires installing thicker layers of conventional insulation materials. This situation causes aesthetic problems regarding the building facades. Moreover, thermal insulation with low cost products or standard materials takes up more space and decreases the volume fraction of inhabitable living space [44]. Therefore, superinsulation is compulsory to obtain the desired, attractive conditions in new constructions and retrofitting of buildings. Insulation performance and cost are the two primary parameters in thermal insulation applications of buildings. Fig. 3 depicts the comparison of three different types of insulation products with respect to the performance, cost and market share. Conventional insulation materials have the largest market potential

since they offer the best performance per unit cost [45]. However, it is estimated for the near future that their cost will slightly increase and market share will reduce. Low cost products offer poor performance and durability and it is predicted that their current situation will not notably change. On the other hand, superinsulation materials like aerogels will dominate the global market in the upcoming future depending on the high performance insulation, extraordinary features and decreasing cost." (Cuce *et al.*, 2014)

2.1 Environmental context

In the following are some quotes of environmental context from referenced studies:

"Thermal insulation concrete building plays an important role in environment sustainability especially energy saving buildings. Buildings are one of the largest consumers of energy worldwide. Therefore, significant energy saving can be realized by buildings with proper materials, design and operation. Thermal insulation systems are nowadays mostly applied for such building envelopes where the materials of load bearing structure such as concrete do not have a substantial thermal insulation capability. Thermal insulation in concrete are materials or combinations of materials that are used to provide resistance to heat flow, should have low conductivity for building application in order to represence of a temperature gradient, has an important effect on the heat exchange between the building interior and the ambiance. The aim of this paper is to review the thermal properties include thermal conductivity and specific heat on various types of concrete."(Shahedan *et al.*, 2017)

"The link between energy consumption and environmental impact is now unquestionable. The building sector accounts for 32% of carbon dioxide gas emissions in Europe, making this sector the second largest source of carbon dioxide pollution, with 120 Mt produced every year. European regulations seek to reduce greenhouse gas emissions by 20% before 2020 with respect to 1990 emissions. At the same deadline, renewable energy will have to constitute 20% of the final energy consumed. These regulations on new buildings are only a part of the solution, because only 1% of the building heritage is renewed each year. Significant improvements could come from the refurbishment of existing buildings. Although energy consumption is mainly due to thermal losses through building envelopes, on a 50-year

lifecycle, one fifth of the energy consumed in buildings is used in the production processes employed to create them (Pacheco-Torgal et al., 2012; Perez Fernandez, 2008).” (Samson, Phelipot-Mardele and Lanos, 2017)

“Energy efficient building is defined as achieving satisfactory internal environment and service with minimum energy consumption. One of the most important parameters that affect the heat transfer through the building envelope is thermal conductivity. The thermal conductivity of lightweight concrete is generally lower than that of normal-weight concrete due to the lower thermal conductivity of air. Although introducing voids in concrete reduces its thermal conductivity and increases its insulation capacity, the mechanical properties are generally compromised.” (Wu *et al.*, 2015)

“Presently, there is an increasing interest and demand for energy savings, reduced strain on material resources and lowered pollution. Energy-efficient buildings with a low negative environmental impact represent an important area in this respect, where zero emission buildings may be part of the path towards a sustainable future.

Thermal insulation for buildings plays an important role to achieve this demand of improved energy efficiency. Recent studies [1] demonstrate that energy efficiency measures like e.g. thermal insulation retrofit are the most cost-effective ones with respect to CO_2 emissions, whereas measures like e.g. solar photovoltaics and wind energy are far less cost-effective than insulation retrofit for buildings. In order to achieve the highest possible thermal insulation resistance, new insulation materials and solutions with low thermal conductivity values are being developed, in addition to utilize the current traditional insulation materials in ever increasing thicknesses in the building envelopes. Noteworthy, very thick building envelopes are not desirable due to several reasons, e.g. considering space issues with respect to both economy, floor area, transport volumes, architectural restrictions and other limitations, material usage and existing building techniques.” (Ng *et al.*, 2015)

2.1.1 Energy consumption Carbon dioxide emission.

“The building sector accounts for approximately 40% of the European energy demand. Space heating and cooling correspond to roughly 60% of the total energy consumed in buildings” (Wu *et al.*, 2015)

2.1.2 Depletion and scarcity of natural resources

In the following are some quotes regarding depletion and scarcity of natural resources environmental context from referenced studies:

“The building sector also has to face the issue of the gradual exhaustion of natural resources and/or the increasing difficulty of gaining access to them. Limestone (the main component of clinker) resources are still large, but the demand for cement is increasing incessantly. The situation has stabilised in industrialised countries, but demand is exploding in emerging countries such as China, India, the Middle East and Latin America (Oliver et al., 2013; Zhang et al., 2014). Taking all sectors into consideration, OPC concrete is the most heavily consumed manufactured product in the world, because of its relatively low cost. It is mainly used for building structures and/or envelopes. OPC production is based on clinker calcination at 1400°C, which is associated with high energy consumption (2900–3300 kJ/t) (Damtoft et al., 2008; Schneider et al., 2011). The corresponding carbon dioxide production is 0·9 t per tonne of cement. Total carbon dioxide gas due to OPC production represents 8% of worldwide carbon dioxide emissions (Oliver et al., 2013). In order to limit these problems, several methods intended to reduce the density of conventional concrete have been developed. In this context, LCs have been developed over the last three decades. Such concretes are obtained by replacing conventional concrete components by lightweight aggregates (LAs) or gas voids. LCs offer the opportunity to reduce the environmental footprint of the building sector by acting on three levers – improvement of building envelope thermal insulation, reduction of carbon dioxide gas emissions and conservation of natural resources. This article references the different production methods employed to make an LC. In the organisation chart of Figure 1, particular attention is paid to thermal conductivity and compressive strength. Two overview graphics (Figures 2 and 3) compare the different LC production methods and the binders employed. Detailed reference is made to the few studies concerning calcium sulfate LC. According to Gartner (2004), this kind of binder is produced with 25% of the energy required for OPC production. Producing gypsum LCs with good thermomechanical performance could thus be very interesting in the current environmental and economic context.” (Samson, Phelipot-Mardele and Lanos, 2017)

“Warming of the Earth's atmosphere and oceans is unequivocal. Earth's average surface temperature has increased by about 0.8 1C and approximately two thirds of this increment has

occurred over just the past three decades [1]. Today, there is a consensus among scientists that global warming is primarily caused by increasing concentrations of greenhouse gases produced by human activities such as the burning of fossil fuels and deforestation [2,3]. Climate model projections indicate that during the 21st century the global surface temperature is likely to rise a further 1.1–2.9 1C for their lowest emissions scenario and 2.4–6.4 1C for their highest [2]. These predictions force the world to rethink global energy strate- gies and consequently take appropriate measures [4]. In this regard, intensive efforts have been made especially in recent years for public awareness on carbon footprint, the trend of carbon dioxide (CO2) concentration in the Earth's atmosphere [5] and its effects on global climate [6,7]. The necessity of the stabilization of atmospheric CO2 concentration below 500 ppm has been often underlined [8]. As a result of the international political efforts, a strong stimulation of research into renewable energy technologies has been observed throughout the world especially in the last decade [9,10,58–62]. The main goal of those studies was to narrow the gap between conventional and renewable energy sources due to the growing significance of environmental issues [11–17]. Currently, renewable energy resources supply about 14% of total world energy demand and their future potential is remarkable [18,19]. However, this notable progress is not still sufficient for the urgent stabilization of greenhouse gas concentration in the atmo- sphere. Therefore, research on energy management and efficient minimization of energy consumption has become vital more than ever in recent years. By the end of the 20th century European Union decided to accept Kyoto-protocol about to decrease the emissions. It was planned to reduce emissions 20% in 2020 compared to the emission levels of 1990 [20].

In the early 21st century, there was an indisputable necessity for the world to recheck the energy consumption levels and their distribution by sector. In 1999, total energy consumption in Europe was reported as 1780 million tons of oil equivalent and 35% of this amount was consumed by residential and commercial sector [21]. One year later, total energy consumption of the United Kingdom by sector and by building type was specified as illustrated in Fig. 1. It was concluded from the report that buildings have a major impact on total greenhouse gas emissions in Europe [22]. Baetens et al. [23] also reported that buildings emitted 8.3 Gt CO2 in 2005 accounting for more than 30% of the greenhouse gas emissions in many developed countries. In this respect, utilization of traditional insulation materials is regarded as a solution to abate the green- house gas emissions in the atmosphere. For instance, Chitnis et al. [151] have evaluated the effects of energy-efficient improvements on potential energy and

emission savings for UK households, and they have concluded the average UK property would achieve a 5.5% reduction in greenhouse gas emissions by using wall insula- tion. However, conventional insulation materials are used in thicker or multiple layers in order to obtain the desired conditions and this situation causes dramatically heavier constructions and complex building details [24]. On the other hand, there is a consensus among scientists that air as an insulator had reached its limit [25,26], and hence developing new, high performance insulation materials is a crucial need for the insulation market. Therefore, several attempts have been made to develop novel thermal insulators meeting the requirements of superinsulation theory.

Although yet discovered in the 1930s [27,28], aerogel as a thermal superinsulation material has undergone great progress and changes in recent years. Aerogel has attracted different sectors and thus it had a wide range of application areas including buildings, automotive, electronics, clothing, etc. Due to its superior physical and chemical characteristic features, aerogel has won great interest especially for energy-efficient retrofitting opportu- nities of residential buildings [29]. The market share of aerogels tripled to 83 M$ in 2008 and is estimated to reach up to 646 M$ by 2013. In this regard, aerogel-based thermal superinsulation has become strategically important for the 29 G$ global insulation market [23]. However, commercialization is still the most challen- ging point of aerogel, and hence aerogel manufacturers focus on cost reduction, performance enhancement and developing new types of aerogels [30–33]. In this paper, a thorough review of the available literature on aerogels is presented. The review is carried out in two main parts. Firstly, current scenario of the insulation market and thermal superinsulation theory is discussed. Secondly, aerogel and its applications in buildings are given in detail. Performance and economic assessment of aerogels, aerogel- based novel materials, safety and health issues, future predictions and recommendations are also considered in the study." (Cuce *et al.*, 2014)

2.1.3 Use of hazardous waste as additives for different concrete recipes

In the following are some quotes regarding use of hazardous waste as additives for different concrete recipes from referenced studies:

“Fly ash from coal power plants and waste incinerators have properties that can be used in concrete production. This has become so common and successful that there may be a shortage of this waste.

Similarly, can be done with other types of hazardous waste. The production of shale gas has been criticized for not being particularly environmentally friendly from different points of view. Recently, a study from China has been published, where contaminated drilling mud from this production is neutralized by being used as an additive for concrete production.” (Wang *et al.*, 2018).

“With the rapid development of China’s economy, energy demand has constantly been increasing, and shale gas, as a new type resource of energy, has become one of the major motivations in the economic development of China. In the course of exploration and development of shale gas, we used oil-based drilling fluid of multi-interval fracturing technology in horizontal well for gas discovery, and then oil-based drillings were circulated to ground which included oil-based cuttings as well as a certain portion of oil-based mud. The pre-processes of oil-based drilling fluid and cuttings are presented in Fig. 1. All the processes were mainly via the vibrating screen system, which made the oil-based drilling cuttings available. In one well, approximately 250 m3 of oil-based cuttings would be generated. Moreover, it is a kind of oily solid waste, thus pyrolysis procedures were used to ensure the safe discharge. The oil-based residues’ oil content would be controlled within 0.3% so that it can guarantee solidification treatment [1,2].

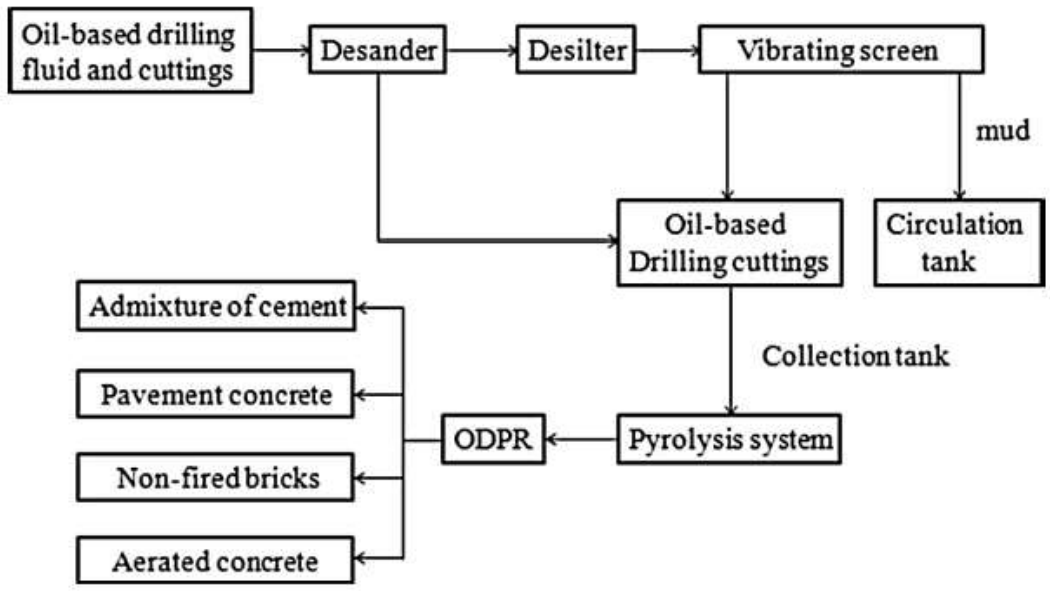

Fig. 1. Pre-processes of oil-based drilling cuttings and comprehensive utilization of ODPR

We can add hardening agent such as cement in ODPR to convert it into solids with certain levels of strength. In this way, the contamination of ODPR can basically be solved within a short period of time. Technically, the absolute majority of contaminants, through solidification [2–5], in the ODPR were mixed in the solidified blocks, so effective treatment could be achieved. However, this process only mixed the pollutants in the solidified blocks rather than completely counteracting them. When buried underground for a long time, the solidified blocks would undergo a series of variations under physical, chemical and biological effects, thus resulting in the formation of secondary-pollution [6–8]. From Fig. 2, we can see that the solidifying processes of ODPR are very tedious. It mainly passes through the first and the second mixture with an agent, then it is solidified in a consolidation tank. In addition, there are also some problems; for example, large areas were occupied, high cost during building among others. What's worse, if construction had not been controlled well, there would be risks of in environmental pollution [2]. So the ODPRs' safe and environmental disposal as well as resource recycling by the exploration and development of shale gas are urgently needed.

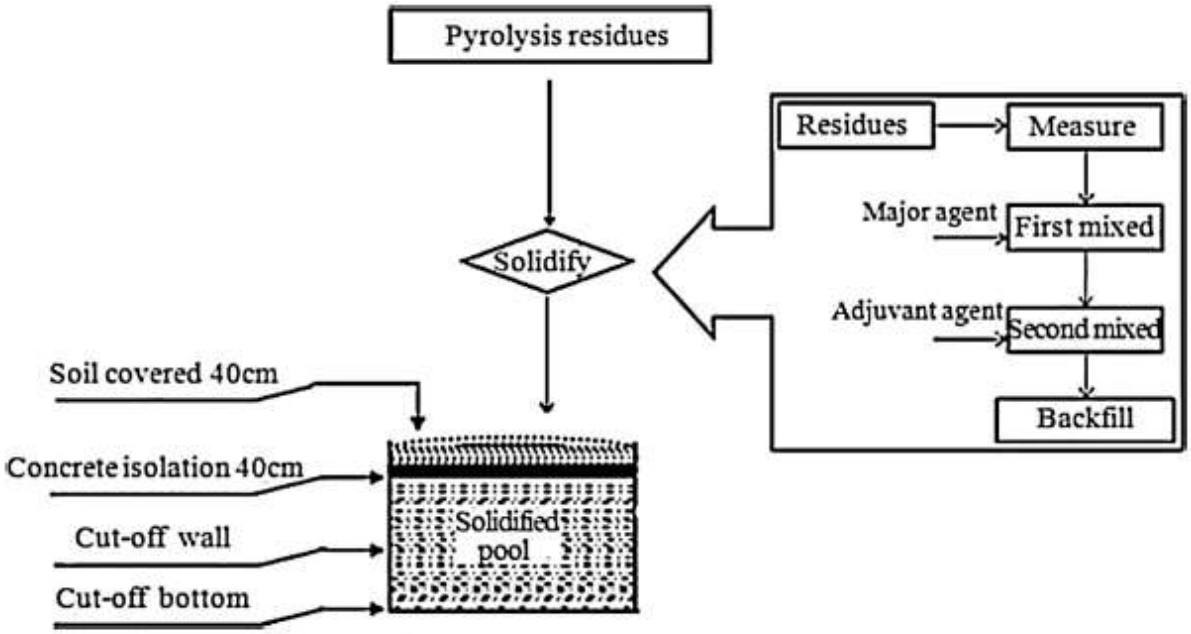

Fig. 2. Solidify processes of ODPR.

Up until now, no studies have been done on the utilization of ODPR for preparing non-autoclaved aerated concrete. A new nonautoclaved aerated concrete was prepared by the ODPR in this study, therefore ODPR was used as a raw material for the preparation of

ONAAC. Besides, this research used the non-autoclaved technology, which can conserve energy and environment.

The present study investigates the ODPR's potential possibility of resource utilization as a partial replacement of cementitious materials to make non-autoclaved aerated concrete will be discussed. The innovation which results from this study is not only produced a new and cost-effective material from drill cuttings, but also mitigated its negative environmental impacts. To achieve the goal mentioned above, mechanical and physical properties, detailed environmental performance, and microstructure analysis were carried out. Meanwhile, modern analytical methods have been used to investigate the early hydration process and hydrated products of ODPR non-autoclaved aerated concrete. This study can effectively solve the problem of ODPRs' safe and environmental disposal and resource recycling. On the other hand, it will play a role of standard guidance in drillings resource utilization by the exploration and development of shale gas in our country. "(Wang *et al.*, 2018)

"Compressive strength

A constant case is we can dry the specimens at the temperature of (105 ± 5)C, then the compressive strength at the loading rate of 2000 N/s, and the testing also refer to Chinese standard GB/T11969-2008. The average test results are given in Table 7 and Fig. 1.

Table 7
Performances of the product and the demand of standard.

Performance	Test result	Standard requirements
Unit weight (kg/m^3)	610	≦625
Compressive strength (MPa)	3.30	≥3.5
Thermal conductivity (W/(m K))	0.124	≦0.16

"

(Wang *et al.*, 2018)

"Conclusions

This study has described a series of experiments that were performed to evaluate the influence of mechanically activated cements on the rate of hydration, structure of the hydrated products, and mechanical properties of ODPR non-autoclaved aerated concrete. The results obtained in the study can be summarized as follows:

(1) According to physical and mechanical tests, an optimal proportion of ONAAC was determined to be 25–30% for Fly-ash, 15–20% for ODPR; 20–30% for Cement, 15–20% for Quicklime and 4% for Gypsum.

(2) Water to solid ratio is an important indicator of the production f ONAAC, the unit weight, aerated effect, compressive strength and production efficiency are related to the water to solid ratio.

(3) Steam temperature directly affected of the mechanical property, which increased with increasing temperature from 65 C to 80 C.

(4) The dry unit weight and thermal conductivity of ONAAC meet the requirements of Chinese standard [19].

(5) In terms of leaching toxicity, the results showed the partial sample of ODPR's pH was slightly above 9.0, other indexes all could meet the First Grade Standard of GB8978-1996, so the environmental performance of ODPR nonautoclaved aerated concrete was very well." (Wang *et al.*, 2018)

3 Results and discussions

The scope of work is rather complicated and consists of several disciplines within science. There are countless different constituents that can be applied for concrete production in infinite combinations. The goal of this study is to find good solutions that can improve the thermal conductivity of concrete for building envelope/external walls purposes while maintaining sufficient strength.

It is a challenge to understand and predict the results of the various ingredients of the compositions. Hajmohammadian Baghban, Kioumarsi and Grammatikos (2018) have presented a study named: “Prediction Models for Thermal Conductivity of Cement-based Composites.”

The different constituents might have effects on each other that can be rather difficult to predict. (Simek and Uygunolu, 2018) have introduced what call “Full factorial design and effect analysis” in order to find the effects of the different constituents together that seems to be very expedient. This might be an advantageous method that will be applied more in the future.

The main findings of this work are presented in Appendix 1, where thermal conductivity and compressive strength are listed. (Samson, Phelipot-Mardele and Lanos, 2017) presented an extensive table from their literature study of 42 articles in their Table 1. The contents of the table consist of the following columns: Reference, Composition, Production process, OPC content: kg/m3, w/c (or w/b) ratio, Paste density: kg/m3, Apparent density: kg/m3, Compressive strength: MPa, Compressive strength test, dimensions (in mm) and age, Thermal conductivity: W/(m.K).

For easier comparisons the mentioned Appendix have adapted this layout. The work of Samson et al. (2018) consists of 44 references and associated data. Approximately 140 more values are added and listed in the Appendix.

In order to visualize the results a few scatter diagrams made in Excel are presented in the following.

Figure 3.1 shows values from (Wu *et al.*, 2015) Table 5 which shows the results of their study compared to concrete. Please refer to Appendix 1 for more information of the constituents. This apply to all of this scatter diagrams.

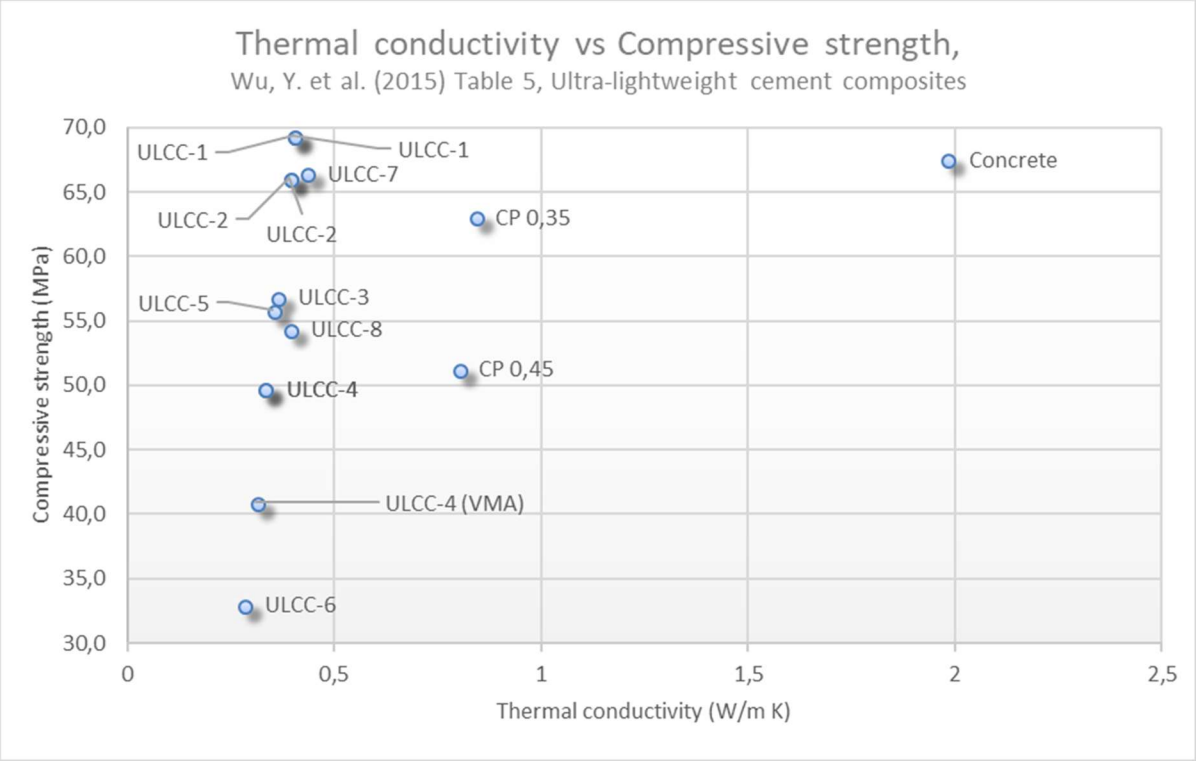

Figure 3.1: Thermal conductivity vs Compressive strength, Wu, Y. et al. (2015). Values from Table 5, Ultra-lightweight cement composites

Figure 3.2 similarly shows the results of (Schnellenbach-Held *et al.*, 2016) Table 1. Unfortunately, the big variations in the results together with some clustered values give small letters. Nevertheless, it gives a good visualization especially when used together with the table in Appendix 1.

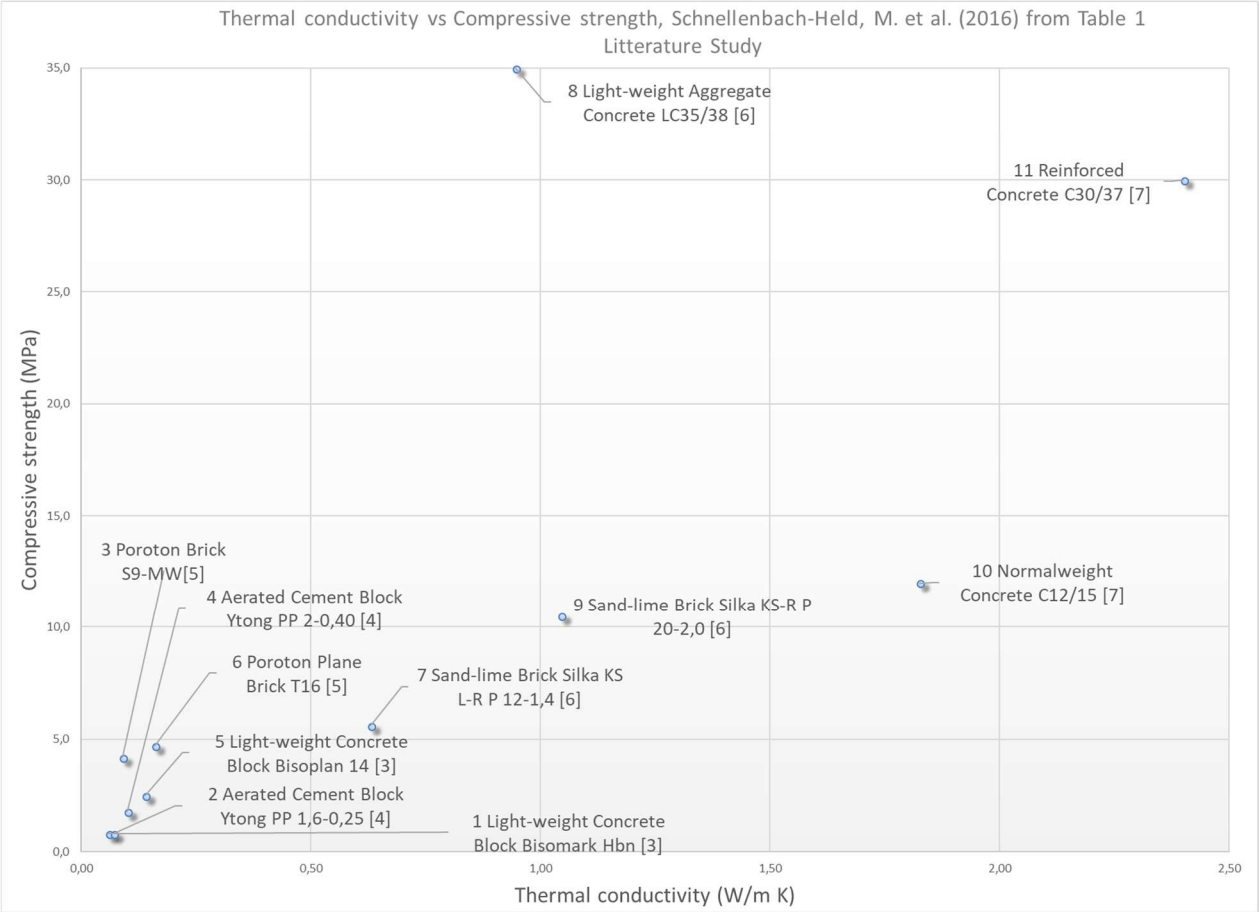

Figure 3.2: Thermal conductivity vs Compressive strength, Schnellenbach-Held, M. et al. (2016) Values from Table 1 (Literature Study)

Figure 3.3 shows data from Appendix 1 where the selection is made from studies that has showed relatively superior results for thermal conductivity and compressive strength.

Figure 3.4 shows the same data from Appendix 1 as Figure 3.3, but the axes are switched. This is for easier comparisons, since some articles have their graphs presented this way.

Thermal conductivity closely adheres to porosity and specific weight, and they are predominantly proportional. The downside is that this reduces the strength of the materials. This has resulted in endless studies to find better inner bonds that are a form of reinforcement at the micro level.

The specific weight is quite important because it reduces actual loads of the structure. There is a considerable gain to apply lightweight materials, since the load on self-supporting walls will be reduced.

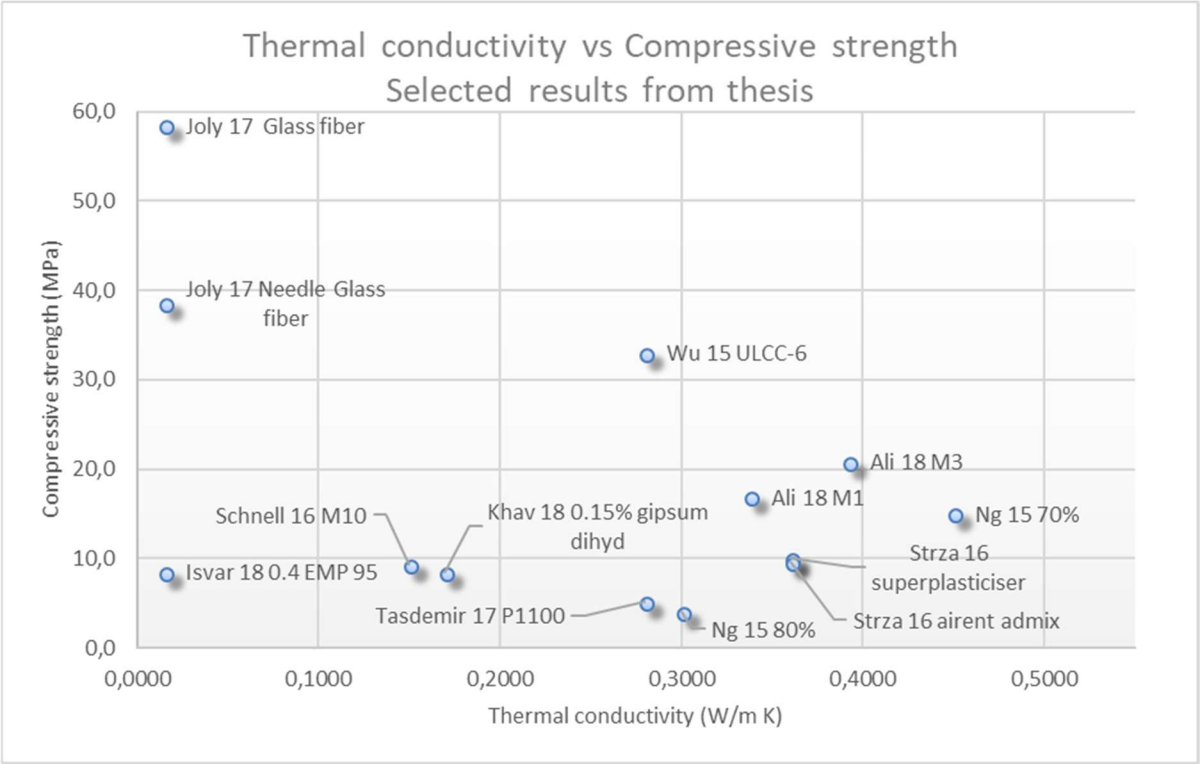

Figure 3.3: Thermal conductivity vs Compressive strength, Selected results from this thesis. (The notation is an abbreviation of the reference, the year of the study and a notation of the constituent).

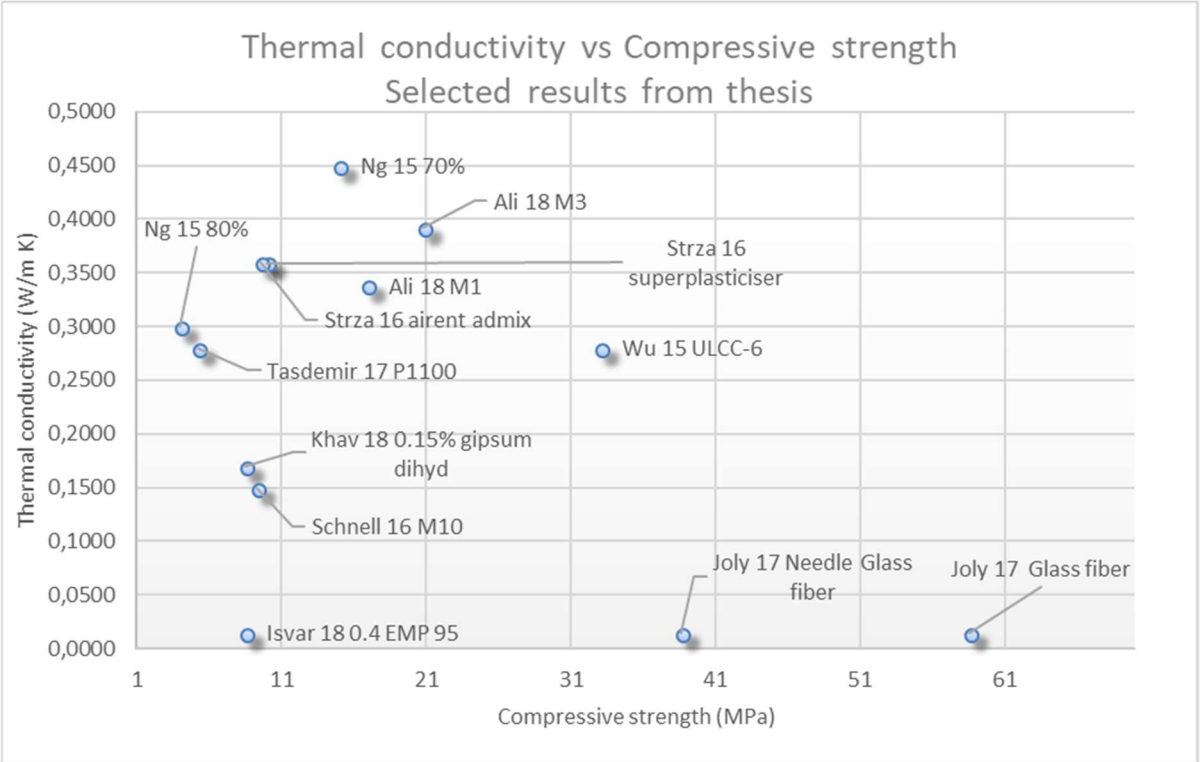

Figure 3.4: Same chart as Figure 3.3, but with switched axis.

In the following are some quotes of results from referenced studies:

“1. INTRODUCTION

Thermal conductivity is an important material property in the energy design process of buildings. While cement-based materials are the most consumed materials in the construction industry, a wide range of thermal conductivity may be desirable for these materials depending on the application areas. Indoor surfaces such as embedded floor heating systems or cementitious materials mixed with phase change materials, may demand high thermal conductivity. On the other hand, materials with low thermal conductivity may be desirable for using as a part of heat insulation or for thermal bridge calculations as well as structural elements.

Moisture content, porosity and constituent materials are the main parameters affecting thermal conductivity of cement-based materials. Thermal conductivity of water is more than 20 times bigger than thermal conductivity of the stagnant air and replacement of air by water can make a notable change in the thermal conductivity of porous materials. While changes in constituent materials and porosity may be neglected after concrete curing for thermal conductivity determination, the moisture content is expected to have considerable changes during lifetime of most cementitious composites. This means that considering one certain value for thermal conductivity of such types of composites may give low accuracy when considering the material performance during the service life of the material. Calculating thermal conductivity as a function of main effective variables such as moisture content, porosity and constituent materials using simplified prediction models can be a practical solution to this challenge. The thermal conductivity of dry material can be adjusted in the mix design, using the knowledge from concrete technology about porosity and constituent materials. Variations in this material property due to moisture content can be estimated based on the saturation degree. Moreover, the water sorption can be controlled by modifying the pore structure as well as internal or surface hydrophobation [1, 2]. The prediction model can for example be introduced to building physic tools, where the thermal conductivity can be updated based on the existing climate conditions.” (Hajmohammadian Baghban, Kioumarsi and Grammatikos, 2018)

4. DISCUSSION

Depending on the application and intended accuracy of thermal conductivity prediction, the appropriate prediction model may be chosen. Theoretical bounds are appropriate tools to approximate the highest and lowest values. When the maximum heat loss through a building envelope due to moisture condensation in the pore structure of the material needs to be estimated or highest thermal resistivity of the cementitious materials in an embedded floor heating system due to drying is under investigation, the theoretical bounds can help providing the answer without conducting experimental investigation. In this case, providing the data for thermal conductivity of individual phases in the composite is sufficient, which can usually be extracted from the existing literature with a reasonable accuracy. While parallel and series model provide the absolute upper and lower limits, H-S model can present tighter bounds. When the thermal conductivity of the phases is not so far from each other (See Figure 1), H-S bounds can even be used for estimating the thermal conductivity of the composite. Figure 4 illustrates a comparison of different prediction models for dried HCPs considering two phases of air (porosity) and solid structure, based on experimental results from Baghban et al. [3]. Since the thermal conductivity of air is more than 20 times lower than the thermal conductivity of water, the difference between H-S bounds are much higher in Figure 4 compared to Figure 1. However, the experimental data is close to the upper H-S bound for this case which can be used for predicting thermal conductivity of the composites with some over estimation. The parallel model is still farther than upper H-S bound and gives considerable difference with the experimental results.

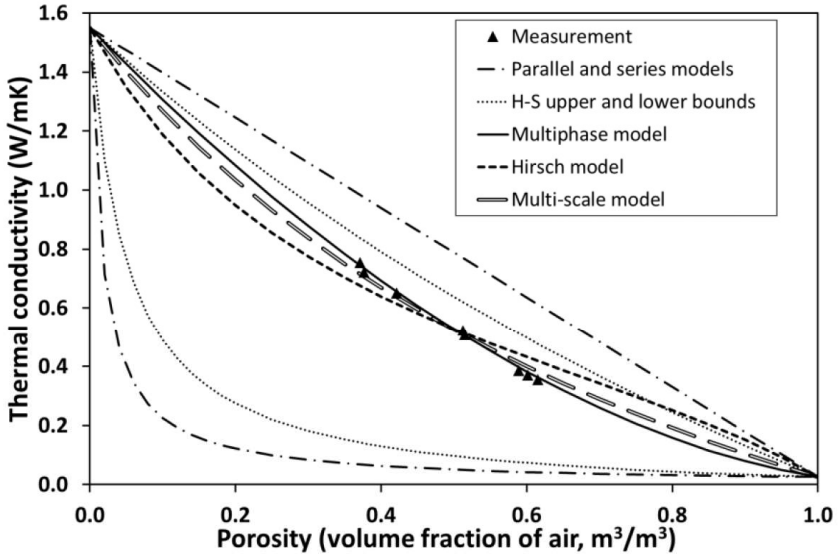

Figure 4 – Comparison of different models with the experimental results of HCPs with two phases of air and solid structure

Multiphase semi-empirical model has shown the best fit to the experimental data in Figure 4 and the three-phase model in Figure 2 is also based on this model which has been in alignment with the experimental results. The multi-scale model also matches for this example and has the potential for accurate prediction. However, increasing accuracy may bring up complications in the modelling, which can make this method difficult to use. On the other hand, the Hirsch model gives some error and makes this model less suitable for this case. Since RSM is an interpolation technique and not a predefined composite model, which uses statistical approaches, it is able to calculate a regression model to predict the response (in this example, thermal conductivity of the composite). The result of RSM is a polynomial of existing variables, which can easily be fitted to the experimental results in figure 4 and especially multiple variables like surfaces such as the one shown in Figure 2. Since this method is not based on a predefined composite model, providing properly distributed experimental data in the actual boundaries of the composite model can facilitate more accurate estimation of the thermal conductivity pattern. Predefined composite models are less sensitive to distribution of the experimental data.

Changes in the mix composition such as incorporating fibers, additives, different types of aggregates or moisture changes, may change the thermal conductivity pattern and prediction models should be investigated for these cases as well. In general, above-mentioned models are expected to have the potential for predicting the thermal conductivity of cementitious composites with intended accuracy." (Hajmohammadian Baghban, Kioumarsi and Grammatikos, 2018)

3.1 Types of Concrete

(Samson et al., 2017, p 202) shows an organization chart of the different partial load-bearing insulation materials

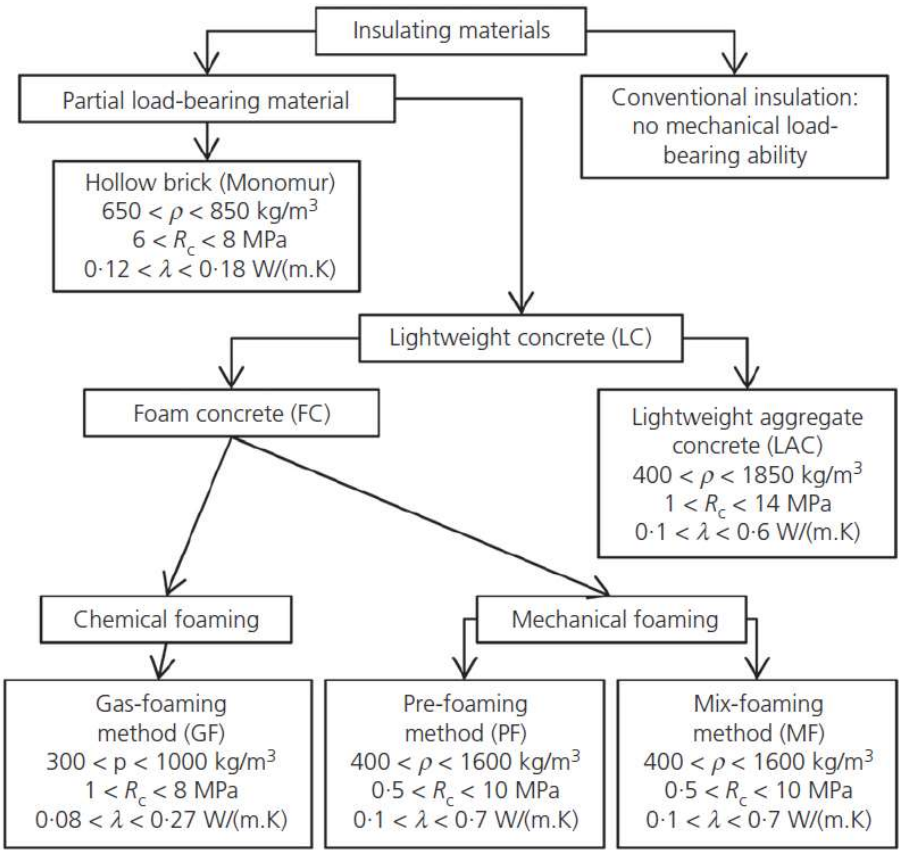

Figure 1. Organisation chart of the different partial load-bearing insulation materials (Samson, Phelipot-Mardele and Lanos, 2017)

3.1.1 Aerogel Concrete

Aerogel concreate is one of the latest developed types of cements and apparently one of the more promising products with respect to the combination of low thermal conductivity and sufficient compressive strength that is highly beneficial for building materials.

"Aerogel is a synthetic porous ultralight material derived from a gel, in which the liquid component of the gel has been replaced with a gas.[1] The result is a solid with extremely low density[2] and low thermal conductivity. Nicknames include frozen smoke,[3] solid smoke, solid air, solid cloud, blue smoke owing to its translucent nature and the way light scatters in the material. It feels like fragile expanded polystyrene to the touch. Aerogels can be made from a variety of chemical compounds.[4]

Aerogel was first created by Samuel Stephens Kistler in 1931, as a result of a bet[5] with Charles Learned over who could replace the liquid in "jellies" with gas without causing shrinkage.[6][7]

Aerogels are produced by extracting the liquid component of a gel through supercritical drying. This allows the liquid to be slowly dried off without causing the solid matrix in the gel to collapse from capillary action, as would happen with conventional evaporation. The first aerogels were produced from silica gels. Kistler's later work involved aerogels based on alumina, chromia and tin dioxide. Carbon aerogels were first developed in the late 1980s.[8]

Aerogel is not a single material with a set chemical formula, instead the term is used to group all materials with a certain geometric structure.[9]" https://en.wikipedia.org/wiki/Aerogel

A recent study from England from 2017 shows that aerogel beads are even better than aerogel powder for replacement materials for sand in this type of application. From the introduction we can read:

"In the present study, a novel concrete material has been investigated with partial replacement of cement with silica fume and Ground Granulated Blast Slug (GGBS), while sand is partially replaced by Aerogel. Aerogel is a synthetic porous ultralight material with very low density and very low thermal conductivity which has been used in some applications in buildings for external insulation. Aerogel can be found in many different types such as powder, beads or blankets." (Tsioulou, Ayegbusi and Lampropoulos, 2017)

Further from the study:

"2 Experimental Procedure

2.1 Materials

The mix designs of the current investigation are based on a previous study (Lampropoulos et al. 2015) on Ultra High Performance Fibre Reinforced Concrete. This mix has been modified by replacing part of the sand with Aerogel, powder and beads and by excluding the steel fibres (Table 1).

Table 1. Aerogel concrete mix design

Sample	Cement (kg/m3)	Silica fume (kg/m3)	GGBS (kg/m3)	Sand (kg/m3)	Aerogel (kg/m3)	Water (kg/m3)	Superplasticizer (kg/m3)
REF	657	119	418	1051	0	185	59
AC-10-P AC-10-B	657	119	418	945.9	7.2	185	59
AC-20-P AC-20-B	657	119	418	840.8	14.4	185	59
AC-30-P AC-30-B	657	119	418	735.7	21.7	185	59

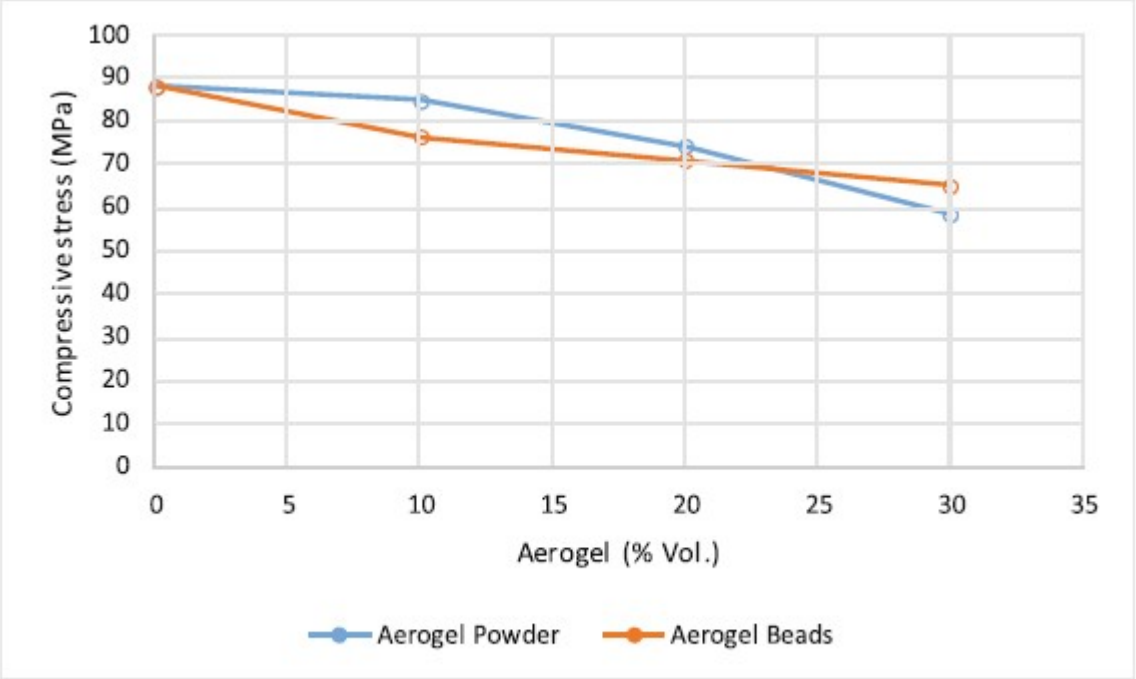

(a)

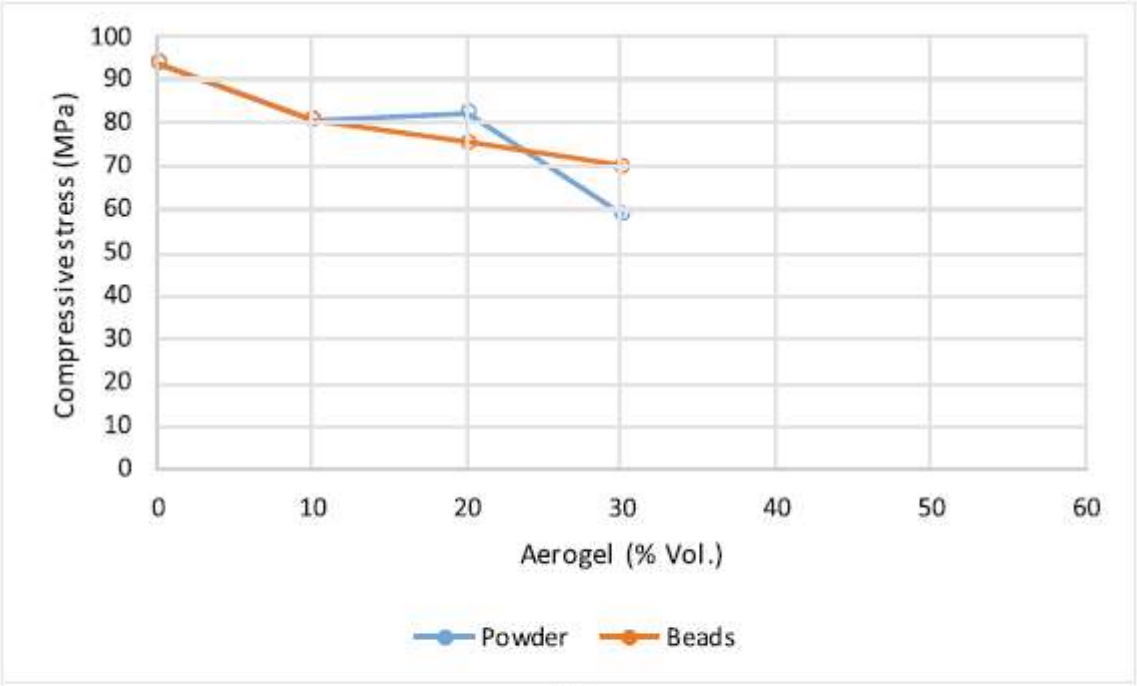

(b)

Fig. 1. Effect of Aerogel content on compressive strength of concrete at the age of (a) 14 days and (b) 28 days

In the above table, AC means Aerogel Concrete, the number next to it (10, 20, and 30) represents the volumetric replacement of sand with Aerogel (in %), and the final letter (P or B) represents the type of Aerogel (i.e. P for powder and B for beads).

The densities of the materials used in the current study are shown in Table 2.

Table 2. Materials and their densities

Material	Density (kg/m3)
Water	1000
Cement	3150
Silica fume	2200
GGBS	1900
Sand	1600
Aerogel	110

2.2 Experimental Results

2.2.1 Compressive Strength

Mixes which are presented in Table 1, using Aerogel powder and Aerogel beads, have been tested in compression on different ages (14 and 28 days after casting) and results for the compressive strength are presented in Fig. 1.

It can be observed than in both cases where Aerogel powder and Aerogel beads have been used as a partial replacement of sand, compressive strength is reduced as the Aerogel amount is increased. Also, based on these results, it seems that the compressive strength is not considerably affected by the type of Aerogel used in the current investigation (i.e. powder and beads), however, mixes with Aerogel beads seem to have higher compressive strength at the age of 28 days.

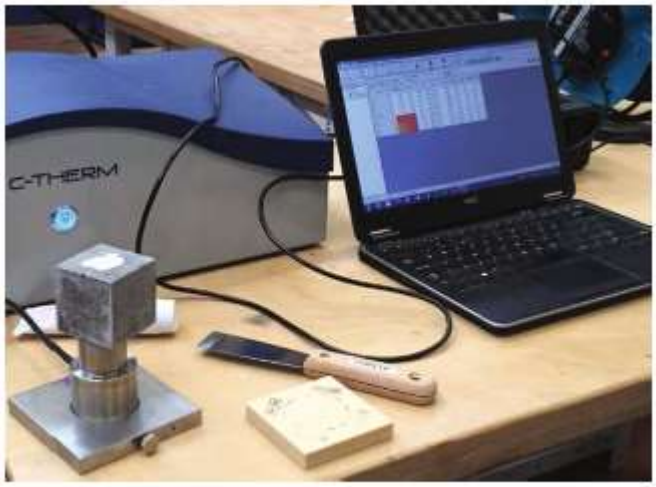

Fig. 2. Thermal conductivity TCi analyser

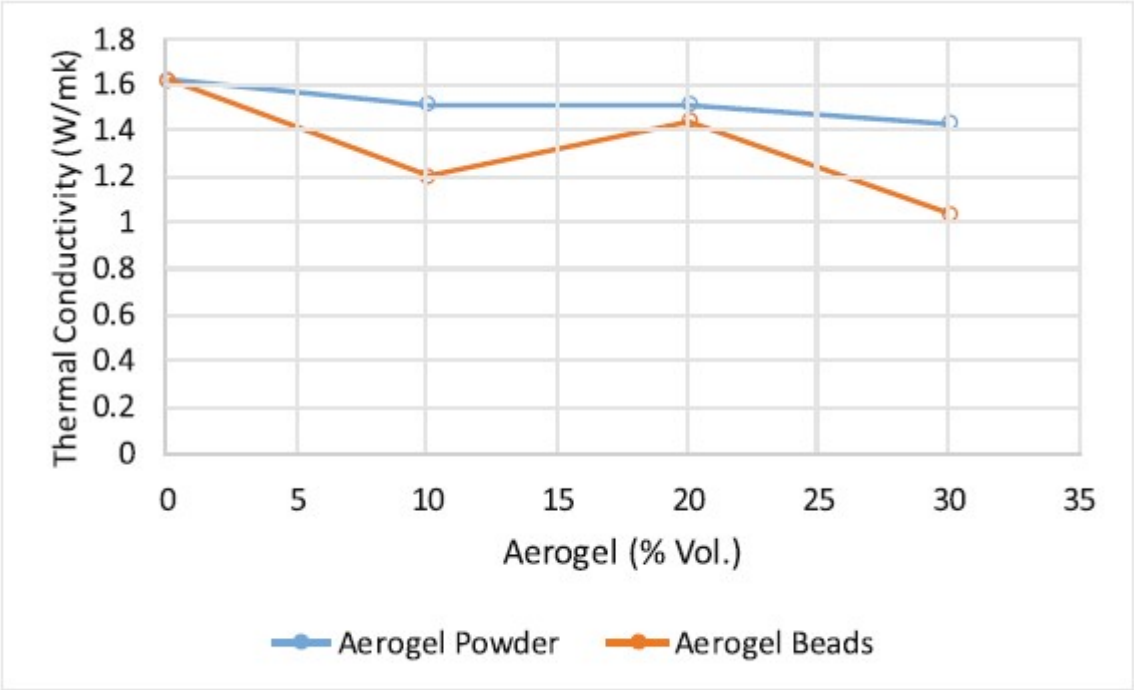

(a)

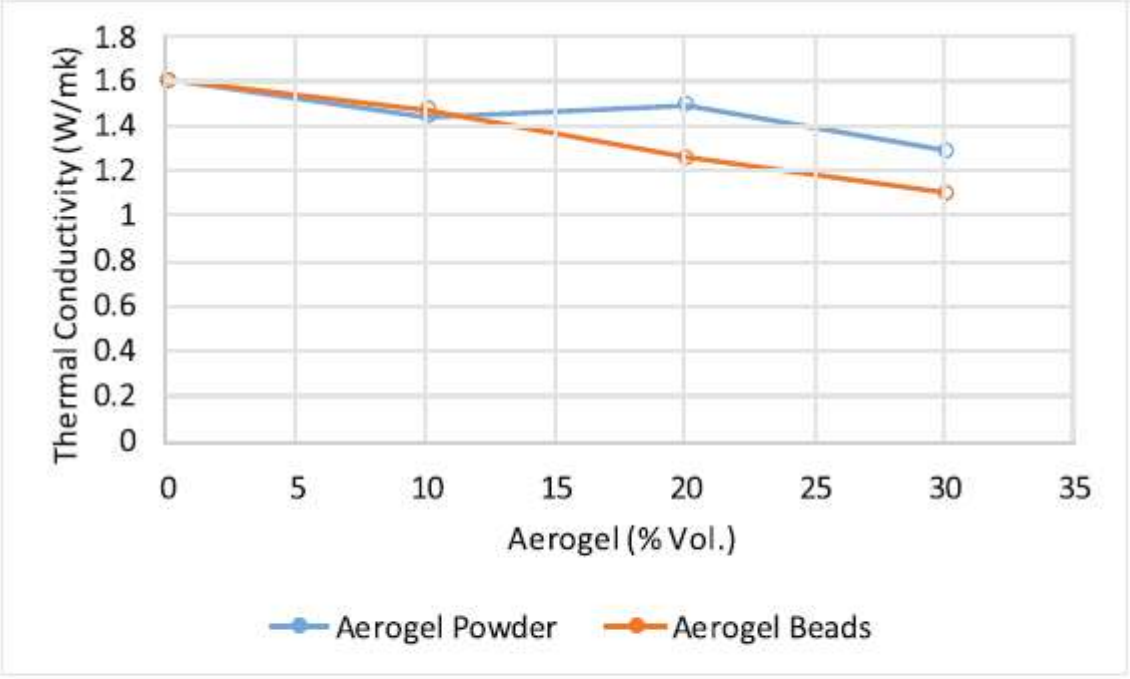

(b)

Fig. 3. Effect of Aerogel content on thermal conductivity at the age of (a) 14 days and (b) 28 days

2.2.2 Thermal Conductivity

Thermal conductivity was measured in all the mixes at the age of 14 and 28 days. For these measurements a Thermal Conductivity Analyser (TCi), which is based on a modified transient plane source method, was used (Fig. 2).

Thermal conductivity measurements for all the examined mixes are presented in the following Fig. 3.

It can be observed that the thermal conductivity in Aerogel beads mixes was, almost in all the examined cases, lower than the respective values for the Aerogel powder mixes.

Also, as the amount of Aerogel in the mix is increased, thermal conductivity is reduced. Hence, the highest reduction of the thermal conductivity in the current study was achieved for 30% sand replacement with Aerogel. In the samples with 30% Aerogel powder, reduction of the thermal conductivity by 11.7% was observed on the 14th day while the respective reduction on the 28th day was found equal to 19%. The respective reductions for the specimens with Aerogel beads were found equal to 35.8% (14th day) and 31% (28th day).

The variation of the thermal conductivity with the age of the concrete is illustrated in Fig. 4. From these results (Fig. 4) it can be observed that change in thermal conductivity is not considerably affected by the age. This is in agreement with previous studies on the effect of the hydration rate on the thermal conductivity properties (e.g. Choktaweekarn et al. 2009).

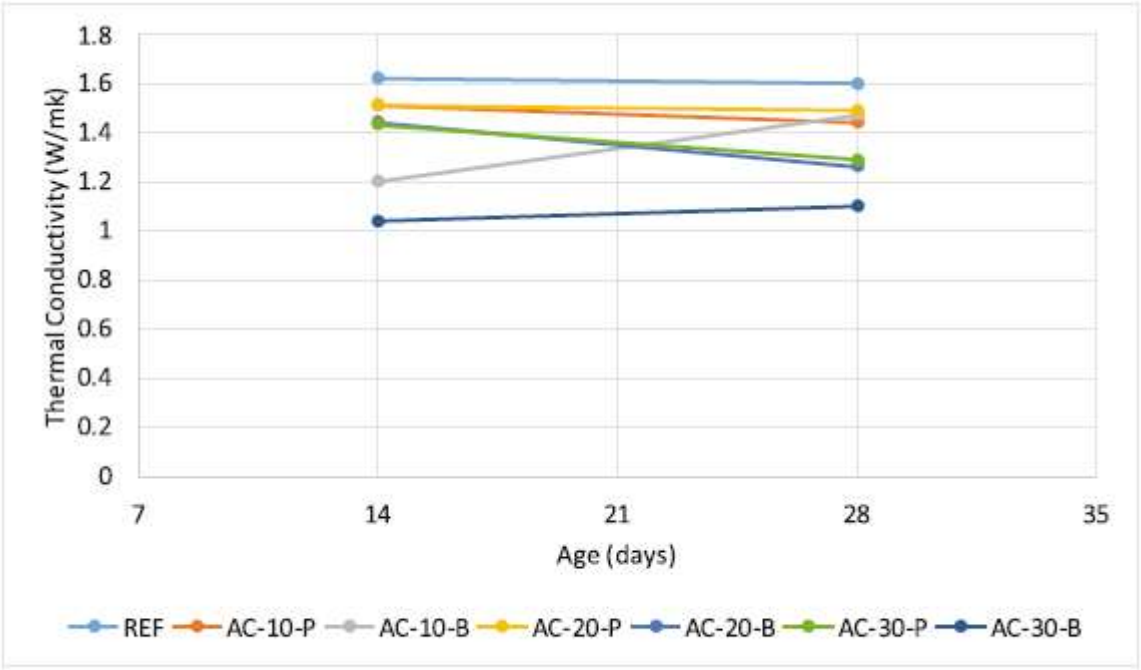

Fig. 4. Thermal conductivity change with concrete's age

3 Conclusions

In the current study the results of an experimental investigation on the development of novel Aerogel concrete with low thermal conductivity and enhanced compressive strength have been presented. Various types (beads and powder) of Aerogel have been used in the mix as partial replacement of the sand. The thermal conductivity of the examined mixes has been measured using a TCi thermal conductivity analyser and compressive tests have also been conducted at 14 and 28 days after casting.

Based on these experimental results the following g conclusions have been drawn:

- The type of Aerogel used in this study (powder or beads) did not significantly affect the compressive strength, while the thermal conductivity was found to be lower for the mixes with the Aerogel beads.

- By replacing 30% (by volume) sand with Aerogel beads, 31% reduction of the thermal conductivity was achieved. The thermal conductivity of this mix was found equal to 1.1 W/mk while at the same time high compressive strength (60 MPa) was achieved.

- Finally, the thermal conductivity of all the examined mixes was not considerably affected by the age of the specimens (14th and 28th day after casting).” (Tsioulou, Ayegbusi and Lampropoulos, 2017)

Another study from Germany, also conducted in 2017 are reporting promising results:

“1 Introduction

The requirements for the thermal insulation of buildings require load-carrying building materials with a low thermal conductivity. One approach is the development of so called Aerogel Concrete which exhibits low thermal conductivities but also a low compression strength. The scope of the research project described (Schnellenbach-Held et al. 2015) was the development of a High Performance Aerogel Concrete with an improved correlation between compression strength and thermal conductivity which allows the construction of single-leaf exterior walls of multi-story buildings without any further thermal insulation.”(Welsch and Schnellenbach-Held, 2017)

Results from previous field research are reported as follows:

“2 State of Research

The first steps in the development of Aerogel Concrete have been undertaken in the year 2008, when Ratke embedded silica aerogel granules in a normal-strength cement matrix for the first time (Ratke 2008). He was followed by researchers in Germany (Hub et al. 2013) and Norway (Gao et al. 2014; Ng et al. 2015), who used matrices of Ultra High Performance Concrete (UHPC) in order to optimize the compression strength of the low-density material Aerogel Concrete. All researchers employed superhydrophobic aerogel with a particle size from 0.01 mm to 4.0 mm or 2.0 mm to 4.0 mm, respectively, which amount was varied between 0 and 80% by volume. It was found that loadings between 50 and 70% by volume can be considered as relevant for the production of an Aerogel Concrete with load-bearing and insulating properties. The findings of the investigations can be summarized as follows: Aerogel Concrete shows excellent building physics properties like a low thermal conductivity, a high sound absorption and a high fire resistance as well as frost resistance. Drawbacks are high material costs, a high tendency to shrink and mechanical properties, which still could be improved: a low compression strength, a low Young’s Modulus and a very low bond stress (Table 1).

Table 1. Properties of aerogel concretes from the literature.

		Ratke (2008)	Hub et al. (2013)	Gao et al. (2014)	Ng et al. (2015)
φ	vol.%	70–50	75–65	60–0	80–0
ρ	kg/m^3	580–1050	500–620	1000–2060	760–2300
f^{*}_{lcm}	MPa	0.6–1.5	1.4–2.5	8.3–62	0–149
$f^{*}_{\mathrm{lct,fl}}$	MPa	-	0.3–0.4	1.2–7.3	0.2–19.0
E_{lcm}	MPa	52–127	1100–1200	-	-
λ	W/(mK)	0.10	0.10–0.14	0.26–1.95	0.31–2.30

*Prisms 40 mm × 40 mm × 160 mm; **Calculated with $f_{\mathrm{lcm,cube150}} = f_{\mathrm{lcm,prism40}} \cdot 0.9$

A more detailed description of the state of research can be taken from (Schnellenbach-Held et al. 2016; Schnellenbach-Held and Welsch 2016).

3 Mixtures for High Performance Aerogel Concrete

A large number of preliminary investigations was performed in order to determine the influence of the mixture composition, the mixing regime and the type of storage (Fickler et al.

2015; Strucka 2016). The mixtures were evaluated by the dry bulk density, the compression strength and the thermal conductivity, using a performance indicator defined by

$$P\,[MNm^2K/Wkg] = \frac{f_{lcm,cube150}[\mathrm{MN/m^2}]}{\rho[\mathrm{kg/m^3}] \cdot \lambda[\mathrm{W/mK}]}$$

In this manner, based on over 100 different mixtures an optimized reference mixture for High Performance Aerogel Concrete was found (Table 2).

Table 2. Reference mixture for High Performance Aerogel Concrete (HPAC).

Portland cement 52.5R	kg/m^3	541.0
Silica aerogel granule	vol.%	61.4
Silica suspension	wt%[a]	13.0
Superplasticizer	wt%[a]	3.6
Organic stabilizer	wt%[a]	0.5
w/c	-	0.29

[a]Based on amount of cement

The cement used for the mixtures was very fine ground, showing a Blaine Value of 5300 cm2/g. The silica aerogel had a particle size from 0.01 mm to 4.0 mm, a thermal conductivity of 0.02 W/(mK) and a porosity > 90%. The amount of the aerogel was varied from 45 to 70 vol.%, the amount of cement was adjusted accordingly. No sand and no coarse aggregate were added. The components were mixed in an intensive mixer in batches of 100 L, using a defined mixing regime. The flow behavior was adjusted by the amount of superplasticizer, resulting in flowable, nearly self-compacting mixtures. Noticeable is the short hydration process: Setting of the HPAC mixtures was observed after 20–30 min, the maximum temperature was reached after 8–9 h, and the hydration process was finished after 24 h. Within these first 24 h, a significant contraction due to shrinkage of 9.5 mm/m was observed. Afterwards the shrinkage curve flattened and reached contractions of about 12.0 mm/m after 28 days.

In order to assess the structure of High Performance Aerogel Concrete, cubes made of HPAC were cut into slices with a thickness of 30 mm. Microsections of these specimens show the complete embedding and the homogenous distribution of the aerogel particles in the high strength cement matrix (Fig. 1).

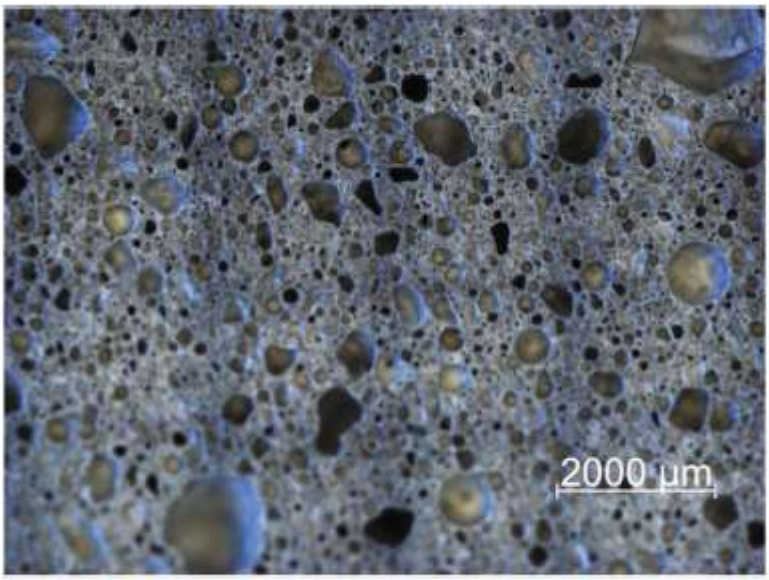

Fig. 1. Microsection of a specimen made of high performance aerogel concrete.

4 Mechanical Properties

4.1 Dry Bulk Density

Due to the absence of sand and coarse aggregate the solid content of HPAC is reduced in comparison to the Aerogel Concretes mentioned in par. 2. Thus, at the same amounts of aerogel granule, the resulting dry bulk densities are also lower (Fig. 2).

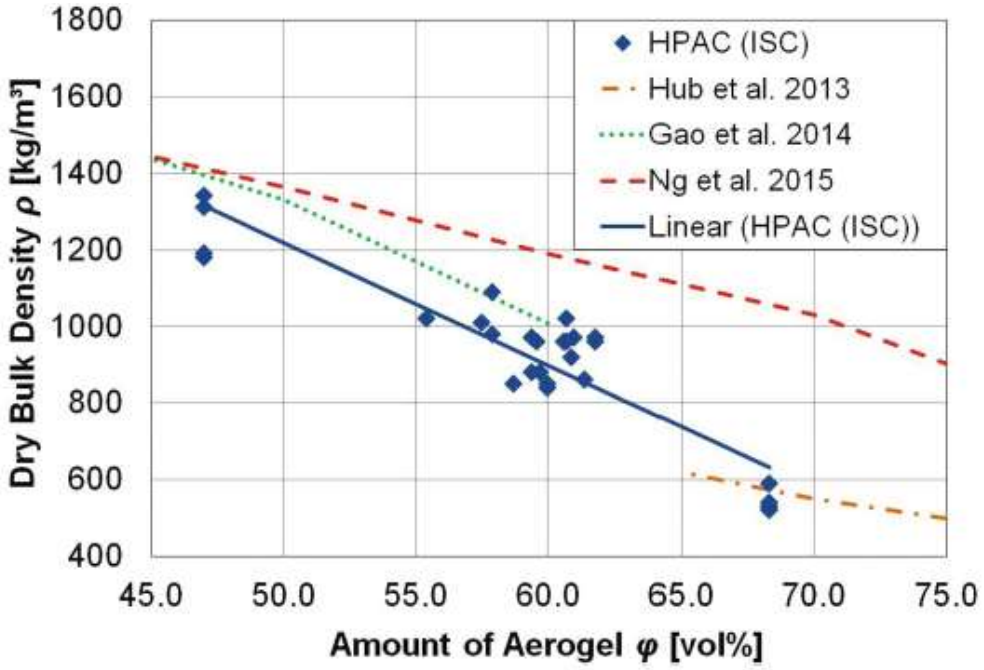

Fig. 2. Relation between aerogel amount and dry bulk density of high performance aerogel concrete compared to aerogel concrete.

4.2 Compression Strength

Compression tests were performed on cubes with 150 mm edge length according to (DIN EN 12390-3 2009), using a 3 MN-two-pillar universal testing machine. The load speed was set to 0.4 N/mm2s (≙ 9 kN/s) and kept constant by the use of an electronic control unit. Figure 3 shows the relation between dry bulk density and compression strength of HPAC, which can be expressed by an exponential function similar to the equation for Aerogel Concrete given in (Gao et al. 2014):

$$f_{lcm,cube150} = 0.37e^{0.0034\rho}$$

Figure 3 also shows that the compression strength of HPAC is considerable higher than that of the Aerogel Concretes mentioned in par. 2. Since the compression strength of these concretes was determined on prisms 160 mm x 40 mm x 40 mm, the values were translated using a conversion factor of 0.9. This factor was found by own tests on Aerogel Concrete cubes of the same batches with an edge length of 150 mm and 40 mm.

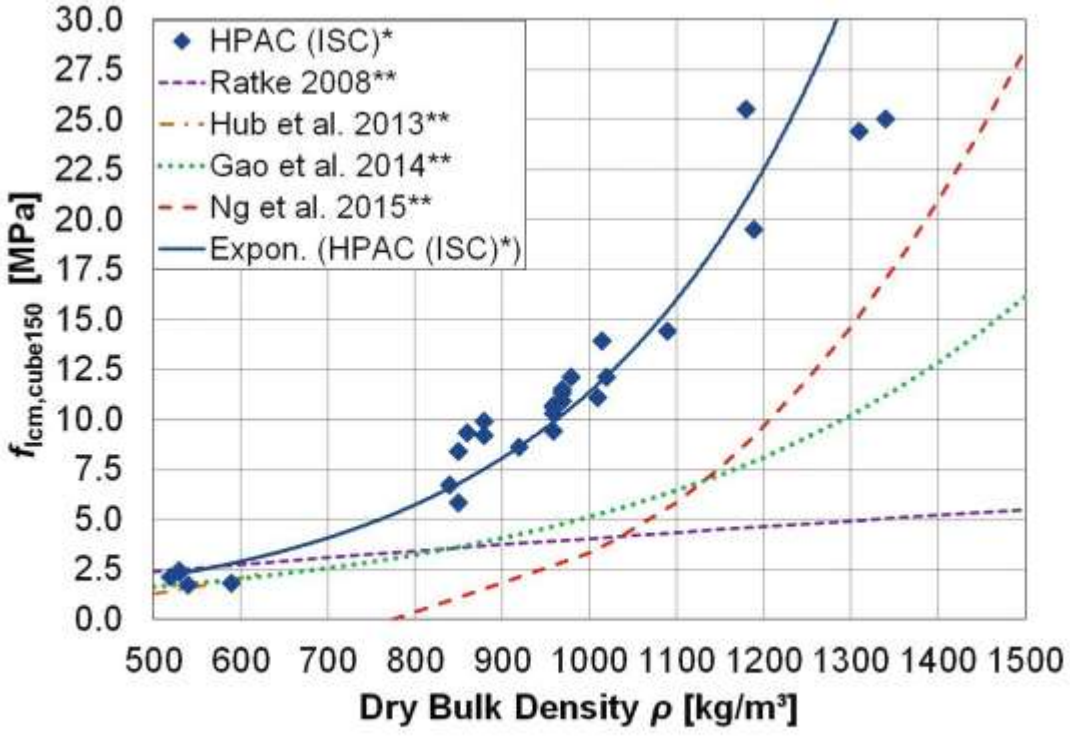

Fig. 3. Relation between dry bulk density and compression strength of HPAC compared to aerogel concrete ($^{*}f_{lcm,\ cube150}$, $^{**}f_{lcm,\ prism40} \cdot 0.9$).

4.3 Flexural Tensile Strength

The flexural tensile strength of HPAC was determined for eight mixtures with amounts of aerogel granule between 45 and 70 vol.% (Table 3). Four-point bending tests according to (DIN EN 12390-5 2009) were performed on samples with dimensions 700 mm x 150 mm x 150 mm.

Table 3. Compression strength, flexural tensile strength and Young's Modulus of different HPAC mixtures (Strucka 2016).

		M7.1	M7.2	M7.3	M7.4	M7.5	M7.6	M7.7	M7.8
φ	vol.%	45.0	50.0	55.0	57.5	60.0	62.5	65.0	70.0
ρ	kg/m^3	1450.2	1406.7	1325.8	1226.9	1133.3	1021.9	888.1	690.4
f_{lcm}	MPa	28.59	26.02	21.63	15.77	13.70	11.17	8.06	5.44
$f_{lct,fl}$	MPa	2.44	1.42	1.03	0.86	0.71	0.6	0.49	0.21
E_{lcm}	MPa	11529	9324	6898	6078	5537	4604	3464	2254

(Welsch and Schnellenbach-Held, 2017)

"5 Thermal Conductivity

The thermal conductivity was identified at the Institute of Materials Research of the German Aerospace Center (DLR), using the Heat Flow Meter Method according to (DIN EN 12664 2001). 14 days after concreting cubes with an edge length of 150 mm were cut into slices of 30 mm thickness and stored in a drying cabinet at 100 °C for 24 h before testing. Deviating from investigations on Aerogel Concrete (par. 2), the relation between compression strength and thermal conductivity of HPAC is nearly linear and can be expressed by (Fig. 4):

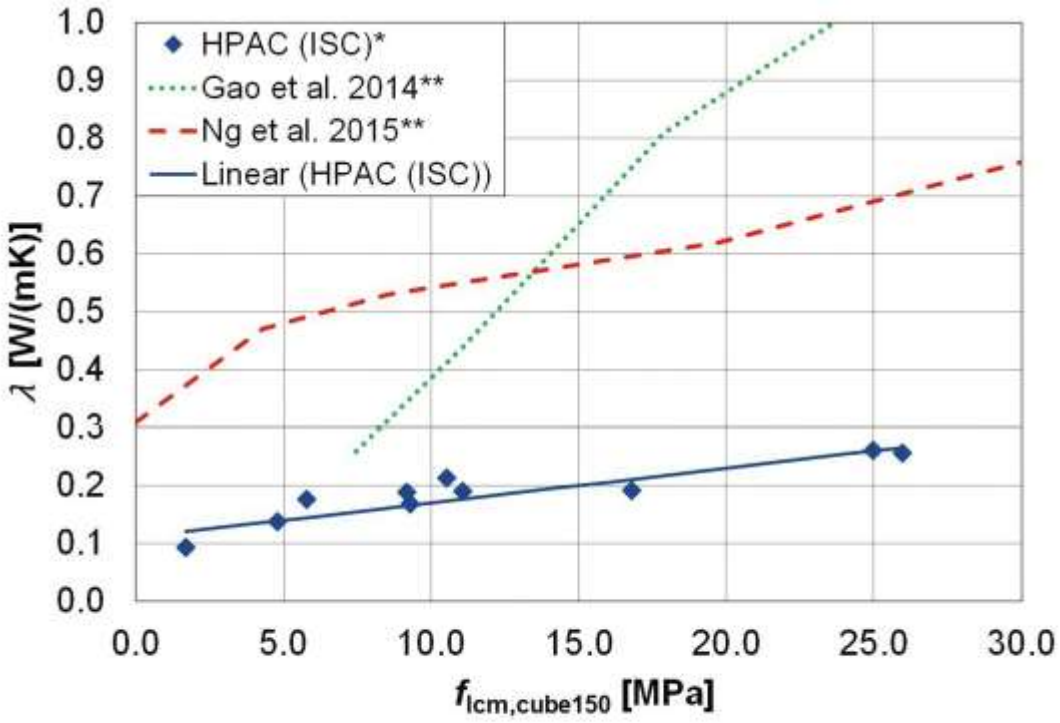

Fig. 4. Relation between compression strength and thermal conductivity of HPAC compared to aerogel concrete ($^{*}f_{\mathrm{lcm,cube150}}$, $^{**}f_{\mathrm{lcm,prism40}} \cdot 0.9$).

$$\lambda = 0.006 \cdot f_{\mathrm{lcm.cube150}} + 0.11$$

From Fig. 4 it is also apparent that the measured thermal conductivities of HPAC are quite lower in the whole considered range of strength compared to the Aerogel Concretes mentioned in par. 2.

6 Conclusions and Outlook

The developed High Performance Aerogel Concrete (HPAC) shows an improved correlation between dry bulk density and compression strength as well as compression strength and thermal conductivity. Compared to previous investigations on Aerogel Concretes, HPAC shows an improved performance over the full spectrum of investigated compressive strength in the range 2 MPa $\leq f_{cm} \leq$ 25 MPa. The performance indicator of HPAC, defined in par. 3 as the ratio of compression strength and the product of dry bulk density and thermal conductivity, amounts 48.7 to 77.7 $\cdot 10^{-3}$ MNm^{2}K/Wkg. This is quite above the performance indicators of Aerogel Concretes mentioned in the state of research, which show values between 9.3 and 28.7 $\cdot 10^{-3}$ MNm^{2}K/Wkg. The comparatively low flexural tensile strength of

HPAC as well as Aerogel Concretes result in the need for reinforcement if HPAC is intended to use for construction members subjected to bending. First investigations on the bond behavior of HPAC showed that it is in principal possible to produce reinforced HPAC (Schnellenbach-Held et al. 2016; Schnellenbach-Held and Welsch 2016). The Young's Modulus of HPAC is slightly below that of Lightweight Aggregate Concrete (LWAC), but can be expressed by a modified equation for LWAC and thus follows the same principles."(Welsch and Schnellenbach-Held, 2017)

3.1.2 Autoclave aerated concrete

A new study from Russia deals with improvement of thermal characteristics of autoclave aerated concrete for energy efficient high-rise buildings application. (Khavanov, Fomina and Kozhukhova, 2018).

"Introduction

The modern regulations require construction materials to meet the strict requirements for thermal and strength performance for construction of polyfunctional energy-saving high-rise buildings and residential complexes. Special requirement are made for materials applied in high-rise buildings. These materials should provide the required level of comfortability and optimal microclimate for human life and activities as well as required heat insulation [1]. Due to a significant environmental impact of construction materials production the energyefficiency of buildings become a problem number one in the construction sector [2]. A "Zero-energy" house is one of the effective approaches in construction was introduced and become very popular in Europe [3].

The new generation composites are the functional materials with improved performance and combine several characteristics such as structural, decorative, thermal-insulation and sound insulation etc. [4]. The application of autoclave aerated concrete as building envelopes is a good way to realize the concept. Aerated concrete performs well in the constructions with steel reinforced-concrete and high-rise monolithic structures [5]. Nowadays, autoclave aerated concrete is a multi-purpose construction material, produced using «green» technology [6]. The aerated concrete is a light-weight structural material with high thermal- and sound-insulation, reduced labor intensity; reduced transportation and others associated costs. Die to its light-weight and plasticity, aerated concrete can be easily cut in simple and more complex

architectural elements, which allows to expand the applicability of the material and be a good fit in high-rise buildings and others complex structures construction where the use of high-density elements is not possible. Moreover, aerated concrete is characterized by low thermal-conductivity providing an optimal air condition control and microclimate.

Development of innovative approaches and energy-efficient and eco-friendly technologies for aerated concrete production with improved thermal characteristics is based on modification of cellular structure saving the strength performance [7–9]. Smart concrete is among of the innovative construction materials. It can work in extreme climate and service conditions [10] considering social and aesthetic aspects [11].

The reduction of density with saving and increasing of strength performance is the key factor for efficiency of production and application of aerated concrete. An effective method to achieve an excellent thermal-insulating characteristics in aerated concrete is the control of hydration process. Often, a low quality autoclave material is associated with uncompleted chemical interaction between lime and quartz components in the binder system. Therefore, intensity and completeness of lime slaking as well as chemical reactivity of Ca(OH)2 are the key parameters at first stage of hydration in order to produce a high quality material.

However, at industrial level of production, it is difficult to precisely control the hydration process. The previous studies [12] showed that slaking of high-reactive lime (reactivity is 86 %, water demand is 32–64%) at the temperature range of 160– 190ºC at the presence of 0.05–0.25 % gypsum, the gypsum dehydration takes place leading to formation of β-hemihydrate of calcium sulfate and Ca(OH)2-particles with higher dispersity. Incorporation of high-dispersed Ca(OH)2 and β-hemihydrate calcium sulfate into the aerated concrete mixture causes the change in hydration kinetics, setting time and rheological performance [13–14]. In addition it helps to combine the periods of intensive structure formation and gas release (blow out of aerated concrete). That provides high-performance matrix structure of the final autoclave composite." (Khavanov, Fomina and Kozhukhova, 2018)

"Results The mix design of aerated autoclaved concrete was developed using design of experiment method considering the following parameters: slaked product content, water/solid ratio and content of β-hemihydrate calcium sulfate (%). The aerated concrete with density of 800 kg/m3 and compressive strength of 4.5 MPa was used as a reference. In order to describe

the binder system response by variation of the given parameters, adequate regression equations and yield surfaces were developed as depicted in Figure 1.

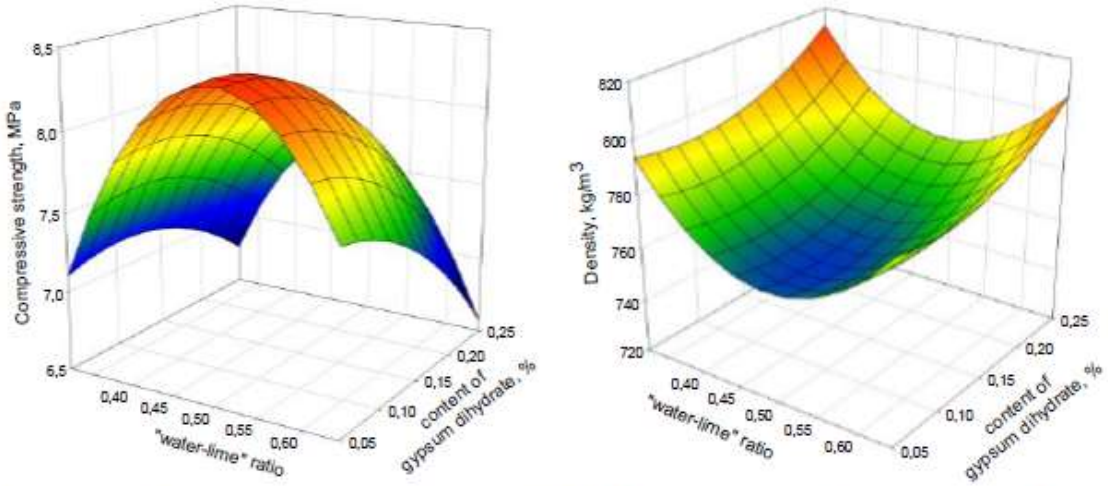

Fig. 1. The effect of water/solid ratio and content of β-hemihydrate calcium sulfate on density and compressive strength of aerated concrete.

Figure 1 demonstrated that the incorporation of previously slaked gypsum-lime binder into the aerated mixture enables to improve compressive strength performance and reduce density and water demand from 0.5 to 0.48 of the specimens. The aerated concrete after autoclave treatment demonstrated the absence of SO□24 ions, confirming the reactivity of β-hemihydrate calcium sulfate during structure formation. Therefore, the optimal mix composition of aerated concrete contented 0.15% of β-hemihydrate calcium sulfate with 0.4 water/solid ratio, resulting in a significant increase of compressive strength from 4.5 to 8.5 MPa, and density reduction from 800 to 760 kg/m3.

Sulfate activation positively effected pore formation in concrete matrix. Structural skeleton of the optimal composition demonstrated porosity increase from 70 to 75% as well as homogeneous pore distribution (Figure 2 b). Pores were spherical with 0.3–0.9 mm in diameter.

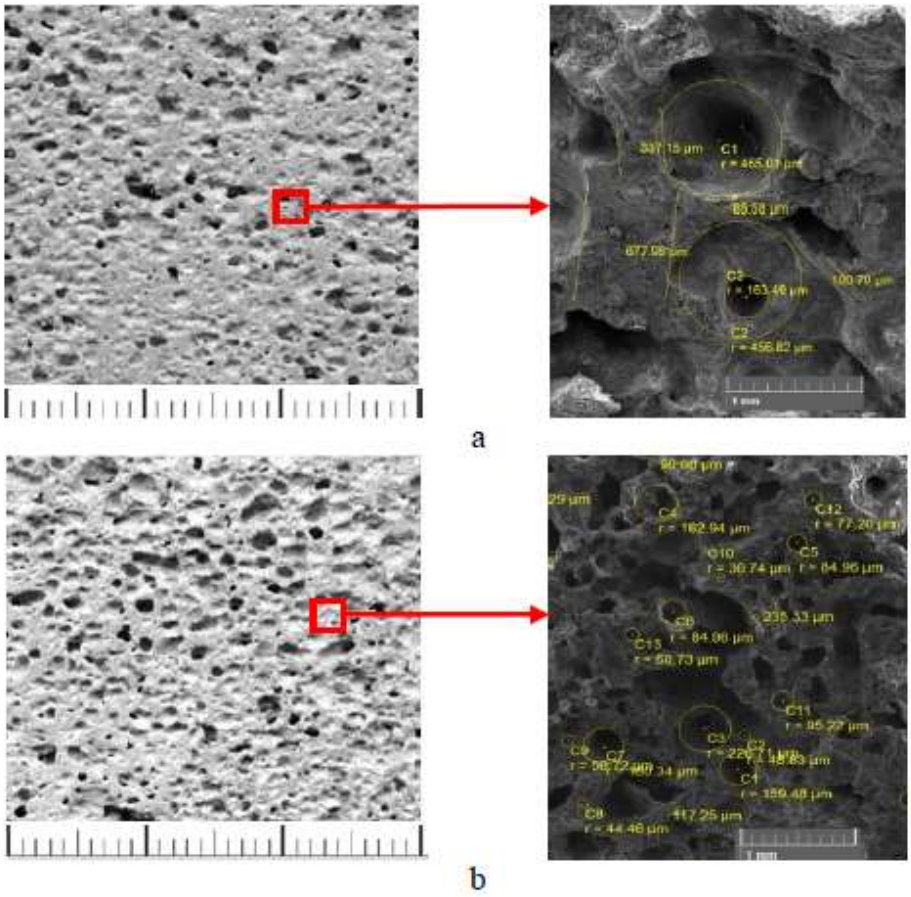

Fig. 2. SEM images of the aerated concrete after autoclave treatment: a – composition 1; b – composition 2 (Table 1).

According to the surface area BET data presented in Table 1, the volume of nanopores in concrete specimens was changed, where the volume of pores less than 94.6 nm was 0.007 cm3/g for reference specimen, and the volume of those for the experimental specimen was 0.018 cm3/g. Formation of proper porous structure is the key parameter to improve thermal characteristics of concrete, because density reduction causes the decrease of thermal conductivity from 0.19 to 0.17 W/(m·C°) (Table 1), improving thermal characteristics of aerated concrete.

Table 1. Characteristics of the aerated concrete after autoclave treatment.

Mix	Content of gypsum dihydrate in previously slaked binder, %	Water/solid ratio	Density, kg/m^3	Compressive strength, MPa	Heat conductivity, W/(m·C°)	Vapor permeability, mg/(m·h·Pa)	Porosity, %	Pore space with pore of 94.6 nm (cm^3/g)
1	0	0.50	800	4.5	0.19	0.14	70	0.007
2	0.15	0.48	760	8.5	0.17	0.16	75	0.018
According to Russian Standard 31359-2007	–	–	800	2.5–7.5	0.19	0.14 at least	–	–

Mix 2 of the produced aerated concrete specimen meets the requirements of the Russian Standard GOST 31359-2007 [19] in terms of vapor permeability, which was 12 % higher than that for reference mix 1 (Table 1). That means it can provide the "breathing wall" effect and keep in-door microclimate optimal.

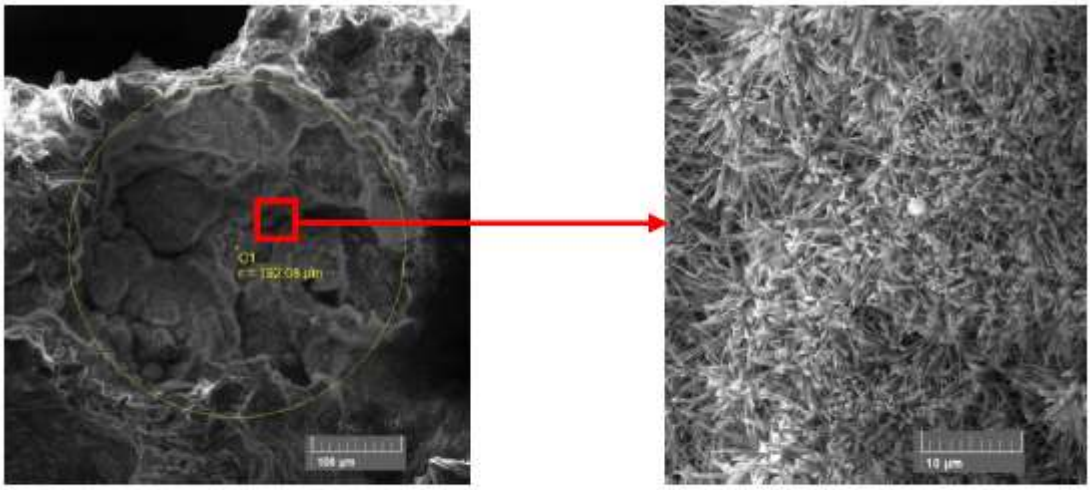

Fig. 3. SEM images of the mix 2 (Table 1).

Microstructure of an interporous zone as the most important zone in aerated concrete matrix responsible for with density and strength performance demonstrated the increase of structural packing density (Figure 3). Hydrothermal curing conditions are favorable for needle-like and stem-like crystal formations, which are typical for 11Å-tobermorite that serves as a reinforcing element at micro level structure strengthening structure of aerated concrete." (Khavanov, Fomina and Kozhukhova, 2018)

“Conclusions

This work demonstrated the opportunity to control thermal- and sound-insulating performance of aerated concrete due to homogeneous pore distribution, required density of interporous zone, required size and shape of particles. It can be achieved by controlling of hydration process in the binder system. Using method of lime sulfate activation allowed maximally intensify lime reactivity and stimulate the chemical interaction between components in the changing and rheological characteristics of fresh concrete mixture and mineral composition of aerated concrete. Increasing porosity, formation of multudispersed pores and their homogeneous distribution led to density reduction of the aerated concrete up to 5 %. The formation of needle-like crystals helps to reinforce matrix structure improving density of interporous zone, reduce structure imperfection and double the compressive strength of aerated concrete.

The developed aerated concrete is characterized by complex of improved thermal characteristics including heat conductivity reduction from 0.19 to 0.17 W/(m·°C), vapor permeability increase from 0.14 to 0.16 mg/(m·h·Pa) and that meets the requirements of modern standards of thermal insulation, energy saving and microclimate parameters. The application of developed concrete is good approach to produce environmentally friendly, sustainable and energy efficient structure at the stage of design, production and operation of high-rise buildings in today’s megapolises.” (Khavanov, Fomina and Kozhukhova, 2018)

3.1.3 Thermal insulating lightweight concrete (TI-LWC)

(Ali *et al.*, 2018) has recently published a well written report on Thermal insulating lightweight concrete (TI-LWC) that is very relevant for this paper.

“1. Introduction

Concrete is the most widely used construction material in the world. Normal weight concrete (NWC) is generally used for building construction despite its relatively high unit weight and limited thermal performance with a thermal conductivity ranging between 1.4 and 3.6 W/m.K [1]. A reduction in the unit weight of concrete and yet providing adequate strength will create a significant economic positive impact to the construction industry. In this regard, lightweight concrete (LWC) offers considerable advantage in terms of its unit weight over NWC.

LWC is a conglomerate of cement and lightweight aggregates. It has a bulk density ranging between 300 and 2000 kg/m3compared to 2200–2600 kg/m3 of NWC. LWC is broadly divided into the following categories based on its bulk density and compressive strength.

a. Thermo insulating lightweight concrete: This type of LWC is used as filling material or as an insulating coating. Its bulk density is in the range of 300–800 kg/m^3 while the compressive strength is in the range of 0.5–7 MPa.

b. Low strength lightweight concrete: This type of LWC is used in structures where the strength of concrete is not important; at the same time, it guarantees an acceptable level of thermal comfort. The bulk density is in the range of 800–1400 kg/m^3 while the compressive strength is in the range of 7–18 MPa.

c. Structural lightweight concrete: This type of concrete is normally prepared with synthetic aggregates. The reduced bulk density of this type of LWC is due to the addition of a void system within the cementitious conglomerate. The bulk density is in the range of 1400–2000 kg/m3 while the compressive strength is normally more than 20 MPa.

LWC can be prepared by utilizing one or more of the following three methods.

a. Utilizing natural or artificial lightweight aggregate with high porosity.

b. Introducing small polystyrene balls, partially or totally, in concrete in lieu of normal aggregates.

c. Adding a substance to the mixture that enables the production of gasses in an alkaline environment, leading to the formation of pores in the concrete.

LWC has many advantages. Some of these include the following:

a. Reduction in the dead load resulting in reduced sizes of structural members, that in turn results in a decrease in the quantity of cement and reinforcing steel,

b. Smaller and less expensive handling and transporting equipment needed to lift and place pre-cast elements,

c. Increase in the utility space due to a reduction in the size of columns, beams, and slabs,

d. Reduced size of the footings,

e. High thermal insulation, and

f. Enhanced fire-resistance.

The construction industry is striving to develop energy efficient buildings and materials, as economic and environmental constraints are bound to increase in the coming years. Improving the thermal insulation properties of concrete is an effective method of achieving this objective. Prevention of transfer of heat through the elements of the building decreases the consumption of energy, thus, decreasing the cost of air conditioning. Less energy resulting from improvements in the thermal insulation properties of concrete helps in a sustainable development of the infrastructure. The higher porosity of the lightweight concrete makes it a suitable material for thermal insulation of structures. In this study, the main aim was to develop a high thermal insulating lightweight concrete." (Ali *et al.*, 2018)

The work of Ali *et al.* also reports from an extensive literature study that will not be reported further here but their experimental program was as follows:

"3. Experimental program

3.1. Materials

TI-LWC mixtures were prepared with a combination of the following materials.

i. Limestone aggregate, produced by crushing large-size limestone rocks,

ii. Scoria aggregate, produced by crushing natural volcanic rocks,

iii. Polyethylene beads,

iv. Oil ash, produced as a waste-product after burning of heavy crude oil in a power plant to generate electricity, and

v. Natural dune sand, primarily comprising of quartz.

The chemical composition of cement, oil ash, and scoria are shown in Table 1 while the physical properties of the selected materials are summarized in Table 2. Figs. 1 through 3 show the polyethylene beads, scoria aggregate and oil ash, respectively, used in this study.

Table 1
Chemical composition of cement, oil ash, and scoria aggregate used in the preparation of TI-LWC.

Constituent, wt%	Type I cement	Oil ash	Scoria aggregate
SiO_2	20.52	1.65	41.47
Fe_2O_3	3.80	0.47	17.53
Al_2O_3	5.64	<0.10	12.81
CaO	64.35	0.45	8.76
MgO	2.11	0.48	8.9
Na_2O	0.19	0.53	3.4
K_2O	0.36	0.03	0.82
SO_3	2.10	–	0.3
V_2O_5	–	2.65	–
Sulfur	–	9.6	–
Loss on ignition	0.70	60.6	–
Moisture	–	5.9	–
Alkalis ($Na_2O + 0.658\ K_2O$)	0.43	0.55	–
C_3S	56.70	–	–
C_2S	16.05	–	–
C_3A	8.52	–	–
C_4AF	11.56	–	–

Table 2
Physical properties of the materials chosen for preparing TI-LWC.

Material	Specific gravity	Absorption, %
Sand	2.56	0.6
Cement	3.15	–
Oil ash	0.6	1.5
Limestone	2.6	1.1
Scoria	1.5	22.2
Polyethylene beads	0.886	0.008

Fig. 1. Polyethylene beads used in the preparation of TI-LWC.

Fig. 2. Scoria aggregate used in the preparation of TI-LWC.

Fig. 3. Oil ash used in the preparation of TI-LWC.

3.2. Specimen preparation

Six trial mixtures were prepared. The details of the trial mixtures are shown in Table 3. Specimens were prepared from the trial mixtures to determine unit weight and compressive strength. Four mixtures exhibiting low unit weight (generally less than 1900 kg/m3) and acceptable compressive strength (More than 14 MPa) were selected for detailed evaluation.

Table 3
Details of trial mixtures, unit weight and 7-day compressive strength.

Trail Mix #	Description of mixture	Ingredients									Flow, cm	Density, kg/m^3	Compressive strength, MPa
		Cement, kg/m^3	Coarse aggregate			Fine aggregate			w/c Ratio	Volume of plasticizer, ml			
			Lime Stone, CA/TA	Scoria, CA/TA	Polyethylene Beads, CA/TA	Sand, FA/TA	Oil ash, FA/TA	Polyethylene Beads, FA/TA					
TM-1	Polyethylene beads as coarse aggregate	370	–	–	0.5	0.5	–	–	0.45	3	12	1370	12.22
TM-2	Polyethylene beads as coarse aggregate with 10% oil ash replacing sand	370	–	–	0.5	0.45	0.05	–	0.45	2	10	1336	7.48
TM-3	50% Scoria and 50% Polyethylene beads as coarse aggregate	370	–	0.25	0.25	0.5	–	–	0.45	2	12	1588	14.55
TM-4	50% Limestone and 50% Polyethylene beads as coarse aggregate	370	0.25	–	0.25	0.5	–	–	0.45	2	16	1644	14.61
TM-5	Limestone as Coarse Aggregate and 50% addition of Polyethylene replacing sand	370	0.5	–	–	0.25	–	0.25	0.4	2	10	1862	2.87
TM-6	Scoria as Coarse Aggregate and 50% addition of Polyethylene replacing sand	370	–	0.5	–	0.25	–	0.25	0.4	2	10	1684	2.08

Table 4 lists the details of the selected mixtures. ASTM C 330 [20] requires a minimum 28-day compressive strength of 17 MPa, and a maximum unit weight of 1840 kg/m3. The various grading combinations and properties of natural LWAs used were considered keeping in mind

Table 4
Details of selected mixtures for detailed study.

Trial mix #	Detailed mix #	Description of mixture	Ingredients							w/c Ratio
			Cement, kg/m^3	Coarse aggregate			Fine aggregate			
				Limestone, CA/TA	Scoria, CA/TA	Polyethylene beads, CA/TA	Sand, FA/TA	Oil ash, FA/TA	Polyethylene beads, FA/TA	
TM-1	M−1	Polyethylene beads as coarse aggregate	370	–	–	0.5	0.5	–	–	0.45
TM-2	M−2	Polyethylene beads as coarse aggregate with 10% oil ash replacing sand	370	–	–	0.5	0.45	0.05	–	0.45
TM-3	M−3	50% Scoria and 50% Polyethylene beads as coarse aggregate	370	–	0.25	0.25	0.5	–	–	0.45
TM-4	M−4	50% Limestone and 50% Polyethylene beads as coarse aggregate	370	0.25	–	0.25	0.5	–	–	0.45

these limits. The concrete mixtures were designed to have approximately similar workability and water to cementitious materials ratio. A variation in the amount of superplasticizer for some mixtures was made to maintain the same degree of workability without adding extra water.

3.3. Testing

The TI-LWC specimens prepared from the selected mixtures were tested to determine the following properties:

i. Unit weight, according to ASTM C138 [21], on 100 mm cube specimens,

ii. Compressive strength, according to ASTM C39 [22], on 100 mm cube specimens,

iii. Modulus of elasticity, according to ASTM C469 [23], on 75 mm diameter and 150 mm high cylindrical specimens,

iv. Flexural strength, according to ASTM C78 [24], on 50 x 50 x 250 mm prismatic specimens,

v. Water permeability, according to DIN1048 [25], on 150 mm cube specimens,

vi. Water absorption, according to ASTM C642 [26], on 75mm diameter and 150 mm high cylindrical specimens,

vii. Drying shrinkage, according to ASTM C341 [27], on 50 x 50 x 250 mm prismatic specimens,

viii. Chloride permeability, according to ASTM C1202 [28], on 100 mm diameter and 50 mm thick disc specimens,

ix. Reinforcement corrosion by measuring corrosion potentials according to ASTM C876 [29] and corrosion current density following the linear polarization resistance method [30]. These tests were conducted on 75 mm diameter and 150 mm high cylindrical specimens with a centrally placed 12 mm diameter steel bar. The specimens were exposed to 5% NaCl to a depth of 100 mm from the bottom, and

x. Thermal conductivity, according to ASTM C177 [31], on 350 mm x 350 mm x 50 mm slab specimens." (Ali *et al.*, 2018)

Ali *et al*. reports their results in 11 subjects and several of the most relevant deserves to be listed in this paper:

"4. Results and discussion

4.1. Unit weight

The unit weight of the selected mixtures, depicted in Fig. 4, was in the range of 1366 to 1744 kg/m3. The least unit weight was measured in Mix # M2 (Polyethylene beads and oil ash) while the maximum unit weight was noted in Mix # M4 (Mixture of limestone aggregates and polyethylene beads). Replacement of normal weight limestone aggregates with lightweight aggregates, such as scoria and polyethylene beads, has resulted in a drastic reduction in the unit weight, being in the range of 24–40%. The reduction in the unit weight will lead to economical construction practices. Lightweight concrete significantly decreases the overall weight of the structure resulting in slimmer structural frames, footing or piles. Also, the decreased dead weight of concrete allows the use of longer spans in turn reducing the cost of propping the supports. The use of LWC may sometimes make it possible to construct structures, which otherwise would not have been possible due to excessive weight. Considerable savings in cost can be accomplished due to the use of the developed LWC in the construction of floors, partitions and external claddings.

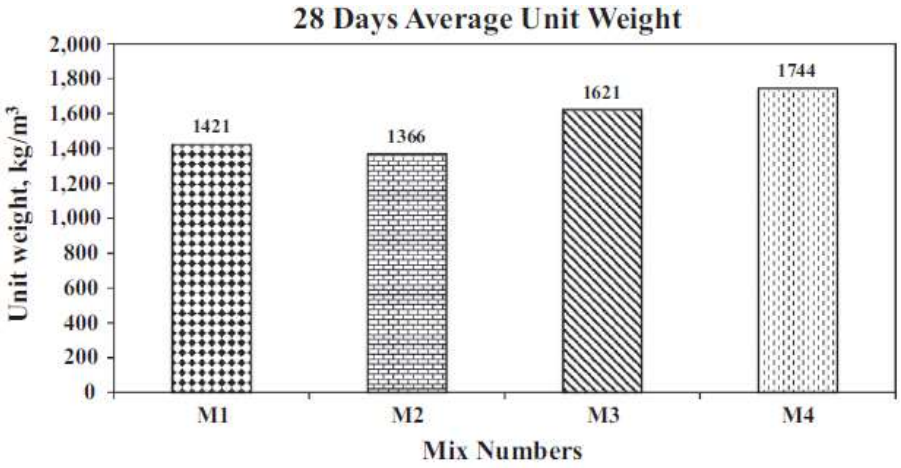

Fig. 4. Unit weight of the developed TI-LWC.

4.2. Compressive strength

According to ASTM standards, structural lightweight concrete should meet the 28-day compressive strength requirements shown in Table 5 without exceeding the corresponding maximum density values. The 28-day compressive strength of the investigated concrete mixtures was in the range of 17–27 MPa. The compressive strength of two mixtures prepared

Table 5
Requirements of compressive strength for structural LWC.

Calculated equilibrium density max, kg/m^3	Minimum average 28-day compressive strength, min, MPa
1840	28
1760	21
1680	17

with full replacement of limestone aggregates with polyethylene beads was 18 MPa (Fig. 5). This reduction in strength is attributed to the low bond between the smooth surfaces of the polyethylene beads and the mortar. The average 28-day compressive strength of NWC to be used as structural concrete should be in the range of 30–35 MPa (ACI-318), while that of

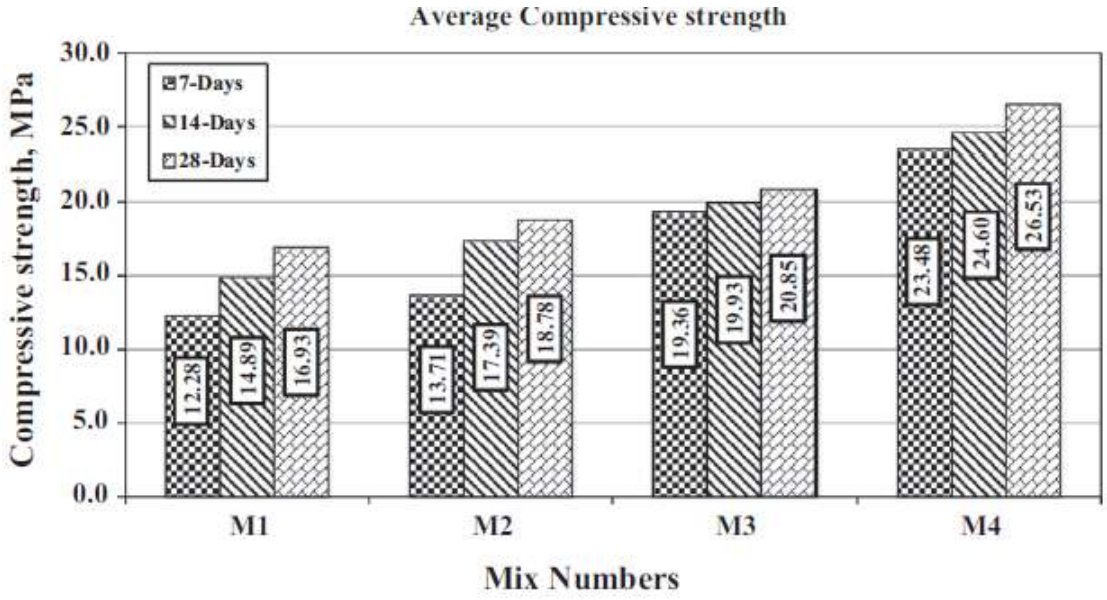

Fig. 5. Compressive strength of the developed TI-LWC.

LWC according to ASTM C 330-02 it should be 17– 28 MPa. Since concrete mixtures incorporating polyethylene beads have exhibited lower compressive strength, these can be used for non-structural purposes that do not require high compressive strength, per se 30 MPa and more. The partial replacement of limestone aggregates with polyethylene beads has increased the strength in the range of 27 MPa. A moderate compressive strength of about 21 MPa was achived by the use of lightweight scoria aggregates and polyethylene beads. The decrease in the compressive strength of LWC may be attributed to increased harshness and a tendency to segregate due to the low cement content and high volume of lightweight aggregates. Furthermore, increasing the volume of porous absorbing lightweight particles,

like scoria, and high volume single graded aggregates of polyethylene beads within the mixture would create a variation in the degree of compaction, and shall have more air entrapped, thus weakening the cementitious matrix resulting in decreased strength. It is suggested that instead of smooth faced new beads, recycled beads with rough surface could be used for increased bond and subsequently increased compressive strength." (Ali *et al.*, 2018)

"4.4. Flexural strength

Three-point loading test was conducted on the prismatic specimens to assess the flexural strength of the developed TI-LWC. These data are presented in Fig. 9. The developed TI-LWC was more ductile compared to the NWC. A ductile concrete will have large deflections in structures, providing a good warning of failure in the form of tensile cracks prior to complete collapse of a flexure member. The modulus of rupture was in the range of 1.75–2.75 MPa in the mixtures incorporating polyethylene beads. The incorporation of polyethylene beads has decreased the modulus of rupture, thus increasing the ductility of the developed TI-LWC. The modulus of rupture of NWC is generally in the range of 5–7 MPa. However, there was an increase in the strain in the mix with full replacement of limestone aggregates with polyethylene beads (Mix M2). The lower flexural modulus in this mix is attributed to the fact that the polyethylene beads with smooth surface do not provide a good bond between the successive aggregate particles leading to weak planes. These weak planes when loaded would not withstand the stresses resulting of early cracking of the specimen.

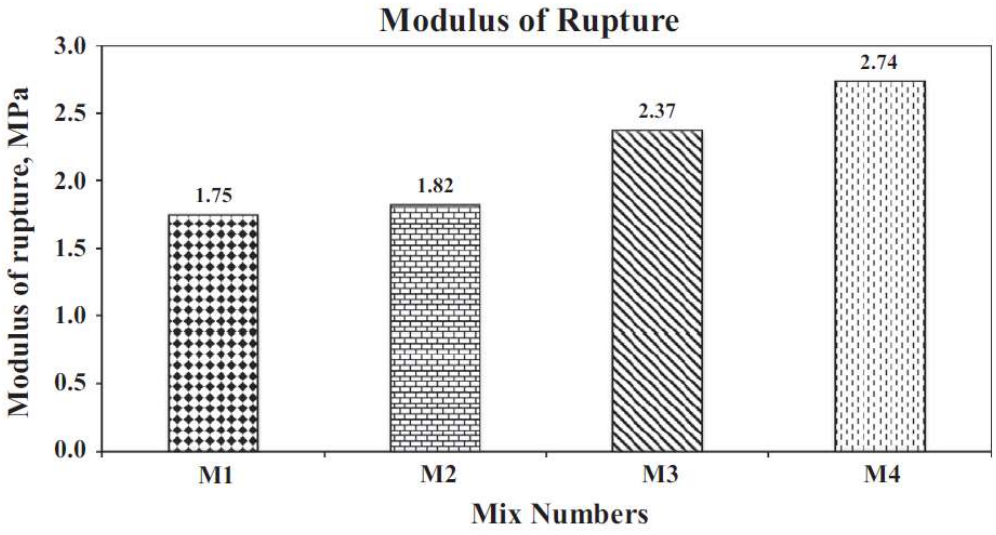

The load-deflection diagrams, as shown in Fig. 10, of the developed lightweight concrete are comparable to that of the NWC. As seen from Fig. 10, mix M2 with 100% polyethylene beads and with 10% oil ash shows more ductile behavior compared to the other three mixes. At the same time, lower ductility was noted in mix in which 100% polyethylene beads were used but without oil ash. This proves that oil ash is beneficial in filling the spaces or voids created due to the weak bond between the polyethylene beads and the cement mortar thus improving the ductility of concrete. The ductility of mixtures with 50% polyethylene beads and 50% scoria or limestone aggregates lies between mixes M2 and M1. It has been suggested that rough

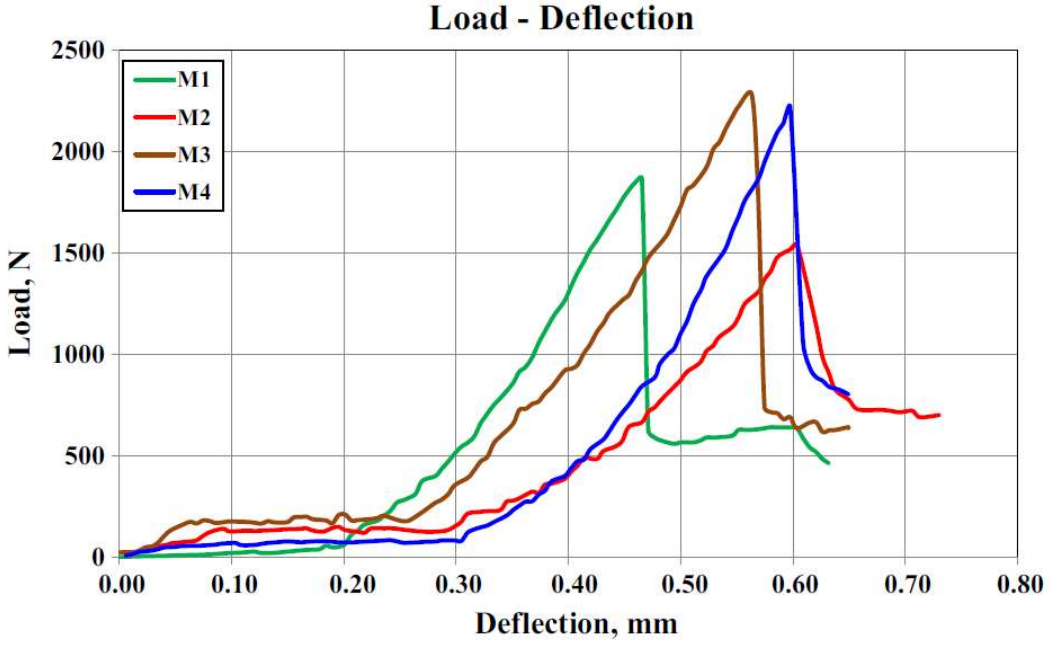

Fig. 10. Load-deflection curves for the developed TI-LWC mixtures.

faced beads could be better than the smooth ones to improve the flexural strength, while it is also established that fine fillers, such as oil ash can improve the ductility.

4.5. Water permeability

The depth of water penetration in the developed TI-LWC mixtures is depicted in Fig. 11. The depth of water penetration was in the range of 103–150 mm. The increased depth of water

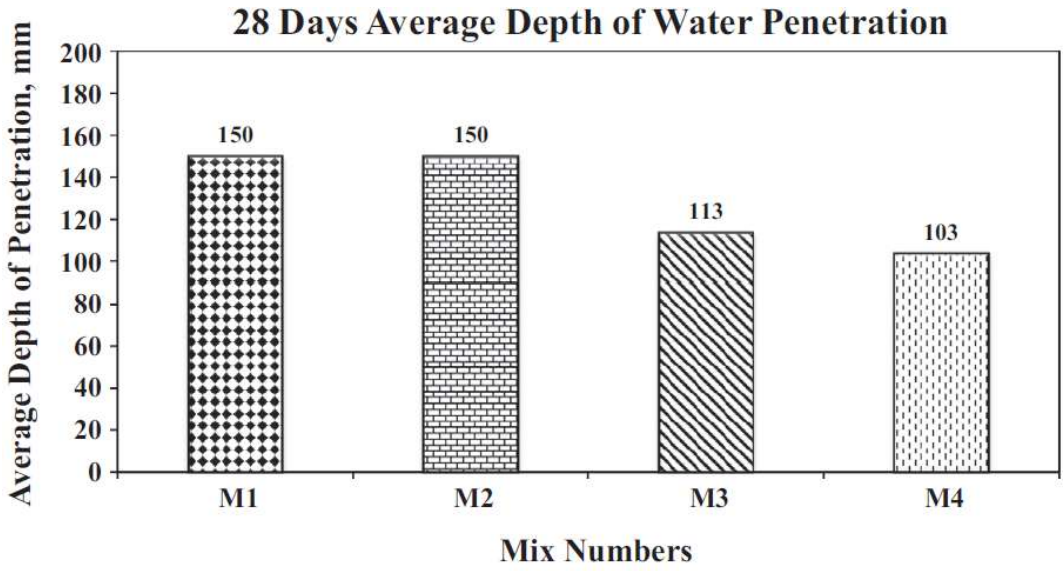

Fig. 11. Depth of water penetration in the developed TI-LWC mixtures.

penetration could be attributed to the porous nature of the aggregates used and due to the weak bond of the polyethylene beads with the cement mortar. Least depth of water penetration of 103 mm was noted in mix M4 prepared with a combination of limestone aggregate and polyethylene beads. The scoria aggregates used are of porous nature and as such it was anticipated that the depth of water penetration in mixture M3 will be high. However, the depth of water penetration was the highest in mixtures M1 and M2 in which polyethylene beads were used as 100% replacement of limestone aggregates. This may be attributed to the presence of weak planes due to a weak bond between the polyethylene beads and the cement mortar.

4.6. Water absorption

The water absorption in the developed TI-LWC mixtures is depicted in Fig. 12. The water absorption was in the range of 4.5–8.3%. Generally, a water absorption of more than 5% is noted in the NWC [35]. A water absorption of more than 5% was measured in mixtures prepared with polyethylene beads as coarse aggregates while it was the least in mix M4 incorporating limestone aggregates and polyethylene beads. The high absorption in case of mixes with full replacement of limestone aggregates with polyethylene may again be attributed to the weak bond between the beads and mortar. Water absorption values were high in mixtures in which polyethylene beads were used as 100% replacement of limestone

aggregates. However, it decreased with a decrease in the quantity of polyethylene beads, indicating a better bond between the aggregates and the cement mortar. The water absorption

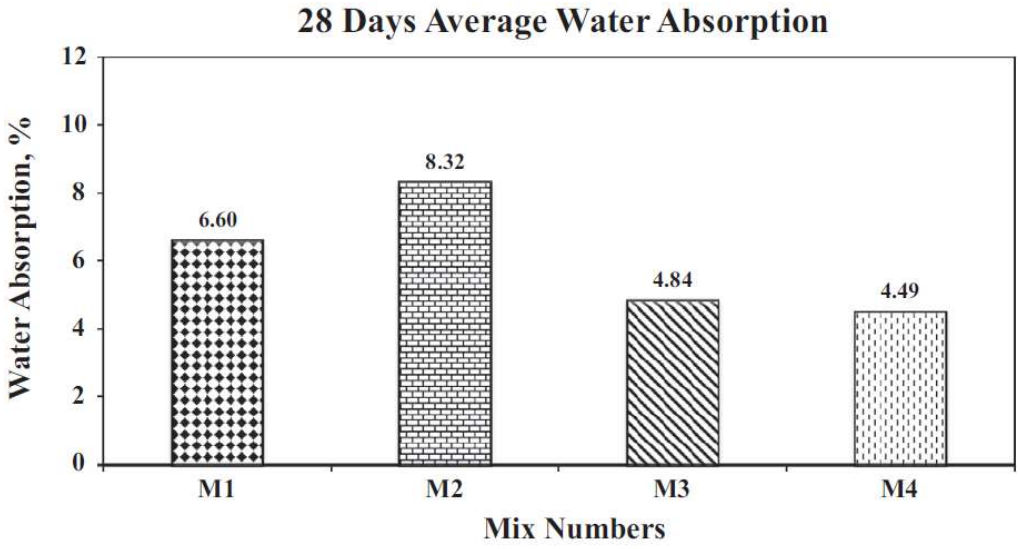

Fig. 12. Water absorption in the developed TI-LWC mixtures.

was even less than the threshold value of 5% [35] in mixtures in which scoria and limestone were used in combination with polyethylene beads.

The increased water absorption in the developed concrete mixtures may be attributed to the air voids in the lightweight aggregates, such as scoria, or weak bond between polyethylene beads and cement mortar." (Ali *et al.*, 2018)

"4.11. Thermal conductivity

The thermal conductivity was measured under steady-state conditions using a guarded hot plate that conforms to ASTM C177 [31]. Slab specimens, measuring 35 x 35 x 5 cm, were prepared and Dynatech guarded hot plate thermal conductance measuring system, TCFG-R4-6, was used to determine the thermal conductivity of the developed TI-LWC. The tests were conducted under steady state conditions. During the tests, the average temperature of the specimens was about 35 ± 2 ºC with the cold surface maintained at about 25 ºC.

The thermal properties (thermal conductivity and thermal resistance) of specimens prepared with the selected mixtures are summarized in Table 8. The thermal conductivity of the developed TI-LWC mixtures was in the range of 0.338–0.510 W/m.K. The lowest thermal conductivity of 0.338 W/m.K was measured in the specimens prepared with 100%

polyethylene beads as coarse aggregates (M1) followed by the other three mixtures. The thermal conductance of normal weight concrete is in the range of 1.3–1.5 W/m.K, which is very high compared to substantially low thermal conductance of the developed TI-LWC. The lowest thermal conductivity was measured in the specimens prepared with 100% polyethylene beads. The thermal conductivity of concrete increases with increasing cement

Table 8
Thermal properties of TI-LWC specimens prepared with selected mixtures.

Mix #	Description of mix	Dimensions, cm	Test thickness, cm	Mean temperature °C	Thermal conductivity W/m.K	Thermal resistance (R) m^2.K/W	1/R
M1	Polyethylene beads as coarse aggregate	35 × 35 × 5	5.70	34.90	0.338	0.169	5.92
M2	Polyethylene beads as coarse aggregate with 10% oil ash replacing sand	35 × 35 × 5	5.16	34.99	0.428	0.121	8.26
M3	50% scoria and 50% Polyethylene beads as coarse aggregate	35 × 35 × 5	5.44	33.60	0.392	0.139	7.19
M4	50% Limestone and 50% Polyethylene beads as coarse aggregate	35 × 35 × 5	5.28	33.75	0.510	0.104	9.61

content and thermal conductivity of the aggregates. The thermal conductivity of aggregates with crystalline structure is more than that of aggregates with an amorphous structure. Polyethylene has an intermediate level of crystallinity that contributes to a decrease in the thermal conductivity of concrete prepared with this type of aggregate.

Fig. 16 shows the comparison between the thermal conductance values from the experimental work and those reported in the literature [36]. As is evident from these data, thermal conductivity of the developed TI-LWC was much less than that reported in the literature. Demirboga and Gul [36] utilized pumice aggregates but the replacement levels were similar to the ones used in the reported work. In addition to the thermal insulation, lightweight concrete provides better fire-resistance than NWC due to its lower thermal conductivity and lower coefficient of thermal expansion.

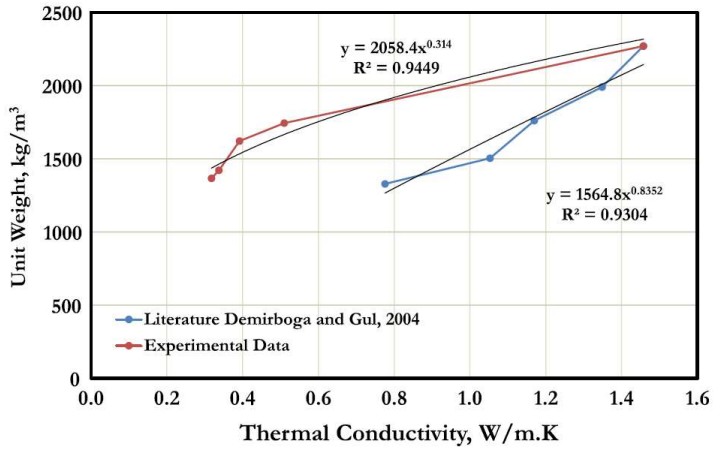

Fig. 16. Comparison of thermal conductance of the selected mixtures with similar studies in the literature [35].

The summary of the results of the tests conducted on the TI-LWC in the reported study is shown in Table 9.

Table 9
Summary of results of the tests conducted on the TI-LWC specimens prepared with selected mixtures.

Mix#	Description of mix	Average unit weight, kg/m^3	Average compressive strength, MPa			Modulus of elasticity, GPa	Modulus of rupture, MPa	Depth of water penetration, mm	Water absorption, %	Total charge passed, Coulombs	Thermal conductivity, W/m.K
			7 days	14 days	28 days						
M1	Polyethylene beads as coarse aggregate	1421	12.28	14.89	16.93	3.95	1.75	150	6.6	2456	0.338
M2	Polyethylene beads as coarse aggregate with 10% oil ash replacing sand	1366	13.71	17.39	18.78	4.09	1.82	150	8.32	3444	0.428
M3	50% Scoria and 50% Polyethylene beads as coarse aggregate	1621	19.36	19.93	20.85	5.62	2.37	113	4.84	4704	0.392
M4	50% Limestone and 50% Polyethylene beads as coarse aggregate	1744	23.48	24.6	26.53	7.50	2.74	103	4.49	2731	0.51

" (Ali *et al.*, 2018)

3.1.4 Lightweight Concrete

A study from turkey in 2017 look at thermal conductivities and mechanical properties of lightweight concretes. "The test results showed that, depending on the amount and type of lightweight aggregate, unit weight of concrete can be reduced and concretes with various physical and mechanical properties of can be achieved. Thermal conductivity was reduced with the use of lightweight aggregates and for all the lightweight concretes considered, a good relationship was obtained between thermal conductivity and unit weight of concrete. Reductions in the compressive strength and modulus of elasticity of concretes have been obtained with decreasing concrete unit weights. The reduction in strength was more for the concrete containing expanded polystyrene beads." (Tasdemir, Sengul and Tasdemir, 2017)

The most relevant results are presented as follows:

Table 2
Mix proportions of lightweight concretes containing pumice (kg/m^3).

Concrete Codes	P 1900	P 1700	P 1500	P 1300	P 1100	P 900	P 700
Cement	348	342	342	291	258	236	209
Water	150	147	147	125	111	101	90
Pre-absorption water	30	44	59	50	45	49	52
Effective water/cement ratio	0.43	0.43	0.43	0.43	0.43	0.43	0.43
Pumice (2–16 mm)	201	296	394	334	297	330	344
Natural sand (0–4 mm)	563	553	553	469	417	191	–
Limestone aggregate (2–16 mm)	677	333	–	–	–	–	–
Superplasticizer	5.2	5.1	5.1	4.4	3.9	3.5	3.1
Air entraining admixture	–	–	–	1.5	2.6	2.4	2.1
Unit weight	1973	1720	1500	1275	1133	913	700

(Tasdemir, Sengul and Tasdemir, 2017)

Table 3
Mix proportions of lightweight concretes containing expanded polystyrene beads (kg/m³).

Concrete Codes	EP 1600	EP 1400	EP 1000	EP 400	EP 300
Cement	223	260	272	223	199
Water	134	156	163	134	120
Pre-absorption water	0	0	0	0	0
Effective water/cement ratio	0.60	0.60	0.60	0.60	0.60
Natural sand (0–4 mm)	1246	979	528	28	0
Expanded polystyrene (2–4 mm)	1.94	6.07	10.31	11.72	10.68
Expanded polystyrene (4 mm)	0.59	1.85	3.15	3.58	3.26
Expanded polystyrene (4–8 mm)	0.35	1.10	1.86	2.12	1.93
Air entraining admixture	0.22	0.26	0.27	0.22	0.20
Unit weight	1606	1404	978	402	335

(Tasdemir, Sengul and Tasdemir, 2017)

Table 5
Properties of the mixtures.

Concrete Codes	Compressive strength (MPa)	Modulus of elasticity (GPa)	Thermal conductivity (W/mk)
P 1900	18.7	19.5	–
P 1700	14.1	13.9	–
P 1500	11.4	11.6	–
P 1300	11.1	7.1	0.36
P 1100	5.2	5.8	0.28
P 900	2.4	3.1	0.23
P 700	1.4	1.6	–
EP 1600	3.4	–	0.45
EP 1400	2.4	–	0.29
EP 1000	1.1	–	0.22
EP 400	0.3	–	0.069
EP 300	0.3	–	0.067

(Tasdemir, Sengul and Tasdemir, 2017)

3.1.5 Polyester-reinforced concrete composites

(Simek and Uygunolu, 2018) has recently presented a relevant study from Turkey that uses polyester to reinforce the concrete named “Thermal, electrical, mechanical and fluidity properties of polyester-reinforced concrete composites”. They also introduce a novel interesting analysis method.

“1. Introduction

In recent years, polyesters have been widely used in resin systems to provide extraordinary mechanical [1], corrosion and water resistance properties to composite materials [2]. These properties of the polymerised polyester resins make it an attractive material in the field of civil engineering application [3, 4]. Inorganic fillers such as cement, sand, silica fume and fly ash, granule blast furnace slag have been incorporated into polyester resins to improve some physical and mechanical properties of concrete composites [2]. Many researchers have investigated polyester resins reinforced concrete properties such as thermal stability and

elastic modulus [2, 5], ultrasonic pulse velocity [6], compressive and flexural strength [7, 8], thermal expansion [9], chemical resistance [10], abrasion resistance [11], thermal conductivity [12], tensile strength [13], durability [14], and morphology [15]. Many of these studies have focused on one or two properties of polyester-reinforced concrete composites (POREC) just as mechanical, thermal or water resistance. However, critical evaluation of all the properties of POREC simultaneously is necessary for real-world applications. In industry, a product is evaluated with multiple features such as thermal, mechanical or workability. In order to get the desired quality of POREC, a systematic analysis approach containing a design of experiment (DoE) methodology has been proposed in this study. The main contribution to the study is that thermal, electrical, workability, mechanical and water resistances of three different types of polyester-reinforced concrete composite have been analyzed simultaneously through full factorial design. Thus, the study aims to explore the effect of polyester granules on concrete using DoE approach.

Polyester resins, which are commercially available in various products with the fillings, fibers and granules [16], are produced with different features such as low melting point for fabrics, which are especially used in the automotive industry [17]; flame retardant for the clothing industry [18]; or fabrics used in the transportation vehicles; and cationic dyeable for the textile industry [19]. Most of researchers have focused on synthesis of polyester with different features. This paper aims to reveal the effect of low melting bonding, flame retardant and cationic dyeable polyester granules properties on concrete composites. Thus, the application areas of these polyester aggregates in the construction industry will become clearer via this research. Moreover, the electrical resistance performance of polyester granules in concrete has not been considered yet in the previous studies. In this respect, it is important for manufacturers to evaluate the performance in concrete. This study provides information to researchers and plastic manufacturers about how to dispose of these polyesters wastes in concrete manufacturing industry.

Polyesters in concrete are preferred because they provide thermal insulation in terms of saving energy, providing water resistance and reducing the compressive strength of the concrete. The study aims to reach the desired level of heat and electrical insulation at an acceptable level of compressive strength using experimental full factorial design. It is important to identify the factors affecting the quality of concrete in designing innovative material and product design. The present study also aims to expose the binary interactions

among polyester on concrete properties using Pareto effect analysis based on the full factorial design.

First, the effect of the factors and their levels on the electrical, thermal, workability, water resistance and mechanical properties of polyester aggregate mixed concrete have been defined. Then, the experiments have been carried out according to the runs determined by full factorial design. The resulting properties have been analyzed systematically by analysis of variance." (Simek and Uygunolu, 2018)

"2. Materials and method

2.1 Materials

Portland cement has a specific gravity of 3.14 and Blaine fineness of 3584 cm^2/g. Class F-type fly ash with a specific gravity of 2.48 and Blaine fineness of 3812 cm^2/g have been procured from Zonguldak Catalagzı thermal power plant. Polycarboxylate ether-based super plasticiser (SP) has been used in all concrete mixtures. Fine aggregate of a size smaller than 4 mm and coarse aggregate (I) of a size between 4 mm and 11 mm and coarse aggregate (II) of a size between 11 mm and 22 mm have used in concrete mixtures. The fine and coarse aggregates have specific gravities of 2.69 and 2.81 and the mean water absorptions of 1.46% and 0.89%, respectively. Polyester granules such as flame-retardant polyester (FRP), cationic dyeable polyester (CDP) and polyester with the low melting point (LMP) have been supplied from a company operating in the engineering plastics production. Their properties are given in table 1 [20, 21].

Table 1. The properties of the polyesters use in this study.

	Values			
Properties	FRP	CDP	LMP	Standard
Elongation at break, %	15–30	15–30	15–30	ISO 527
Specific gravity	1.35–1.40	1.35–1.40	1.35–1.40	ISO 1183
Tensile strength, MPa	40–45	40–45	35–40	ISO 527
Tensile modulus, GPa	1–2	1–2	1–2	ISO 527
Hardness, Shore D	70–75	75–80	75–80	ISO 868
Flexural strength, MPa	40–45	40–45	35–40	ISO 178
Thermal conductivity, W/m*K	0.2–0.3	0.2–0.3	0.2–0.3	ASTM D5930
Electrical resistance, ohm-m	10^8–10^{10}	10^8–10^{10}	10^8–10^{10}	ASTM D257
Purity, %	100	100	100	N/A
Granule size, mm	0–4 mm	0–4 mm	0–4 mm	N/A
Granule type	Cylindrical	Cylindrical	Cylindrical	N/A
Granule color	Dark grey	Smoky	Beige	N/A

2.2 The full factorial design and Pareto effect analysis

The experimental design techniques play an important role in developing a new process and enhancing product performance. The objectives of the experimental design applications can be summarized as identifying the most effective input factors on the quality characteristics and determining the factor levels which can optimize the quality characteristics.

Interaction effects of factors can be investigated with the help of full factorial designs [22]. The factorial design consists of all possible combinations of all levels of each factor in the experiment. The most important advantage of full factorial experiment designs is that the main and interaction effects of the factors on the quality characteristics can be measured and analyzed easily via the experiment design method. The Pareto charts obtained by the full factorial design provide information about the magnitude and significance of a factor's effect [23]. These charts show the absolute value of the effects and the importance of the factors can be evaluated using absolute values. Moreover, a Pareto chart is an effective tool that helps us identify the variance source, and thus it is possible to design a product with the desired quality characteristics. A Pareto chart based on full factorial design, which is a simple statistical tool, can also be used to analyze and sort the individual, two-way and three-way interaction effects.

2.3 Methodology

Factor analysis of the polyester-reinforced concrete composites includes five flow steps (figure 1). First, electrical resistance, thermal conductivity, slump flow, 3-day compressive strength, 7-day compressive strength and 28-day compressive strength, the 28-day splitting tensile strength and the percentage of water absorption of hardened concrete have been determined as POREC quality criteria. FRP, CDP and LMP have been replaced in 0–4 mm fine aggregate, which is defined as the factors' effect on POREC properties. POREC properties have been determined by the full factorial design–based DoE approach. Finally, Pareto charts and main effect plots, which are obtained with the full factorial design, have been used to analyze the importance levels of factors." (Simek and Uygunolu, 2018)

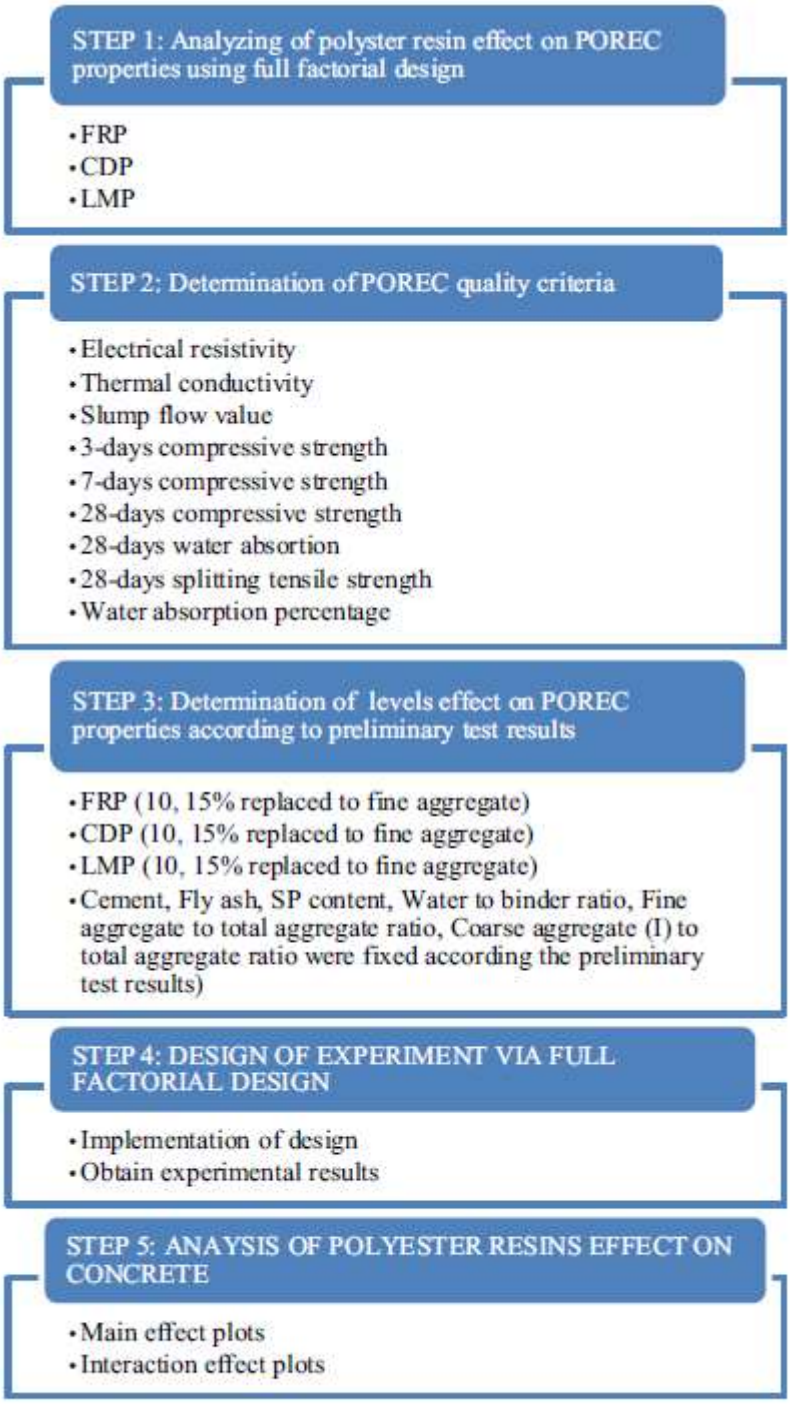

Figure 1. Proposed methodology for analyzing polyester-reinforced concrete composite properties.

"3. Identifying performance optimization properties of POREC

3.1 POREC's performance criteria

Thermal conductivity selected as the first criterion provides information on the heat loss between an environment and building [24, 25]. Using concrete with low thermal conductivity

in buildings provides the thermal comfort for residences and energy savings for manufacturers. TCI–Thermal Conductivity Analyzer was used in the study to determine the thermal conductivity of concrete by hot wire method as given in ASTM C 1113 standards [24, 26].

Electrical resistivity of concrete is affected by the pore size distribution and interconnection, degree of saturation, conductivity of pore fluid and temperature. The two methods of probe are a simple yet reliable as they measure the bulk electrical resistivity in laboratory-based quality control tests. The same concrete specimens, which are prepared for the physical and mechanical tests, can be used for resistivity measurement. In the measurements, the concrete sample is placed between two parallel metal plates with moist sponge contacts at the interfaces to ensure proper electrical connection.

A DC current is applied, and the resistivity of concrete between electrodes is measured on the dry specimens. The two-probe method is used to determine the POREC electrical resistivity and all measurements are carried out at room temperature [27]. Electrical resistivity of POREC is calculated as follows [27]:

$$\rho = \frac{RS}{L} \qquad (1)$$

Where ρ is the electrical resistivity as Ω.m; the internal electrode distance is symbolized as L (m); the electrode conductive area is defined as S (m^2) and R is the measured resistance as Ω [27]. Electrical resistance values also give information about corrosion risk [28]. High electrical resistance means low corrosion risk and high corrosion endurance [28].

The 3-, 7-, 28-day compressive strength of POREC was determined according to the EN 12390/3 [29]. The 28-day splitting tensile strength of POREC was also determined by the EN 12390/6[30]. Slump flow value, the percentage of water absorption POREC was determined according to EN 12350-2 [31] and EN 12390-7 [32]. Eight performance criteria and their desired properties are presented in table 2.

Table 2. POREC characteristics.

Quality criteria	Exemplar	Definition	Type of concrete test	Desired properties
1	R1	Thermal conductivity (W/m K)	Hardened concrete test	Minimise
2	R2	Electrical resistivity (ohm*m)	Hardened concrete test	Maximise
3	R3	Slump flow (cm)	Fresh concrete test	Maximise
4	R4	Compressive strength (N/mm^2) 3 days	Hardened concrete test	Maximise
5	R5	Compressive strength (N/mm^2) 7 days	Hardened concrete test	Maximise
6	R6	Compressive strength (N/mm^2) 28 days	Hardened concrete test	Maximise
7	R7	Splitting tensile strength (N/mm^2) 28 days	Hardened concrete test	Maximise
8	R8	Water absorption (%)	Hardened concrete test	Minimise

3.2 Definition of factors and experiment conditions

Three factors that each has two mix levels affect the POREC quality were determined as flame retardant, cationic dyeable and polyester with the LMP amount taking into account preliminary experiments. Polyester aggregates FRP, CDP and LMP were used instead of fine aggregate (table 3). In all experiments for 1 m^3 concrete; amount of cement, amount of fly ash, water to binder (cement and fly ash) ratio, super-plasticizer content defined for one

Table 3. Factors and their levels.

		Bounds± (%)		Bounds* (kg)	
Factors	Definition	First level	Second level	First level	Second level
FRP	Flame-retardant polyester	10	15	70	105
CDP	Cationic-dyeable polyester	10	15	70	105
LMP	Polyester has low melt point	10	15	70	105

±defined replaced to fine aggregate.

*Defined according to preliminary test results.

hundred kilograms binder (SP), the percentage of fine aggregate to total aggregate ratio (FA), coarse aggregate (I) to total aggregate ratio (CA1) and coarse aggregate (II) to total aggregate ratio (CA2) are fixed at 450 kg, 120 kg, 0.45, 1.25, 60, 20 and 20, respectively, considering preliminary test results."(Simek and Uygunolu, 2018)

"4. Full factorial design and effect analysis

A 23 full factorial design was chosen to implement the experiments in this study. In table 4, columns 2–4 represent the three control factors and their codified levels. Columns5–7 show

Table 4. Full factorial design and sample properties.

Exp. no.	Factors (coded)			Factors (uncodified)			Properties of sample		
	FRP	CDP	LMP	FRP (kg)	CDP (kg)	LMP (kg)	Unit weight of fresh concrete (kg/m^3)	Fresh concrete temperature °C	Unit weight of dry concrete (kg/m^3)
MR0*	–	–	–	–	–	–	2419	23.0	2370
MR1	− 1	− 1	− 1	70	70	70	2170	20.2	2150
MR2	1	− 1	− 1	105	70	70	2147	21.1	2107
MR3	− 1	1	− 1	70	105	70	2284	21.3	2254
MR4	1	1	− 1	105	105	70	2103	20.6	2070
MR5	− 1	− 1	1	70	70	105	2124	26.2	2081
MR6	1	− 1	1	105	70	105	2093	26.1	2068
MR7	− 1	1	1	70	105	105	1770	21.2	1746
MR8	1	1	1	105	105	105	2003	20.2	1969

*MR0: Reference concrete.

uncodified levels belonging to factors. Columns 8 and 10 illustrate the unit weight of fresh and dry concrete. Fresh concrete temperature of POREC in all experiments has been also given in column 9. The actual contents of all the ingredients per cubic meter of concrete for all experimental runs can be seen in table 5.

Table 5. Quantity of mixture for all experiments (1 m^3).

Exp. no.	Cement (kg)	Fly ash (kg)	Water (kg)	SP (kg)	FA (kg)	CA1 (kg)	CA2 (kg)	FRP (kg)	CDP (kg)	LMP (kg)	Total polyester (kg)
*MR0	450	120	219.6	5.98	898	305	305	0	0	0	0
MR1	450	120	219.6	5.98	449	305	305	70	70	70	210
MR2	450	120	219.6	5.98	374	305	305	105	70	70	245
MR3	450	120	219.6	5.98	374	305	305	70	105	70	245
MR4	450	120	219.6	5.98	299	305	305	105	105	70	280
MR5	450	120	219.6	5.98	374	305	305	70	70	105	245
MR6	450	120	219.6	5.98	299	305	305	105	70	105	280
MR7	450	120	219.6	5.98	299	305	305	70	105	105	280
MR8	450	120	219.6	5.98	225	305	305	105	105	105	315

*MR0: Reference concrete.

The experimental results obtained by full factorial design of experiments are illustrated in table 6. All main and Pareto effects analysis were computed by MINITAB® version 17.

Table 6. Experimental results.

Exp. no.	R1 (W/m*K)	R2 (ohm*m)	R3 (cm)	R4 (N/mm^2)	R5 (N/mm^2)	R6 (N/mm^2)	R7 (N/mm^2)	R8 (%)
*MR0	1.65	202.650	17	42.30	47.62	58.16	3.96	2.14000
MR1	1.06	327.973	16	30.97	39.36	41.72	1.85	0.93000
MR2	1.29	525.244	17	33.58	34.97	36.00	2.45	1.84955
MR3	1.60	583.216	17	31.93	36.40	34.25	2.63	1.32330
MR4	1.39	605.628	17	31.69	33.98	34.00	1.84	1.53608
MR5	1.44	528.737	18	33.37	34.99	37.67	2.14	1.99498
MR6	1.53	494.550	17	31.14	32.47	33.14	1.82	1.16098
MR7	1.11	476.613	16	34.35	35.80	37.09	1.72	1.38912
MR8	1.09	638.126	20	32.12	33.10	33.77	1.96	1.68664

*MR0: Reference concrete.

" (Simek and Uygunolu, 2018)

“4.3 Improvement ratios in the POREC properties

The thermal conductivity value of the POREC decreased from 1.65 W/m*K to 1.09 W/m*K with the addition of 105 kg of each polyester type compared to the reference concrete. The electrical resistivity value of the POREC increased from 202.65 ohm*m to 638.13 ohm*m with the addition of 105 kg of each polyester type compared to the reference concrete. Meanwhile, the 28-day compressive strength of the POREC decreased from 58.16 MPa to 33.77 MPa. Although there is a decrease with 41.94% [(58.16–33.77)/(58.16)] (please see table 4; M8-numbered mixture) by the reference concrete (table 4; M0-numbered mixture) at 28-day compressive strength, a recovery with 33.94% [(1.65–1.09)/(1.65)] is obtained at thermal conductivity value and an improvement ratio with 214.89% [(638.13–202.65)/(638.13)] is obtained at electrical resistance value (please see table 4; M8-numbered

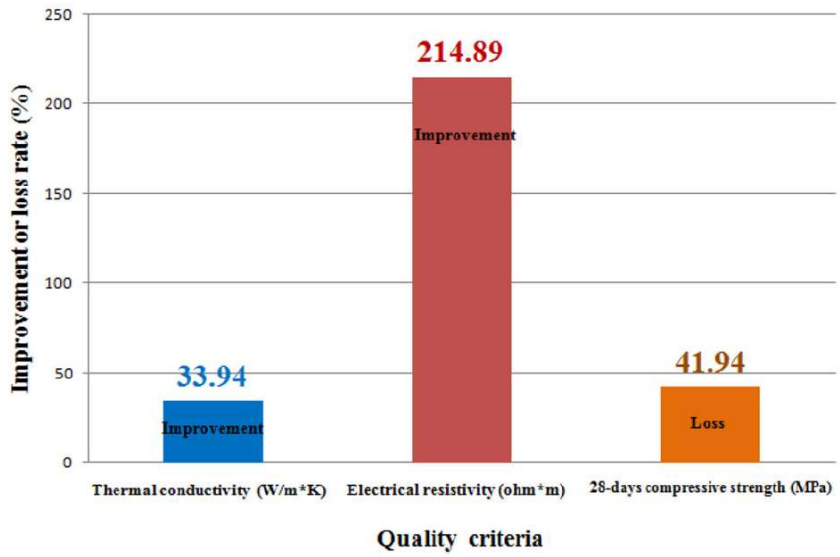

Figure 5. Improvement or loss rate (%) for the selected quality criteria.

mixture). Improvement rates for POREC compared to the reference concrete have been given in figure 5.” (Simek and Uygunolu, 2018)

“5. Conclusions

A full factorial-based design of experiment approach has been first used to analyze the polyester-reinforced composite concrete’s properties systematically. Both the main and Pareto effects on the selected responses such as the thermal conductivity, electrical resistivity, slump flow, 3-day compressive strength, 7-day compressive strength, 28-day compressive strength,

28-day splitting tensile strength and the percentage of water absorption have been analyzed statistically via the full factorial design.

The effect of the most influential factors on the polyester-reinforced composite concrete's thermal conductivity has been determined as the interaction between the cationic dyeable and low-melt-point polyester. These two polyester–mixed concrete composites are suitable for the production of thermal insulating concrete. Moreover, it is concluded that the CDP has the highest electrical resistance, in other words, corrosion resistance, product among polyesters that are used in this study. Furthermore, the CDP and polyester with the low melt point increase with the 3-day compressive strength. Considering these results, the CDP, which has high thermal, water and corrosive resistance, is found to be a more attractive polyester.

Another remarkable result is that despite the lack of individual effect on responses, polyester fillers have a significant effect on responses as two or three interactions. To illustrate, the CDP and polyester with low-melt point have a little individual effect on thermal conductivity. However, they have significant reducing effect on thermal conductivity (figure 2) together. This result demonstrates that an experimental design should be used to analyze quality criteria that contradict each other.

The recovery rate of 33.94% in the thermal conductivity and 214.89% in the electrical resistivity of polyester-reinforced concrete composites has been obtained with a 28-day compressive strength loss of 41.94% according to the reference concrete (polyesters have not been used in concrete) in the full factorial design application. This improvement in the thermal conductivity value is important for the building sector, which is the largest energy consumer in terms of energy saving and reduction of the carbon emissions. The improvement ratio in the electrical resistivity value is quite remarkable to obtain such concrete that has high corrosion endurance compared to the reference concrete.

The polyester-reinforced concrete composite has 1.09 W/m*K thermal conductivity value and 638.13 ohm*m electrical resistivity value, which is obtained with full factorial design study, is included in C 25/30 compressive strength class as it has 28-day compressive strength at 33.77 MPa value. These results indicate that the polyester-reinforced concrete composites are quite effective for achieving thermal and corrosion resistance concrete with an acceptable compressive strength loss." (Simek and Uygunolu, 2018)

3.1.6 Magnesium potassium phosphate cement

Xu, Ma and Li, 2015, from China presents a study of Magnesium potassium phosphate cement paste with large water-to-solid ratio.

“Introduction

Magnesium phosphate cement (MPC) is a type of chemically bonded ceramic, in which the chemical bonding is formed by a through-solution acid-based reaction between magnesia and phosphate. Development of chemically bonded ceramics with phosphate bonding was originally spurred by the need for a fast setting binder for dental or bone restorations [1]. Further investigations on MPC showed that this bonding material has a number of superior properties over ordinary Portland cement, such as rapid setting [1–16], high early strength [1–6,8,11–13,15], strong bonding strength [5,6,9,15], high deicer-scaling resistance [9] and low drying shrinkage [15]. It has thus been popularly used as a repair material in the field of civil engineering for many years. More recently, applications of MPC have been further explored, like waste stabilization/solidification [17,18] and 3D printing for biomedical implants [19].

Traditionally, MPC was produced by using dead-burnt magnesia, ammonium phosphate and water [2–10]. However, ammonium gas that has an unpleasant tangy odor is released as a reaction byproduct during the MPC fabrication process. This serious disadvantage of MPC prepared with ammonium phosphate greatly hindered its wider application. As a result, investigations on seeking a better phosphate salt as the ammonia phosphate replacement have been undertaken [1, 11–16]. As documented in these previous investigations [1,11–16], potassium dihydrogen phosphate (KH2PO4, KDP)with a smaller dissociation constant and lower solubility, is regarded as a better and more suitable phosphate for MPC fabrication. The principal chemical reaction that occurs in the MgO–KDP–H2O ternary system can be expressed as follows:

$$MgO + KH_2PO_4 + 5H_2O \rightarrow MgKPO_4 \cdot 6H_2O. \quad (1)$$

As shown in the above reaction formula, magnesium potassium phosphate hexahydrate (MgKPO4·6H2O, i.e. MKP) is the resultant principal reaction product, which is also known as K-type struvite due to its struvite isostructure. Previous studies [1,11–16] demonstrated that the performance and microstructure of this latterly developed magnesium potassium

phosphate cement (MKPC)-based composite could be evidently affected by magnesia reactivity, magnesia-to-phosphate (M/P) molar ratio, fine aggregate to binder ratio, water usage and the setting retarders, such as boron compounds used. Chau et al. [1] explained the M/P ratio influence on compressive strength of MKPC pastes through systematic microstructure investigation. They concluded that a higher M/P ratio could facilitate better MKP crystal formation and growth, which in turn led to stronger compressive strengths. Nevertheless, the M/P ratio influence on the mechanical strengths of MKPC-based composites was differently interpreted in other previous studies [12,15]. Li et al. [12] investigated the mechanical strengths of a series of MKPC pastes with M/P ratios ranging from 3 to 6, and showed that an M/P ratio of 4 could be considered as optimum, as it contributed to the highest compressive and flexural strengths. Qiao et al. [15], however, demonstrated that among a series of MKPC mortars with M/P ratios ranging from6 to 12,mortarwith an M/P ratio of 8 exhibited the highest compressive and flexural strengths. In addition, they also observed that a decrease of the M/P ratio could lead to clear bonding strength enhancement, which was explained by the specimen with a lower M/P ratio having better fluidity and more MKP hydrate that led to improved lubrication of the bonding interface, thus resulting in superior bonding strength. Aiming for use as a repair material, the previous investigations [1,12,15] regarding M/P ratio influence have frequently focused on those MKPC-based composites with quite low water-to-solid (w/s) ratios lower than 0.30. With the on-going developments, MKPC based composites with large w/s ratios have now also been used as waste stabilization/solidification binders [17,18] and injectable biomedical materials [20]. However, the influence of M/P ratio on the performance and microstructure of these MKPC-based composites with large w/s ratios has received little focus.

According to the MKPC reaction shown in Eq. (1), the theoretical w/s ratio among the starting raw materials, for an M/P ratio of 1, can be calculated as 0.51. Hence, it can be deduced that, as the normally used M/P ratio is larger than 1, the theoretically required w/s ratio would be smaller than 0.51. In order to guarantee high reaction levels, a large w/s ratio of 0.50 was selected in this work for the fabrication of a series of MKPC pastes with a wide range of M/P ratios from 4 to 12. This work started from the characterization on the dead-burnt magnesia used, as its properties would greatly affect the performance of the fabricated MKPC pastes. Setting behavior, in terms of the paste final setting time and the temperature evolution during setting was then investigated. Thereafter, properties, including mechanical strengths and thermal conductivity, and the microstructure of the MKPC pastes were

systematically investigated. It should be pointed out that the thermal conductivity of MKPC-based composites, to the best of knowledge of the authors, has not been reported so far. This study would offer useful information for the potential thermal applications of the MKPC-based composites in the future." (Xu, Ma and Li, 2015)

They found some interesting results regarding thermal conductivity

"3.4. Thermal conductivity property

The performance of MKPC-based composites has already been widely investigated and reported [1,11–15]; nevertheless, little attention has been paid to their thermal conductivity so far. Such investigation would provide sound information for adoption in fields related to thermal engineering in the future. In this work, the thermal conductivity of the MKPC pastes at 28 days was studied, and is presented in Fig. 10(a). It can be clearly seen from Fig. 10(a) that an increase of the M/P ratio leads to higher thermal conductivity of the MKPC pastes. As compared to P-MP4, the thermal conductivity improvement percentages are calculated as 14.57%, 17.59% and 25.09%, respectively, for P-MP8, P-MP10 and P-MP12. The thermal conductivity of composite materials largely depends on the thermal characteristics of their components and their microstructures. Generally, more thermally conductive composite components and denser composite microstructures have higher composite thermal conductivity [26,27]. Although MKPC pastes with lower M/P ratios have denser

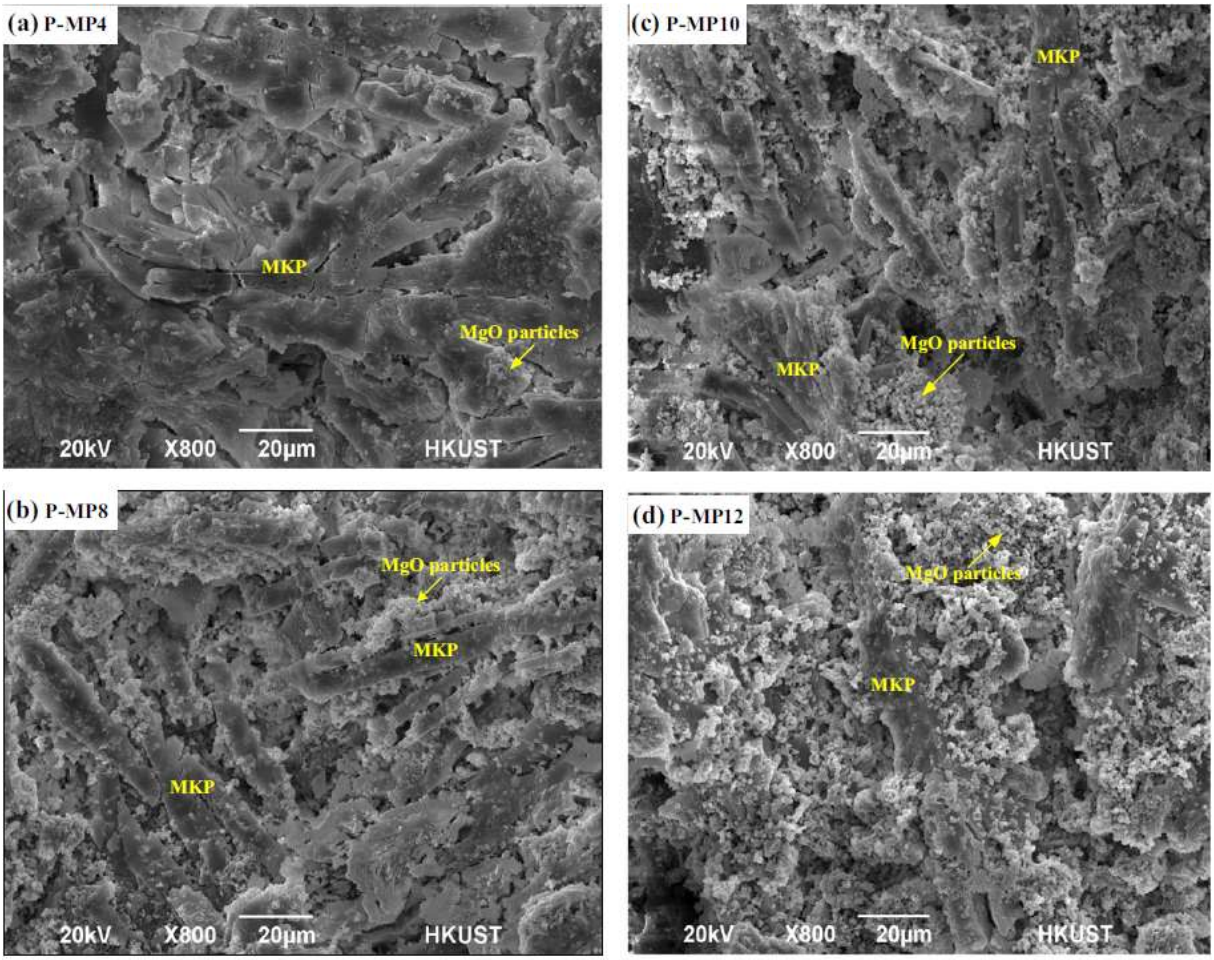

Fig. 7. SEM morphologies of the MKPC pastes at 28 days.

microstructures, as shown in Fig. 7, they have lower thermal conductivities. This indicates that the thermal conductivity of MKPC pastes could be more related to the thermal characteristics of the components in the MKPC reaction system. As aforementioned, the 28-day hydrated MKPC pastes are mature with little unreacted residual KDP; it, therefore, is suggested that the thermal conductivity of MKPC pastes could be greatly affected by the volume ratio (φ_{TC}) of the unreacted magnesia and the resultant MKP, which can be written as

$$\varphi_{TC} = \frac{(1-\partial_R) \times V_{MgO-total}}{\partial_R \times \tau_E \times V_{MgO-total}}. \qquad (11)$$

The calculated results of φ_{TC} are given in Table 4, which are 0.22, 0.51, 0.64 and 0.77, respectively, for P-MP4, P-MP8, P-MP10 and PMP12. The correlation between the thermal conductivity of the MKPC pastes and the φ_{TC} was analyzed and is shown in Fig. 10(b). It can be seen from the figure that the thermal conductivity of the MKPC pastes is strongly related to the φTC through the following relationship

$$Y_{TC} = 034\varphi_{TC} + 0.74;\ \ R^2 = 0.95 \qquad (12)$$

where YTC is 28-day thermal conductivity of MKPC paste in W/(m·K). From this linear regression analysis, it is suggested that magnesia can offer more favorable characteristics for better enhancing the thermal conductivity of the MKPC pastes as compared to the resultant MKP.

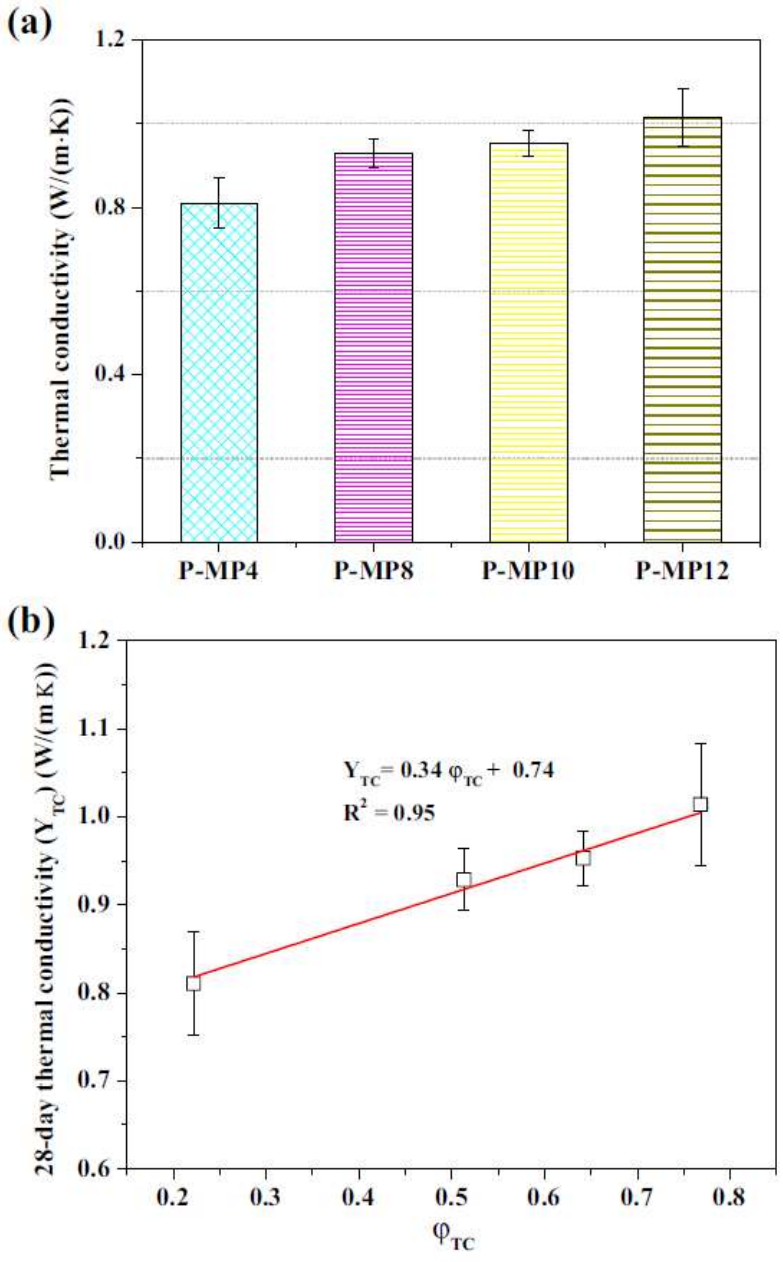

Fig. 10. Thermal properties of the MKPC pastes: (a) thermal conductivities of the MKPC pastes at 28 days; (b) linear regression between thermal conductivity (Y_{TC}) and φ_{TC} of the MKPC pastes at 28 days.

"(Xu, Ma and Li, 2015)

3.1.7 Foam Concrete

(Fernando, Jayasinghe and Jayasinghe, 2017) found in their resent study the following: “It is shown that the use of this foam concrete along with cement fiber boards produces a lightweight wall panel that can be used very effectively for load-bearing walls of single story houses and non-loadbearing walls of multi-story buildings. These lightweight panels can allow rapid construction while reducing the overall weight of the building.” (Fernando, Jayasinghe and Jayasinghe, 2017)

Even though the thermal conductivity is not reported in their study, the product they chose to test can easily be put into industrial production. Because of that this study is reported in my paper.

“1. Introduction

The development of alternative building materials that use waste materials or recycled materials is becoming beneficial due to over exploitation of natural resources as building materials. Expanded Polystyrene (EPS) is one such material generally used for packaging or insulation. EPS is non-biodegradable and hence if released into the nature after its use, it may not decay through natural means [1]. Hence, reuse of EPS is beneficial in terms of environmental protection. The reuse could be in its natural form consisting of beads or in a modified form obtained with heat treatment [2,3] or it could be various other forms of polystyrene waste [4].

EPS bead is a material that contains 98% air and only the rest is polystyrene. Therefore, it has a very low density in the range of 20–30 kg/m3 and also does not have a compressive strength of useful magnitude. The individual EPS beads have a spherical shape and the size could vary from about 1 mm to 8 mm. It has a closed cell structure and hence would not absorb water. One possible use of EPS beads is as an ultra-lightweight aggregate to produce light weight concrete. Several research studies have looked at many different aspects. In the study by Babu et al. [5], lightweight aggregate concretes have been made with densities varying from about 550 kg/m^3 to 2200 kg/m^3. All the lightweight concretes have been designed with a fly ash replacement of 50% by weight of the total cementitious material. The strengths at 28 days of casting varied from 1.1 N/mm^2 to 18.4 N/mm^2 for the density range given above. Due to the presence of fly ash, the strength gain could continue beyond 28 days and the 90-day strengths

obtained varied from 1.5 N/mm^2 to 23.4 N/mm^2. In this study, two types of EPS beads have been used. Type A (4.75–8 mm) with mostly 6.3 mm size beads and Type B (1–4.75 mm) with mostly 4.75 mm size was used in concretes." (Fernando, Jayasinghe and Jayasinghe, 2017)

They report earlier studies and continues: "The above researches indicate various uses of EPS that can be utilized to produce lightweight concrete with possible applications as a structural material or a non-structural material. In the research presented in this paper, the use of mechanically recycled EPS beads is explored to produce a durable lightweight panel of adequate strength that can be used as a walling material for buildings and houses. The panel consists of two cement fiber boards of 5 mm thickness. These boards can be used to produce wall panels of 100 mm thickness by using EPS based foam concrete as an infill material. Since the wall panel has a size of 2.4 m x 0.6 m, the ability to lift and handle the panels during construction is a major criterion. This is addressed by obtaining a sufficiently low density in the range of 650–750 kg /m3 for the foam concrete. With such low densities, the strength characteristics of the composite panel consisting of cement fiber boards and foam concrete infill has been determined experimentally.

The main objective of this research is to investigate the structural properties and constructability of a lightweight concrete wall panel which uses mechanically recycled EPS as one of the raw materials along with cement fiber boards on either side.

In order to develop the lightweight wall panel, the following methodology was used:

1. A foam concrete mix that uses EPS was developed experimentally to obtain a mix with a lower density while having sufficient strength.

2. The wall panels were constructed and tested to determine the compressive strength and the flexural strength.

3. The structural adaptability was checked using the above results."(Fernando, Jayasinghe and Jayasinghe, 2017)

"3. The experimental program

The experimental program consisted of the following:

1. Comparison of a mix containing non-recycled EPS in terms of density and that of a mix containing 50% of the EPS mechanically recycled while maintaining the same mix proportions.

2. The testing of EPS based lightweight concrete sandwich wall panels for compressive strength and buckling characteristics.

3. The testing of the proposed wall panels for flexural strength.

3.1. Selection of a mix

In order to control the weight of the panel, it was necessary to have a foam concrete having a density in the range of 600–700 kg/m^3. For this, a number of trial mixes were compared. Table 1 presents one such mix with ratios worked out with respect to the weight. With a low density of 25–30 kg/m3, EPS in this mix can dominate the volume occupied.

The mix indicated in Table 1 gives a total weight of 918 kg giving a wet density of 918 kg/m^3.With the hydration of cementitious material, part of the water will be consumed and the rest will evaporate. Hence, the dry density would be in the range of the target density of 650–750 kg/m^3 that is obtained about 2–3 weeks after casting the panel when it is ready for installation. Though the quantity of EPS used was only 2.4% by weight, it can easily occupy a significant portion of the total volume due to a very low density of EPS beads.

Table 1
A sample mix proportions for lightweight EPS based concrete.

Materials	Content (kg/m^3)	By weight
Cement	380	41.4%
Sand	136	14.8%
Water	282	30.7%
EPS	22	2.4%
Fly ash	98	10.7%

A comparative study was carried out using test cubes to determine the effect of mechanically recycled EPS beads. When the cubes were made, machine mixing was used to represent the true situation during the actual production of wall panels. As the first step, a part of sand and cement was mixed with water to form a consistent mortar mix. To this, EPS beads were added along with the rest of the sand, cement and water and mixed thoroughly to produce a

homogeneous mix. This mix has been used to cast 150 mm x 150 mm x 150 mm cubes. The mix was hand compacted into the cubes as usually done in other research studies [5,6,10]. Once removed from the mould, the cubes were kept immersed in water for 7 days. In the same mix, two types have been used. Sample 1 had all EPS as non-recycled type. Sample 2 had 50% of EPS as mechanically recycled. A series of cubes was cast and tested for each mix and the average values of density were determined which are presented in Table 2.

Table 2
Density of samples of EPS based lightweight concrete mix.

Sample number	Average density (kg/m^3)
Sample 1	738
Sample 2	629

It can be seen that the use of mechanically recycled EPS has resulted in a lower density. Non-recycled EPS has a spherical shape and recycled EPS has granular shape and also a larger size of about 5 mm. When used in the same mix, it can result in different compaction and hence could give different values for density. One of the key parameters that could be affected by this reduction in density is the compressive strength. Since the intention was to use recycled EPS, the strength properties have been determined when the above mix is used with 50% recycled EPS.

In order to determine the strength properties of the wall panels, two different types of panels were cast. The actual panels proposed for the construction is cast between two cement fiber (asbestos free) sheets (identified as Type 1 and shown in Fig. 1a). In addition, panels have been cast without the cement fiber boards as well (Identified as Type 2 and shown in Fig. 1b) for comparison purposes with respect to some important behavior characteristics.

The panels can be cast for thickness of 75, 100 or 150 mm. The height of the wall panel is 2.4 m and the width are 0.6 m. For the study presented, a thickness of 100 mm has been used, since it is the appropriate thickness for most of the applications.

3.2. Compressive strength of short panels

One of the questions that can be raised is the actual role played by the cement fiber boards in carrying compressive loads in the panels. In order to determine this effect, both Type 1 and Type 2 panels have been cut to a height of 690 mm. For a thickness of 100 mm, this gives a

Fig. 1. (a) A Type 1 wall panel. (b) A Type 2 wall panel.

slenderness ratio of less than 7 and hence the slenderness effects are unlikely to be dominating. The loads were applied in steps of 0.5 tones using a Universal Compression Testing machine. The deformations were recorded by using dial gauges. The instrument set up is shown in Fig. 2. Three panels were tested under each type. For all the panels, the failure mode was observed as crushing of the panels either at the top or bottom. The results are presented in Table 3. The panel with cement fiber boards did not disintegrate and this is an encouraging observation where the composite action was available until failure.

Table 3
Test results of the compression test on short panels.

Panel	Panel identification number	Failure load (kN)	Failure stress (N/mm^2)	Average strength (N/mm^2)
Panels with board (Type 1)	1	237.4	3.89	4.06
	2	247.2	4.05	
	3	258.9	4.25	
Panels without board (Type 2)	1	142.4	2.33	2.13
	2	112.8	1.84	
	3	135.4	2.22	

Fig. 2. A Short Wall panel being tested for compressive strength.

It can be seen from Table 3 that the presence of cement fiber boards of 5 mm thickness on either side allows a greater load carrying capacity. This could be due to some confinement effects by the cement fiber boards or the boards carrying some part of the load or both the

above reasons. Hence, the presence of cement fiber boards can be considered beneficial, though it would add an extra cost to the panels.

Another important characteristic that needs attention is the degree of shortening that a composite panel consisting of foam concrete and cement fiber sheets would suffer under the axial loads. The elastic deformation of the panel was determined by obtaining the actual movement of the platens using dial gauges mounted on a self-standing steel channel. Hence, the movement obtained is the actual shortening of the panel. Thus, these actual shortening can be used to determine the elastic modulus from the load deformation curve. One such curve is given in Fig. 3a. The initial part shows a nonlinear deformation prior to indicating a reasonably linear deformation. This is due to the various deformations that take place in cross heads until the loads are properly applied to the panel and hence, the important part will be the linear portion shown in Fig. 3b.

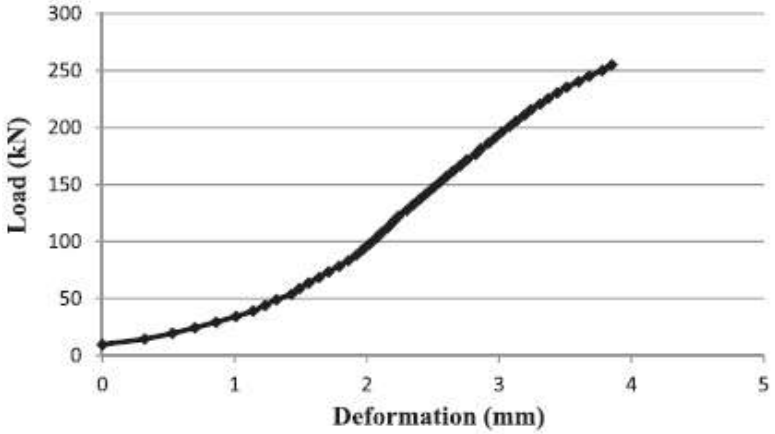

Fig. 3a. Load Deformation curve for short Type 1 panels.

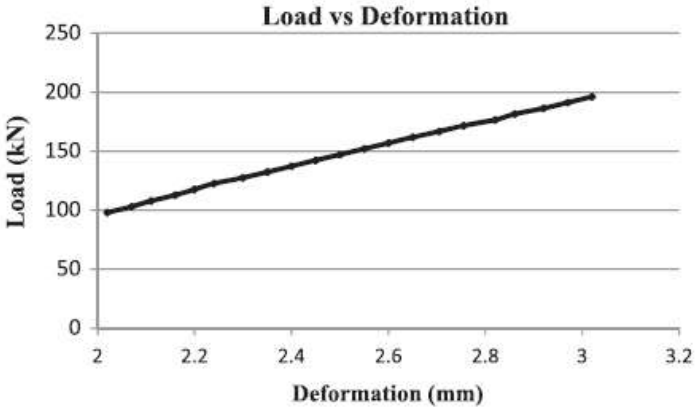

Fig. 3b. Linear portion of the Load Deformation curve for short Type 1 panels.

Fig. 3b can be used to determine the elastic modulus of the Type 1 panel by assuming that the cross section remains the same at 600 mm x 100 mm. Fig. 3b indicates that when the load is increased from 100 kN to 200 kN, the panel has shortened by 1 mm, giving an Elastic modulus of 1.15 kN/mm2. As expected, the elastic modulus is not high and hence, its effect on the deformation under working stresses should be assessed.

The load deformation curve for Type 2 panel is given in Fig. 4a and b. The cross section is the same as for the Type 1 panel. When the load is increased from 50 kN to 115 kN, it has shortened by about 1 mm. This gives an elastic modulus of 0.75 kN/mm2. This indicates that the presence of cement fiber boards of Type 1 can provide an additional stiffness to the panel resulting in a higher elastic modulus.

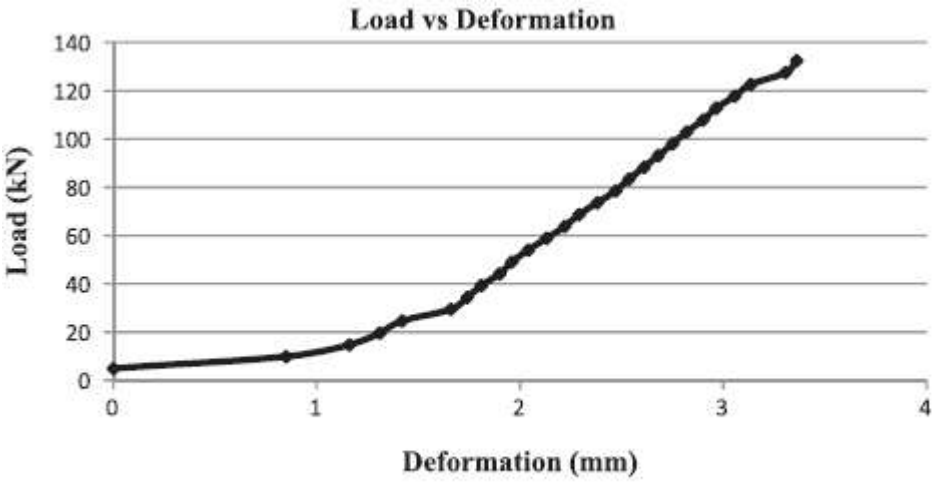

Fig. 4a. Load Deformation curve for short Type 2 panels.

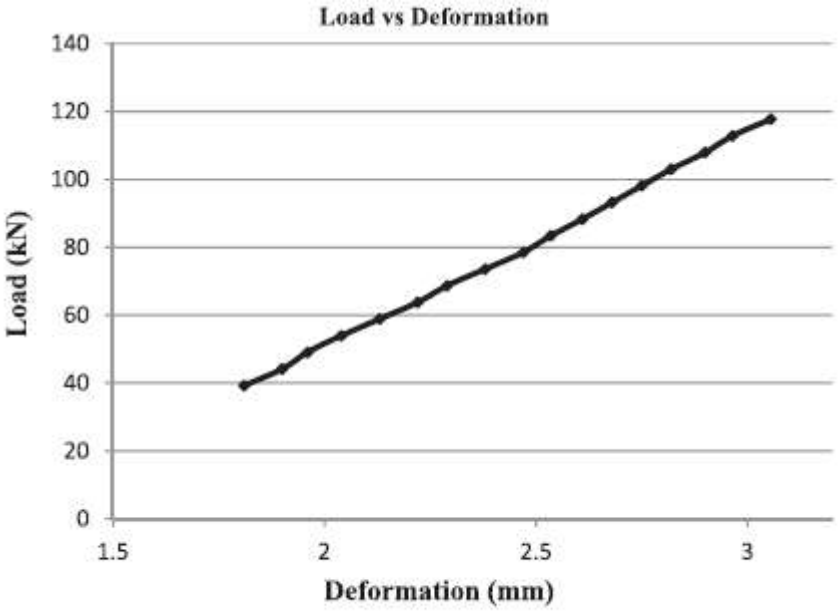

Fig. 4b. Linear portion of the Load Deformation curve for short Type 2 panels.

When two materials act together in a composite wall, it is important to know whether it could disintegrate when the loads are increased. The panels failed due to crushing at the top and hence, it could be stated with confidence that the bond between the cement fiber sheets and the foam concrete is strong enough to have the full composite action until failure.

3.3. Behavior of the full height panels

As the height of a panel increases, the slenderness ratio will also increase, thus having a higher possibility of failure by buckling. The height of the panels tested was 2400 mm. The instrument setup is shown in Fig. 5.

Table 4 presents the results of the compression test for Types 1 and 2 panels, of full height. The failure load was less than that of the shorter panel, indicating some contribution from buckling towards the failure, in addition to crushing, since the panel is having a slenderness ratio of 24.

When used as a partition wall, the stress in the panels at the bottom level will be very small since the self-weight of the panel is only about 100 kg for 2.4 m height and a length of 600 mm. This will give a very low stress due to self-weight and it is in the range of 0.017 N/mm^2. Hence, the panel with a strength in excess of 2.75 N/mm2 (Table 4), when used as a partition material could have a significantly large factor of safety. Hence, both Types 1 and 2 will be able to provide adequate strength as partition walls. However, the robustness of the Type 1

panel that has cement fiber boards will be higher. Another application of the wall panel is the internal and external walls of single story houses. In these, the additional load on the panels

Fig. 5. Wall panel being tested for compressive strength.

will be the weight of the roof. A typical design load of a roof will generally be 1.0–1.5 kN/m^2. Hence, the roof would mean an additional load of 6–8 kN per meter length of the wall thus

giving rise to an extra stress of 0.08 N/mm^2. Such additional stress can be easily resisted by the composite wall panels. Hence, the composite wall panels (Type 1) can be recommended for load bearing walls single story houses as well.

3.4. Flexural strength of panels

In order to determine the lateral load resistance, the panels were tested for flexure. As illustrated in Fig. 6, the wall panels were placed horizontally and tested for its flexural strength according to ASTM C78- simple beam with third-point loading [15].

Fig. 6. Wall panel being tested for flexural strength with third point loading.

The initial failure location was observed carefully and found that the failure location of all the panels was within the middle third. Hence the equation Eq. (1), found in ASTM C78 [15] simple beam with third-point loading was used to determine the stress at failure.

$$R = Pl/bd^2 \quad (1)$$

where

R = Bending stress in MPa

P = Maximum applied load indicated by the testing machine in N

l = Span length in mm

b = Average width of the specimen in mm

d = Average thickness of the specimen in mm

All the panels displayed brittle failure. The failure stress for panels without cement fiber board was very low compared to the panels with the board. The results of the test are indicated in Table 5.

Table 5
Test results of the flexural test on panels.

Panel	Failure Location	Failure load (kN)	Failure stress(N/mm^2)
Type 1	Within middle third	4.3	1.64
Type 2	Within middle third	0.8	0.31

As can be seen in Table 5, the flexural strength of Type 2 panels was significantly less than that of Type 1 panels. Hence, Type 1 panel with cement fiber boards on either side are recommended for load bearing walls of single story buildings and for the nonloadbearing walls of multi-story buildings. The flexural strength of Type 1 panel (1.64 N/mm2) is comparable with that of burnt clay brick walls [16] and other alternative walling materials [17,18].

4. Constructability and applications

The constructability of these lightweight panels would need addressing of few issues. Its connectivity can be assured to a greater extent by having a tongue and groove joint in the panels (Fig. 7) that will allow a strong bond when a suitable cement-based grout is used during erection. It is possible to finish the walls without any plaster due to the presence of cement fiber boards on either side. The walls will also need a thin fiber-based tape at the

joints to provide a neat finish. The controlling of the weight of a 100 mm thick panel to be in the range of 100 kg allows two workers to handle the panels.

Fig. 7. The tongue and groove arrangement.

In addition, it would be necessary to have various custom made galvanized steel components to have sufficient connectivity to the floor and the soffit of the beams. The applications include loadbearing walls in single story construction and non- loadbearing walls in other buildings. Fig. 8 shows an application of the EPS based lightweight concrete walls in a single-story house.

Fig. 8. Application of the EPS based lightweight concrete wall panels in a single storey house.

Moreover, the EPS based lightweight panels can be used in the other applications which include apartment buildings, hotels, commercial buildings and many other diverse buildings needing partitions. These foam concrete boards are not affected by moisture and tend to gain more strength when moisture is present. This is also an encouraging factor that will allow less restricted use.

In tall buildings, the repetitive use of lightweight partitions could reduce the self-weight at each floor level, thus giving a significant advantage in the foundation." (Fernando, Jayasinghe and Jayasinghe, 2017)

3.1.8 Aerogel-incorporated ultra-high-performance concrete

"The last few years we have focused on exploring the properties, requirements and possibilities of the state-of-the-art thermal insulation materials and solutions for buildings. These include vacuum insulation panels (VIP), gas-filled panels (GFP), aerogels and also phase change materials (PCM). PCM by itself is not an insulation material in principle but may still be an important part of the thermal building envelope. At our lab, both theoretical [2–7] and experimental work [8–23] were conducted alongside to derive new materials that go beyond these state-of-the art materials, thus dawning the birth of the concepts such as nano insulation materials (NIM) through the utilization of the Knudsen effect [24–30], where experimental investigations so far have concentrated about making hollow silica nanospheres (HSNS) [30–38], thus enabling thermal insulation and improved energy efficiency from a 'nano' perspective.

Application of nanotechnology is an important tool for research on new construction and building materials, addressing both ecoefficiency (economic and ecological) and energy-efficiency issues [39–41]. Accordingly, nanotechnology has found a niche in the field of concrete and cement composites [42–49] where common ingredients in construction such as chemical admixtures are often coined as nano materials nowadays. It is determined that other than thermal insulation, nanotechnology is also essential in addressing the needs of other building applications. In general, nanotechnology in buildings and construction has been researched upon [50–55], and a development roadmap for utilizing nanotechnology in construction has also been given [54–55]. Various nanoparticles [56–61] and carbon nanotubes [62–67] have been applied in different cement and concrete materials, typical for studying and attempting to enhance the mechanical properties. Further information concerning carbon nanotubes may be found in the literature [68–73], where their application in the construction industry may also be addressed in particular [68]. Other studies which are of interest in this respect involve structure and properties of aerated concrete [74], measured thermal conductivity of concrete [75], polymer nanocomposite foams [76] and aerogel incorporated into concrete [77]."(Ng *et al.*, 2015)

“The first attempts to reach such a NanoCon material may be tried by engaging composite materials, i.e. with a final material product which on a nanoscale is not homogeneous. As an example, joining NIM and carbon nanotubes (CNT) in one single material might enable a very low thermal conductivity due to the presence of NIM, while a very large tensile strength arising from the contribution of CNT. In this regard it should be noted that CNTs have a very large thermal conductivity along the tube axis, and that the very large tensile strength of CNTs (63,000 MPa measured and 300,000 MPa theoretical limit) surpasses even that of steel rebars (500 MPa) by more than two orders. In comparison, concrete itself without rebars has a tensile strength of 3 MPa and a compressive strength of 30 MPa. Hence, the potential impact of NanoCon is tremendously huge. Even if the very ambitious goal of as low thermal conductivity as 0.004 W/(mK) for NanoCon is not reached within a foreseeable near future, every order of magnitude the thermal conductivity may be lowered from the high value of concrete down towards the values of the traditional and the state-of-the-art thermal insulation building materials, while still being able to maintain substantial parts of the construction properties of concrete, will be very important.” (Ng *et al.*, 2015)

3.2 Type of filler materials

In this context lightweight filler materials are used to reduce weight, increase porosity and decrease thermal conductivity. Aerogels, PVA polymers and waste -based aggregates are described in more detail in the next chapters. There are also aggregates that is used to establish a form of reinforcement or armoring by develop chemical bounds, crystalline structures and local armoring. Other popular aggregates are also mentioned. There are also useful additives that can control float and water absorption that is outside this scope.

3.2.1 Lightweight aggregates

(Samson et al., 2017) have prepared a complementary well-comprehensive summary of plentiful commonly used lightweight aggregates that is quoted from in the following:

“The easiest way to produce an LC is to replace part of the OPC concrete components by LA (density, ρ<1200 kg/m3) inserted in a fresh mineral suspension. The resulting materials are

referred to as LACs. A wide density range is accessible (1350–1850 kg/m3). LAs are usually produced locally, depending on available resources." (Samson et al., 2017)

"Different LAs exist, and they are classified according to their provenance: natural mineral (directly as extracted or after a thermal treatment), plant-based or synthetic LAs. The incorporation of plant-based LAs in mineral binders is an ancient technique (Arnaud and Amziane, 2013) and several plant-based LAs are employed: hemp (Aït Oumeziane et al., 2016; Arnaud and Amziane, 2013; Collet and Pretot, 2014), flax (Aamr-Daya et al., 2008), wood (Mohammed et al., 2014) and rice husk (Torkaman et al., 2014). These resources have the advantage of being by-products or waste. Using these resources decreases the environmental footprint of the material. Unfortunately, the mechanical performance of plant-based LACs is usually poor because soluble components of bio-based aggregate can alter the hydration kinetics of hydraulic binders (Diquelou, 2013).

Natural mineral LAs such as pumice (Anwar Hossain, 2004), diatomite or volcanic slag (pozzolan) (Demirdag and Gunduz, 2008) are commonly used directly after extraction to produce LAC. These LAs are usually crushed to reduce their size and to control the grain size distribution, so energy consumption increases. Unfortunately, they are only available in some particular places in the world. Natural mineral LAs enable medium density LAC to be produced (density of 1100–1500 kg/m3 for volcanic slag LAC and 500–1300 kg/m3 for pumice LAC). Most of the LAs employed in LAC production come from the transformation of mineral resources, usually by thermal treatment (Tassew and Lubell, 2011). These mineral materials (shale, slate, clay) are heated to their fusion point (between 1000 and 1200°C), at which point they expand as released gases are trapped by the materials' viscosity. These LAs have densities of 300–900 kg/m3 and enable LAC to be produced with a wide range of densities (700–1850 kg/m3). The density of expanded clay LAC is between 700 and 1600 kg/m3 and is associated with a compressive strength of 4 to 30 MPa. LAs can also be modified by adding phase change materials (e.g. paraffin) to modify their thermal inertia (Sukontasukkul et al., 2015).

Other natural materials such as perlite (silica volcanic rock) or vermiculite (aluminum–iron–magnesium silicate) are produced with a material expansion phase due to thermal treatment. These LAs differ from the previous ones by their very low densities: 30–240 kg/m3 for perlite and 60–130 kg/m3 for vermiculite. Schackow et al. (2014) used vermiculite LA to produce LAC having medium thermal conductivity (0·34–0·50 W/(m.K)), intermediate compressive

strength (6·3–14·3 MPa) and density ranging from 1130 to 1250 kg/m3. Sengul et al. (2011) partially substituted the sand of OPC concrete by perlite LA. The first sample was made without perlite LA and this represented the OPC concrete control sample. The amount of perlite was gradually increased by 20% steps. The thermomechanical results are presented in Figures 2 and 3. A significant drop in compressive strength appeared with increasing sand substitution by perlite, while the thermal conductivity decreased. Other Las are industrial byproducts. The most commonly used are blast furnace slag and fly ash. These LAs have a spherical pellet shape and usually lead to good mechanical performance of the LAC (Kayali, 2008). Expanded blast-furnace slag is a metal industry waste. It is produced by adding water that vaporizes when it comes into contact with the high-temperature blast-furnace slag, and this phenomenon creates porosity (Tan and Pu, 1998). The process of fly ash LA production is similar. Using this LA leads to LAC with a density of 1000–1800 kg/m3 and compressive strength of 4–25 MPa. Synthetic LAs have also been produced. The most widespread synthetic LA is expanded polystyrene (Chen and Liu, 2013; Li et al., 2013), which gives low-density LAC.

The quality of LA is judged by its lightness or thermomechanical properties, but not only these factors. The shape of the LA can have a strong impact on the fluidity of fresh paste. According to Turhan Erdog˘an and Fowler (2005), spherical LA is preferred because it preserves sufficient paste fluidity. Another important parameter is permeability, as a highly porous LA captures a large amount of water, which can be detrimental for binder hydration. According to Nguyen et al. (2014), LAs that present impermeable shells are preferred." (Samson et al., 2017) (Samson, Phelipot-Mardele and Lanos, 2017)

"In recent years, structural concrete mixtures with low thermal conductivities have been developed using aggregates other than some commonly used manufactured LWA or industrial by-product such as expanded clay, expanded shale, or foamed slag etc. Examples of the LWAs include pumice [6,7], perlite [8,9], cenospheres [10,11], polyurethane foam [12], diatomite [7], expanded glass [13], aerogel [14], and high-impact polystyrene [15]." (Samson, Phelipot-Mardele and Lanos, 2017)

"Thermal insulation materials of the future

The concept of nano insulation materials (NIM) seem to represent a leap forward for the next generation of thermal insulation materials. One such example is found through the studies

conducted by Gao et al. [12,17], Jelle et al. [5] and Sandberg et al. [6] where hollow silica nanospheres (HSNS) may be a possible foundation or stepping-stone for the development of the NIM of tomorrow. One distinctive advantage of HSNS NIM over conventional thermal insulators is the controllability of thermal properties by modifying their structural parameters like e.g. particle size, porosity, inner diameter and shell thickness. HSNS utilize physical principles such as the Knudsen effect to reduce the thermal conductivity of the material to a minimum. Nevertheless, it must be noted that turning the laboratory-made HSNS NIM into practical thermal insulation materials for building applications may require substantial research efforts dedicated to this field. One may also imagine to apply hollow silica nanofibers (HSNF) in such NIMs, e.g. for increased mechanical strength purposes.

A thermal insulation material should be light-weight and have a certain strength for transport and handling on the building site. Fibre reinforcing of aerogel is one principle that is well documented [10,11], and the right combination of fiber material and aerogel could result in a stronger and, at the same time, a material with a reduced thermal conductivity. Reinforcement often leads to a higher thermal conductivity, as seen from Table 1. Hence, a new material should consist of a homogenous, porous substance. To implement pores in already uniform materials would be an interesting research topic. Possible ways to perform this could be to implement closed pores individually using small valves or by implementing a membrane with holes of the desired size (which is removed at a later stage). Another solution may be to create a material that becomes open-porous when inflated. An inflation process, e.g. by chemical means, from within a bulk material creating a closed nanopore structure could also be imagined and feasible in the future.

In summary, one may categorize some of the promising experimental methods into membrane foaming, internal gas release and sacrificial template methods. The membrane foaming method is using a membrane to prepare a foam with nanoscale bubbles, followed by hydrolysis and condensation of a precursor within bubble walls to make a solid structure. The internal gas release method uses a controlled decomposition or evaporation of a component to form nanobubbles in a liquid system, followed by formation of a solid shell along the bubble perimeter. The sacrificial template method is based on the formation of a nanoscale liquid or solid structure, followed by reactions to form a solid shell along the template perimeter. The sacrificial template core is then chemically or thermally removed, thus resulting in a hollow sphere. Scanning electron microscope (SEM) images of the different steps in the template

method when synthesizing HSNS are depicted in Fig.1, where polystyrene (PS) is used as the sacrificial template material." (Gangassaeter *et al.*, 2017)

3.2.2 Aerogels

"Aerogels

Aerogels were discovered in 1931 by Samuel S. Kistler and are a silica gel where all the liquid components are replaced by air through a complex drying process. The remaining material creates a nanoporous structure with low thermal conductivity [9]. The solid thermal conductivity of silica is relatively high, but the silica aerogel has only a small fraction of solid silica. With a good purity and production method pore sizes of 5 to 70 nm are possible, where the air-filled pores will take up between 85 to 99.8% of the volume [4]. Pure aerogels have a low thermal conductivity typically between 12-20 mW/(mK).

Aerogels are constantly being developed, both regarding the production process and the final material product itself. Challenges with the material for building purposes have been inherent low density and thus high fragility, which complicates the handling process without fracturing the aerogel products. Therefore numerous different composites have been made in order to create a more robust material [10]. Mineral wool and aerogel have been mixed, with a resultant thermal conductivity of 19 mW/(mK) [7]. Hayase et al. report a development of another composite aerogel with a density of 20 kg/m3 and a thermal conductivity of 15 mW/(mK) [11]. Also note that as aerogels may be produced as either opaque, translucent or transparent materials, these products may be used for several different building applications, e.g. in opaque walls, translucent solar walls or glazing systems and transparent windows or glazing systems. Table 1 gives an overview of the findings of several different variants of aerogels and their characteristics."(Gangassaeter *et al.*, 2017)

Table 1. Examples of aerogels, listed with important characteristics.

Aerogel	Density (kg/m^3)	Thermal conductivity (mW/(mK))
Stone wool and aerogel [7]	-	19
Polymethylsilsesquioxane-cellulose nanofibre bicomposite aerogels [11]	20	15
Aramid fibre reinforced silica aerogel [10]	150	22.7
Monolithic silica aerogels [12]	-	≈ 13

(Gangassaeter *et al.*, 2017)

"Aerogels are a special class of extremely low density, amorphous, mesoporous materials with a nanostructure. In the case of aerogels, the 'nano' designation refers to the size of the pores within the material rather than the actual particle size. Pore sizes in aerogels are generally between 5 and 70 nm and have a pore density of between 85 and 99.8% by volume [9], resulting in a very low thermal conductivity, a low gaseous conductivity and a low radiative infrared transmission, making them an extremely efficient insulating material." (Westgate, Paine and Ball, 2018)

"Aerogel possesses a very high strength to mass ratio and can support up to 1600 times its own mass [11]; however, as manufactured, it is a brittle material, having a fracture toughness of only ~0.8 kPa $m^{1/2}$. Although easily crushed, this does not destroy its porous structure; aerogel that has been ground into a powder occupies approximately the same space as the original sample, demonstrating that the pore structure of the material does not change significantly [12].

In addition to its low weight and lower space requirements, aerogel's higher durability makes it an attractive alternative to fiber and foam insulation materials [13]." (Westgate, Paine and Ball, 2018)

"Aerogel's contribution to energy efficiency

Energy saving and lowering CO_2 emissions are topics of great actuality with great impact on many areas of science and economics worldwide. Energy spent for heating in total accounts for over 50 % of the total demand, of which roughly two-thirds go into buildings and one-third into the generation and distribution of industrial process heat.

Heating, ventilation and air conditioning (HVAC) of buildings (including industrial and commercial buildings) account for approximately 40 % of the global energy consumption. The energy consumption of HVAC systems in buildings can be lowered by up to 75 % with minimal effort by installing a proper thermal insulation, which results in a comparable, cost-effective reduction in CO_2 emissions. Aerogel materials offer great potential as thermal insulation materials of the future and have already began to enter niche markets in building and pipe insulation industries.

In terms of economic potential and potential climate impact, building insulation represents a tremendous opportunity given the shear market size and immediate need for better building

envelopes [2]. The standard approach to decrease thermal losses of buildings is to install thicker layers of conventional insulation materials. Heat loss through a fine porous insulation material can occur via three transport pathways, namely conduction through the pore gas, conduction through the solid skeleton and radiation. There is naturally an esthetic disadvantage linked to such thick insulation layers: the insulated object occupies more space and the usable living space decreases. This is a problem of growing concern in the context of increasing urbanization and highly densified district planning in city centers where each square meter of floor area counts. Silica aerogel insulation materials can achieve the same thermal insulation performance with only half of the thickness of the conventional insulation materials (Fig. 1). This extremely low thermal conductivity is due to the combination of low density (skeletal conductivity) and small pores (reduced gas conductivity) [4]. Aerogels are the only class of non-evacuated insulation materials that offer ‘‘super-insulating’’ properties without the need for a special pore gas [2, 5]. Nowadays, silica aerogels are commercially available that combine extremely low thermal conductivity values on the order of 0.012–0.018 W/(m K) under ambient conditions with water vapor permeable, hydrophobic as well as nonflammable materials properties.

Saving space is the most important reason for the use of superinsulation. Typical application scenarios in buildings are interior insulation solutions for retrofit as well as thin facade insulation for the renovation of old and historical buildings, side-on balcony and flat roof balcony constructions. In the construction industry, the thermal resistance of a construction element is expressed in terms of the U value, which describes the heat loss through a given thickness of a specific element or single component. Figure 1 shows a comparison of the material thickness required to achieve a U value of 0.2 W/(m2 K) for various insulation materials and their respective materials cost per m2 area. Aerogel insulation requires less than half the materials thickness when compared with polystyrene foam or mineral wool, but also costs roughly 8–9 times more for the same effect than a standard solution.

Furthermore, the mechanical properties of today’s commercial aerogels still leave to be desired, as they are generally known as fragile and brittle materials. In comparison with polymer foam materials, e.g., r10 (compressive stress at 10 % strain) and tensile strength of pure silica aerogels are significantly lower than those of polymer foams (Fig. 1). Therefore, it does not come as a surprise that current efforts in aerogel materials research primarily target production processes to reduce cost of production and the improvement of mechanical

properties of the material. This work is a short review of recent developments in cost reduction and mechanical strengthening efforts superinsulating aerogel materials from the perspective of today's commercially available silica aerogels." (Koebel *et al.*, 2016)

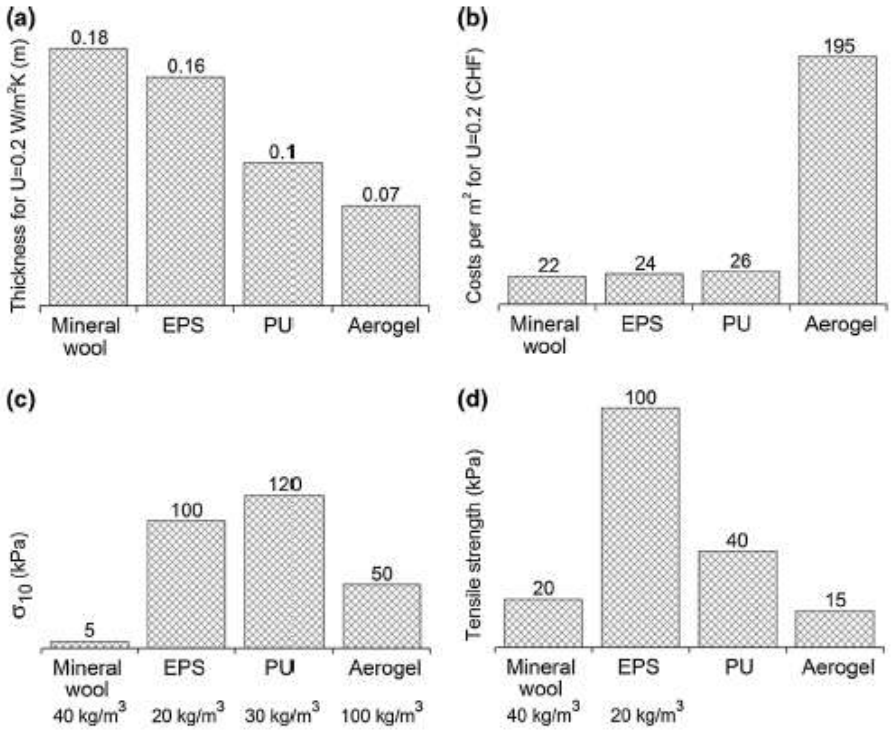

Fig. 1 Comparison of **a** thermal insulation performance expressed as material thickness to reach a U-value of 0.2 W/(m2 K), **b** materials cost per m^2, **c** stress at 10 % strain (σ_{10}) and **d** tensile strength of the most common thermal insulation materials

(Koebel *et al.*, 2016)

"Whilst aerogel may have the potential to help reduce energy usage in buildings, it is also important to consider the properties of the binder material. Prior to the introduction of hydraulic cements, non-hydraulic lime putty was routinely used as a binder material for mortars, plasters and renders in building construction and has proved to be durable over many centuries [17]. It has a significantly lower environmental impact than that of the more commonly used Portland cement, which requires higher temperatures during production, and hence results in higher CO_2 output, than lime. But the case for lime as a low carbon material is strengthened further by the fact that it actually reabsorbs CO_2 whilst setting; a non-hydraulic lime putty can absorb nearly its own weight in CO_2 [18]." (Westgate, Paine and Ball, 2018)

"Thermo-mechanical properties of reinforced aerogel materials

Figure 5 shows a direct comparison of the thermal conductivity of various classes of aerogel materials as a function their mechanical properties. Polyisocyanate (PU) aerogels as well as

X-aerogels, depending on density, can give rise to extremely high E-moduli. However, superinsulating properties (k\20 mW/(mK)) are only achieved at rather low densities (typically below 0.2 g/cm3) with correspondingly weaker mechanics. Pure biopolymer aerogels such as aerocellulose [43, 61] or aeropectin [42] display E-moduli similar to those of pure silica aerogels but with significantly higher thermal conductivities. As discussed above, our recent silica-biopolymer hybrids combine excellent mechanical properties with very low thermal conductivities.

Clearly, a common goal of aerogel research is to achieve maximum mechanical strength and superinsulating properties in one and the same material. In other words, the ultimate aerogel is located on the bottom right hand side of Fig. 5a and b. Current development efforts could be summarized as follows: synthetic polymer and X-aerogel materials feature excellent mechanical properties at higher densities. The primary development in this field is to produce

novel materials with significantly lower thermal conductivity. This is of course most easily accomplished by lowering the material density which, however, automatically leads to a reduction in mechanical performance. Silica aerogel composites are being investigated with the primary goal of improving the mechanical strength while retaining the ultralow thermal conductivity of silica aerogel. This strengthening requires the addition of a secondary phase which inevitably leads to an increase in density and thermal conductivity. From this simple logic, it is clear that there are inherent physical limitations to the extent of strengthening given simply by the (nano-)structural constraints of the aerogels themselves. However, the last decade has brought significant progress in this field and opened up many avenues to explore and develop. (Koebel *et al.*, 2016)

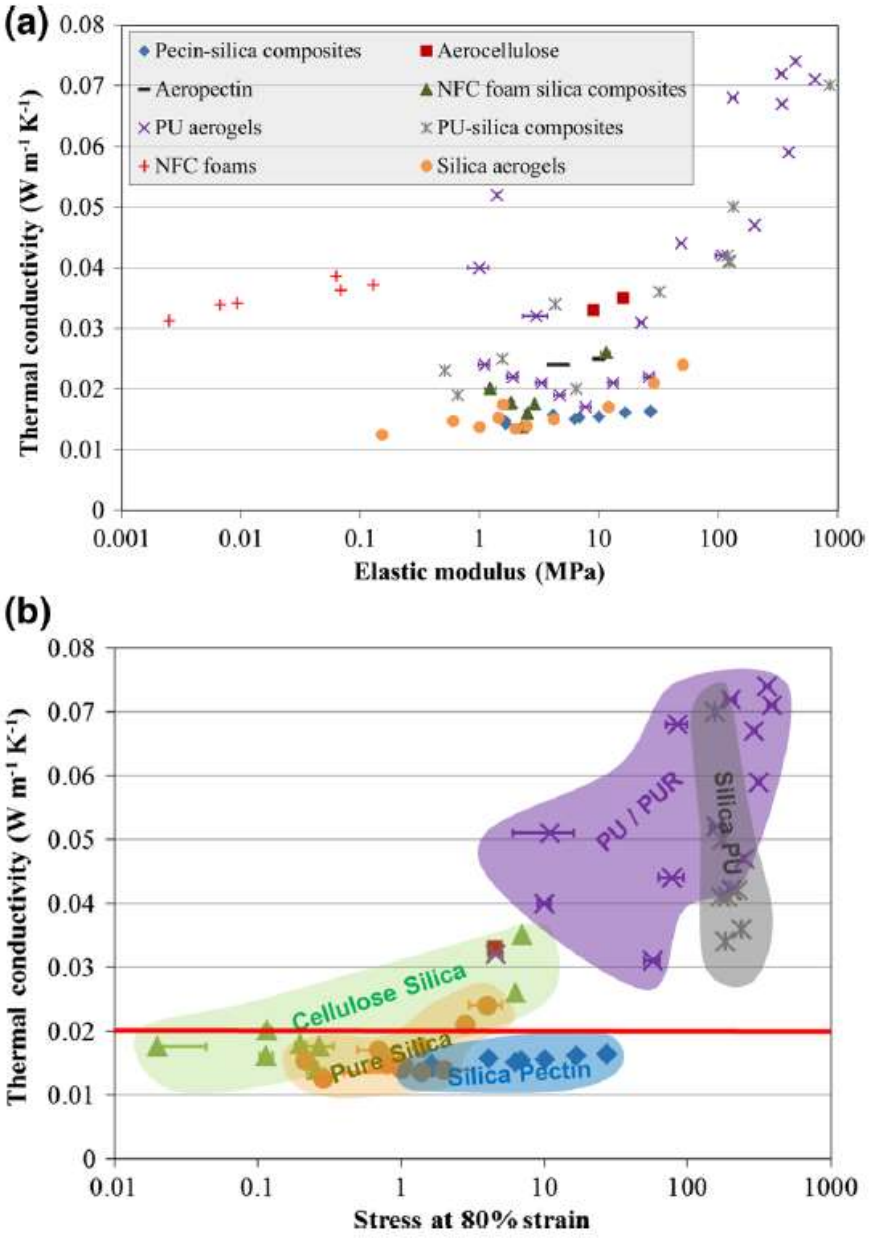

Fig. 5 A comparison of the thermal conductivity of various classes of aerogel materials as a function their respective **a** compressive modulus and **b** stress at 80 % strain

(Koebel *et al.*, 2016)

"A further advantage of non-hydraulic lime is its long shelf life. It is common for manufacturers to recommend that, once opened, bags of lime are used within a specified time or discarded. In practice, practitioners may keep lime from a few days to one year depending on the storage conditions and risk of excessive hydration and carbonation within the bag. Non-hydraulic lime putty, however, can be stored for significantly longer due to the effectiveness of the milk-of-lime layer on the surface of the putty at preventing carbonation.

The carbonation rate and plasticity of lime putty have been found to be still improving after periods in excess of five years [19].

The use of a lime putty as a binder is also advantageous for the recycling of materials. Hardened lime binder can be removed from masonry relatively easily, whereas the high strength bonding of cement mortars and renders can prevent recycling of materials, as it cannot be removed easily from brick and stone without causing damage.

An additional benefit to using lime is its superior water vapor permeability compared to modern commercial plasters [20]. When used as a render, the higher permeability of lime plaster helps moisture to escape from within the walls, preventing freeze thaw damage [21]. When used as a plastering material, its ability to release moisture helps to prevent mould formation and reduction in thermal resistance. Although there is little published data on the permeability of aerogel plasters, one study by Ibrahim et al. reported a figure of 5.1 x 10^{-11} kg/s m Pa for an experimental aerogel based external render [22]. This figure is significantly higher than was found in a study by Wang et al., where five commercially available gypsum plasters were found to achieve figures of between 1.62 and 2.53 kg/s m Pa [23].” (Westgate, Paine and Ball, 2018)

“Compared to other insulation materials such as glass and natural fiber, aerogel is still of higher cost. However, it should be noted that it is still a relatively new material for construction applications. As its use becomes more widespread, higher production quantities and economies of scale will help lower the cost [24]. Aerogel is the insulation material of choice for applications where the space available for insulation is limited but performance cannot be compromised.” (Westgate, Paine and Ball, 2018)

“Toxicity, safety and health issues of aerogels

Silica aerogels are produced by drying aqueous solutions of sodium silicate. They are very light, hydrophobic powders which are effective at lower rates than diatomaceous earths. The very low dust density has prevented the widespread application of these materials in the past because of the potential health hazards which would occur as a result of inhalation. The application of amorphous silica presents a minimal health hazard but inhaled dusts which contain crystalline silica can result in silicosis and other respiratory diseases such as

emphysema and pneumoconiosis [145]. Aspen aerogels presented a report about the potential health problems which may be caused by aerogels as shown in Table 8 [146].

Recommendations to avoid health problems caused by aerogels

Aerogels may cause some potential health problems especially during installation. To avoid that, some simple modifications may be performed. As an instance, aerogels may be inserted in rubber, plastic or aluminum covers to prevent them from direct contact with hands. These kind of materials are called aerobels. Inhalation during installation may cause mechanical irritation of the upper respiratory tract. Therefore, breath masks should be used and installation should be completed as soon as possible. Protective eyewear and glove should be used in order to avoid eye and skin damage. Airborne dusts during installation may cause some allergic reactions so unless it is compulsory, people with allergy should not stay in the installation environment for a long period, of time." (Cuce *et al.*, 2014)

"Predictions for future of aerogels

It is a clear fact that aerogels have extraordinary characteristic features like very low thermal conductivity, translucent structure, good sound insulator etc. However, they need to be more cost effective to compete with the traditional insulation materials. It is understood from the literature that intensive efforts are made to reduce their manufacturing costs and if it is succeeded, aerogels have the potential to be one of the most attractive material of the century. Aerogels have a great deal of application areas such as spacecrafts, skyscrapers, homes, automobiles, electronic devices, clothing etc. With the inevitable needs and developments on the prescribed areas, it is expected that aerogels will be improved and novel high technology materials based on aerogels will be discovered." (Cuce *et al.*, 2014)

3.2.2.1 Reinforced and superinsulating silica aerogel

Reinforced and superinsulating silica aerogel is described in an article from 2018 (Iswar *et al.*, 2018).

"Here, we introduce strong and superinsulating silica hybrid aerogels with an unprecedented combination of properties, prepared by co-gelation of an ethanol-based silica sol and silane terminated prepolymers. This route does not depend on a post gelation modification step

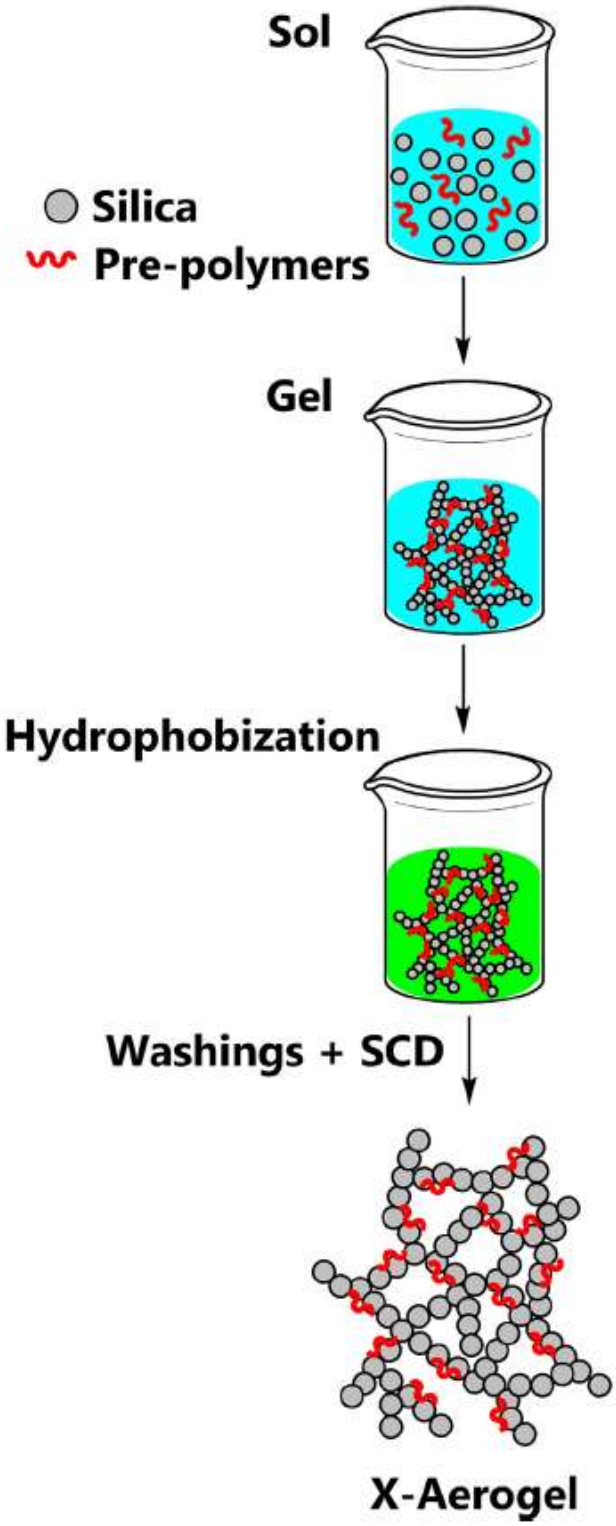

Fig. 1. Synthesis of hybrid aerogels by co-gelation. The length of the polymer chains varies from ~2 to ~100 nm depending on prepolymer type and the diameter of the primary silica particles is ~4 nm.

typical for classical X-aerogels, but introduces the reinforcement by co-gelation with isocyanatoalkoxysilane based cross-linkers (Fig. 1; Table 1). Because the silane terminated

prepolymers are fully compatible with the ethanolic gelation and hydrophobization solvent, no additional solvent exchanges are required." (Iswar *et al.*, 2018)

Table 1
Properties of prepolymers and corresponding hybrid aerogels (for $X:SiO_2 = 0.3:1$).

Name	Source	'R2'	MW (g/mol)	λ ($mW \cdot m^{-1} \cdot K^{-1}$)	σ_{max}[a] (MPa)	avg. WCA (°)
*$(MeO)_3$-Si-$(CH_2)_3$-(NH)-(C=O)-O-**R2**-O-(C=O)-(NH)-$(CH_2)_3$-Si-$(OMe)_3$ (commercial)*						
Vestanat® EP-M 95	Evonik	Aliphatic	~600	14.7	6.4	147
Geniosil® STP-E 15	Wacker	Polyether	~11000	17.3	5.2[b]	100
Geniosil® STP-E 35	Wacker	Polyether	~14000	17.4	6.2[b]	113
*$(EtO)_3$-Si-$(CH_2)_3$-(NH)-(C=O)-O-**R2**-O-(C=O)-(NH)-$(CH_2)_3$-Si-$(OEt)_3$ (lab. Synthesized)*						
Empa 2033	Empa	fatty acid dimer diol (Pripol™ 2033, Croda)	~1100	16.6	6.3	133
Empa 1990	Empa	dimer diol (Radianol 1990, Oleon)	~1100	17.0	4.4	144
Empa D-140	Empa	castor-oil derived polyol (Polycin® D-140, Vertellus®)	~1300	16.9	4.6	137
Empa D-265	Empa	castor-oil derived polyol (Polycin® D-265, Vertellus®)	~900	17.0	4.2	138
Empa D-290	Empa	castor-oil derived polyol (Polycin® D-290, Vertellus®)	~900	16.3	3.6	143

[a] Stress at 80% strain.
[b] For $X = 0.25$ ($X:SiO_2$); X stands for the mass ratio of prepolymer to silica.

(Iswar *et al.*, 2018)

"Thermal conductivity, thermogravimetry and uniaxial compression

Thermal conductivity (EN 12667 at 10 ºC) was determined from monolithic, square plate specimens with a custom built guarded hot plate device (Figure S2) designed for small samples of low λ materials [38]. Estimated uncertainties for thermal conductivity are 2% relative. Thermogravimetric Analysis (TGA) was investigated on 4e6mg samples using a Netzsch TGA 209 F1 instrument in 80% v/v O_2 and 20% v/v N_2, and with a heating rate of 5 ºC/min from 30 ºC to 900 ºC. Uniaxial compression tests were performed on monolithic cylindrical samples (10mm diameter, 20-30mm high) using a universal mechanical testing setup (Zwick/Z010, Zwick/Roell, Germany), with a 10 kN force transducer (KAP-S, AST Gruppe GmbH, Germany) at 23 ºC and 50% RH. Samples were compressed at a rate of 1 mm/min up to 80% strain and elastic moduli were calculated from the linear regime of the compression curves (at 7 ± 3% strain)." (Iswar *et al.*, 2018)

"Results and discussion

The addition of the prepolymers increases the envelope density (r) up to 0.179 g/cm^3 and decreases the specific surface area from 850 to 650m^2/g (Figure S8 and Table S3), but hybrid aerogels with excellent thermal and mechanical properties can nonetheless be produced from a wide range of silane-terminated prepolymers (Table 1; Figures S4, S5, S6, S7a and S7b). The process is relatively insensitive to the type of prepolymer, as demonstrated by the use of eight different kinds of prepolymers with a wide range of molecular weights and chain lengths, including those from natural oil-based polyols (Table 1). However, the EP-M 95

prepolymer, comprised of a short aliphatic chain between the silane terminations, yielded hybrid aerogels with better thermal and mechanical properties, compared to the polyether and NOP based prepolymers. Presumably, the short length of this prepolymer, with a separation of

~2-3 nm between the silane terminations, is optimal to reinforce the inter-particle necks between the primary silica particles (~4 nm diameter) that make up the aerogel backbone (Fig. S13). Longer prepolymer chains somewhat reduce the strengthening capacity, particularly in the case of the NOP based prepolymers (Figures S15 and S16), and lead to higher shrinkage, density and thermal conductivity, particularly for the polyether based prepolymers (Table S3). Note that the variations of the thermal and mechanical properties discussed above are relatively minor compared to the much larger variation in molecular weight (Table 1) and all prepolymers enable the synthesis of hybrid aerogels with excellent thermal and mechanical properties. The reinforcement effect is also not directly proportional to the number of covalent Si-O-Si bonds formed between the prepolymer and silica particles: for example, the addition of the short EP-M-95 prepolymer (MW ~600) instead of the much longer STP-E-35 (MW ~14000) introduces over 20 times more possible covalent crosslinks, but has a similar effect on the maximum stress (s_{max}) and E modulus, and only leads to a modest difference in thermal conductivity (Table 1, Fig. 5). The aerogels based on the EP-M prepolymer were selected for a more detailed characterization and are discussed in detail below. An extensive description of the data for the other samples can be found in the supplementary information." (Iswar *et al.*, 2018)

"Thermal and mechanical properties

All hybrid aerogels can sustain uniaxial compression without rupture to at least 80% strain (Fig. 5a, Figures S15, and S16), regardless of the prepolymer type or concentration, and can be recovered as a cohesive, flattened disk after testing. In contrast, prepolymer free reference silica aerogel typically breaks up into multiple small pieces below 50% strain. The addition of prepolymers increases the compressive (E) modulus, compressive strength at 10% and 50% strain (σ10, σ50) and final compressive strength (σ_{max}), which corresponds to the strength at 80% for the hybrid aerogels as none of them failed at lower strain (Fig. 5b and c, Figures S17a-d and S18a-d). The increase in σ_{max} is a linear function of the prepolymer concentration (Fig. 5b), whereas the E-modulus follows a power-law dependence on sample density (Figure S19; Tables S2 and S3). The hybrid aerogels prepared with the EP-M 95 prepolymer exhibit

the best mechanical performance with a final compressive strength as high as 21MPa and an E modulus of up to 3.4 MPa. Remarkably, the EP-M 95 derived materials also display the lowest thermal conductivities with λ between 14.7 and 16.8mWm^{-1} K^{-1} for densities in the 0.10 and 0.18 g/cm^3 range (Fig. 5d). The thermal conductivity displays a minimum in λ around X~0.4 and ρ~0.12 g/cm^3, consistent with the well-known dependence of λ on ρ for silica aerogels [2,4] (Fig. 5d and Figure S8; Table S3). At lower prepolymer concentrations and densities, the gas phase conduction is higher because of larger pores. At higher prepolymer loadings and densities, the solid conduction through the skeleton increases, even though this increase is minimal for the EP-M 95 based hybrid aerogels.

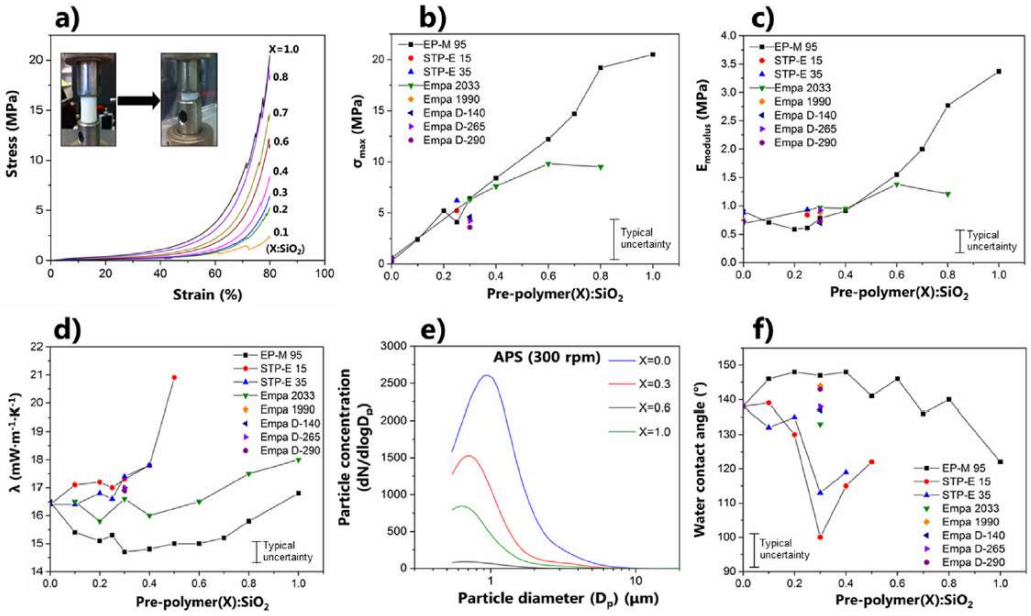

Fig. 5. (a) Stress-strain curves of EP-M 95 hybrid aerogels for variable prepolymer concentrations; (b) Final compressive strength (σ_{max}); (c) E modulus; (d) λ; (e) Particle release of EP-M 95 hybrid aerogels (300 rpm, APS - 0.54–19.8 μm); and (f) Water contact angle. Note that the hybrid aerogels with Empa 1990, Empa D-140, Empa D-265 and Empa D-290 prepolymers were synthesized for only one concentration (X = 0.3).

The ability to improve silica aerogel's mechanical properties without a penalty in thermal conductivity positions this new class of polymer modified ormosil/silica aerogels at the leading edge of what is possible in aerogel reinforcement (Fig. 6). Indeed, previous reinforcement strategies have consistently increased thermal conductivity, negating the unique selling point of aerogels as thermal superinsulation materials, with only one exception, the pectin silica hybrid aerogels recently developed in our laboratory [21]. Compared to the latter, the materials presented here use a simpler, more scalable production processes, with faster gelation times and fewer solvent exchanges.

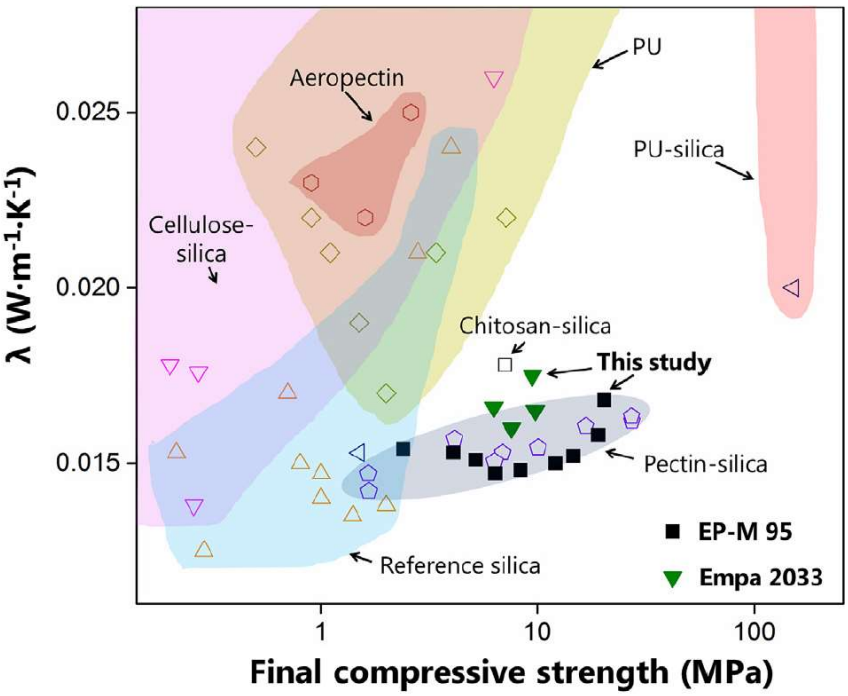

Fig. 6. λ versus final compressive strength for aerogel-like materials: [4,8,11,15,16,21,22,40–45]. Data on the polyrotaxane-silica hybrids [33] were not included because λ was determined indirectly.

"(Iswar *et al.*, 2018)

"Conclusions

Mechanically strong, superinsulating aerogels are produced by a one-step sol-gel process. In contrast to other reinforcement strategies, no additional solvent exchanges or post-modification steps, compared to standard silica aerogel synthesis, are required. The ability to produce materials with improved properties from a wide variety of prepolymers, including those from renewable precursors, highlights the flexibility of the approach. The reinforced, hydrophobic hybrid aerogel materials can sustain uniaxial compression to at least 80% strain, display a high compressive strength and stiffness and have all but eliminated the particle release. Crucially, the reinforced aerogels maintain the ultra-low thermal conductivity typical for silica aerogel (15-17 mWm-1 K^{-1}). This new class of polymer modified ormosil/silica aerogels offer a superior insulation performance, when compared to the current state-of-the-art, and uses a simpler and more scalable production process." (Iswar *et al.*, 2018)

3.2.3 Poly (vinyl alcohol) (PVA) polymer

Another promising resent study: “Thermal, mechanical, and surface properties of poly(vinyl alcohol) (PVA) polymer modified cementitious composites for sustainable development)”(Lu *et al.*, 2018) deserves to be presented in this dissertation.

“INTRODUCTION

Polymer modified cement and concrete have been rapidly developed and widely used in civil infrastructure, such as thermal insulating mortar and self-healing concrete,[1–7] because the good cohesion and adhesion of polymer enable it as not only a reinforcing filler in the cement matrix to regulate the microstructure and improve the mechanical behavior, but also an effective surface modifier to adjust the surface nature of cement-based materials. The addition of polymer benefits to enhance many properties of cementitious materials, including fluidity,[8] water permeability,[9] mechanical properties,[10] and dimensional stability.[11] Moreover, the addition of very small amount of polymers leads to an enhancement of adhesion strength and durability of cementitious composites, which makes it as a good candidate of repair materials.[12]

Poly(vinyl alcohol) (PVA), as one of the major water-soluble polymers, has been widely used to reinforce cementitious materials in terms of physical and engineering properties due to its superior chemical resistance and excellent mechanical properties. [13–16] It has been reported that PVA with a large amount of hydroxyl groups can be used as a reinforcing filler,[17] aggregate surface modifier,[18] or fiber reinforcement[19,20] to cementitious materials. Among them, PVA fibers reinforced cement-based materials have become one of the most promising materials for high-performance structural and functional application with the merit of high ductility, enhanced toughness, and favorable strength to weight ratio. Based on the basic principle of micromechanics and fracture mechanics,[21,22] the strain hardening cementitious composites with pseudo strain hardening and multiple cracks less than 100 μm have successfully developed, which can meet the high requirements of safety and durability in developing sustainable infrastructure.[23]

In addition, many attempts have been conducted to investigate the mechanical strength and microstructures of PVA-modified cement-based materials. Allahverdi et al.[24] indicated that PVA-modified cement mortar had a better workability due to the surface activity present in water soluble polymer that can increase the viscosity of the water phase in the cement mortar. Kim et al.25 found that the compressive strength of cement mortar decreased with the

increasing amount of PVA because the mild surfactant properties of PVA led to generate the small air voids and bubbles in cement matrix. However, Singh and Rai[26] indicated that the compressive strength of cement mortar was enhanced with the addition of PVA since some new compounds filled in the pores of cement matrix and improved the chemical interaction between the PVA and cement hydrates. Until now, most of studies only revealed the influence of PVA polymer on the mechanical, microstructural, and engineering properties of cement-based materials. However, to our best knowledge, as a kind of mild surfactant agent with amphiphilic property, PVA should have a great influence on the functionalization of cement-based materials, such as thermal inertia and surface hydrophobicity, which benefits to the improvement of cement-based materials in terms of thermal insulation and self-cleaning properties but has been rarely investigated. More importantly, it still lacks of investigation on the relationship between the functional and mechanical properties of the PVA-modified cementitious materials. Therefore, in this study, the effect of PVA on the thermal properties of cement paste was first investigated by conducting steady heat conduction test and thermal conductivity test. The porosity of the PVA-modified cement paste was measured by mercury intrusion porosimetry and then correlated with its thermal insulation property.

Moreover, the influence of PVA on the surface wettability of cement paste was investigated using contact angle meter. Also, the compressive and tensile strength of the PVA-modified cement paste were investigated by compression test and indirect tensile splitting test. Finally, the relationship between the thermal insulation, surface hydrophobicity, and mechanical properties of the PVA-modified cement-based materials was established." (Lu *et al.*, 2018)

"MATERIALS AND SAMPLE FABRICATION

Materials

Ordinary Portland cement type 52.5 (Green Island, Hong Kong) was used to fabricate cement paste. The PVA 1788 with the molecular weight of 72,800–83,500 and the degree of hydrolysis of 87%–89% was supplied by Yingjia Industrial Co., Ltd. (Shanghai, China). The superplasticizer based on polycarboxylate polymers (PCE, ADVA 189) with a concentration of 28–30 wt % were purchased from Grace Concrete Admixture Products, Hong Kong.

Fabrication of PVA-Modified Cement Paste

Table I lists the mix proportions of the PVA-modified cement paste. The water to cement (w/c) ratio was fixed at 0.31. The addition of PVA was 0.5%, 1.0%, 2.0%, and 3.0% by the weight of cement. The amount of PCE was adjusted to satisfy the workability of the fresh

Table I. Mix Proportions of the PVA-Modified Cement Paste

No.	Cement (g)	w/c	PCE (g)	PVA (wt %)
1	5000	0.31	18.0	0.0
2	5000	0.31	18.0	0.5
3	5000	0.31	18.5	1.0
4	5000	0.31	19.0	2.0
5	5000	0.31	19.5	3.0

mixture. The mixing procedures were as follows:

1. cement particles and PVA powders were first dry mixed for 2 min at 300 rpm by a mixer (Habort 5-Quart Mixer) to make a uniform dispersion of PVA in cement;

2. water with premixed PCE was added into the mixture above and mixed together for 2 min at 300 rmp and another 2 min at 1000 rmp;

3. the paste splashed on the side of the bowl should be scrapped down during the mixing process;

4. the fresh mixture was cast into cylinder molds with diameter of 100 mm and height of 200 mm for indirect tensile splitting test and cubic molds with 40 x 40 x 40 mm for compressive test. Specimens with dimensions of 200 x 100 x 40 mm were used for both the steady heat conduction test and thermal conductivity test, respectively. The specimens were demolded after 1 day and cured in the ambient environment (20 ºC, 40% humidity) until test." (Lu *et al.*, 2018)

EXPERIMENTAL

Thermal Characterization

Steady Heat Conduction Test. Figure 1 shows the schematic diagram of the steady heat conduction test facility. The facility consists of three main parts: an infrared red lamp as the heating resource, a hollow PVC tube (green) with reflective paper for creating a uniform

temperature field, and a hollow wooden-box (bottom black box). The testing specimen (red) was placed in the center-top of holder in the wooden box, and gaps between the holder and

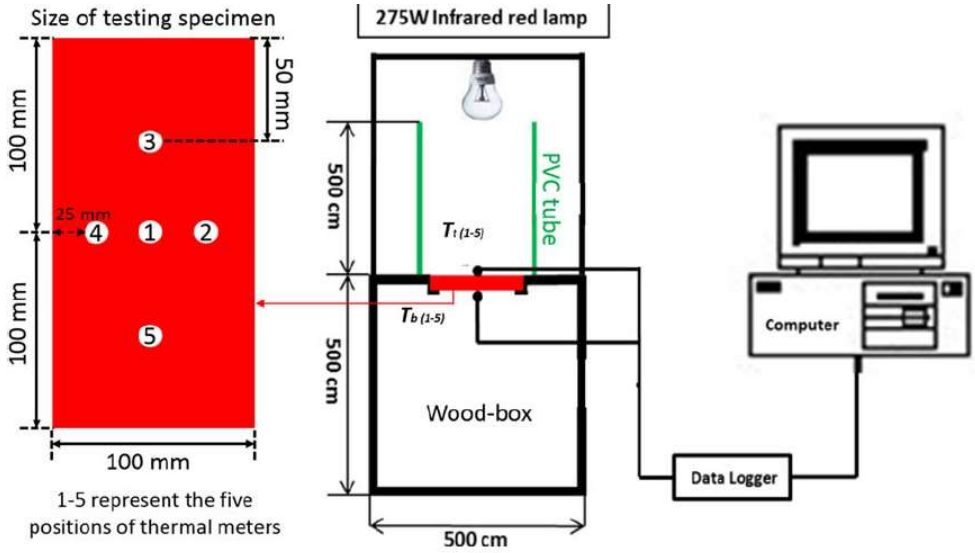

Figure 1. Schematic diagram of the steady heat conduction facility. [Color figure can be viewed at wileyonlinelibrary.com]

specimen was filled with thermal insulating materials and sealed by adhesive tapes to prevent heat leakage. There were five thermocouples [$T_{t(1–5)}$ and $T_{b(1–5)}$] attached to each side of the specimen, and the average value indicated the surface temperature variation, and the data can be collected by a data acquisition in every 0.17 s. The testing specimens at the curing age of 28 days were used for the steady heat conduction test, which was carried out in a controlled room with constant temperature of 25 °C and humility of 50%.

Thermal Conductivity Test. The thermal conductivity test was carried out using a quick thermal conductivity meter based on ASTM C1113-90 Hot Wire Method (QTM 500, Kyoto Electronics Manufacturing, Japan).[4] The experimental setup consists of a temperature test chamber and data acquisition system. The measurement temperature range is from 2100 to 1000 °C with the precision of 65%. The testing specimen at 28-day was firstly oven-dried at 110 °C for 8 h and then vacuum dried for 3 days to remove moisture in the pores before the thermal conductivity test.

Mechanical Test

The compressive test was conducted using a universal testing machine (MTS Alliance) with a loading of 1 kN/s. The indirect tensile splitting test was conducted on cylindrical specimens at

the age of 28 days, in accordance with ASTM C496. At least, three specimens were cast and tested for each mix and each property.

Microstructural Analysis

The porosity of the PVA-modified cement paste was determined by mercury intrusion porosimetry (Pascal 140 + 440, POROTEC). After the compression test, the broken sample was crushed into smaller pieces with the dimension of 3–6 mm, which were then vacuum-dried to constant weight and used for porosity measurement. Scanning electron microscope (SEM, JEOL 6300) was used to characterize the failure surface after the specimens broke in the mechanical test. In addition, the surface wettability of the PVA-modified cement paste was measured by contact angle meter (DIGIDROP, GBX). The testing specimens for contact angle measurement were firstly vacuum dried for 24 h to remove all the surface water, and then conducted for 10 times for each mix, and the average value was used to reflect the surface wettability of the testing specimens." (Lu *et al.*, 2018)

"**RESULTS AND DISCUSSION**

Thermal Insulation Property of the PVA-Modified Cement Paste

In this study, both the steady heat conduction and thermal conductivity test were measured to investigate the effect of PVA on the thermal properties of cement paste. For the steady heat conduction test, ΔT is the temperature difference between the inner and outer surface temperature of the testing specimen, and the larger ΔT is usually considered as a key parameter to indicate the better thermal insulation property of the specimen.

Table II. Surface Temperature of the PVA-Modified Cement Paste in the Steady Heat Conduction Test

Parameter	Surface temperature (°C)	Temperature difference (°C)	Thermal conductivity [W/(m K)]	
No.	Outer	Inner		
1	61.60	52.30	9.27	0.862
2	63.35	52.48	10.87	0.728
3	63.97	51.26	12.72	0.575
4	66.39	53.07	13.32	0.492
5	71.08	58.89	12.49	0.558

Table II lists the value of ΔT corresponding with the thermal conductivity of PVA-modified cement paste, and two representative temperature–time curves for normal cement paste and cement paste with 2.0% PVA in the steady heat conduction test are shown in Figure 2. The

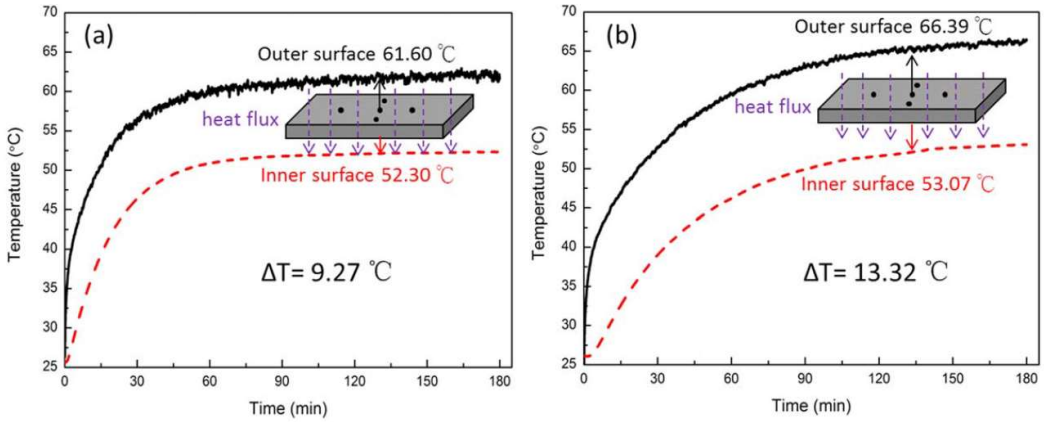

Figure 2. Temperature–time curves for normal cement paste and cement paste with 2.0% PVA in the steady heat conduction test. [Color figure can be viewed at wileyonlinelibrary.com]

experimental results demonstrate that the reference specimen (normal cement paste without PVA) has the smallest ΔT (9.27 °C). When the amount of PVA increases from 0.5%, 1.0% to 2.0%, ΔT increases from 10.87, 12.72 to 13.32 °C, correspondingly. The increasing ΔT indicates that there is less heat transferring from outside to inside of the specimen per time during the steady heat conduction test. This phenomenon can be explained by the increased porosity of cement paste with the addition of PVA. PVA, as an anionic action of surfactant, consists of a hydrophobic backbone and a hydrophilic end. The negative charged hydrophobic end can attach on the surface of cement particles with positive charge due to the electrostatic

attraction, which benefits to reduce the surface tension and generate stable bubbles in cement matrix,[27] as shown in Figure 3. Due to the moderate surfactant properties and viscoelasticity

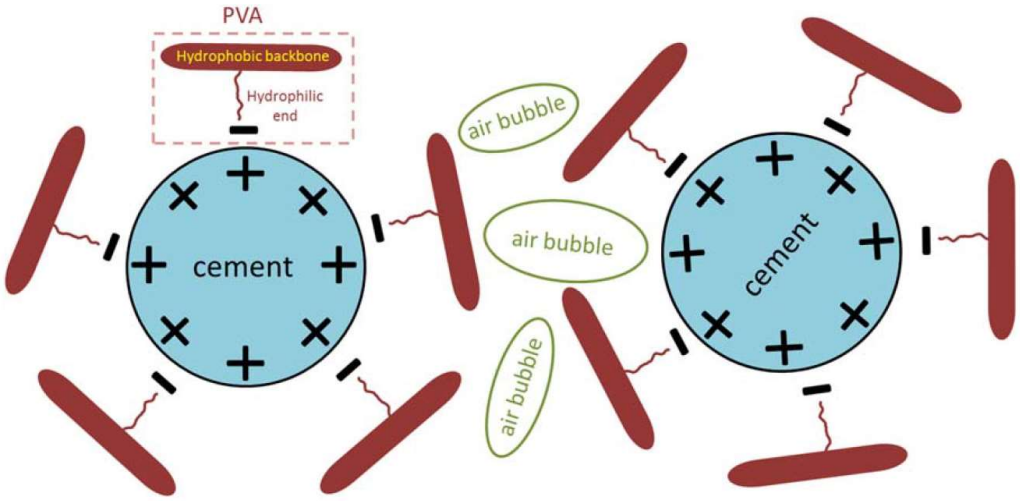

Figure 3. Mechanism of PVA as an air entrainment. [Color figure can be viewed at wileyonlinelibrary.com]

of PVA, air bubbles in the cement matrix are hardly to be removed, which can increase the porosity and improve the thermal insulation property of cement paste. However, when the amount of PVA reaches up to 3.0%, the ΔT and thermal conductivity of the testing specimen decreases and increases, which means that the higher addition of PVA plays a negative effect on the thermal insulation property of cement paste. This is attributed to that the excessive addition of PVA in cement paste reduce the viscosity of cement paste at the mixing and fresh stage, which is not beneficial to the formation and stability of the air bubbles in the cement paste, so the porosity and thermal insulation properties of the cement paste are reduced. Figure 4 shows the total porosity of the PVA-modified cement paste. It clearly indicates that

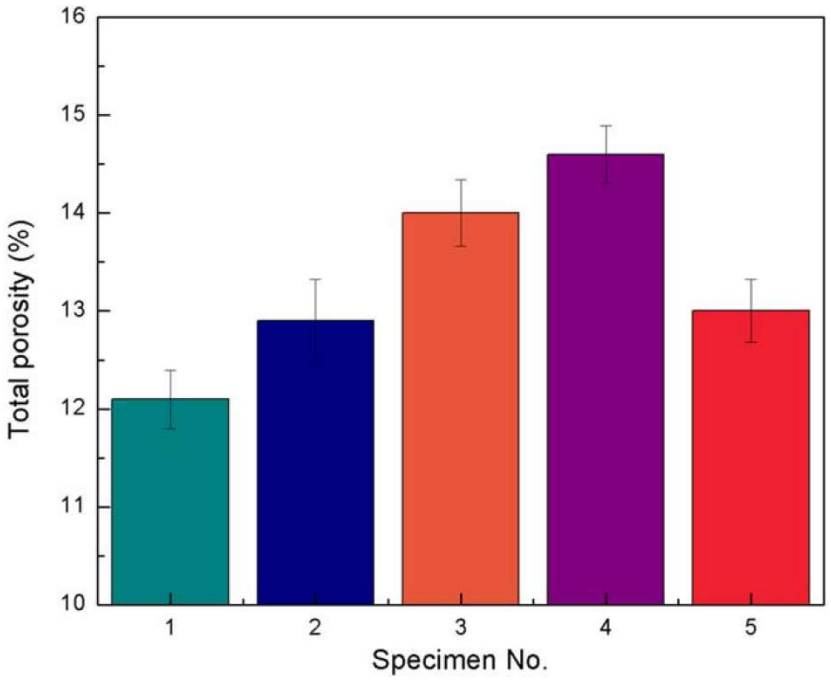

Figure 4. Total porosity of cement paste with different amount of PVA.

when the amount of PVA is less than 2.0%, the porosity of the cement paste increases with the increasing amount of PVA; however, excessive PVA (higher than 2.0%) leads to a reduction in the total porosity, which is the major reason leading to the smaller ΔT and increased thermal conductivity of cement paste. In summary, based on the results obtained from steady heat conduction test and thermals conductivity test, 2.0% addition of PVA is the optimum to achieve the best thermal insulation property of cement paste by reducing the thermal conductivity by 42.9% and increasing the porosity by 20.7%, respectively.

However, it seems not reasonable to use the ΔT to evaluate the thermal insulation property of the PVA-modified cement paste in this study. In most cases, the larger ΔT usually leads to the lower indoor surface temperature when the testing specimen is irradiated under a constant heat source. However, in this study, the largest ΔT of the specimen appears when the addition of PVA is 2.0%, but the lowest indoor surface temperature of the specimen appears when the addition of PVA is 1.0%. For example, sample 4 (2.0% PVA) shows the largest ΔT of 13.32 ℃, and the outer and inner surface temperature are 66.39 and 53.07 ℃. Compared with sample 4, sample 3 (1.0% PVA) shows a lower value of ΔT (12.72 ℃), and both the outer (63.97 ℃) and inner surface temperature (51.26 ℃) are lower than that of sample 4. In terms of ΔT, it can be concluded that sample 4 shows a better thermal insulation property than sample 3 due to the larger ΔT. However, in terms of inner surface temperature, sample 3 has a lower value than sample 4, which means that the thermal insulation property of sample 3 is

better. The contradictory conclusions result from the different thermal energy absorption ability and changed outer surface temperature of the specimen with different amount of PVA. Although ΔT of sample 4 is larger than that of sample 3, the outer surface temperature of sample 4 is also higher (2.42 ℃) than that of sample 3, indicating that more thermal energy is captured at the outer surface of the cement paste with the increasing amount of PVA, and that is the major reason leading to that the larger ΔT does not stand for the lower inner surface temperature of sample 4. In order to figure out the mechanism behind, thermal analysis of PVA was carried out using DSC. Figure 5 shows the DSC curve of PVA polymer. It reveals that when 1 g of PVA is heated from 36 to 96 ℃, there are totally 46.42 J energy can be absorbed by PVA. Based on the mix proportions listed in Table I, when the addition of PVA increases from 1.0 to 2.0 wt %, 50 g more PVA is added into cement paste, leading to that more thermal energy (50 g 3 46.42 J/g52321 J) can be collected by cement paste with 2.0% addition of PVA, comparing that with 1. 0% PVA, and that is the reason leading to the higher outer surface temperature of sample 4. Therefore, it can be concluded that thermal conductivity can only reflect the thermal insulation property of the PVA-modified cement paste when the outer surface temperatures are almost the same. However, it is not believable to use thermal conductivity as an indicator to reflect the thermal insulation property of PVA-modified cement paste in this special case because more thermal energy can be collected at the surface of cement paste with the increasing amount of PVA. In summary, the effect of PVA on the thermal insulation property of cement paste has two sides, and the optimum balance to obtain the lowest inner surface temperature of testing specimen can be achieved by adding 1.0% PVA into cement paste." (Lu *et al.*, 2018)

3.2.4 Waste based aggregates

Aerogels were discovered

3.2.4.1 Crushed Sand Concrete containing Rubber Waste

Aerogels were discovered in 1931 by Samuel S. Kistler and are a silica gel where all the liquid (Mohamed and Djamila, 2018)

"1 Introduction

Rubber waste management is one of the serious environmental problems in the world and it has many challenges for the recycling process. The recycling and disposing of some waste rubber types have many challenges. These are attributed to the difficulty of making separation, type of rubber used, incineration problems, environmental regulations, and increasing the cost of recycling. Use of such waste rubber materials in civil and construction engineering applications has become an attractive alternative to disposal to reduce both the cost of disposal and waste quantities. Many authors [1-9] have reported the properties of concrete with used tyre rubbers and plastics waste. Their results indicate that the size, proportion, and surface texture of rubber particles affect the strength of used tyre rubber contained in concrete [1–9].Eldin and Senouci [3] conducted experiments to examine the strength and toughness properties of concrete made with rubber waste. They noted that the mechanical strength decreases when the rubber waste content increase. Several authors [1,3,4] used tyre chipped rubber containing Portland cement concrete for uses in sound/crash barriers, retaining structures, and pavement structures has been extensively studied. Test results founded that the use of used tyre chipped rubber considerably increases toughness and resistance. Khatib and Bayomy [1] studied the influence of adding two rubbers, crumb and chipped on performances of concrete. They found that the compressive strength of concrete would decrease with increasing rubber content.

This work aims to study the possibility of using waste rubber of shoes in sand concrete without any transformation except grinding, to minimize the cost of the final material. The influence of the proportion of waste used on the physical, mechanical and thermal properties of the new material has been studied and analyzed.

2 Experimental

2.1 Materials

The used sand in this work was extracted from the south of Algeria, near the city of BOUIRA. The particle size distribution is shown in Figure 1, and the physical properties are presented in

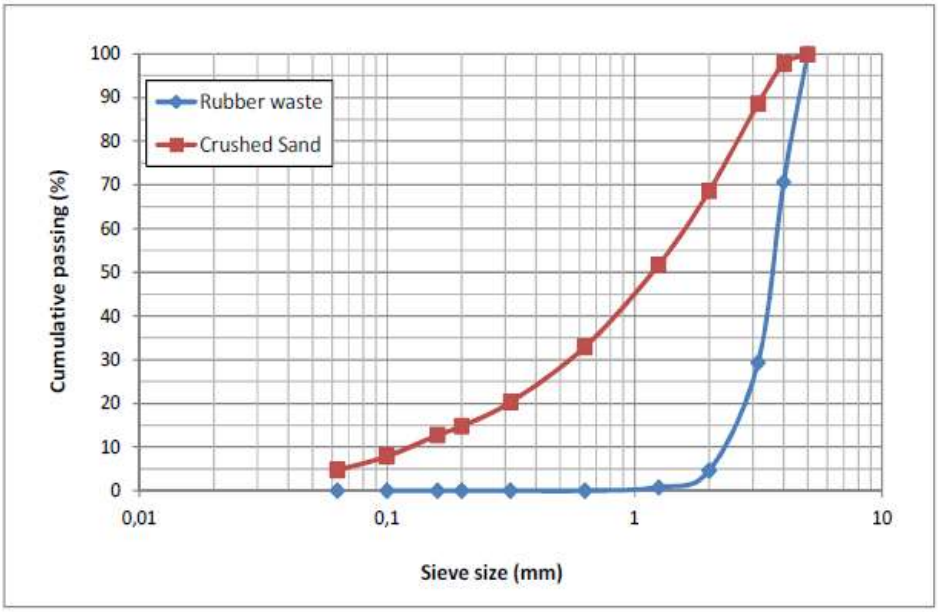

Fig. 1. Particle size distribution of used sand and rubber waste.

Table 1. The X-ray Diffraction analysis of used sand demonstrates their essentially limestone nature “Figure 2”. A SEM investigation reveals the crusaded shape of the grains “Figure 3”.

Table 1. Physical properties of used sand.

Properties	Sand	Norm
Apparent density (kg/m^3)	1490	NP EN 1097-3
Specific density (kg/m^3)	2500	NP EN 1097-6
Water absorption (%)	1.5	NP EN 1097-6
Sand equivalent (%)	63.50	NP EN 933-8
Fineness modulus	3.14	NP EN 933-1
Compactness (%)	0.60	NF P 18-555
Porosity (%)	0.40	NF P 18-555

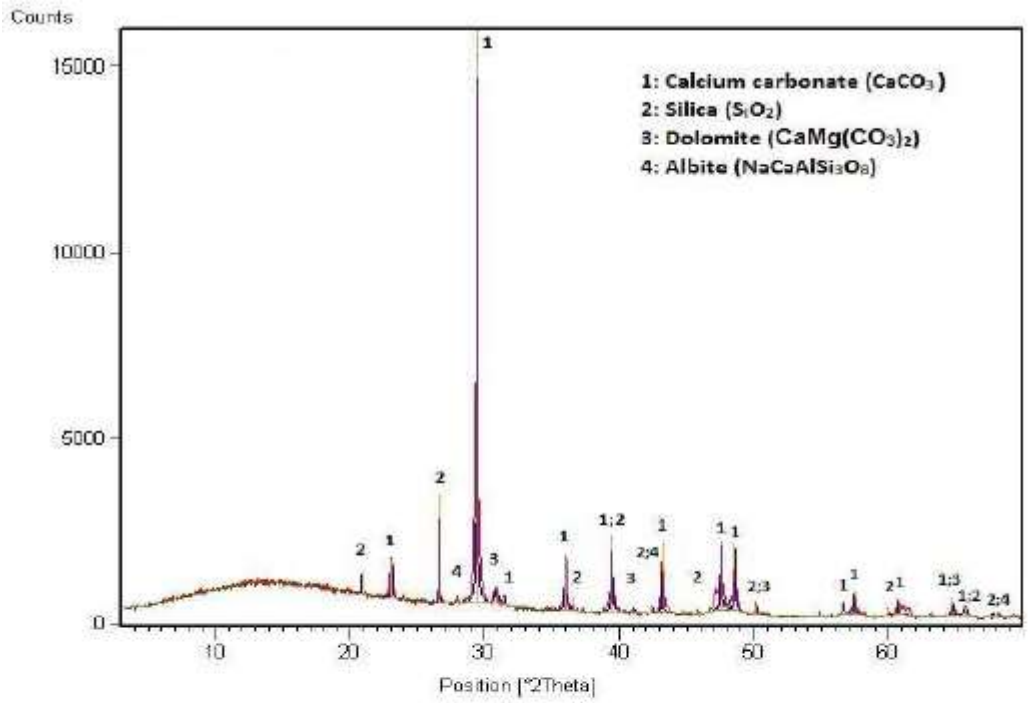

Fig. 2. X-ray diffractogram analysis of used crushed sand.

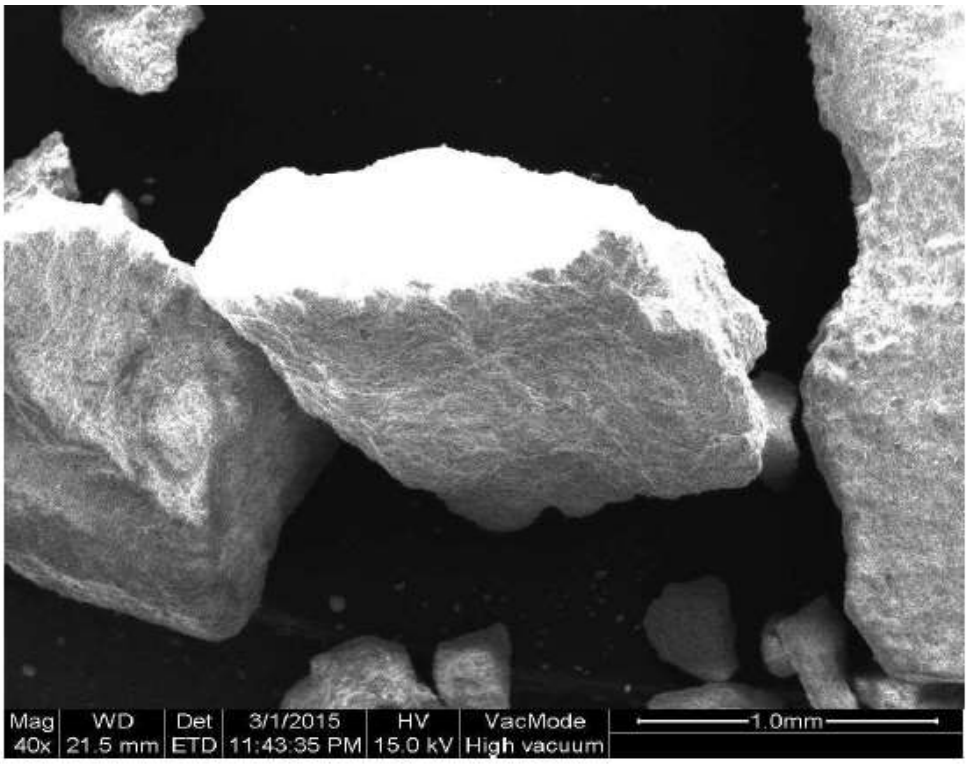

Fig. 3. Scanning electron micrographs of used crushed sand.

Portland cement CEM II/A 42.5 from CHLEF Factory in Algeria was used throughout this study, with a density of 3100 kg/m^3. Moreover, the chemical analysis revealed the existence of the chemical products shown in Fig. 3 with the proportions presented in Table 2.

Table 2. The chemical composition of used cement (%).

Materials Oxides	Cement
SiO_2	21.89
Al_2O_3	6.15
Fe_2O_3	3.95
CaO	58.76
MgO	1.13
K_2O	0.67
Na_2O	0.57
SO_3	1.62
CaO_{Free}	0.45
P.F	4.67
Total	99.86

The use of fillers in sand concrete composition is essential [10]. Their use is intended to complete the grading curve of sand in its finest part in order to obtain more compact concrete and reduce the cement content and therefore the cost of concrete [11]. In this work the fillers used are the limestone powder. Their specific density is 2,857 kg/m^3, and specific surface area 310 m^2/kg.

The rubber waste used in this work to obtain by the recycling the waste of shoes discharged into the environment after were collected, are washed, compressed, crushed and extruded in the form of grains, and added in the mass of sand concrete with percentage 10%,20%,30% and 40%. Figure 4 shows the general aspect of used rubber waste in this work. The sieve analysis results are given in Figure 1 and the table 3 lists the set of physical, mechanical properties.

Fig.4. General aspect of used rubber waste.

Table 3. Physical and thermal properties of used rubber wastes.

Table 3. Physical and thermal properties of used rubber wastes.

Properties	Rubber waste
Diameter	1.5
Apparent density (kg/m^3)	0.8
Bulk density (kg/m^3)	1.28
Compactness (%)	62.5
Porosity (%)	37.5
Water absorption (%)	0.1
Thermal conductivity (W/m K)	0.15

The admixture used is an Algerian plasticiser of 'MEDAFLUID 104', liquid form; color chestnut; a PH equal to 6, density 1,04 ± 0,01 and a content of chlore < 1g/L.

The mixing water used for the different mixes is the distribution drinking water.

2.2 Mix design

The optimal compositions of the sand concrete studied, without rubber waste, is based on the experimental method of project of Sablocrete [11]. This gave for cement proportioning of 350 kg/m^3, 1560 kg/m^3 of sand, 130 kg/m^3 of fillers, and a water/cement ratio of 0.75, a percentage of plasticizer of 1% of weight of cement. The rubber waste is added in sand

concrete at dosages (0%, 10%, 20%, 30% and 40%). Literary codes identify each mixture in a precise way:

• CSC: Control sand concrete (without rubber).

• SCRW: Sand concrete with rubber waste.

The specimens produced were cured in air at 20°C and 50% RH. After 24 h, they were removed from the molds and placed in water for another 24 h and then open-air stored until the day of testing. Such curing has been chosen according the normal manufacturing of sand concrete in Algeria. This procedure was respected for all compositions and all tests." (Mohamed and Djamila, 2018)

"3 Results and discussion" (Mohamed and Djamila, 2018)

"3.2 Bulk density

Figure 7 give the bulk density of crushed sand concrete as a function of rubber waste. The results displayed that the incorporation of rubber waste in crushed sand concrete contributes to reduce the bulk density. This reduction probably due to the lower density of the rubber compared with the dune sand and the air content caused by the grain of RW, which in turn reduces the unit weight of the mixtures. Khatib and Bayomy [1] concluded that because of low specific gravity of rubber particles, unit weight of mixtures containing rubber decreases with the increase in the percentage of rubber content.

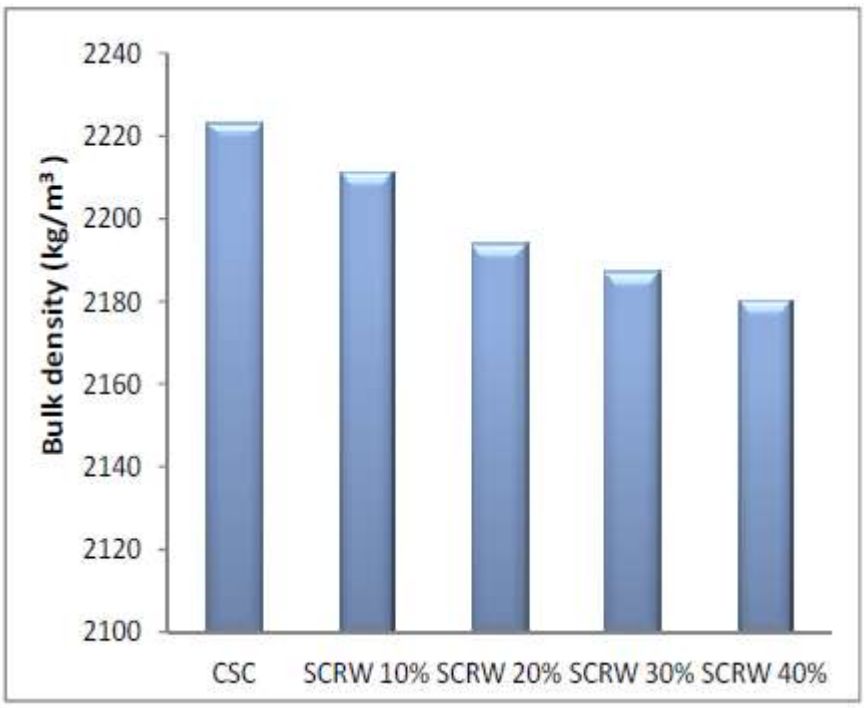

Fig.7 Bulk density of crushed sand concrete as function of spent rubber waste content.

3.3 Mechanical strength

The compressive and flexural strength tests of hardened crushed sand concrete were performed at the age of 28 are showed in figure 8 and 9. The results displayed in that compressive strengths of crushed sand concrete decrease 20 % respectively for addition of 40% natural crushed sand by rubber waste. Even thing in the case of the flexural strengths, which indicates that the addition of 40 % of the rubber waste in a crushed sand concrete represents decrease the performances of new materials. This trend may be related a poor adhesion between the surface of the rubber aggregate and binder paste is likely to have contributed to such a strong decay of mechanical properties. This reduction in performance of SC can be also caused by the great porosity and hardness of grain of rubber waste compared with natural crushed sand. Several authors [3] reported that the addition of rubber waste in the concrete, involves a significant reduction in the mechanical strength of concrete.

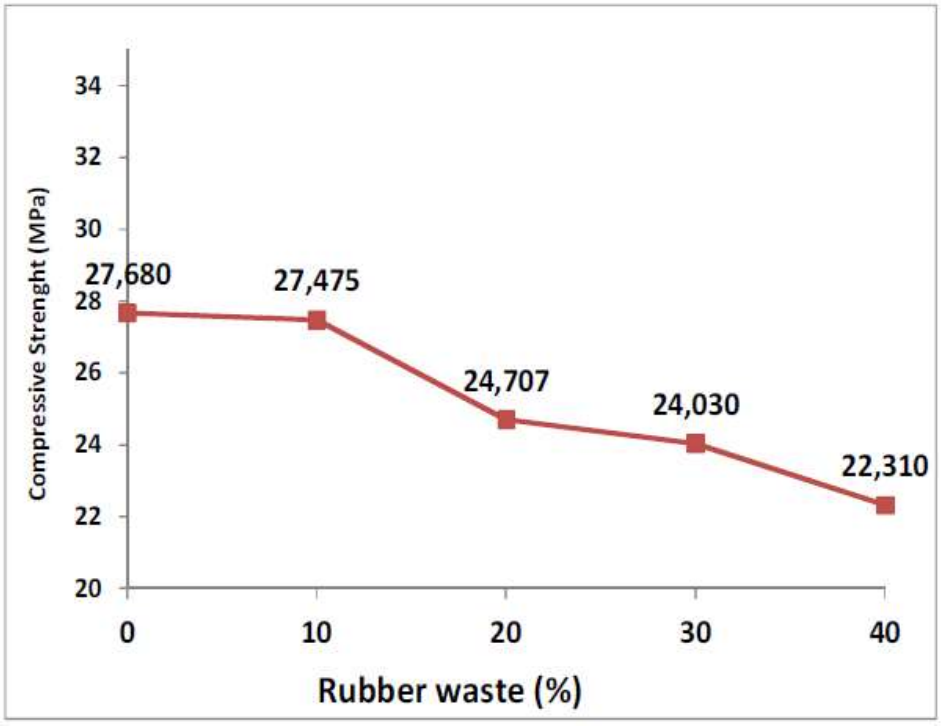

Fig.8. Compressive strength of crushed sand concrete as function of rubber waste content.

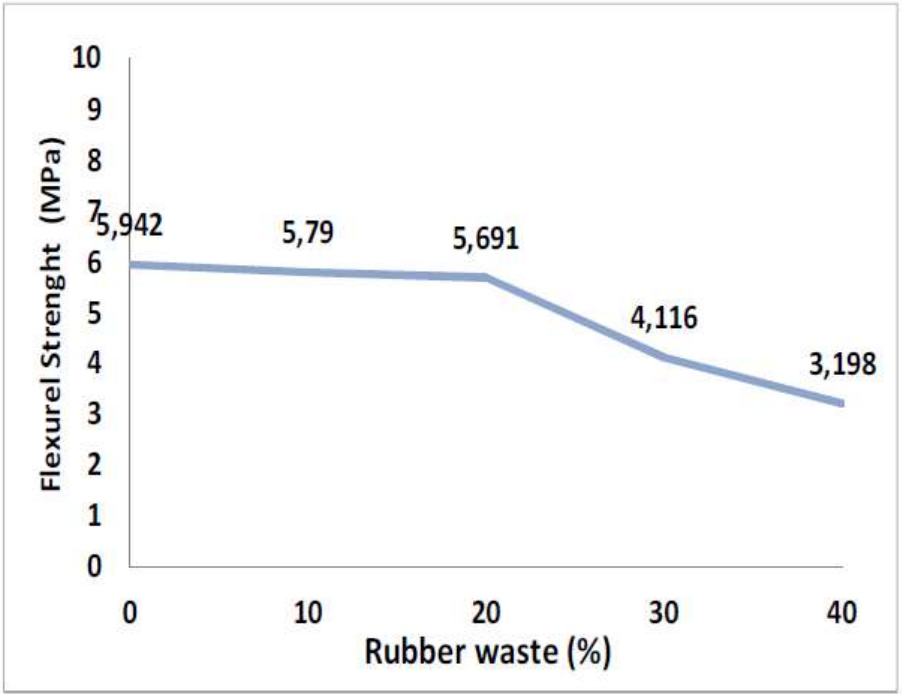

Fig.9 Flexurel strength of crushed sand concrete as function of rubber waste content.

3.4 Thermal properties

The thermal conductivity values of the specimens measured at 28 days are showed in figure 10. The results show that the thermal conductivity of crushed sand concrete decrease when

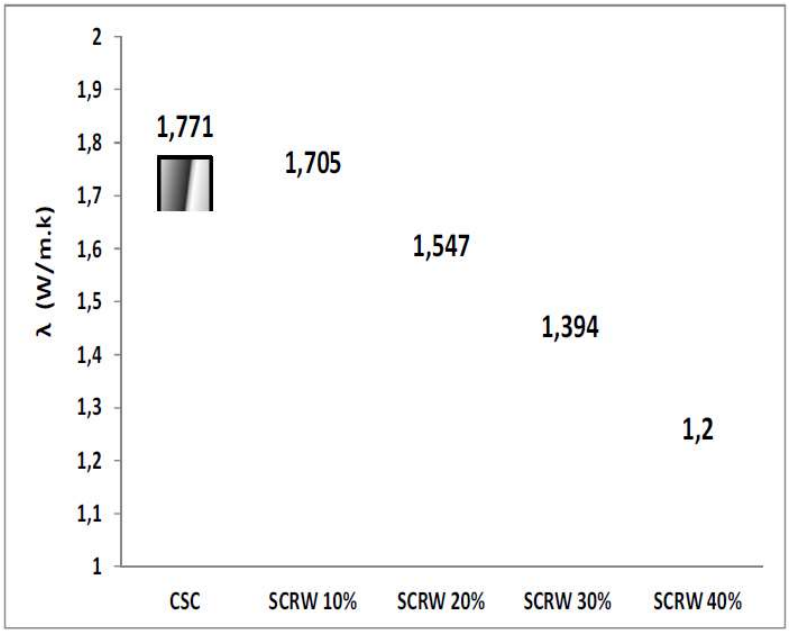

Fig.10. Thermal Conductivity of crushed sand concrete as function of rubber waste content.

the percentage of addition of rubber waste increase. It is thought that, this situation caused by the lower TC coefficient of the rubber (0.15 W/m K) than natural aggregate (2 W/m K) [12]. So the decreasing thermal conductivity came also from the increase in porosity induced by the rubber waste. In fact the pores contain air which has a TC (0.024 W /mK) much lower than all the other components of the SC. Similar results were observed by several authors in composite systems, for example F. Iucolano et al. [13] in a study on plastic waste in mortar composites, and it's showed a decreased in value of thermal conductivity of mortar containing PET about 50% lower than a traditional mortar." (Mohamed and Djamila, 2018)

3.3 Alternative types of Aerogel applications

"Aerogel is most often incorporated into buildings in the form of blankets for loft insulation or boards for wall and ceiling insulation. However, insulating boards can be wasteful of material due to the requirement to be cut to size. Also, insulating boards have the

disadvantage of requiring a flat surface for fixing onto. As a solution to these limitations, several organizations are developing plaster mixes that incorporate aerogel in granular form. One experimental product developed by Stahl et al. [3], comprised of a mineral and cement free binder and hydrophobized granular aerogel at up to 90% by volume, has achieved a thermal conductivity value of 0.025 W/mK. A similar composite material developed by Burrati et al. [4] reportedly achieved a thermal conductivity value of 0.05 W/mK with 90% aerogel by volume; the equivalent material without aerogel had a value of 0.5 W/mK. To date, however, there is only one known commercially available plaster that incorporates aerogel granules as the insulating element: the Fixit 222 Aerogel Insulating Plaster System. Fixit 222 is a highly developed product, comprising aerogel granules, light weight mineral aggregate, natural hydraulic lime, white cement and calcium hydroxide. Despite the use of cement and mineral aggregate, it still claims to achieve a thermal conductivity value of 0.028 W/mK [5]. These new plasters have significantly better thermal insulation performance than traditional cement or gypsum plasters with sand aggregate, which typically have thermal conductivity values of between 0.22 and 0.72 W/mK [6]. Interestingly, though, there appears to be no published information relating to strength or flexibility for any of these new insulating lime plaster materials. Two studies, involving cementitious mortars incorporating aerogel, which did investigate strength, reported compressive strength, flexural strength and thermal conductivity all reducing with increased aerogel content [7,8].” (Westgate, Paine and Ball, 2018)

Hasan *et al* report also some applications for silica aerogels: “The aerogel composite blankets are widely used as thermal insulation for various ground and aerospace applications [42, 43]. The aerogel composite thermal insulator blanket or wrap are commercially available from vendors such as Aspen Inc., Cabot etc. and they are mainly used in industrial pipeline for gas and oil. Further, in construction and building fields [4, 44, 45] aerogel based thermal insulation elements are often used in the current decade. Aerogel thermally insulated composite panels are now widely used, particularly in European countries and North America [4], which saves energy and thus global warming can be minimized. Recently, aerogel is also reported to be used as thermal insulation in textile industry [46].

Apart from the ground thermal insulation application, bulk aerogel and aerogel composite blankets are also used in space applications [42, 47]. For example, aerogel based thermal insulation blankets are successfully implemented in cryogenic propulsion tank [48, 49], Mars

rovers e.g., Sojourner in 1997, Spirit and Opportunity in 2003 by NASA [42]. Further, the possibility of replacement of Kapton based multilayer insulation (MLI) blanket is also studied and reported by several researchers [32, 50, 51]. The aforesaid research results [32, 50, 51] concluded that MLI shows much effective thermal insulation behavior in high vacuum environment as compared to aerogel blanket. However, because of the presence of an environment rich in CO_2 at Martian surface, aerogel based thermal insulation may perform better than conventional MLI [32, 50, 51]. Further, due to light weight, superior outgassing behavior and flexibility made aerogel blankets more attractive for spacecraft thermal control applications. It is also reported that aerogel blankets can be applied for micrometeorite protection particularly for the spacecraft in low earth orbit (LEO) besides its thermal protection [32, 50, 51].” (Hasan *et al.*, 2017)

3.3.1 Granular aerogel incorporated into non-hydraulic lime-based plasters

Some very promising results are reported in the following for an application for rehabilitation of old and listed buildings that will improve the environmental issues in a very good manner.

”This paper investigates the use of granular aerogel incorporated into non-hydraulic lime-based plasters with the aim of developing a product that is highly insulating and has good vapor permeability, with the capability of reducing the operational energy consumption of buildings.”(Westgate, Paine and Ball, 2018)

Materials and results are presented in the following:

“2 Experimental materials

2.1. Lime putty

The binder material used for this work was a lime putty supplied by J J Sharpe, which was matured for at least 6 months. The lime putty was weighed before and after drying in an oven to remove the water content and was found to have a solids content, assumed to be calcium hydroxide of 51%. This allowed accurate batching of the mix constituents.

2.2. Aerogel granules

The silica aerogel was supplied by Aerogel UK. The material comprised open cell, hydrophobic aerogel granules ranging in size from 125 mm to 5 mm.

2.3. Standard sand

The sand used in this investigation was a dry siliceous natural sand conforming to BS EN 196-1 and ISO 679: 2009. This grade of sand comprises particles that are generally isometric and rounded in shape and having a particle size distribution as shown in Fig. 1. This type of sand was specified for this investigation to facilitate consistency and repeatability of experimental conditions.

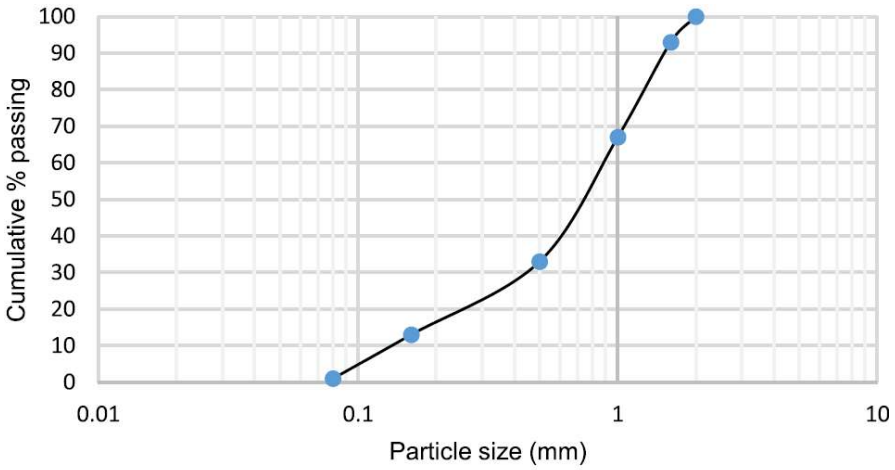

Fig. 1. Particle size distribution for standard sand.

2.4. Polypropylene fibres

Polypropylene monofilament fibres from Adfil [26] having lengths 12 and 18 mm and a diameter of 20 mm were added to the experimental plaster mixes at 0.5% by volume, to help reduce shrinkage and cracking. The fibres had been treated with a surfactant for optimum dispersion and bonding. No details of the surface treatment were provided by the manufacturer.

The volume fraction was kept at 0.5%, as it was considered that higher proportions of fibres might negatively affect the rheology of the plaster and that strength per se was not the most important physical property for a plaster." (Westgate, Paine and Ball, 2018)

2.5. Sample preparation

Five different plasters were prepared for testing using a mix ratio of 1:1 aggregate to lime putty by volume, giving a ratio ≈2:1 aggregate to lime by volume after allowing for the water content of the putty. The five specimens all contained fibres and varying ratios of aerogel and sand. The corresponding mix ratios and resulting bulk densities are presented in Table 1.

The lime and sand were prepared using a paddle mixer for a minimum of twenty minutes to ensure the plaster was suitably workable. Fibres were added to the mixture in small amounts during the mixing process to help ensure an even distribution throughout the matrix. The aerogel was added afterwards and mixed into the plaster by hand using a trowel. This was to avoid subjecting the aerogel to prolonged stress during mixing and possible degradation of the granules. The experimental mixes were then added to the prism molds in small quantities and tamped down as the material was added, to reduce the occurrence of trapped air bubbles within the specimens. For each experimental mix, three standard 40 x 40 x 160 mm prisms were prepared for strength testing, six discs of diameter 100 mm and thickness 25 mm for thermal conductivity testing and three discs of diameter 175 mm and thickness 15 mm for water vapor permeability testing.

After molding, the specimens were stored in a climate chamber regulated at a constant temperature of 20 °C ± 2 °C and relative humidity of 65% ± 5% as specified in standard EN 1015-11:1999 [27]. The specimens were covered with a thin plastic wrap for the first week to maintain a high level of humidity, as exposure to ambient atmospheric conditions during this period can result in significant reduction in strength due to premature drying and subsequent cracking [28]. The specimens were then left in the molds for a further week to allow them to achieve sufficient rigidity to facilitate demolding." (Westgate, Paine and Ball, 2018)

"4. Results

4.1. Compressive and flexural strength

Figs. 2 and 3 show stress as a function of strain during compressive and flexural testing respectively. The data was reported up to a strain value of 0.03 as a consequence of the failure mode behavior of specimens containing fibres. At higher values of strain the test data indicates that the specimens did not fail in a brittle manner even though their condition was such that they would have been considered to have failed as a building element.

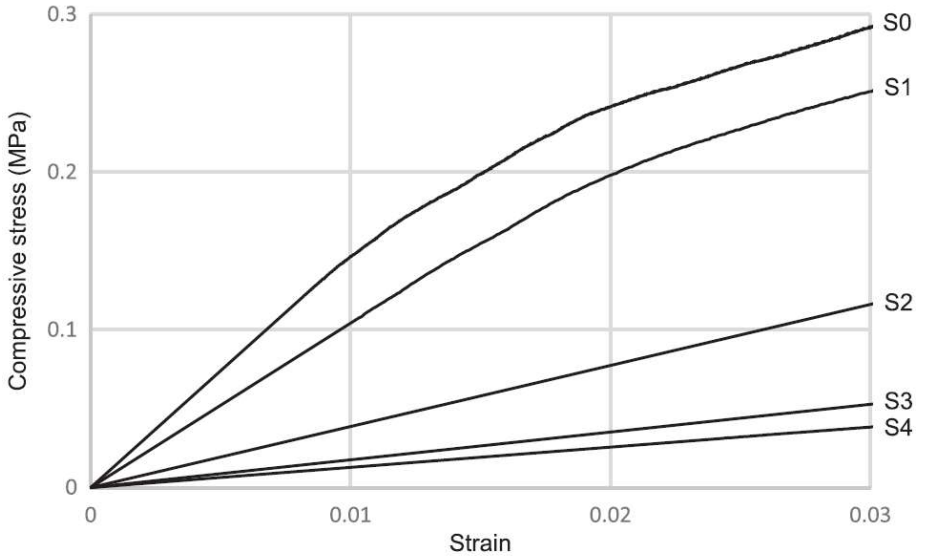

Fig. 2. Average compressive strength test results for each of the five plasters.

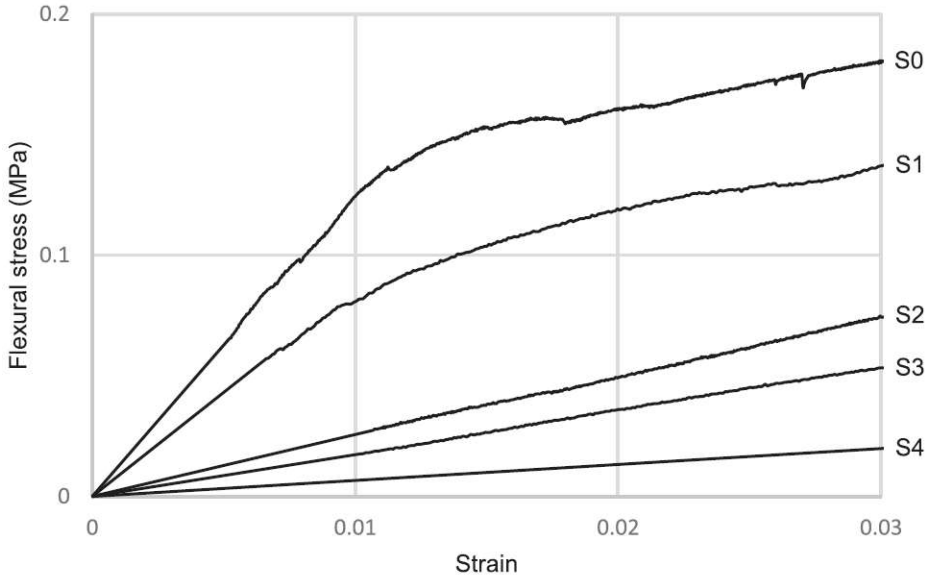

Fig. 3. Average flexural strength test results for each of the five plasters.

As the flexural test caused test specimen deformation but did not fracture it, the deformed specimen was manually broken in half after the test, and fibres and binder were removed from the fracture faces for further testing.

4.2. Effect of fibres on failure mode

Fig. 4 shows the different behaviors under stress of lime mortars with and without fibres added. Fig. 4(A) shows a typical behavior for a standard lime mortar (without fibres) under compression. At failure, the specimen fractures and fails at a distinct point in the test. In Fig. 4(B) it can be seen from the degree of compression at the base of a specimen containing aerogel (S1) that the addition of 0.5% fibres by mass permits the lime mortar to achieve a high strain capacity, and that the fibres have prevented fracturing and have helped to maintain the integrity of the specimen.

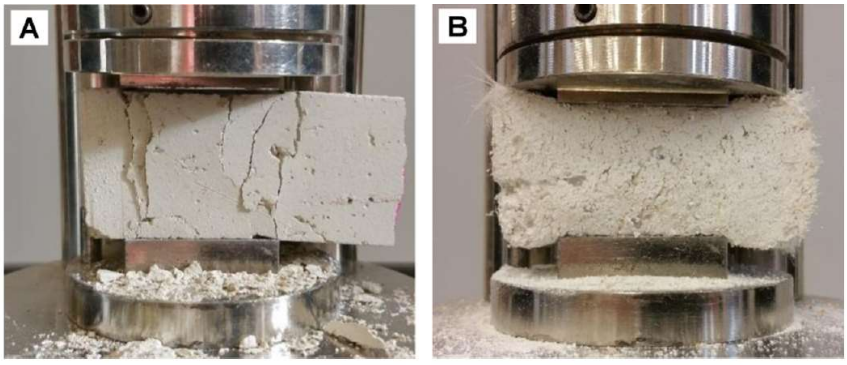

Fig. 4. Compressive fracture of a reference mortar without fibres (A) and typical deformation of a specimen (S1) containing fibres and aerogel (B).

Similarly, during flexural testing a significant difference is observed between the specimens with and without fibres added. The standard mix lime specimen cracked at the point of maximum stress (Fig. 5(A) and broke into two halves. Fig. 5(B) shows that the specimen containing fibres endured a significantly higher strain without failing and has considerably greater flexibility.

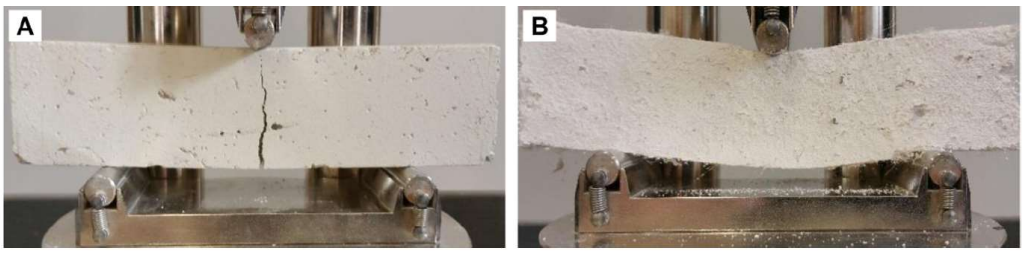

Fig. 5. Flexural fracture of reference mortar without fibres (A) and deflection of a specimen (S1) containing fibres and aerogel (B).”

(Westgate, Paine and Ball, 2018)

“4.5. Thermal conductivity

Fig. 12 shows the thermal conductivity for each experimental mix. To provide statistically significant results, an average of three separate test runs using a different pair of specimens for each test is reported. The thermal conductivity decreased significantly with increased aerogel content. Thermal conductivity values as a function of aerogel content by volume show an exponential relationship as per Eq. (3) where, k is thermal conductivity, Ae is aerogel content and k is the rate of change.

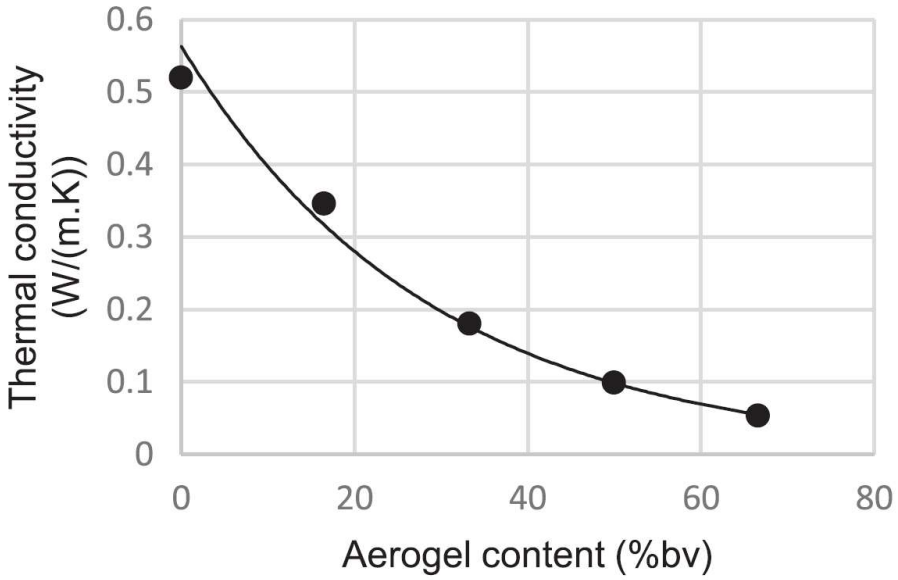

Fig. 12. Effect of aerogel content on thermal conductivity.

$$\lambda_{(Ae)} = \lambda_{(0)} e^{k \cdot Ae} \qquad (3)$$

Using a value of 66.6 for Ae gives a value of -0.034 for k. This exponential relationship can be explained by the fact that as the volume fraction of low density aerogel was increased, the volume fraction of high density quartz sand was decreased proportionally. The thermal insulating performance of the plaster mix comprising only aerogel as aggregate (S4) was only marginally inferior to other experimental insulating plasters being developed using aerogel; however, the plaster mixes investigated here utilized a significantly lower proportion of aerogel compared to those materials developed by Stahl et al. [3] and Burrati et al. [4].

4.6. Water vapor permeability

Fig. 13 shows the weight loss data for each specimen measured over a period of ten hours. The data, when plotted, shows a linear relationship between time elapsed and weight of moisture lost by diffusion through the specimen under test. The permeability clearly increased with higher aerogel content and remained constant throughout the test. This tendency was attributed to the hydrophobicity of the aerogel preventing the blockage of the pores with moisture.

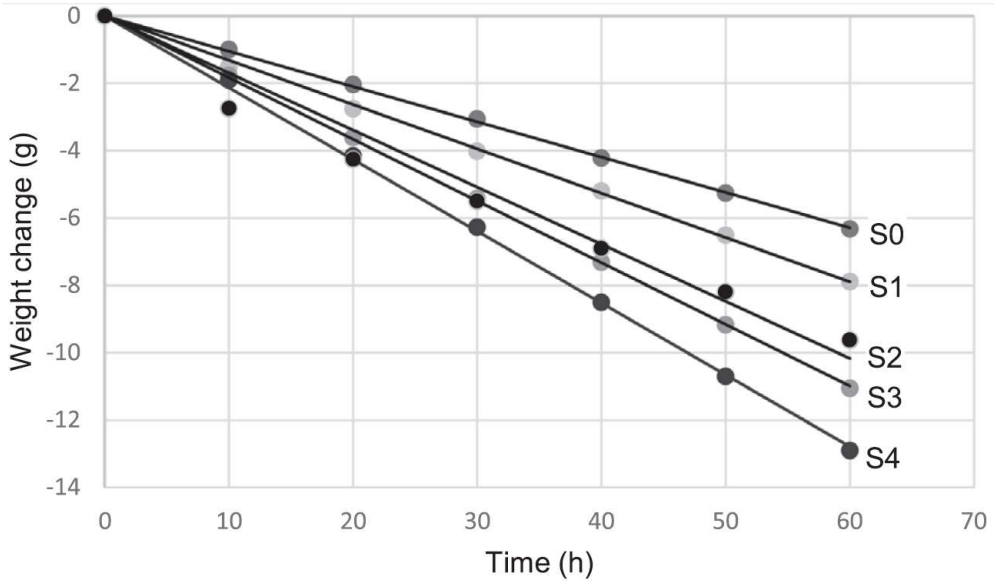

Fig. 13. Graph of weight loss against time during wet cup permeability test. " (Westgate, Paine and Ball, 2018)

"5. Discussion

Whilst the inclusion of aerogel clearly improves the thermal efficiency of the plaster mixes, the only specimen that achieved thermal efficiency comparable to similar aerogel plasters currently reported in the literature was the specimen comprising purely aerogel as the aggregate material (S4). When sand is incorporated into the mix, thermal conductivity rises significantly due to its high density compared to the aerogel. It should be taken into consideration, however, that the proportions of aerogel used in these experimental mixes was lower than those used in the other studies.

As initial attempts at incorporating aerogel into lime binders produced plasters that suffered shrinkage, cracking and very low strength, it is interesting that other similar investigations have not reported data for compressive and flexural strength. The strength values obtained during this investigation, even with fibres added to the binder, were significantly lower than

that which would normally be expected for a lime plaster. However, the high degree of plastic deformation without fracturing demonstrated the superior flexibility and toughness of these experimental mixes in comparison to the more commonly used lime/sand mixes without added fibres. These experimental mixes clearly sacrifice strength for flexibility and toughness, but for a plaster, this can be a distinct advantage because the plaster can accommodate building movement, which helps to avoid cracking.

The specimen comprising only aerogel as the aggregate material exhibited permeability significantly superior to conventional gypsum plasters and comparable to a similar developmental aerogel product. This effect can clearly be attributed to the aerogel. The linear relationship between permeability and aerogel content indicates that changes in the sand proportions had a negligible effect on permeability compared to changes in the aerogel content. This is of particular benefit when using non-hydraulic lime, which sets purely through carbonation and depends on the pore structure of the plaster for diffusion of CO2. This property of aerogel containing plasters is also beneficial to the 'breathability' of a building, as it can assist the release of moisture absorbed by walls that could otherwise freeze and expand, causing damage to masonry.

The permeability of lime-based construction materials is the physical property that is probably most responsible for the long-term durability of these materials. The fact that aerogel has also

proven to be a durable material when compared to more conventional insulation materials suggests that these experimental mixes should possess long-term durability. The experimental work carried out did not reveal any reaction between the lime and aerogel that might cause deterioration in the plaster. Furthermore, being hydrophobic and inorganic, there is no chance of moisture causing decay to the aerogel, as is possible with some natural insulating materials.

The SEM images obtained from the polypropylene fibres support the assumption that they are responsible for imparting flexibility to the plaster. The surface of the new polypropylene fiber is clearly very smooth; however, the surface condition of fibres extracted from the fracture face of test specimens shows score marks along the length of the fiber, which is consistent with there being a physical bond between the binder and the fibres. The nature of the surface damage to the fibres is consistent with the gradual failure mode observed during strength testing, whereby the physical bond between binder and fibres provides resistance to pull-out and hence improved plastic deformation. It is also evident from the measurements taken from

these images that the fibres are not stretching and thinning under tension. The absence of any evidence of chemical bonding between the lime and fibres, and the nature of the linear marking along the axis of fibres extracted from test specimens, is also consistent with resistance to fiber pull-out being responsible for the high levels of flexibility.

The low strength and rough surface texture (Fig. 4b) of these experimental mixes would not make this a practical choice for a surface plaster coat. However, they could be utilized as the first coat in a multi-coat plaster. Traditionally, the first coat is the thickest, which would be the ideal location for incorporation of the aerogel plaster. The subsequent top coats would then provide the required protection and quality of finish.

The number of permutations of different mixes using the materials considered here is vast and beyond the scope of one study. There exists, therefore, significant scope for further work in this area, specifically the investigation of different binder to aggregate ratios, volume fraction and types of fibres and volumetric proportions of aerogel.

6. Conclusions

- The results of this investigation confirm that aerogel granules can be successfully incorporated into non-hydraulic lime putty to produce viable lightweight, thermally insulating plasters.

- The thermal performance and permeability of the plaster containing only aerogel aggregate was superior to conventional plasters on the market and comparable to similar aerogel based insulating plasters being developed that contain higher proportions of aerogel.

- Previous investigations into aerogel-based plasters have not considered strength or flexibility, which are important factors for in service use. The viability of the plasters developed in this investigation was strongly dependent on the inclusion of fibres, which improved flexibility and toughness and reduced shrinkage and cracking.

- There is considerable scope for further work by investigating different mix proportions and different specification materials.

- Further work is required to investigate the use of these insulating plasters as part of a multi-coat plaster system in order to optimize layer thicknesses to provide the required combination of cost, thermal efficiency, physical strength and quality of finish." (Westgate, Paine and Ball, 2018)

3.3.2 Advanced Aerogel-Based Composite (AABC) material

This material can be applied quite similar to aerogel blankets, but the innovative and effective production method and installation method is quite different.

"1. Introduction

The world energy consumption for building space heating is rising. The need of new materials to decrease the thermal losses is therefore essential. The Advanced Aerogel-Based Composite (AABC) material shows a great potential as a new efficient insulation system solution [1-3]. In an experimental study E. Cuce et al. [4] shows that aerogel insulation system can provide slimmer constructions in buildings with higher mitigation in greenhouse gas emissions compared to the conventional insulation materials.

In the frame of the Horizon 2020 European research program [5], the HomeSkin project [6] aims to develop and introduce on the European market a new silica AABC material with competitive performances compared to current insulations. In order to control the production costs, the new process is fulfilled without the need of the supercritical drying production step. Many efforts were necessary to reach properties that were targeted in the project: ultra-low thermal conductivity and excellent moisture regulation with high water vapor permeability.

This article describes the main steps to produce the new aerogel insulation material and presents its current properties. Thermal conductivity is compared using different kind of matrix materials. The microstructure of the material is analyzed with SEM (Scanning Electron Microscopy) technique. The mechanical properties are tested as well as the vapor permeability of the aerogel material. In order to prove the practical use of this new aerogel insulation, two different systems are actually applied in the FACT [7] facilities of the CEA in France and described in this article.

2. Material and method

2.1. Production process

An innovative process methods used for manufacturing xerogel and insulating composite materials is developed in the frame of the project. The main steps of this production process are represented in the Figure 1. A silica sol obtained by hydrolyzing alkoxysilane in the presence of hydrochloric acid and then adding ammonia, is poured on sheets of melamine foam, Polyethylene terephthalate (PET) fiber, Glass fiber or Needle glass fiber (NGF) introduced in a tailor-made reactor. The thickness of these matrix materials can vary from 7 mm to 30 mm. After gelation, the reinforced alcogel is aged. Hydrophobization agent is then introduced into the chamber. The reaction mixture was then separated from the hydrophobic silica alcogel composite. Finally, the condensed alcogel reinforced by the melamine foam, the PET fiber or the glass fiber is dried in a pilot scale dryer.

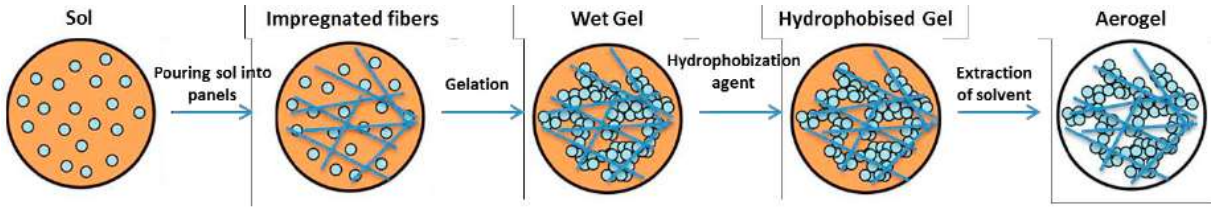

Fig. 1. Description of the process steps to produce silica aerogel panels (inspired form [8]).

2.2. Structural and thermal characterization techniques

The thermal conductivity values were measured on the samples obtained using the guarded hot plate method according to ISO 8301:1991 standard [9] at 23°C, 50% relative humidity and atmospheric pressure. The specimens' dimensions were 300mm by 300mm and thickness of samples were included between 10mm to 30mm.

Water vapor permeability was determined according to EN 12086 [10] and EN ISO 12572 standards [11]. Testing was performed on round samples with a diameter of 80mm. Samples were preconditioned at 23°C and 50% relative humidity prior to testing. For each material "dry-cup-method", for the humidity range from 0% to 50% relative humidity, and "wet-cup-method", for the range from 50% to about 100%, were performed.

Testing of Compressive stress (10% deformation) and tensile strength perpendicular to faces were performed. All samples were preconditioned at 23°C and 50% relative humidity prior to testing. Results are compared to requirements given by product standard EN 13162 for

mineral wool [12] and EN 13500 for External Thermal Insulation Composite Systems (ETICS) [13].

Scanning electron microscopy (SEM) was used to provide information on the microstructure of aerogels. This characterization technique was used to visualize the aerogel matrix and its interaction with the matrix material. The images were taken with a SEM Philips XL30 on representative small cubic samples (10mm by 10mm by 10mm) cut from larger panel. During the sample preparation, a special attention was given not to distort the structure of the aerogel blanket."(Joly *et al.*, 2017)

"3. Results

The described production process allows the production of 300mm by 400mm samples with a maximum thickness of 30mm. In order to improve the insulation physical characteristics, different kinds of matrix were tested: melamine foam, Polyethylene terephthalate (PET) fiber, Glass fiber or NGF.

The produced samples were tested through different kinds of analysis. For insulation material, the thermal conductivity is crucial. The Table 1 shows the measured thermal conductivity of aerogel panel for different kinds of matrix material and density. This physical property is varying as a function of the matrix material as well as a function of the density of the material itself. The initial densities of the used matrix can be rather different. For instance, these densities for PET fibers and NGF are respectively 0.035 kg/m3 and 0.096kg/m3. Adding aerogel material to the matrix leads to an increase of the density and a decrease of the thermal conductivity. The lowest thermal conductivity is reached with melamine matrix with a thermal conductivity lower than 0.014W/(m.K). For PET fiber, Glass fiber and NGF matrices, the thermal conductivity is slightly higher but remains lower than 0.016W/(m.K). For all kind of matrix material, the reached values of the thermal conductivity are competitive with regard to commercial aerogel-based insulating materials, which is currently between 0.015W/(m.K) for the product Spaceloft from Aspen [14] and 0.0190W/(m.K) for the product Aerorock ID from Rockwool [15].

Table 1. Thermal conductivity of aerogel panel for different kinds of matrix material. Density of the samples is indicated.

Composite based (Thickness)	Density ρ [kg/m3]	Thermal conductivity λ [W/(m.K)]
Melamine (10mm)	98.7	0.0137
	101.0	0.0136
PET fiber (13mm)	118.2	0.0148
	116.6	0.0155
Glass Fiber (30mm)	98.0	0.0148
	106.1	0.0151
Needle glass fiber (7mm)	182.5	0.0142
	194.9	0.0156

The Table 2 shows the water vapour resistance factor μ measured for aerogel insulation material. This property is essential to calculate the water vapour fluxes trough the material during winter and summer periods and to estimate the condensation risks. For AABC material, the measured factor varies between μ=4-9. This property can be compared to common insulation materials – mineral wool μ=1, wood fiber insulation μ=1-3, polystyrene (EPS), extruded polystyrene (XPS) and polyurethane foam (PUR) μ=60-150. The water vapour permeability of the developed aerogel composite is thus lower than the vapour permeability of wool and higher than common insulation materials such as polystyrene.

Table 2. Water vapour diffusion resistance factor of aerogel composite.

Composite based	Method	Water vapour diffusion resistance factor μ [-]
Glass Fiber	Dry-cup-method - 23°C, 0/50% RH	8.6
	Wet-cup-method - 23 °C, 50/93% RH	4.1
Needle Glass Fiber (NGF)	Dry-cup-method - 23°C, 0/50% RH	6.1
	Wet-cup-method - 23 °C, 50/93% RH	4.2

The compressive stress (10% deformation) and tensile strength perpendicular to faces were performed with Glass fiber and NGF composite. The results are shown in the Table 3. Comparing these two materials, the compressive stress at 10 % deformation is better for compound with Glass Fiber. On the other hand, the tensile strength perpendicular to faces is significantly better for composite with NGF. These measurements show that aerogel composite with Glass fiber does not fulfill the requirement to be used in external thermal insulation composite systems (ETICS). It was noticed that compound with Glass Fiber had a tendency to delaminate, so that low tensile strength perpendicular to faces for this material is

expected. NGF can be applied in ETICS, but it must be anchored to the main structure. For further characterization tests, NGF was preferred because of its better mechanical properties.

Table 3. Compressive stress and tensile strength measured values for Glass fiber and Needle glass fiber.

Test type	Parameter [kPa]	Test method	Measured value (NGF) [kPa]	Measured value (Glass Fiber) [kPa]	Requirements or classification acc. to EN 13162	Requirements acc. to EN 13500 (ETICS)
Compressive stress (10% deformation)	σ10	EN 826 [16]	38.6	58.5	Value >30kPa (CS(10)30); value >50kPa (CS(10)50)	>10kPa
Tensile strength perpendicular to faces	σT	EN 1607 [17]	15.2	0.8	Value >15kPa (TR15); min. load level 1 kPa	Fixing: - adhesive ≥80 kPa - anchors ≥7.5 kPa - anchored grid ≥5 kPa

During the optimization process, selected samples were characterized by SEM. The Figure 2 shows typical images resulting from back scattered electron analysis. This technique allows the visualization of the fibers of the glass wool and the silicium aerogel grains. These images show on one side the aerogel composite obtained with Glass fiber and on the other with Needle glass fiber. For the glass fiber matrix, the size of the aerogel granulate microstructure varies between 10 to 200µm. This picture indicates air gaps of 50-200µm between the aerogel grains. For the Needle glass fiber, the aerogel grains are much smaller and the air gaps between the grains decrease as well. This observation is in good agreement with the density measurements, shown in Table 1, where the Needle glass fiber can be twice as dense as Glass fiber aerogel composite.

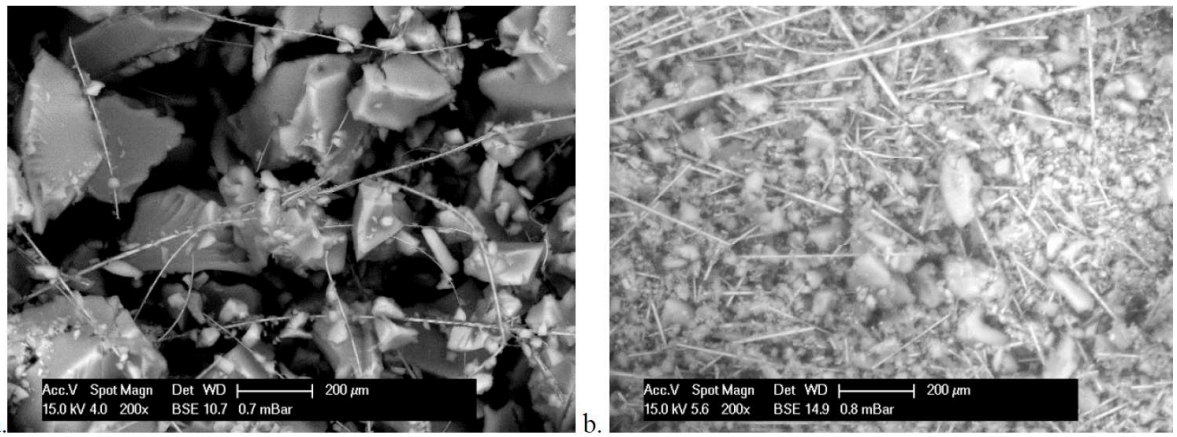

Fig. 2. SEM characterization of aerogel. AABC materials with Glass fiber matrix on the left and Needle glass fiber on the right. “

(Joly *et al.*, 2017)

“Conclusion

In the frame of the h2020 horizon program, the Homeskin project has developed a new family of AABC material which has been tested and applied in real size facilities. The produced aerogel material shows competitive properties with a thermal conductivity below 0.016W/(m.K). The microstructural analysis shows a structure composed of fibers, coming from the matrix, and aerogel grains. This superinsulation material is produced with a simplified production process which should reduce production costs and allow HomeSkin product to be competitive on the current European superinsulation market.

To show feasibility and measure in-situ hygrothermal behaviors of the new material, AABC are tested in an experimental facility. These ongoing measurements will be used to eventually validate the data obtained by numerical simulations."(Joly *et al.*, 2017)

3.3.3 Flexible and Transparent Silica Aerogels

Parale, Lee and Park, 2017 list some applications for Flexible and Transparent Silica Aerogels.

"Thermal Insulation Applications of Flexible Aerogels

Flexible aerogels are promising materials for a variety of thermal insulation related applications, such as building insulation, cryogenics, and vacuum insulation. [133,134)] The

properties, such as high surface area, sharp pore size distribution, very low thermal conductivity, high flexibility, and transparency, can make these materials useful for different industrial and energy related applications. An overview of the important properties of some reported flexible silica aerogels is given in Table 2. The application of flexible and transparent aerogels in buildings as well as in cryogenic insulation is explained in the present section.

4.1. Building insulation

For building insulation, due to their low thermal conductivity and high temperature insulation performance, flexible and transparent silica aerogels are an alternative to traditional insulation materials. Reports are available on the application of transparent aerogels for daylighting purposes in new buildings.[135)]

Recently, Aspen Aerogels, Inc., developed an aerogel based insulation material that is known as Spaceloft®.[136] This is a flexible aerogel blanket with room temperature thermal conductivity of approximately 0.013 W/m·K. In daylighting and solar energy applications, due to their transparent nature, aerogels are applicable. For this purpose, research on the development of highly insulating aerogel windows has been conducted over the last decade. In one European Union project named HILIT,[3] monolithic aerogelbased windows were developed with a combination of vacuum glazing technology and the application of 1 to 10 mbar pressure. The prepared 13.5 mm aerogel glazing showed an overall heat loss coefficient Uwindow of 0.66 $W/m^2 \cdot K$ and solar transmittance TSOL of more than 0.85. Also, to allow for high thickness of the aerogel glazing, the heat loss coefficient was decreased, while a solar transmittance was observed. Cabot Aerogel commercialized two aerogel products, Nanogel™ and Okagel.[136] In 30 and 60 mm samples, Okagel has thermal conductivity of 0.018 W/m·K and heat transmittance coefficients between 0.6 and 0.3 W/m2·K, respectively." (Parale, Lee and Park, 2017)

3.4 High-Performance Thermal Insulation Materials

During the last years there has been a tremendous research and development on High-Performance Thermal Insulation Materials but there is still challenges in order to develop promising insulation systems for the building industry that can be applied in big commercial and industrial scale.

Thermal insulation concrete is experiencing fierce competition from stand-alone systems where the insulation materials are not mixed within the concrete, but are used as internal, intermediate or external layers.

Gangsåssæter *et al*,2017 are presenting a study that concern two of these potential solutions:

"State-of-the-art thermal insulation solutions like vacuum insulation panels (VIP) and aerogels have low thermal conductivity, but their drawbacks may make them unable to be the thermal insulation solutions that will revolutionize the building industry regarding energy-efficient building envelopes. Nevertheless, learning from these materials may be crucial to make new and novel highperformance thermal insulation products. This study presents a review on the state-of-the-art air-filled thermal insulation materials for building purposes, with respect to both commercial and novel laboratory developments. VIP, even if today's solutions require a core with vacuum in the pores, are also treated briefly, as they bear the promise of developing high-performance thermal insulation materials without the need of vacuum. In addition, possible pathways for taking the step from today´s solutions to new ones for the future using existing knowledge and research are discussed. A special focus is made on the possible utilization of the Knudsen effect in ail-filled nanopore thermal insulation materials." (Gangassaeter *et al.*, 2017)

"4 Thermal insulation materials

Materials used as thermal insulation in buildings try to benefit from solutions that create products with low thermal conductivity. This can be achieved by reducing one or several of the contributions shown in Eq.1. In mineral wool, i.e. glass and rock wool products, such a reduction is achieved by bounding fibres together with the use of suitable resins, hence creating complex pore structures with limited/obstructed ways for heat transfer through the material [7]. Manufacturers have come a long way in creating porous materials with low

thermal conductivities, e.g. mineral wool products with thermal conductivity values down to 32 mW/(mK).

The drawback with these materials appear together with the higher requirements to thermal insulation in buildings. For example, to achieve a U-value of e.g. 0.22 W/(m2K) (minimum requirement for wall insulation in Norway per 26th of November 2016 [8]) with a standard mineral wool material, a thickness of approximately 150 mm is needed. For low-energy or zero emission buildings the requirements are even lower U-values. This may result in an insulation layer of more than 250 mm in thickness, which hence takes up valuable space and introduces challenges with convection between the wind and vapour barrier enclosing the insulation layer.

An increased research in the field of thermal building insulation materials have resulted in new materials with better performance in some areas. Aerogels and VIP are examples of materials that have noticeably lower thermal conductivity values [7].

4.1 Aerogels

Aerogels were discovered in 1931 by Samuel S. Kistler and are a silica gel where all the liquid components are replaced by air through a complex drying process. The remaining material creates a nanoporous structure with low thermal conductivity [9]. The solid thermal conductivity of silica is relatively high, but the silica aerogel has only a small fraction of solid silica. With a good purity and production method pore sizes of 5 to 70 nm are possible, where the air-filled pores will take up between 85 to 99.8% of the volume [4]. Pure aerogels have a low thermal conductivity typically between 12-20 mW/(mK).

Aerogels are constantly being developed, both regarding the production process and the final material product itself. Challenges with the material for building purposes have been inherent low density and thus high fragility, which complicates the handling process without fracturing the aerogel products. Therefore numerous different composites have been made in order to create a more robust material [10]. Mineral wool and aerogel have been mixed, with a resultant thermal conductivity of 19 mW/(mK) [7]. Hayase et al. report a development of another composite aerogel with a density of 20 kg/m3 and a thermal conductivity of 15 mW/(mK) [11]. Also note that as aerogels may be produced as either opaque, translucent or transparent materials, these products may be used for several different building applications,

e.g. in opaque walls, translucent solar walls or glazing systems and transparent windows or glazing systems. Table 1 gives an overview of the findings of several different variants of aerogels and their characteristics.

Table 1. Examples of aerogels, listed with important characteristics.

Aerogel	Density (kg/m³)	Thermal conductivity (mW/(mK))
Stone wool and aerogel [7]	-	19
Polymethylsilsesquioxane-cellulose nanofibre bicomposite aerogels [11]	20	15
Aramid fibre reinforced silica aerogel [10]	150	22.7
Monolithic silica aerogels [12]	-	≈ 13

4.2 Vacuum insulation panels

Vacuum insulation panels (VIP) consist of a multilayer envelope that encloses an open-porous material, also known as the VIP core. To increase the thermal resistance of the panel, vacuum is formed inside the core [7]. The core material could consist of glass fibre, open-cell polyurethane foam, open-cell polystyrene foam, precipitated silica or aerogel. For achieving the lowest thermal conductivity, precipitated silica, fumed silica or aerogel should be used [13]. Numerous VIP are produced, and many of them can be purchased on the market from various suppliers [14].

VIP have several challenges that may make it difficult for them to become the thermal insulation material of the future. One of the main disadvantages is to keep the vacuum intact. This makes it hard to adapt panels at the building site, and the risk of punctures is always present. Thus, the VIP must be handled carefully [15]. Furthermore, the VIP envelope creates a thermal bridging effect [16]. A solution to reduce this problem is to put double, overlapping layers of panels, but this creates more work and higher material usage. Another problem with the envelope is that it is not absolutely air and vapour tight, thus air and water vapour will diffuse into the core as time passes, hence reducing the insulation performance substantially over time. Research is being carried out on how to create better envelopes with respect to the tightness. However, for most of these there will still be a diffusion process of air and water vapour through the VIP envelope and into the VIP core, which may be decreased but not fully stopped.

If the panel is perforated, the core material will still have a rather low thermal conductivity, i.e. VIP with an airfilled fumed silica core will have a thermal conductivity of around 20 mW/(mK). Note then that the difference between 4 mW/(mK) (pristine condition) and 20

mW/(mK) (punctured) of 16 mW/(mK) is due entirely to gas thermal conductivity (not considering any changes to the solid due to loss of vacuum). That is, the combined solid state and radiation thermal conductivity of fumed silica is as low as 4 mW/(mK) or in principle lower (as there is still a very small concentration of air inside a VIP, a small part of the 4 mW/(mK) value is due to gas conduction). Hence, as it is possible to make materials with such a very low solid state and radiation conductivity, lowering the gas thermal conductivity should be a good opportunity to make an air-filled nanopore based high-performance thermal insulation material at atmospheric pressure." (Gangassaeter et al., 2017)

3.5 New Type of Prefabricated Concrete Sandwich Wall Panel

Prefabricated concrete sandwich wall panels have been widely used for more than 30 years, but have been restricted to 3-4 story building due to lack of axial stress capacity. Xie Qun et al (2018) have recently presented remarkably positive results for axial strength for a new type of prefabricated concrete Sandwich wall panel by applying 3D slender and flexible steel armoring to the concrete.

"1. Introduction

Concrete sandwich panel is a widely used prefabricated wall element in residential and office buildings which is usually composed of two concrete layers separated by an insulation layer. Within each concrete layer there is a steel wire mesh and a serial of continuous rebar trusses as transverse connectors running along the full height of panel are adopted to attach concrete layers together which could provide resistance to horizontal shear. Sandwich panel has several advantages such as light self-weight, heat insulation and fast erection [1]. The sandwich wall panel system was initially developed and manufactured as non-load-bearing cladding or compartment elements in office building in U.S in the 1990s. Since the sandwich panels exhibit fully comparable performance to those of precast concrete solid panels, an interest in sandwich panels using as load-bearing structural elements in low-story buildings has been observed in the past decade years. A. Benayoune [2] has investigated the behavior of

precast concrete panels subjected to eccentric compressive load and the results show that the load-bearing capacity of panels will nonlinearly raise with the increase of height-to-thickness ratio. Finally a semi-empirical formula has been proposed for strength prediction. Junsuk Kang [3] has adopted FEM method to study the structural performance of concrete sandwich panel with foam insulation under axial compression. Fabrizio Gara [4] has illustrated experimentally and numerically both the flexural and compressive behavior of fabricated sandwich panels without shear connectors. The aim is to determine the behavior of panel with different slender ratios under the axial and eccentric load. The result indicate that the strength of panels will decrease with the increase of slender ratios. With the development of housing industrialization and prefabricated building construction in China recently, some studies have been carried out on the structural behavior of concrete sandwich panel currently. Mohamad N [5, 6] has used foamed concrete as an alternative material to produce a new type of precast sandwich panel and a double symmetrical truss-shaped connectors are employed in this panel. The experimental and theoretical results of axial and eccentric compression show that the slender ratio H/t has significant effect on the axial behavior of panel. Compared with the panel with single connectors the panel with double connectors presents better compressive strength and ductility. Olsen M D [7] has investigated the structural performance of concrete sandwich panels with carbon fiber connectors and the results show that the carbon fiber connector can effectively minimize the influence of thermal bridge due to its excellent property of heat isolation. Woltman G D [8] has adopted glass fiber reinforced polymer (GFRP) connectors as an alternative to metallic connectors and the load-slip behavior of sandwich panel has been established through a serial of shear tests. Hopkins P [9] has developed an innovative fiber reinforced polymer (FRP) shear plate connector and studied its effects on the flexural behavior of insulated concrete sandwich panels in terms of stiffness, strength, and applicability for constructions. Liew J Y R [10] has proposed a new concept for designing composite structures comprising a lightweight concrete core sandwiched between two steel plates which are interconnected by J-hook connectors. Tests confirms that the shear transfer capability of J-hook connector is superior to the conventional headed stud connector.

Based on the existing research results, as a structural system traditional sandwich panels are only employed in buildings with three stories below due to the limitation of load-bearing capacity, stiffness and connection type. In order to the possible application for multi-story buildings even high-rise buildings, a new prefabricated sandwich panel has been presented in this work, compared with the common sandwich panels, there are several typical

characteristics for this new panel which includes core columns confined by spiral stirrup along the panel cross-section with 600mm spacing, foamed concrete block between external structural layers as internal insulation layer, and self-compact fine aggregate concrete applied in external layers with high flow performance. To improve the strength and stiffness of panels, a 3D steel wire skeleton in each layer which is composed of two vertical steel mesh connected with horizontal steel bar has been employed. A detailed configuration of panel is shown in figure 1. All steel elements of this panel are mechanically and automatically manufactured in factory, then transported to construction site for the overall steel skeleton assembly. Concrete in layers and core columns is needed to be casted in site. The thickness of concrete layer is adjustable according to the strength requirement of structural system and the existence of 3D steel wire skeleton and core columns is expected to contribute to greatly enhance the structural performance of panel. A test of full-scale specimens subjected to axial compressive load has been carried out in order to understand the actual behavior of this new sandwich panel." (Qun, Shuai and Chun, 2018)

"2. Test program

With the purpose of performance comparison, two full-scale panels are designed with same height and width but different panel thickness, wire diameter as well as steel wire type, for specimen ZY1 planar steel wire mesh is used in concrete layers while a 3D steel wire skeleton is employed for specimen ZY2. The compressive strength of concrete is 36.8 MPa and the yield strength of rebar is 417 MPa. The detailed information of specimens is shown in table 1.

Table 1. Specimens information (unit:mm).

No.	Height	Width	Thickness Concrete layer	Insulation thickness	Total	Steel wire mesh	Diameter of steel wire	Slenderness ratio	Reinforcement ratio
ZY1	2400	1300	25	60	110	planar	3	21.8	1.17%
ZY2	2400	1300	40	60	140	three-dimension	2	17.1	0.97%

All the specimens are vertically installed with an unconstrained end on the top and a fixing end on the bottom. Two 2500kN hydraulic jacks are setup at the top beam of specimen whose function was to transmit the centralized load to a uniformly distributed load along the full width of specimen. The axial load has been applied monotonically with a constant increment of 50kN. A lateral support system consisting of a serial of 50mm-diameter solid steel rollers

and 20mm-thick steel angles is installed close to the side face of top beam to restrain lateral movement. The test setup is presented in Figure 2.

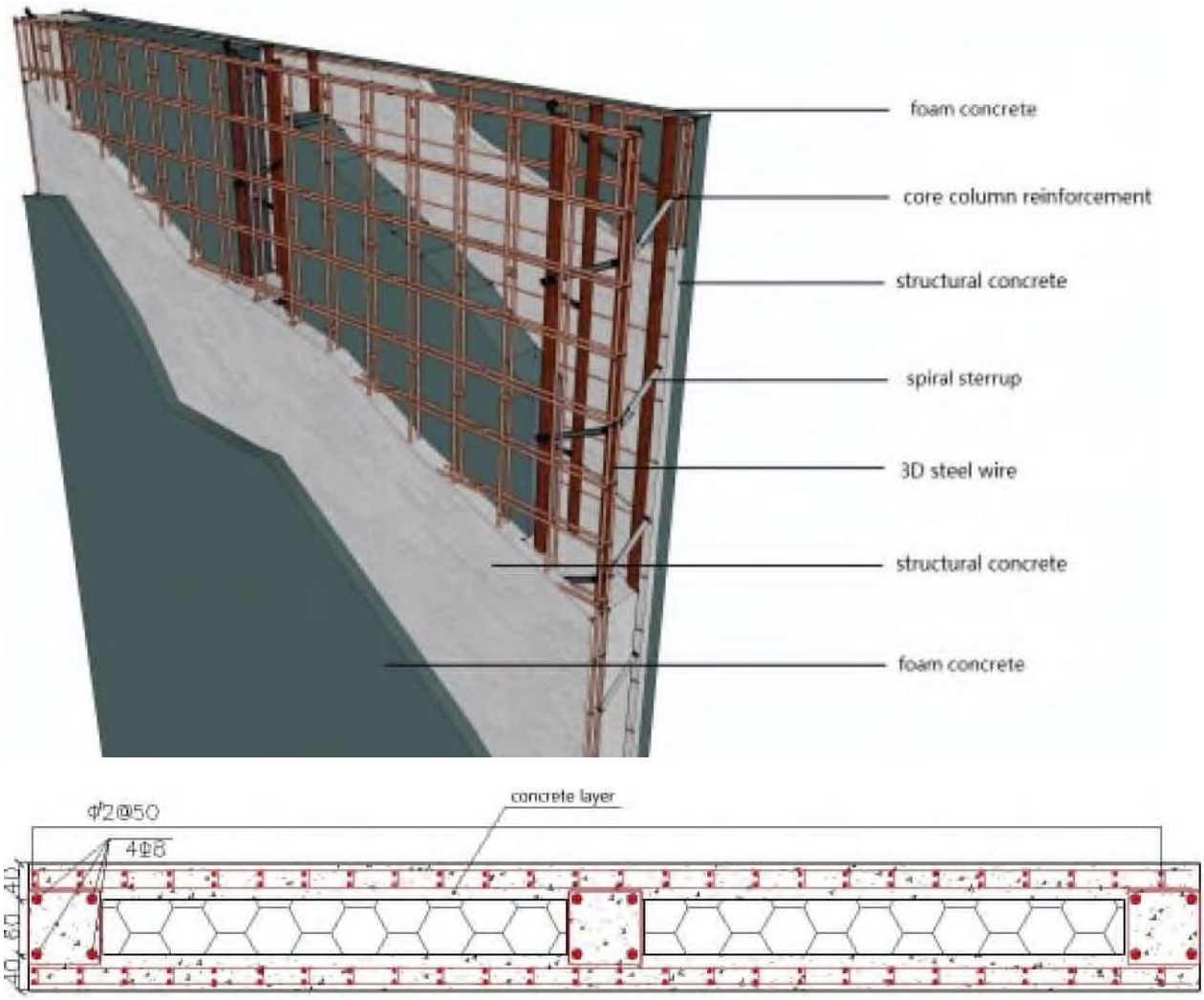

Figure 1. Section of the new fabricated sandwich panel.

Figure 2. Test setup. ” (Qun, Shuai and Chun, 2018)

“3. Experimental results

In the early stage of loading, the strains for both steel reinforcement and concrete have a linear increase with the growth of load, and the vertical and horizontal displacements slowly develop within a very small value. For ZY1 the first visual crack occurs in the mid-height of panel under the axial load of 1060 kN. Under load of 1280 kN another inclined crack appears at the corner of panel bottom which develops obliquely upwards following the load increment. With the increase of axial loads, several new cracks vertically occur in the middle of panels and the existing diagonal cracks extend and widen quickly. At the ultimate load of 1420kN a sudden failure occurs with a main vertical crack almost thorough the panel height. The specimen ZY-2 had similar structural performance with ZY-1 in the process of loading. The peak strength was 4280 kN with severely local concrete crush in the top of concrete layer. For two specimens there were no massive cracks found in the surface of panel even in the ultimate state. The main test results were listed in table 2.

Table 2. Experimental results.

Specimen No.	ZY-1	ZY-2
Crack load	1060 kN	4000kN
Ultimate load	1420 kN	4284kN
Maximum lateral displacement	3.2mm	8.9mm
Failure mode	Vertical through crack	Local concrete crush

4. Results analysis

4.1. Load-deformation analysis

The lateral deflections obtained from the data of five LVDTs along the specimen height under axial load have been presented in figure 4. For ZY-1 the lateral deflections approximately kept a linear growth in the initial loading stage. While the load exceeds 800kN lateral deformation began to develop towards inverted direction since the excessive displacement of panel top triggered the restriction function of lateral bracing system. After then with the load increased, the lateral displacement at HD5 which is near the bottom end of panel gradually decreased back to zero in the final failure, while the displacement at HD1 which is near the loaded end of panel developed much faster than other measured points. The farther distance away from the panel top, the less lateral displacement was expected which could be attribute to the second-order effect. Similar to the deformation characteristic of ZY-1, the load-lateral deflection curves of ZY-2 developed almost elastically in the early stage of loading.

Compared with ZY-1, the curves of ZY-2 measured at different positions show a monotonic development towards one direction mainly due to the smaller slenderness ratio.

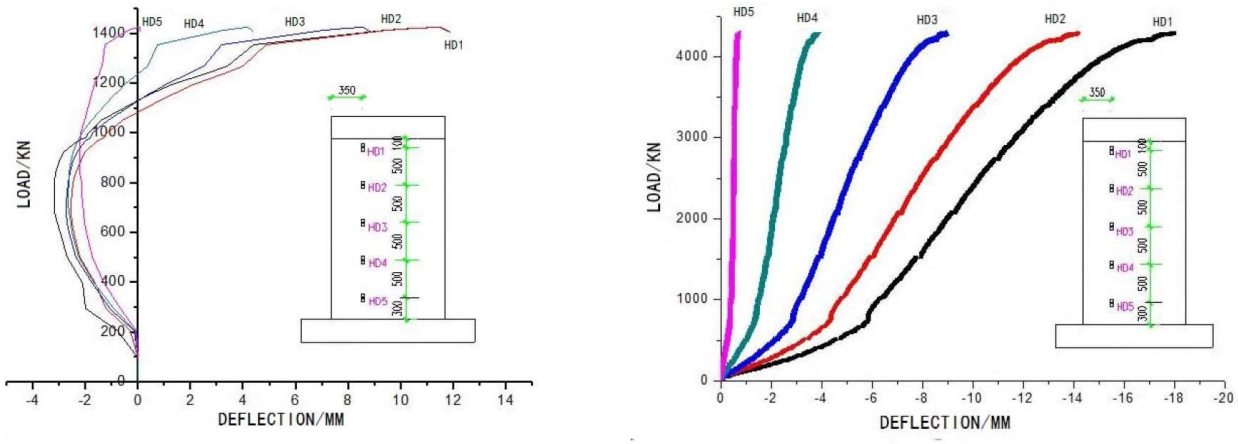

(a) ZY-1 (b) ZY-2

Figure 4. Load-lateral displacement curves.

4.2. Load-strain analysis

The load-concrete strain curves of ZY1 were presented in figure 5 (a). There are two measured points in the mid-height of specimen and one at the bottom corner. All the data recorded by concrete strain gauges indicated that the full cross-section of specimen was in compression. However due to the lateral flexure caused by high slenderness ratio even under the axial compression, there actually were a concrete layer of specimen in the combined action of tension and compression and another layer in pure compression. Based on this

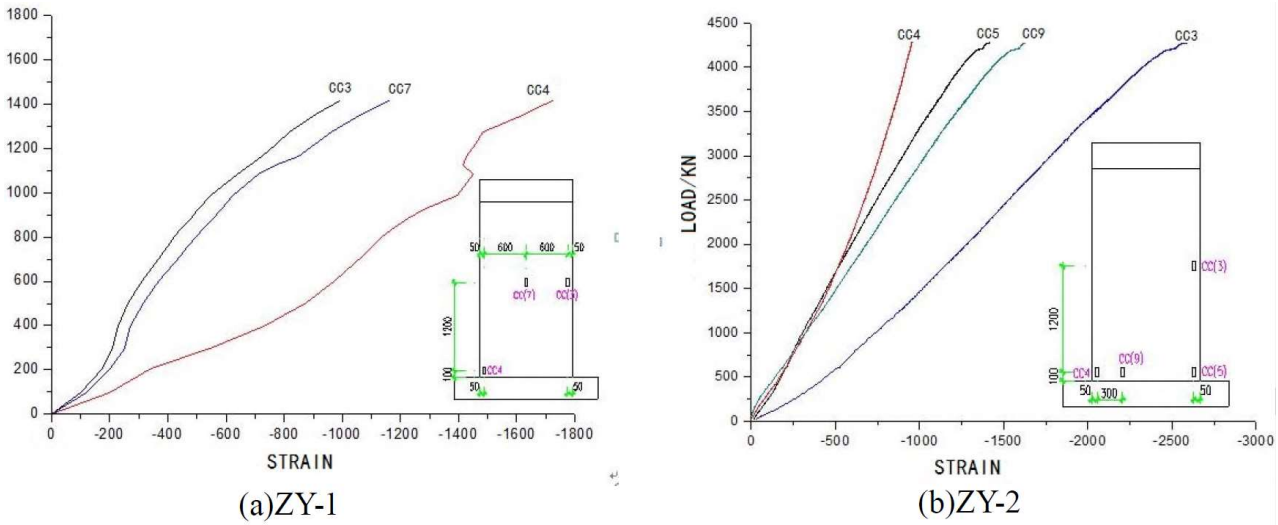

(a)ZY-1 (b)ZY-2

Figure 5. Load-concrete strains curves.

analysis, the strains of CC3 and CC7 in tensile layer had smaller values than that of CC4 in compressive layer under the same axial load. All concrete strains developed within relatively

small values during the loading program and the peak strains is about 1500με which was much lower than the ultimate compressive strain of concrete. In figure 5 (b) there were four load-concrete strain curves for different measure points of ZY2. Compared with ZY1, the growth of concrete strains in ZY2 was almost proportional to the increment of axial load. The strain linearly developed up to 4000με and much exceeded the ultimate concrete strain in uniaxial compression which verified that the excellent confinement of 3D steel skeleton system.

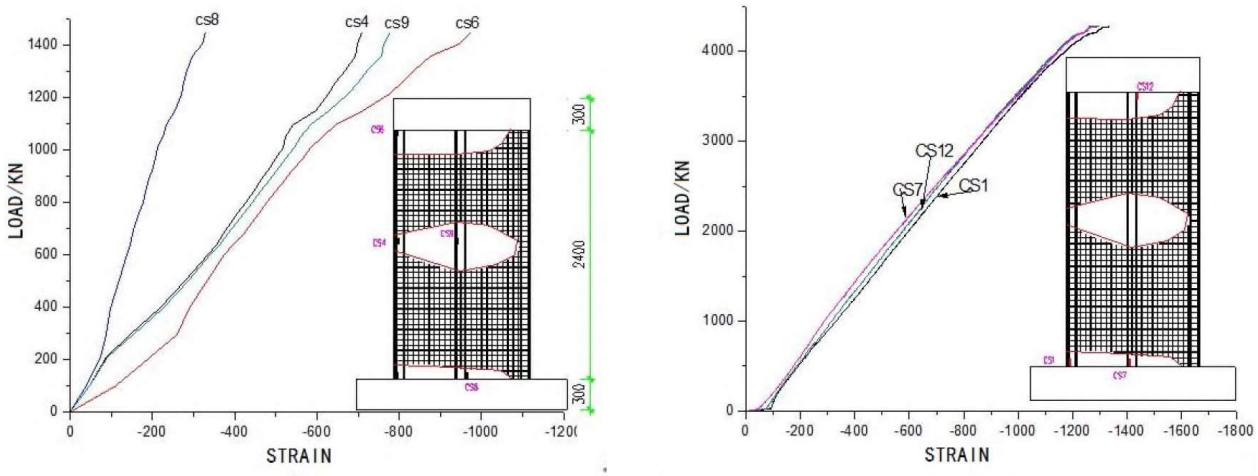

(a)ZY-1 (b)ZY-2

Figure 6. Load-reinforcement strains curves.

5. Conclusions

The structural behavior of a novel prefabricated sandwich panel under axial load has been experimentally investigated in this work. Some conclusions could be drawn as following:

1) A brittle failure occurred with a main vertical crack almost thorough the full height for specimen ZY-1 and severe local concrete crush in the panel top appeared in the final state for specimen ZY-2. No massive cracks were found in the surface of panels during the whole process of loading.

2) Compared with ZY-1 with planar steel wire mesh, the specimen ZY-2 with 3D steel wire skeleton presented better structural performance with greatly higher strength and robustness due to the smaller value of slenderness ratio even with less reinforcement ratio.

3) The lateral deflections almost kept a linear growth in the initial loading stage and due to the existence of core columns there was no obvious out-of-plane

deflection generally seen in traditional sandwich panel subjected to axial compression. The strain curves both for concrete and reinforcement approximately presented a proportional growth with the development of axial load." (Qun, Shuai and Chun, 2018)

3.6 Essential properties

Samson, Phelipot-Mardele and Lanos (2017) have made an impressive compilation of results which contains the most essential data for this thesis. An illustration of the table (which is not ment to be readable) is shown below:

"

Reference	Composition[a]	Production process[b]	OPC content: kg/m³	w/c (or w/b) ratio	Paste density: kg/m³	Apparent density: kg/m³	Compressive strength: MPa	Compressive strength test, dimensions (in mm) and age	Thermal conductivity: W/(m.K)
Neville (2011)	Various	LA, GF, PS	Various			300–1850	0·3–70	Cubic, 28 d	0·1–0·65
Othuman Mydin (2010)	OPC, S, surf (protein)	PF		w/c = 0·5 w/b = 0·33	800	650–1850	3·2–15·3	Cylindrical 28 d	0·226–0·484
Aamr-Daya *et al.* (2008)	OPC, LA SP, surf	LA		0·3 < w/c < 0·55	1955–1370	1560–985	10·5–32	4 × 4 × 16	
Anwar Hossain (2004)	OPC, LA, S	LA	430–490	w/c = 0·45	Spreading	1831–2515	24–40	Cubic 28 d	
Demirdag and Gunduz (2008)	OPC, LA	LA	41–162	2 < w/c < 10	1254–1505	1185–1472	0·49–8·48	Cubic 28 d	0·44–0·65
Schackow *et al.* (2014)	OPC, LA, S, surf (Microair®), SP	LA		0·5 < w/c < 1·10		1070–1290	6·31–15·55	Cubic 28 d	0·34–0·56
Sengul *et al.* (2011)	OPC, LA, S, surf, SP	LA	295–317	w/c = 0·55	696–2015	392–1992	0·1–28·8	Cubic 28 d	0·13–0·6
Chen and Liu (2013)	OPC, SF, high alumina content cement, polypropylene fibres, LA, SP, surf	LA	1230	w/c = 0·26	395–810	400–800	1·58–11	Cubic 28 d	0·07–0·3
Kayali (2008)	OPC, FA, LA, SP	LA	300–370	0·56 < w/c < 0·64	1722–2280	1602–2290	44·6–66·75	Cubic 28 d	
Bumanis *et al.* (2013)	Several cements, LA	LA		w/c = 0·5	734–781	490–555	2·8–4	4 × 4 × 16 28 d	
Nguyen *et al.* (2014)	OPC, S, G, LA	LA	426	w/c = 0·45		1170–2030	22·2–45·3	Cylindrical 28 d	0·43–1·6
Uysal *et al.* (2004)	OPC, LA	LA	200–500		Spreading	1970–2040			0·776–1·458
Liu *et al.* (2014)	FA, oil palm shell, SP	LA	0			1291–1791	8·3–30·1	Cubic 28 d	0·47–0·49
Lo *et al.* (2004)	OPC, FA, LA	LA	338–420	0·54 < w/c < 0·56	Spreading	1617–1851	29·19–38·58	Cubic 28 d	
Cui *et al.* (2012)	OPC, S, LA	LA		w/c = 0·35			18·9–59·1	Cubic + Cylindrical 28 d	
Haque *et al.* (2004)	OPC, LA	LA	280–536	0·42 < w/c < 0·80	Spreading	1775–2355	38–57	Cubic 28 d	
Bogas and Gomes (2013)	OPC, LA, S, SP	LA	300–594	0·3 < w/c < 0·55	Spreading	1494–2358	28·1–81·6	Cubic 28 d	
Ke (2008)	OPC, S, SF, LA, SP	LA	414–826	0·29 < w/b < 0·46	1605–2156	1453–2107	24·91–85·93	Cylindrical 28 d	
Gencel *et al.* (2014)	G, polypropylene fibres, LA	LA	0	w/b = 0·65		890–1010	1·98–3·56	Cubic 28 d	0·42–0·55
Serhat Baspinar and Kahraman (2011)	G, LA	LA	0	w/b = 0·5		890–1130	2·38–3·21	Cubic	0·16–0·31
San-Antonio-González *et al.* (2015)	G, LA	LA	0			690–980	1·47–5·64	4 × 4 × 16 7 d	0·088–0·141
Jiménez Rivero *et al.* (2014)	G, LA	LA	0	0·7 < w/b < 0·76		560–1090	0·70–13·36		
Cherki *et al.* (2014)	G, LA	LA	0	w/b = 0·7		446–803			0·098–0·302
Gutiérrez-González *et al.* (2012)	G, polyamide powder	LA	0	0·4 < w/b < 0·5		751–1477	1·47–15·64	4 × 4 × 16 28 d	
Yu and Brouwers (2012)	G, LA, SP	LA	0	0·6 < w/b < 0·75	Spreading	690–800		4 × 4 × 16	0·12–0·15
Dolton and Hannah (2006)	OPC, FA, surf	MF				400–600	0·71–1·98	Cubic	0·075–0·097

Table 1. Review of LC composition, fresh paste density and thermomechanical properties (continued on next page)

" (Samson, Phelipot-Mardele and Lanos, 2017)

The table continues on the next page, and it is also further extended in this thesis in Appendix 1, with other findings featured in this thesis. For a readable version, please see Appendix 1.

“

Reference	Composition[a]	Production process[b]	OPC content: kg/m³	w/c (or w/b) ratio	Paste density: kg/m³	Apparent density: kg/m³	Compressive strength: MPa	Compressive strength test, dimensions (in mm) and age	Thermal conductivity: W/(m.K)
Tikalsky *et al.* (2004)	OPC, FA, S, surf	PF	57–629	0·40 < w/b < 0·57		497–629	0·71–1·77	Cubic 28 d	
Cabrillac *et al.* (2006)	OPC, L, S, surf	GF		0·4 < w/c < 0·45				Cubic 28 d	
Yang and Lee (2015)	OPC, SF, G, SP, surf	PF	400–650	0·2 < w/c < 0·3	Spreading	491–694	2·4–6·9	Cubic 3, 7 and 28 d	0·118–0·199
Just and Middendorf (2009)	OPC, aluminium powder, SP, SF	GF		0·45 < w/c < 0·6	Spreading	450–1300	2–24		
Kearsley and Wainwright (2001a)	OPC, FA, surf (protein)	PF	193–1620	0·3 < w/c < 1·17 0·3 < w/b < 0·6		1000–1500	5·8–85·7	Cubic 28 d	
Jones and McCarthy (2006)	OPC, FA, S, SP, surf	PF	210–600	0·32 < w/c < 0·58		610–1230	1–6·8	Cubic 28 d	
Awang *et al.* (2012)	OPC, S, FA, L, polypropylene fibres, surf	PF		w/b = 0·45	700–1530	600–1400	0·3–11·8	Cubic	0·35–0·6
Bogas *et al.* (2013)	OPC, FA, S, SF, LA, surf, SP	LA	300–525	0·3 < w/b < 0·65		1458–2430	25·2–81·6	Cubic 28 d	
Aldridge (2005)	OPC, S, FA, SF, surf	PF				400–1600	0·5–10		0·1–0·64
Panesar (2013)	OPC, S, three surfs (one protein, two synthetic)	PF	361–611	w/c = 0·29	Spreading	1600–2240	2–58	Cylindrical 28 d	0·78–1·1
Kearsley and Wainwright (2002)	Fast-setting Portland cement, FA, surf (protein)	PF	320–1000	0·3 < w/c < 1·17 0·3 < w/b < 0·6		772–1972	5·8–85·7	Cubic 365 d	
Nambiar and Ramamurthy (2007)	OPC, S, FA, surf (organic)	PF				600–1200	1–15		
Visagie (2000)	OPC, FA, surf	PF		0·3 < w/c < 1·6 0·27 < w/b < 0·33		536–1235	1–24·2	Cylindrical 28 d	
Wei *et al.* (2013)	OPC, FA, SP, surf (protein)	PF	80%	w/c = 0·32 w/b = 0·18		252–1870	0·42–45·5		0·065–0·50
Vimmrová *et al.* (2011)	G, OPC, calcium carbonate, LA, microsilica, surf	LA and GF		0·53 < w/b < 1·07		547–945	2–12	4 × 4 × 16	0·12–0·39
Çolak (2000)	G, marble powder, aluminium sulfate, aluminium potassium, surf	LA and GF	0	0·55 < w/b < 85		756–1086	0·35–2·2	Cubic	
Yang *et al.* (2013)	OPC, G, OPC, L, ground granulated slag, sodium sulfate, aluminium powder	GF	15–45%	0·43 < w/b < 0·55		590–740	2·2–6·4	Cubic 28 d	
Umnponpanarat and Wansom (2015)	G	GF	0	0·6 < w/b < 0·7	Spreading	640–1200	0·72–11·44	Cubic	0·188–0·498

[a]OPC, ordinary Portland cement; LA, lightweight aggregate; L, lime; FA, fly ash; SF, silica fume; S, sand; G, gypsum; F, filler; SP, superplasticiser; surf, surfactant;
[b]LA, lightweight aggregate; GF, gas-foaming method; MF, mix-foaming method; PF, pre-foaming method

Table 1. Continued

” (Samson, Phelipot-Mardele and Lanos, 2017)

“The utilization thermal insulation of building becomes a great potential to reduce the building thermal load and consequently its energy consumption especially in hash weather [1]. Thus, thermal insulation systems lead to improvement of economical aspects of buildings due to increased awareness and increased electric energy tax. Insulation materials can be made in different forms including loose-fill form, block form, board form,blanket form, pipe form, rigid form, foamed in place, or reflective form [2]. The choice of the proper insulation material form and type depends on the type of application as well as the desired material physical, thermal and other properties. Thermal insulation materials, like other natural or synthetic materials which exhibit temperature dependence properties that vary with their characteristics and the influencing temperature range [3]. Thermal insulation are very important in a wide variety of scientific and industrial applications especially building construction where a number of different experimental techniques have been developed to

measure the thermal conductivity for different experimental conditions and for different materials in concrete.

Concrete generally exhibits good fire resistance properties and thus finds wide applications in buildings and other built infrastructures, where fire safety is one of the primary considerations.The properties of concrete that are needed for fire-resistanceanalysis are thermal, mechanical, deformation, and special properties. Thermal properties are mainly determined by thermal conductivity, specific heat, thermal diffusivity, thermal expansion, and mass loss.Thermal conductivity is defined as the ratio of heat flow rate to the temperature gradient, and represents the uniform flow of heat through concrete of unit thickness over a unit area subjected to a unit temperature difference between the two opposite faces.The thermal conductivity value of normal concrete ranges from 0.62 to 3.3 W/m/K across more than five folds of magnitude depending on the types of coarse aggregate, moisture condition and temperature [4-7]. However, the lightweight insulating concrete with polystyrene bead or cellular lightweight concrete even exhibits the thermal conductivity of 0.07 to 0.33 W/m/K[8]. Specific heat is the amount of heat per unit mass required to change the temperature of a material by 1°, and is generally expressed in terms of thermal (heat) capacity, which is the product of specific heat and density. Specific heat is highly influenced by moisture content, aggregate type, and density of concrete [9-11]. This aim of this paper is to review significant research in thermal insulation performance in concrete application." (Shahedan *et al.*, 2017)

"Since the beginning of the millennium the requirements for the thermal insulation of residential and nonresidential buildings have led to a number of developments in the field of building materials for massive outer walls. To fulfil the requirements of national regulations resulting from the EU-directive on the energy performance of buildings [1] for the heat transfer coefficient (such as the U-value in the German Energy Saving Ordinance 2014 [2]), only masonry blocks with low bulk density can be used for single-leaf walls. The thermal conductivities of such heat insulation masonry are in the range $\lambda = 0.06$ W/(mK) to $\lambda = 0.16$ W/(mK) (Table 1, lines 1-6), so that in general wall thicknesses between 36.5 cm and 49 cm are necessary to achieve the required U-values.

Table 1. Bulk densities, thermal conductivities and compressive strength of selected massive wall-building materials.

	Material	ρ (kg/m³)	f_k / $f_{(l)ck}$ (MPa)	λ (W/(mK))
1	Light-weight Concrete Block Bisomark Hbn [3]	315-335	0.8	0.06
2	Aerated Cement Block Ytong PP 1,6-0,25 [4]	250	0.8	0.07
3	Poroton Brick S9-MW [5]	810-900	4.2	0.09
4	Aerated Cement Block Ytong PP 2-0,40 [4]	400	1.8	0.10
5	Light-weight Concrete Block Bisoplan 14 [3]	600	2.5	0.14
6	Poroton Plane Brick T16 [5]	710-800	4.7	0.16
7	Sand-lime Brick Silka KS L-R P 12-1,4 [6]	1210-1400	5.6	0.56-0.70
8	Light-weight Aggregate Concrete LC35/38 [6]	1500-1600	35.0	0.89-1.00
9	Sand-lime Brick Silka KS-R P 20-2,0 [6]	1810-2000	10.5	0.99-1.10
10	Normalweight Concrete C12/15 [7]	2200-2400	12.0	1.65-2.0
11	Reinforced Concrete C30/37 [7]	2300-2400	30.0	2.3-2.5

As it is apparent from Table 1, the characteristic compressive strength of these materials, which are optimized in respect of a low thermal conductivity, is in the range fk ≤ 4.7 MPa. Therefore multi-story buildings cannot be erected with these materials even if the wall thickness is high. Thus, if a higher compressive strength is required (Table 1, lines 7-11), typically an exterior wall construction without additional insulation is no longer feasible due to the higher densities and the associated higher thermal conductivities. In most cases, a load bearing layer of normal weight concrete, lightweight aggregate concrete or sand-lime bricks with an external thermal insulation system or with core insulation and facing layer (cavity wall) is implemented in this case." (Schnellenbach-Held *et al.*, 2016)

"Due to the weakness in structural properties of the designed AIC, a new formulation to achieve higher strength is desired. Commonly, the mechanical properties of concrete are enhanced by a reduction in water/cement ratio (w/c) or improvement in packing densities. An optimized model of this system is the ultrahigh performance concrete (UHPC) where a mixture of coarse, fine and micro fine aggregates, very low amounts of water, silica fume and high amounts of cement are utilized [87]. Silica fume is an essential ingredient of UHPC which increases packing due to their nano size nature, but also further enhance the bond between the cement paste and aggregate particles through their hydration reaction with cements [88]. Further information concerning miscellaneous aerogel investigations, also including aerogel windows, may be found in the available literature [89–102].

Based on these reasons, this investigation utilizes the UHPC model for the modification of aerogel-incorporated mortars (AIM) to improve the structural properties such as compressive strength while maintaining the thermally insulating properties achieved by the aerogel incorporation. The optimal target is to produce AIMs with a minimum compressive strength

of 20 MPa while maintaining as low a thermal conductivity as possible, with a target in the range of 0.1 W/(mK) or below. To highlight the feasibility of the application of the UHPC model on this system, the mechanical and thermal properties of the AIM samples are clarified, and a comparison between them and that achieved via normal mortar mix is highlighted."(Ng *et al.*, 2015)

"Figs. 5 and 6 display the compressive strengths and thermal conductivities of AIM samples containing 60 and 80 vol% aerogel at different w/c ratios. For AIM samples containing 60 vol% aerogel, it can be observed that w/c plays a role in influencing the properties of the sample. When w/c is increased to 0.225, the compressive strength attained a maximum at 12.7 MPa, though at the expense of the highest thermal conductivity (0.61 W/(mK)). This change in properties of the AIM samples could be explained by the higher degree of hydration of the cement matrix. When w/c increased further to 0.25, excess water was present which could be explained by the possibility that increase water amount in the matrix acted to weaken the hydrating cement matrix and thus reduce the strength once again.

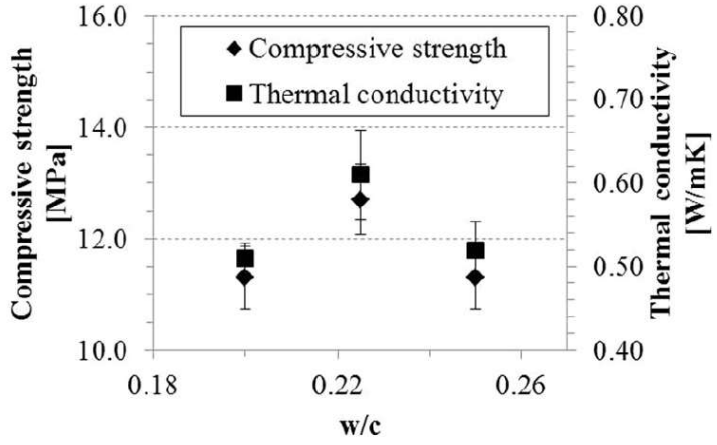

Fig. 5. Compressive strength and thermal conductivity of AIM samples containing 60 vol% aerogel as a function of w/c. Standard deviation calculated to 95% interval.

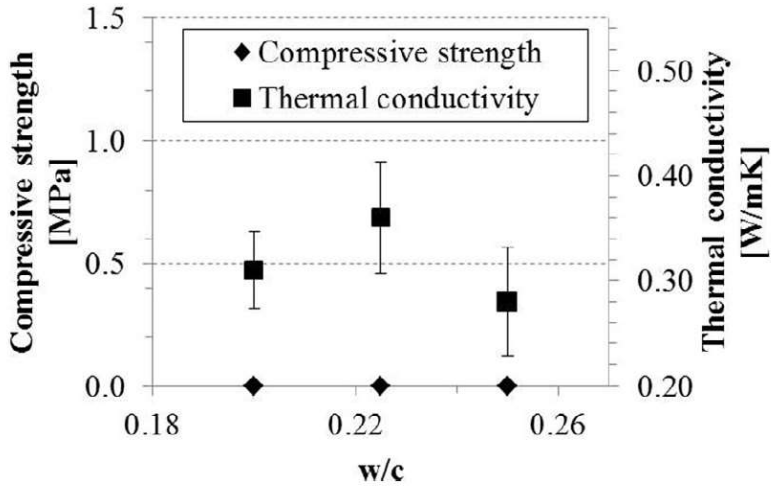

Fig. 6. Compressive strength and thermal conductivity of AIM samples containing 80 vol% aerogel as a function of w/c. Standard deviation calculated to 95% interval.

In the case of AIM samples containing 80 vol% aerogel, a similar trend in thermal conductivity of the samples was observed. However, compressive strengths of all three samples were negligible. These findings signified that the amount of effective binder is a crucial factor in determining compressive strengths of AIM samples, particularly at higher aerogel loadings. Therefore, a threshold maximum of 70 vol% aerogel loading should be employed in these systems. Below that, e.g. with 60 vol% aerogel, the amount of water plays likely a significant role in affecting the properties of the sample." (Ng *et al.*, 2015)

3.6.1 Thermal properties

3.6.1.1 Specific Heat

"The specific heat for all the concrete types as shown in FIGURE 1 remains almost constant up to 300°C, and then increases between 650°C and 800°Cindicates the specific heat has linear relationship with the temperature. Fly ash concrete exhibit slightly highest values of specific heat throughout the temperature compare to others type of concrete. This could be attributed to varying permeability characteristics of concrete. This result refer to the permeability of fly ash concrete are less permeable compare to the others concrete [11, 12].

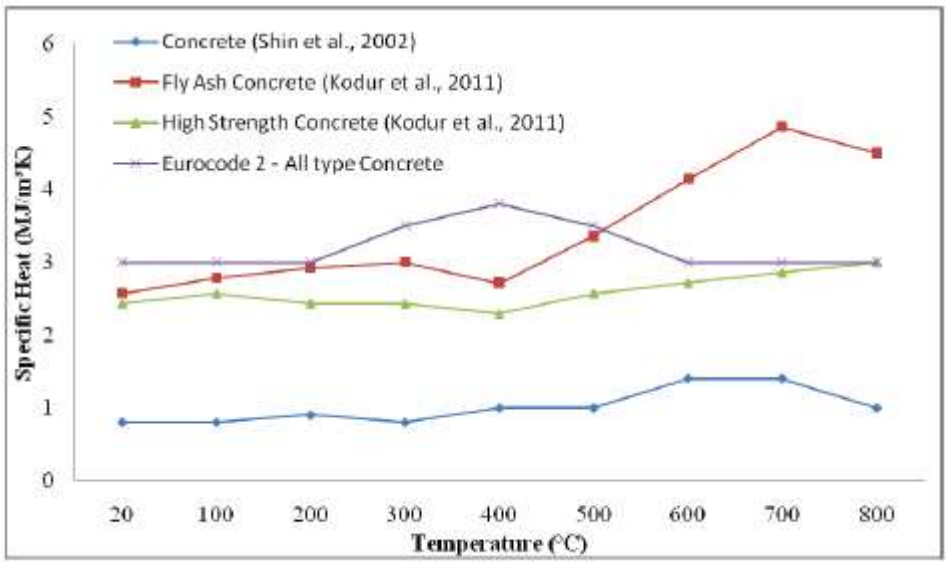

FIGURE 1. Specific heat at elevated temperature of various type of concrete.

Hence, extra heat is absorbed for releasing bound water in less permeable concretes, whichexhibit fly ash concrete to thehigher specific heat values. The specific heat for all concrete decreases from 700°C to 800°Cexplains that beyond higher temperature the concrete itself decomposition from solid to liquid. Previous research has also observed that the specific heat of concrete is affected by physiochemical processes that occur in the cement paste and aggregate above 600°C [12]." (Shahedan *et al.*, 2017)

3.6.1.2 Thermal Diffusivity

For concrete application, thermal diffusivity is also one of the thermal properties. High thermal diffusivity in concrete will ensure its temperature to equivalent with the surroundings. Thus, concrete with thermal insulation behaviour require low thermal diffusivity to lead concrete can drop the temperature or barrier temperature extremes happened during a harsh weather. Thermal diffusivity is defined as the ratio of thermal conductivity to volumetric heat capacity:

$$\alpha = \frac{k}{\rho C} \quad (1)$$

where α is the thermal diffusivity, kthermal conductivity, density and C specific heat capacity.According to previous research, the thermal diffusivity of concrete has decreased with an increase intemperature except for the specific heat [7, 15, 16]. FIGURE 3 shows other studies on thermal diffusivity on various type of concrete.

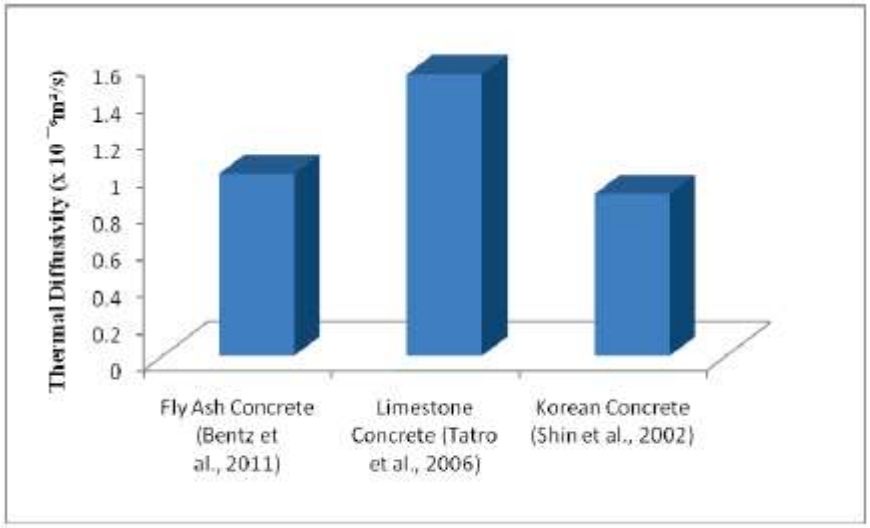

FIGURE 3. Thermal diffusivity of various type of concrete

A reduced of thermal diffusivity will reduce thermal conductivity, which may due to the reduction in density as described in formula 1." (Shahedan *et al.*, 2017)

3.6.1.3 Thermal conductivity

Thermal conductivity all type of concrete is decreases with the increases of temperature as shown in FIGURE 2. There are approximately 50% of the thermal conductivity reduce at 800°C compare at normal temperature. The result of thermal conductivity decreases with temperature, and this decrease is dependent on the concrete mix properties, specifically moisture content and permeability. Subsequently, thermal conductivity for fly ash concrete follows a similar trend to the high strength concrete. The result of thermal conductivity

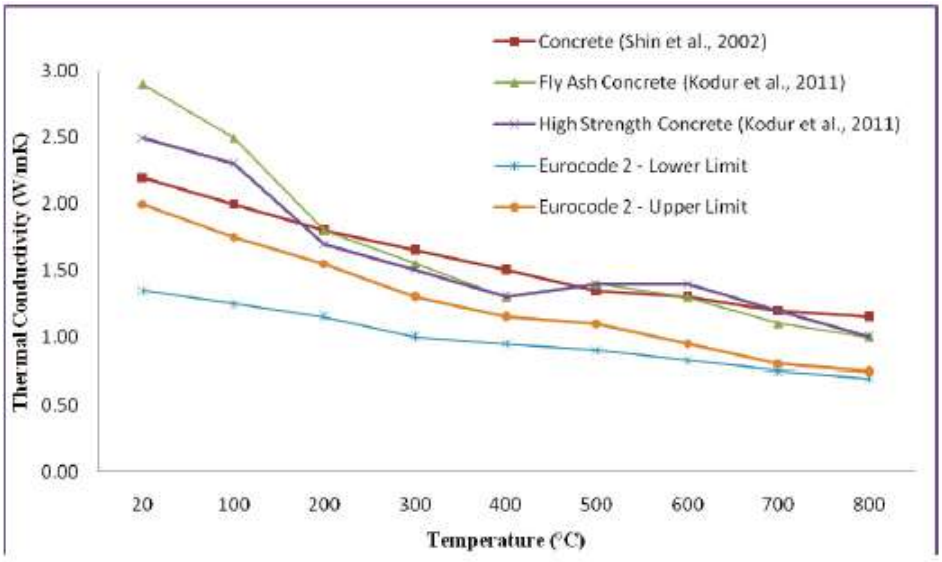

FIGURE 2. Thermal conductivity at elevated temperature of various type of concrete.

smoothly decreases can be attributed to the moisture loss anddissociation of small amounts of physically bound water present in concrete due to the increases of the temperature [12]. These properties are strongly dependent on temperature.In general, the density, the conductivity and the diffusivity decrease with an increase in temperature [12, 14, 15]. Eurocode provides two limits for the thermal conductivity of concrete but with no reference to concrete type. The thermal conductivity in Eurocode 2 lower and upper limit based on predictions for the fire resistance show that the constitutive property models in the Eurocode manual of practice." (Shahedan *et al.*, 2017)

"Few studies have been conducted on the thermal performance of FC. Aldridge (2005) presents some FC typical thermal conductivity values, ranging from 0·1 to 0·7 W/(m.K) for densities between 600 and 1850 kg/m3. The thermal conductivity of a 1000 kg/m3 FC was reported to be one sixth that of an OPC concrete (Aldridge, 2005). However, other authors have stated that thermal conductivity is more or less proportional to density (Aldridge, 2005; Samson et al., 2016), with a decrease of 100 kg/m3 being associated with a 0·04 W/(m.K) decrease in thermal conductivity. Yang and Lee (2015) studied the thermal conductivity of OPC FC produced by the pre-foaming method and found values ranging from 0·118 to 0·199 W/(m.K) for densities of 400–600 kg/m3. Figure 2 references all the data on LC thermal conductivity collected in this literature review. There is a clear correlation between density and thermal conductivity. The results were obtained with a variety of measurement techniques. To correctly compare these results, a tolerance (difficult to evaluate) should be applied. A similar overview of mechanical properties follows." (Samson, Phelipot-Mardele and Lanos, 2017)

The thermal conductivity was determined for some of the mixtures (M5, M8, M9-M13) with the Transient Hot Bridge (THB) measurement principle. The results of the ISC and the results of [10] are shown in Fig. 3. A correlation between thermal conductivity and compressive strength becomes obvious. For both studies the thermal conductivity rises with an increase of the compressive strength (as well as the dry bulk density). The test results represented in [10] stretch across compressive strength between 8 MPa and 62 MPa with corresponding thermal conductivities between 0.26 W/(mK) and 1.9 W/(mK) while the currently determined values for compressive strength and thermal conductivity are located in a range between 6 MPa and 23 MPa as well as 0.17 W/(mK) to 0.37 W/(mK). This means that the scope of testing at the ISC delivered smaller values for the thermal conductivity – which imply a better heat

insulating property – at a comparable compressive strength.) (Schnellenbach-Held *et al.*, 2016)

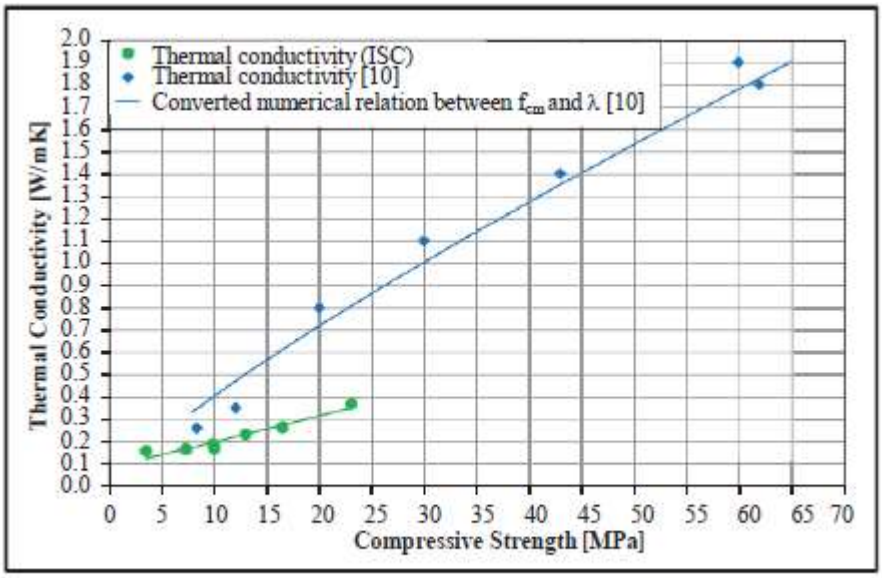

„ Fig. 3. Correlation between compressive strength and thermal conductivity “ (Schnellenbach-Held *et al.*, 2016)

“As noted earlier, tests for thermal parameters were conducted with an Isomet 2104 apparatus using the non-stationary method. Figure 8 shows the thermal conductivity coefficients (λ) for the variants of the composite with superplasticiser. The correlation between water content during the first few days of composite curing and the value of λ can be clearly seen. Despite that, in the later period, the concrete with additional water (L/18/SP) demonstrated the lowest value of λ. Samples with aerogel tended to dry out much more quickly in comparison with the composite of a dense cement matrix without aerogel, for which λ changed only slightly during the first 28 d of concrete curing.

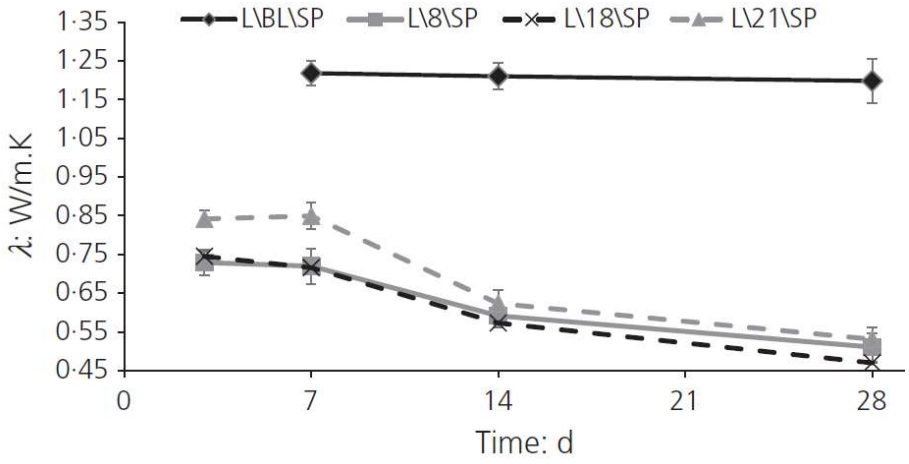

Figure 8. Thermal conductivity coefficients in the first 28 d of curing of composites with superplasticiser

The addition of aerogel resulted in a significant reduction of thermal conductivity. After 28 d of curing, values of the thermal conductivity coefficient were approximately two times smaller for composites with aerogel compared with the control sample.

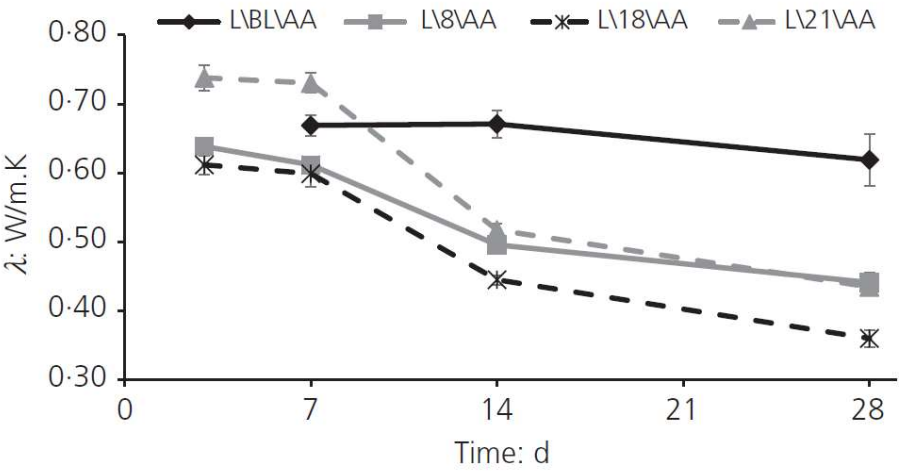

Figure 9. Thermal conductivity coefficients in the first 28 d of curing of aerated composites

The composite materials aerated with an air-entraining admixture presented even lower values of the thermal conductivity coefficient (Figure 9). Similarly to the concretes with superplasticiser, the sample with additional water achieved the lowest λ values. However, the differences in thermal conductivity between samples with aerogel and the control sample were not as substantial as for the samples with superplasticiser. This is the result of the very high level of the air-entraining admixture, which aerates the cement matrix significantly.

However, concretes with aerogel again dried significantly faster than the control." (Strzalkowski and Garbaliska, 2016)

"One of the most important parameters that determine the heat transfer through building envelope is the thermal conductivity. It is a measure of the rate at which heat is transferred through a material, and is defined as the ratio of heat flux to temperature gradient. Concrete has low thermal conductivity compared with other building materials, and can be further reduced by introducing air voids to resist heat flow between indoor and outdoor environment. There are several ways to introduce air voids into concrete: (1) voids in aggregates of various sizes, (2) voids in cement paste, (3) elimination of sand in the concrete mixture leading to voids in between the coarse aggregate, and (4) combinations of the above. Among them, the first one is typically used to achieve higher specific strength and low permeability." (Wu *et al.*, 2015)

"Thermal conductivity of concrete is affected primarily by the thermal conductivity of the raw materials used, mixture proportion, void content, and moisture condition of the concrete. The thermal conductivity of most natural rock aggregates is much higher than that of the cement pastes, and it varies depending on the rock type. In general, rocks with crystalline structure show higher thermal conductivity than amorphous and vitreous rocks of the same composition [4,5]. The thermal conductivity of cement pastes increases with the reduction of water/binder (w/b) and capillary porosity. Due to the lower thermal conductivity of air (in the order of 0.03 W/m K), the thermal conductivity of lightweight concrete (LWC) is generally lower than that of normal weight concrete. For a given type of lightweight aggregate (LWA), the reduction in the concrete density results in a decrease in the thermal conductivity. Moisture content is another major factor that influences the thermal conductivity of concrete because the thermal conductivity of water (0.5 W/m K) is higher than that of air." (Wu *et al.*, 2015)

Table 8
Comparison of experiment and estimated thermal conductivity of the ULCCs.

Mix ID	w/b	λ_{cp} (W/m K)	V_{ceno}	Thermal conductivity of ULCCs (experiment) (W/m K)	Estimated thermal conductivity of ULCCs			
					From H–S lower bound		From series model	
					Estimated thermal conductivity of cenospheres = 0.133 W/m K	Error of estimation (%)	Estimated thermal conductivity of cenospheres = 0.209 W/m K	Error of estimation (%)
ULCC-1	0.35	0.835	0.383	0.398	0.392	1.6	0.389	2.3
ULCC-2	0.35	0.835	0.387	0.388	0.389	0.3	0.387	0.3
ULCC-4	0.45	0.804	0.487	0.327	0.322	1.5	0.337	3.0
ULCC-4 (VMA)	0.45	0.804	0.486	0.308	0.323	4.8	0.337	9.5
ULCC-3	0.37	0.829*	0.443	0.355	0.352	0.9	0.358	0.9
ULCC-7	0.35	0.835	0.386	0.425	0.390	8.3	0.387	8.9
ULCC-8	0.35	0.835	0.381	0.39	0.393	0.8	0.390	0.0

* Calculated by linear interpolation.

(Wu *et al.*, 2015)

3.6.1.4 Heat transfer in materials and The Knudsen effect

Gangassaeter et al., 2017 explains Heat transfer in materials and The Knudsen effect:

"Heat transfer in materials

All materials have specific properties when it comes to conduction of heat, and this is irrespective to whether one are looking at solids, liquids or gases. Heat flows spontaneously from a higher temperature body to a lower temperature body, and this will happen as a result of solid state and gas conduction, radiation and convection [1]. The relation between the different contributions are often described as in the following [2]:

$$\lambda_{total} = \lambda_{solid} + \lambda_{gas} + \lambda_{rad} + \lambda_{conv} + \lambda_{coup} + \lambda_{leak} \quad (1)$$

where λ_{solid} is solid state conductivity, λ_{gas} is gas conductivity, λ_{rad} is radiation conductivity, λ_{conv} is convection conductivity, λcoup is conductivity due to coupling effects between the other terms in Eq.1, and λ_{leak} is (air) leakage thermal conductivity.

In addition, it is important to identify which of the terms contribute most to the thermal transport. As we will see later for vacuum insulation panels (VIP), the gas conduction part is very large and the most dominant when the VIP is punctured.

The Knudsen effect

Conventional thermal insulation materials are produced so the effects of conduction, radiation and convection are minimized. Using low-radiative surfaces and porous structures reduces radiation, convection and solid conduction, but due to the size of the pores and the open-porous material, the gaseous thermal conduction is limited to the conductivity of air [3]. A solution to this is to utilize the Knudsen effect. This effect is explained by the equations in the following, and implies that a reduction of the pore size in the material to the nano range will effectively reduce the thermal conductivity [4]:

$$\lambda_{gas} = \frac{\lambda_{gas,0}}{1+2\beta Kn} \tag{2}$$

Where

$$Kn = \frac{\sigma_{mean}}{\delta} = \frac{k_B T}{\sqrt{2}\pi d^2 p \delta} \tag{3}$$

where λ_{gas} is a combination of thermal conductivity of the gas inside the pores on nanoscale and the energy transfer when molecules collide with pore walls (the latter from the β factor), $\lambda_{gas,0}$ is the thermal conductivity for air at standard temperature and pressure (STP), β is a unitless number between 1.5 and 2.0 which describes the (in)efficiency of energy transfer between molecules and pore walls when colliding [5], Kn is the Knudsen number, σ_{mean} is the mean free path of gas molecules, δ is the pore size of the material, d is the collision diameter of the gas molecules, p is the gas pressure inside the pores, k_B is the Boltzmann's constant, and T is the temperature [6]. It is clear from Eq.2 and 3 that for pores only a few nanometres in diameter the Knudsen number becomes large. This results in a low λ_{gas}. For example, a material with pore size of about 100 nm would achieve a λ_{gas} of somewhat below 8 mW/(mK). Note that the value for stagnant air at STP is 26 mW/(mK) [6].

The Knudsen effect is achieved when the pores have a dimension comparable or smaller than the mean free path of the gas molecules inside the pores. Knowing how to utilize and exploit the Knudsen effect will be very important in the development of high-performance thermal insulation materials based on air-filled pores for building applications." (Gangassaeter *et al.*, 2017)

3.6.2 Compressive strength

“Use as partial load-bearing material imposes a minimum compressive strength that must be defined for each use and construction project (Chen and Liu, 2013). Several experiments linking density, binder composition (Bogas et al., 2013), w/b ratio, production methods and associated mechanical performances have been conducted on FC. Kearsley (1996) and Kearsley and Wainwright (2002) indicate that the compressive strength of LC decreases exponentially with density. According to Nambiar and Ramamurthy (2007), FC can be classified into two categories depending on density. Between 500 and 1000 kg/m3, compressive strength decreases with increasing diameter of gas occlusions. For higher densities, compressive strength mostly depends on the mineral paste formulation, because the bubbles are far apart from each other. Aldridge (2005) confirmed that compressive strength decreases with a decrease in density, as shown by Kearsley and Wainwright (2001a). However, constituents and content can change, and density is not necessarily the most elevant compressive strength indicator – the w/b ratio, cement choice, porous structure and curing conditions drastically impact mechanical properties.

All the LC mechanical performance information collected is given in Table 1 and Figure 3. The relation with density is not as clear for compressive strength as it is for thermal conductivity (Figure 2). Density is not a sufficient parameter to characterise mechanical performance, but it remains significant. A study on the effect of porosity is presented next. Like the thermal conductivity results, compressive strength results have been obtained with a variety of methods. To correctly compare these results, a tolerance should be applied. “ (Samson, Phelipot-Mardele and Lanos, 2017)

“Due to the weakness in structural properties of the designed AIC, a new formulation to achieve higher strength is desired. Commonly, the mechanical properties of concrete are enhanced by a reduction in water/cement ratio (w/c) or improvement in packing densities. An optimized model of this system is the ultrahigh performance concrete (UHPC) where a mixture of coarse, fine and micro fine aggregates, very low amounts of water, silica fume and high amounts of cement are utilized [87]. Silica fume is an essential ingredient of UHPC which increases packing due to their nano size nature, but also further enhance the bond between the cement paste and aggregate particles through their hydration reaction with cements [88]. Further information concerning miscellaneous aerogel investigations, also including aerogel windows, may be found in the available literature [89–102].” (Wu *et al.*, 2015)

“The results of the strength tests and the related dry bulk densities are shown table 2.

Table 2. Compressive strength ($f_{cm,cube,150}$) of the optimized mixtures after 28 days (7 days)

Mixture	M8	M5	M7	M1	M10	M9	M6	M12	M2	M11	M3	M4	M13
Dry bulk density ρ [kg/m³]	730	750	810	850	860	880	940	1010	1015	1050	1070	1130	1170
Dry Storage: f_{cm} [MPa]	3.1	6.2	7.9	7.4	8.9	9.9	9.8	13.0	11.5	15.3	13.8	17.1	21.1
Heat Treatment: f_{cm} [MPa]	3.0	6.6	7.2	7.8	10.0	9.5	9.2	12.0	12.7	16.3	12.8	12.7	23.6
Mix Storage: f_{cm} [MPa]	3.7	7.3	7.9	8.4	9.3	9.2	10.1	11.7	13.9	16.5	12.7	15.8	23.1
Mix Storage: $f_{cm,7\ Days}$ [MPa]	3.7	5.6	7.4	8.1	8.9	6.6	7.7	11.6	10.3	14.5	10.9	16.2	19.2

Most of the mixtures achieved the highest compressive strength by using the mix type of storage. The early heat treatment did not lead to a significantly higher compressive strength. Regarding the relation between the compressive strength at concrete ages of seven days and 28 days no clear trend could be observed.

A further important aspect, which has been discovered in the scope of testing, is the correlation between the drybulk density and the compressive strength. The compressive strength for the 13 mixtures by using mix storage is shown in Fig. 2. For this purpose, a linear regression analysis was performed. The coefficient of determination was calculated to a value of 0.93 which shows a high correlation between the bulk density and the compressive strength. In [16] the compressive strength of porous bodies can be calculated as a function of the bulk density. In this case the values ρ_0 and σ_{cr} of the employed Portland Cement have been used.

$$\sigma_{cr} = 0{,}2 \cdot \sigma_{cr}^{0} \cdot (\rho / \rho_0)^{(3/2)} \tag{1}$$

Regarding the investigations of aerogel concrete in [8] the factor 3/2 in the equation should be replaced by 0.75. Both functions are represented in Fig. 2. In the experimental investigations of the Institute of Structural Concrete (ISC) most of the optimized mixtures achieved a higher compressive strength than expected according to equation (1) regarding [8] and [10].) (Schnellenbach-Held *et al.*, 2016)

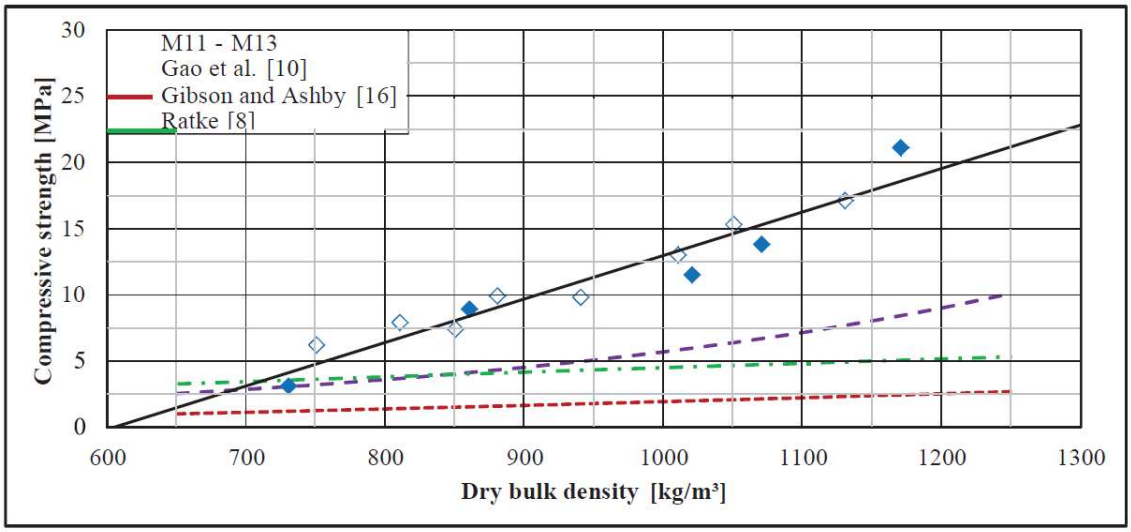

Fig. 2. Compressive strength at a concrete age of 28 days of 13 mixtures in relation to the dry bulk density

(Schnellenbach-Held *et al.*, 2016)

"Compressive strength tests were conducted after 7 and 28 d, and the results for the composites with superplasticiser are presented in Figure 12. It is clear that the impact of aerogel addition is substantial. The mean compressive strength of samples with aerogel was approximately only 30% of that of the control samples. The highest strength values from the composites with aerogel particles were observed for the concretes with natural-moisture aggregate. Unfortunately, due to the aggregate absorbability, it was difficult to produce a larger amount of concrete mix with this recipe because the aggregate absorbs water from the cement grout: this could hinder the correct thickening and production of a larger number of samples.

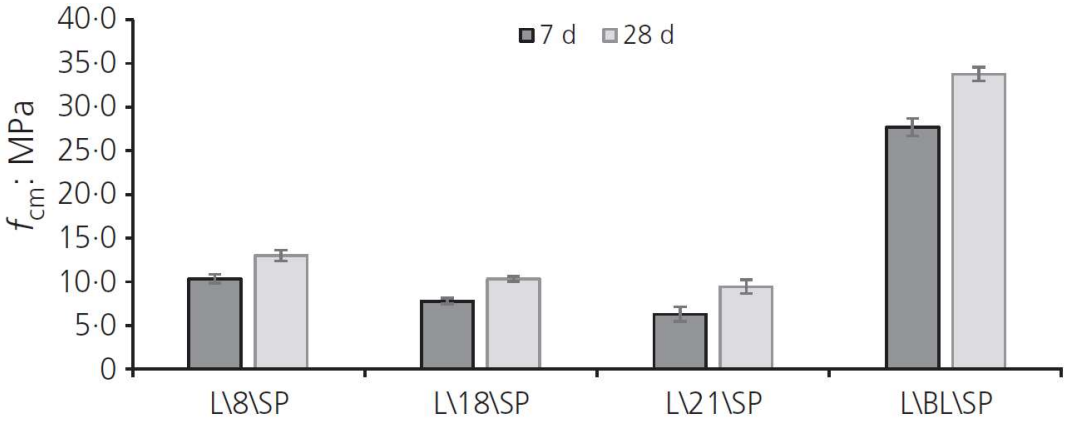

Figure 12. Average compressive strength of composites with superplasticiser

As expected, the aerated concretes showed lower values of mean strength (Figure 13). Similar issues regarding the aggregate absorbing water from the grout were observed upon forming the samples of concrete L\8\AA. Nevertheless, the effect of the water/cement ratio on strength is clearly seen, regardless of how the water is delivered. It can be stated that the best results were obtained for the concretes with some additional water: their workability and consistency were acceptable, and their strength was higher than that of the concretes with pre-moistened aggregate. The compressive strength values of the samples with aerogel were higher than the results for the control concrete samples. This means that the aerogel granules fill the pores of the aerated structure of the cement matrix.

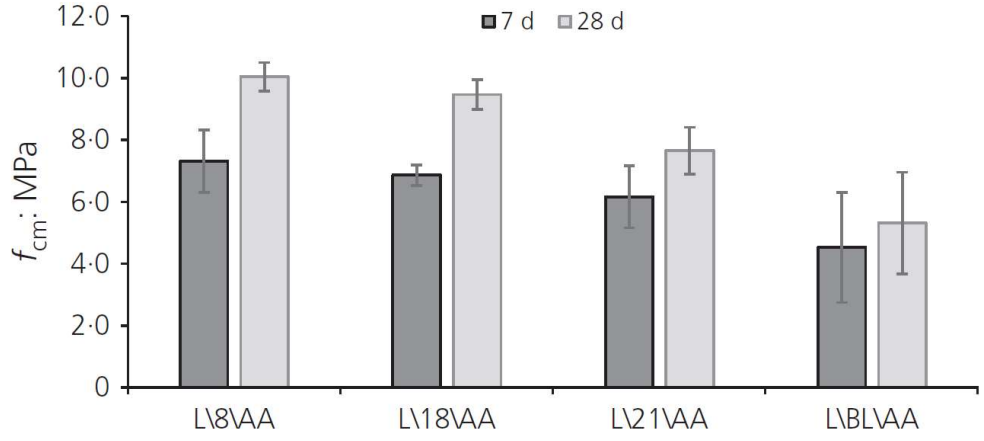

Figure 13. Average compressive strength of composites with air-entraining admixture

Furthermore, the standard deviations are much smaller in comparison with the control aerating admixture sample, which means that the structure of composites with aerogel is more uniform in comparison with the control aerated samples. “(Strzalkowski and Garbaliska, 2016)

“Fig. 3 clearly shows that the density of the ULCCs and concrete is affected by the density of the aggregates embedded in the cement paste matrices. The ULCCs had significantly lower density (1154 to 1471 kg/m3 after demold) due to the incorporation of hollow cenospheres

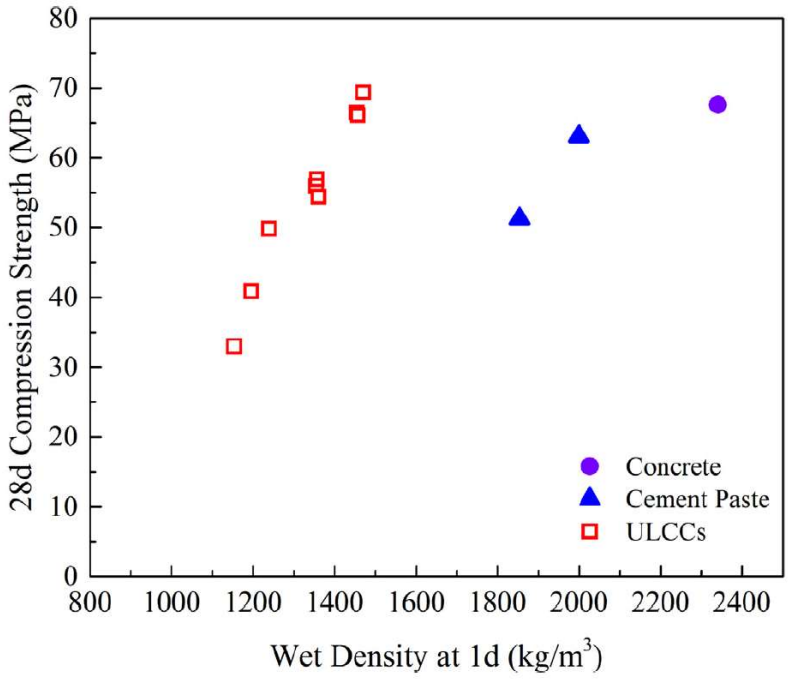

Fig. 3. 28-day compression strength vs wet density after demold.

(particle densities = 615 and 908 kg/m3) as micro aggregates compared with the concrete (2341 kg/m3 after demold) which included granite coarse aggregate and natural sand with densities of 2650 and 2630 kg/m3, respectively. The compressive strength of the ULCCs, cement pastes, and concrete samples was affected by their density. The compressive strength of the ULCCs and cement pastes was reduced with the decrease in density (Fig. 3). evertheless, 28-day compressive strength of 69.4 MPA was achieved for the mixture ULCC-1, similar to that of the cement paste with w/b of 0.35 and the concrete. The specific strength (strength/density) of the ULCC-1 is 0.047 MPa/kg/m3, which is equivalent to a normal weight concrete with compressive strength of about 110 MPa. Flexural tensile strength of the ULCCs, cement pastes, and concrete increased with the increase in the compressive strength (Fig. 4a).

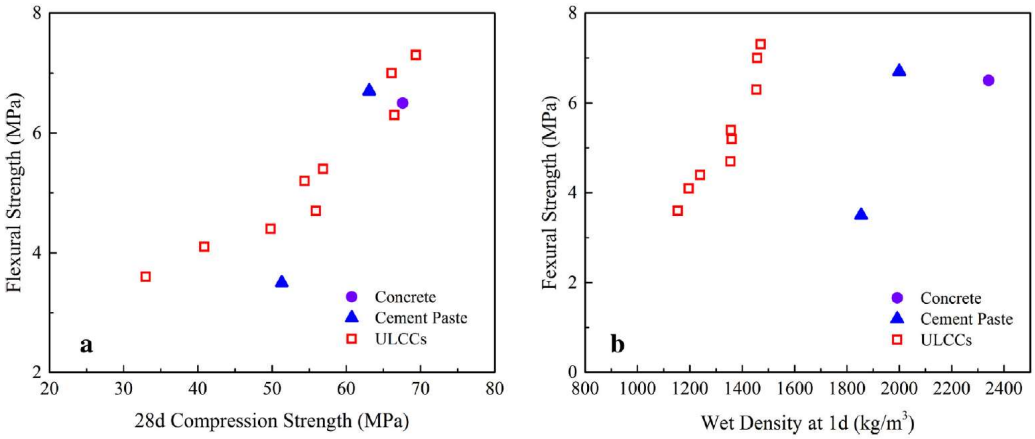

Fig. 4. (a) Flexural tensile strength vs compressive strength; (b) flexural tensile strength vs wet density after demold.

The flexural tensile strength of the ULCCs was about 8.4–10.9% of their 28-day compressive strength, which is comparable to that of the cement pastes and concrete. The flexural tensile strength of the ULCCs and cement pastes also decreased as the density decreased (Fig. 4b).

The elastic modulus of cement composites and concrete was generally affected by their compressive strength and density. As shown in Fig. 5a, the elastic modulus of the ULCCs increased with an increase in the compressive strength. With the 28-day compressive strength within a range from 33.0 to 69.4 MPa, the elastic modulus of the ULCCs, cement pastes, and concrete decreased with the density (Fig. 5b). The elastic modulus of the ULCCs and concrete were also affected by the density of cenospheres and aggregates incorporated in the cement paste matrices." (Wu *et al.*, 2015)

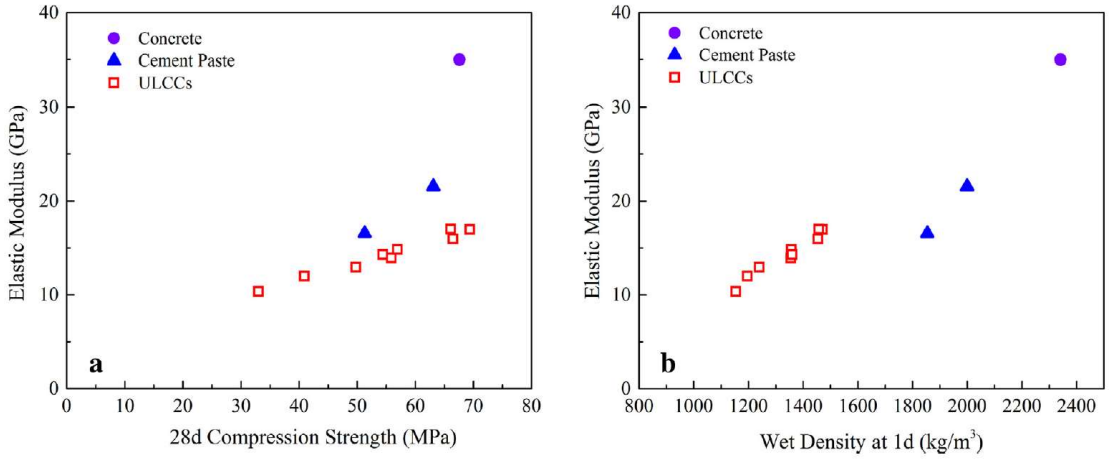

Fig. 5. (a) Elastic modulus vs compressive strength, (b) elastic modulus vs wet density after demold.

(Wu *et al.*, 2015)

3.6.3 Porosity

“Controlling the occlusion size distribution is the most critical step during FC production. Porosity and porous structure seem to condition LC thermomechanical behaviour just as much as the matrix properties. According to Visagie (2000), high porosity severely reduces compressive strength, especially if the occlusions are large. Like conventional cementitious materials, FC contains nano-pores or gel pores (diameter, d<0·01 μm), capillary pores (0·01 μm<d<10 μm) and macro-pores (10 μm;trapped and entrained air). Gel pores make up 40–55% of the total LC pore volume but do not affect water permeability or compressive strength. However, the water in these gel pores is physically linked to the cement by the hydration process. This water controls creep and shrinkage phenomena. Pores obtained by a gas-foaming method are usually bigger than pores obtained with other methods. A few interesting studies reference methods for analysing different porous structures. Nambiar and Ramamurthy (2007) used black ink and talc to obtain a good contrast between the solid matrix and occlusions. The experiments revealed that the occlusion volume percentage was lower than the percentage obtained by weighing the samples. There are three possible explanations for this: the occlusions were not cut in middle, the occlusions could overlap, or edge occlusions were excluded. In order to compare and quantify the porous structure of arious LC compositions, two quantitative parameters are introduced, r50 and r90, corresponding to 50% and 90% of the total cumulative area. With the pre-foaming method, these two parameters increase with an increase in aqueous foam, the growth of the r90 parameter being less rapid. The r90 radius is better correlated with compressive strength. Big pores primarily affect FC compressive strength. From images of this type of FC, some calculation algorithms can be written to obtain surface occlusion size distributions. Soroushian and Elzafraney (2005) showed that only simple morphological operations (dilatation, erosion, opening, closing, filling holes etc.) are necessary. As there is a good contrast between the black matrix and the occlusions, they can be easily separated and, after image treatment, the occlusion area, perimeter and equivalent diameter are determined for each occlusion.

Wei et al. (2013) created a large density range of FC (252–1870 kg/m3) with the pre-foaming method. A threedimensional characterisation was obtained by tomography analysis, which revealed that the medium radius of occlusions decreased with an increase in apparent density, as was also determined by previous surface analysis (Nambiar and Ramamurthy, 2007). Finally, a two-dimensional analysis was proposed using a random draw model that enabled a representative occlusion size distribution to be created. This model led to excellent thermal

conductivity predictions when the porosity was smaller than 35%. Wei et al. (2013) assigned the differences observed between model predictions and measurements to significant differences between the surface images and the real volume of the porous structure. Another possible source of error is that radiative effects are neglected in the model. Radiative effects are more important when porosity is high. Just and Middendorf (2009) studied the influence of several parameters on FC porous structures made with OPC cement. As demonstrated by Yang and Lee (2015), decreases in the w/b ratio tend to decrease the medium occlusion size. Occlusion sizes can also be reduced by the addition of fly ash. Yang and Lee also revealed that occlusion sphericity decreased when occlusions became larger." (Samson, Phelipot-Mardele and Lanos, 2017)

4 Conclusions

Materials described in the literature study with low thermal conductivity are often characterized by low specific gravity and frequently they are porous. This also means that they have low compressive strength and are crisp and no ductile. For earogel, it is often a matter of improving the different bindings. We have seen that this has been done successfully in the two studies of Iswar, S. et al. (2018) with reinforced and superinsulating silica aerogel through in situ cross-linking with silane terminated prepolymers and Joly, M. et al. (2017) with aerogel in combination with Glass Fiber and Needle Glass Fiber.

Aerogel shows very good insulation properties and recent research also shows good mechanical properties. In addition, aerogel can be transparent and emit light. When mixing aerogel in concrete the studies show that both thermal conductivity and compressive strength are worsened. Further research still appears to be necessary before we see a breakthrough in this area.

Prefabricated walls have been used for a long time and involve quick and practical construction methods. Concrete has been reinforced with steel armoring for a long time. P. L. N., Jayasinghe, M. T. R. and Jayasinghe, C. (2017) has shown that foam concrete along with cement fiber boards that works as armoring have yielded promising results.

Qun, X., Shuai, W. and Chun, L. (2018) also shows very good results for sandwich elements using three-dimensional steel reinforcement instead of flat reinforcement mesh. This happens even though the degree of armor reduces. This seems to be a brilliant idea, although this is far from surprising. Rather, it is use of known technology within a slightly different field of application.

Prefabricated Concrete Sandwich Wall Panel represent a very efficient and proven construction method. Qun, X., Shuai, W. and Chun, L. (2018) reported that the three-dimensional steel reinforcement

“The thermal properties that influence the temperature rise and distribution in a concrete are thermal conductivity, specific heat, and mass loss. A good insulator has a higher specific heat capacity because it takes time to absorb more heat before it actually heats up (temperature

rising) to transfer the heat. A low thermal conductivity and thermal diffusivity results in a good thermal performance which can reduce energy losses and drop the temperature equivalent with the surroundings through the concrete of a building."(Shahedan *et al.*, 2017)

"The present economic and environmental context motivates the elaboration of construction materials that are usable as both insulation and partial load-bearing material. This review indicates that several LCs, lightened by means of LA or gas occlusions, are being created and examined by the scientific community. The different LCs can be classified according to their production method, as shown in the organisation chart presented in Figure 1. One particular characteristic of LCs is a very wide range of available densities.

The referenced works are numerous and differ by several parameters, such as LA presence (or absence), binder nature and content, production process, w/b ratio and surfactant content. The thermomechanical performances obtained for each work are listed (Table 1) and presented graphically in Figures 2 and 3.

Analysis of these data enables the following observations.

- Thermal conductivity mostly depends on density. At the same apparent density, the previously outlined parameters only slightly impact thermal conductivity.

- At the same apparent density, compressive strengths are more dispersed. Huge variations can be observed for some LCs produced with the same binder. These dispersed results cannot be explained only by the choice of binder. The influence of the porous structure might be able to explain these marked variations.

Gypsum LAC and FC with interesting thermal and mechanical properties have been successfully produced (Samson et al., 2016; Figures 2 and 3). As a binder, gypsum has a smaller environmental footprint than OPC, but few works have investigated the suitability of such building solutions. Furthers investigations into the durability of gypsum LC are required to prove the relevance of this solution." (Samson, Phelipot-Mardele and Lanos, 2017)

"The effects of the addition of aerogel particles on the thermal properties and compressive strength of composite materials based on lightweight fly ash aggregate were examined. Concretes with superplasticiser and aerating admixture were also tested. For both groups of composites, the tests were performed on three moisture variants of the lightweight aggregate.

The test results support the idea of adding aerogel particles to improve thermal properties. Relatively low values of the thermal conductivity coefficient (λ) were obtained, within the range 0·36–0·53 W/mK (compared with control sample without aerogel, λ= 1·198 W/mK), and high values of the volumetric specific heat (cv) were also obtained, 1·44–1·68 10^6 J/(m^3.K), depending on the concrete mix type. This explains why concrete composites containing aerogel used as a load-bearing layer would improve the insulating properties of whole external partitions. High values of volumetric specific heat would also have a positive impact on the stabilisation of internal building temperature and these advantages should be exploited for improving the energy-saving potential of structures.

The influence of aerogel granules on compressive strength was also assessed. The composites produced had a mean compressive strength of 6–13 MPa after 28 d of curing. Therefore, this material can be compared to hollow ceramic bricks or autoclaved aerated concrete and could be used for selfsupporting elements of a building or even for small loadbearing structures such as walls in detached houses or other single-storey buildings.

This study also investigated the structure of pure aerogel particles and how they act on a cement matrix. SEM images demonstrated the results of stirring a fresh mixture: some of the granules were abraded and crushed into smaller granules due to the stirring action. The images taken also showed clear boundaries between the grout and individual aerogel granules.

The impact of aerogel on the distribution of air pores in concretes was also discussed. A method for taking aerogel into account in the pore structure of the whole composite material was presented. It was diagnosed that a 20% volumetric share of aerogel in the composite resulted in an increase in total porosity of 8·63% and, in particular, the appearance of additional pore volume within the nano-porosity range of 10–30 nm.

The results discussed in this paper justify the application of aerogel particles as an admixture to concretes. Each of the composites in the study had an identical volumetric share of 20% of aerogel and thus significantly different values of the thermal and strength parameters were obtained. This indicates the substantial influence of the aggregate moisture content and the simultaneous action of the plasticising or aerating admixtures. In the application of aerogel for the modification of concrete composites, the main issue is the aerogel price barrier. However, this is expected to fall with an increase in widespread production technology."(Strzalkowski and Garbaliska, 2016)

“Based on concrete formulas of HPC, UHPC and LC an aerogel concrete was optimized at the ISC with the goal to increase the compressive strength while maintaining good heat insulating properties.

Three types of storage have been investigated. The influence of a heat treatment on the compressive strength is negligible. The concrete core reached up to 80 °C during the hydration process depending on the cement and silica fume content. The hydration process was completed after approximately 26 hours.

The compressive strength reached values up to 23.6 MPa and increased with bulk density. No trend can be identified for the difference of compressive strength between seven and 28 days. The thermal conductivities are in the range $0.16 \leq \lambda \leq 0.37$ W/(mK) representing good insulating properties. The most suitable mixture achieved a compressive strength of 10 MPa, a density of 860 kg/m³ and a thermal conductivity of 0.17 W/(mK). Compared to heat insulation masonry, the developed High Performance Aerogel Concrete achieves higher compressive strength at comparable thermal conductivities.” (Schnellenbach-Held *et al.*, 2016)

“For comparison between various mix proportions, it is desirable to define a merit number M = compressive strength/(thermal conductivity／density). Higher values of the merit number indicate better optimization between mechanical and thermal properties. The histogram shown in Fig. 11b indicates that the merit number of the ULCC is basically one order of magnitude higher than most of the results from Sengul et al. [52], Mounanga et al. [12], Gül et al. [8], and Yun et al. [53].” (Wu *et al.*, 2015)

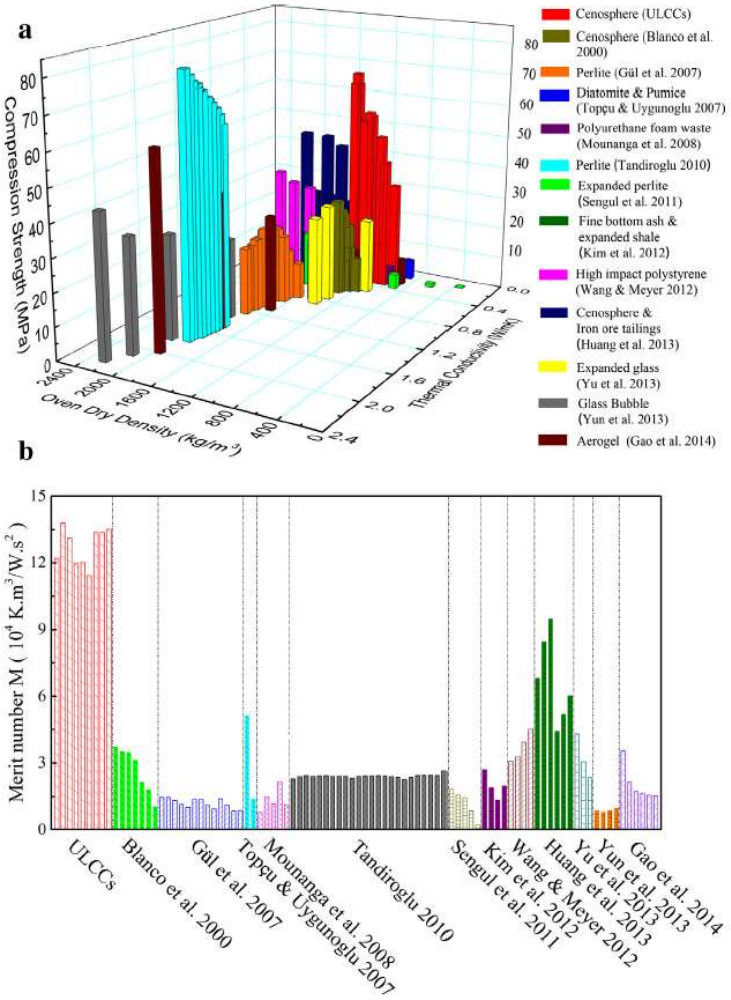

Fig. 11. (a) Density, compressive strength, and thermal conductivity of the ULCCs in comparison to concrete with various lightweight aggregates reported in literature, (b) merit number defined as M = compressive strength/(thermal conductivity * density) (MPa/(W/m K) * (kg/m^3) = 10^4 K m^3/W s^2) of various lightweight concretes mentioned in (a).

(Wu *et al.*, 2015)

"Mechanical properties and thermal conductivity of ultralightweight cement composites (ULCCs) with 1-day density from 1154 to 1471 kg/m3 and 28-day compressive strength from 33.0 to 69.4 MPa were studied. The low densities of the ULCCs were achieved by incorporating hollow cenospheres from fly ash generated in thermal power plants. The properties of the ULCCs were compared with those of cement pastes with w/b of 0.35 and 0.45 and those of a concrete with 28-day compressive strength of 67.6 MPa. Based on the experimental results, numerical calculation, and discussion, following conclusions can be drawn:

1. Compressive strength, flexural tensile strength, and elastic modulus of the ULCCs were reduced with decrease in density. However, the compressive and flexural tensile strength of 69.4 and 7.3 MPa were achieved for the ULCC-1, respectively, similar to those of the cement paste with w/b of 0.35 and the concrete. The specific strength of the ULCC-1 is 0.047 MPa/kg/m3, equivalent to that of a normal weight concrete with compressive strength of about 110 MPa. The density and elastic modulus of the ULCCs and concrete were affected by the density of aggregates embedded in the cement paste matrices. The ratio of the flexural tensile strength/compressive strength of the ULCCs is comparable to that of the cement pastes and concrete.

2. Thermal conductivity of the ULCCs was reduced with decrease in the oven-dry density and it was significantly lower than that of the cement pastes and concrete due to the incorporation of hollow cenospheres. With similar 28-day compressive strength, the thermal conductivity of the ULCC was 54% and 80% lower than that of the cement paste and concrete, respectively.

3. Compared to the properties from various lightweight concretes reported in literature, the ULCCs have an optimum combination of low thermal conductivity, lightweight, and high specific strength. The low thermal conductivity of the ULCCs is due to the incorporation of hollow cenospheres as micro-aggregate which effectively introduce voids and decrease density of the ULCCs. The high specific strength of the ULCCs may be attributed to (1) the presence of hard and stiff shell in the cenospheres, (2) the ‘‘control’’ of void sizes in the cenospheres, and (3) the creation of strong cement paste matrices that provide ‘‘three dimensional’’ confinement to the cenospheres.

4. The incorporation of polyethylene fibers reduced the brittleness observed in the ULCC samples, but did not have significant effect on the strength and elastic modulus if the density and w/b were kept constant. However, the fiber reinforced ULCC had higher thermal conductivity than that without fibers, which may be due to the higher thermal conductivity of the polyethylene fibers. The shrinkage reducing admixture and viscosity modifying agent did not have significant effect on the mechanical properties and thermal conductivity of the ULCCs.

5. The thermal conductivity of the ULCC can be estimated by usingValore’s equation (1980) with a multiplication factor of about 1.2.

6. The estimated average thermal conductivity values of the cenospheres based on H–S lower bound and Series model are significantly higher than that provided by manufacturer due to the effect of void space among the cenosphere particles.

7. Based on the estimated thermal conductivity of cenospheres, the thermal conductivity of the ULCCs can be estimated using H–S lower bound and Series model with error of estimation less than 10%. Overall, the H–S lower bound gives lower error of estimation than the Series model." (Wu *et al.*, 2015)

"Insulation mortar ultra-high performance concrete (I-UHPC) formulation was utilized to optimize the structural properties of insulation composite materials based on aerogel incorporation. It was observed that increased aerogel content, especially under higher loadings resulted in a drastic drop in the mechanical strength of these aerogel-incorporated mortar (AIM) samples, owing to a decrease in packing effectiveness and effective binder. At an aerogel loading of 50 vol% where a minimum compressive strength of 20 MPa was maintained, the AIM samples registered a thermal conductivity value of 0.55 W/(mK), rendering such an UHPC modified AIM system to be unsuitable as a standalone system for insulating purposes. Nevertheless, the ability to bring down thermal conductivity by a factor of 5 signifies that much less insulation materials are needed to cover the concrete building envelope in obtaining the desired thermal resistance, thus slimmer building blocks are to be expected, and may also be viewed as a stepping-stone towards the ultimate goal of a concrete or construction material exhibiting both satisfactory thermal and mechanical properties.

Due to the limitation of the applicability of the UHPC formulation on the AIM model, it is thus proposed to improve these AIM samples by first maintaining a maximum aerogel content of up to 50–60 vol% for maximum structural properties at 28 days after curing, whereas further improvement of the insulation of the mortar may be achieved through other means such as e.g. incorporation of other binder materials possessing lower thermal conductivities. Additionally, the binding force between aerogel and cement matrix may be improved by mixing procedures or incorporating amphiphilic materials or even fibers, which can act as intermediates for the surfaces. (Ng *et al.*, 2015)

5 Further Work

This study can be advantageously improved by including material from suppliers. The development is also happening quickly in this field and it is very relevant to look at what can actually be delivered to the construction industry today.

There are also still new articles being published, and there are also some good articles that are not found or omitted on a too thin basis.

As mentioned earlier, the specific weight of the material is very important for how appropriate they are for use in the building shell. By looking at thermal conductivity and compressive strength only, without looking at the effect of the material's specific gravity, one gets a misleading picture of their usefulness.

Therefore, a factor for specific weight should be added that will make the collected data a better work tool.

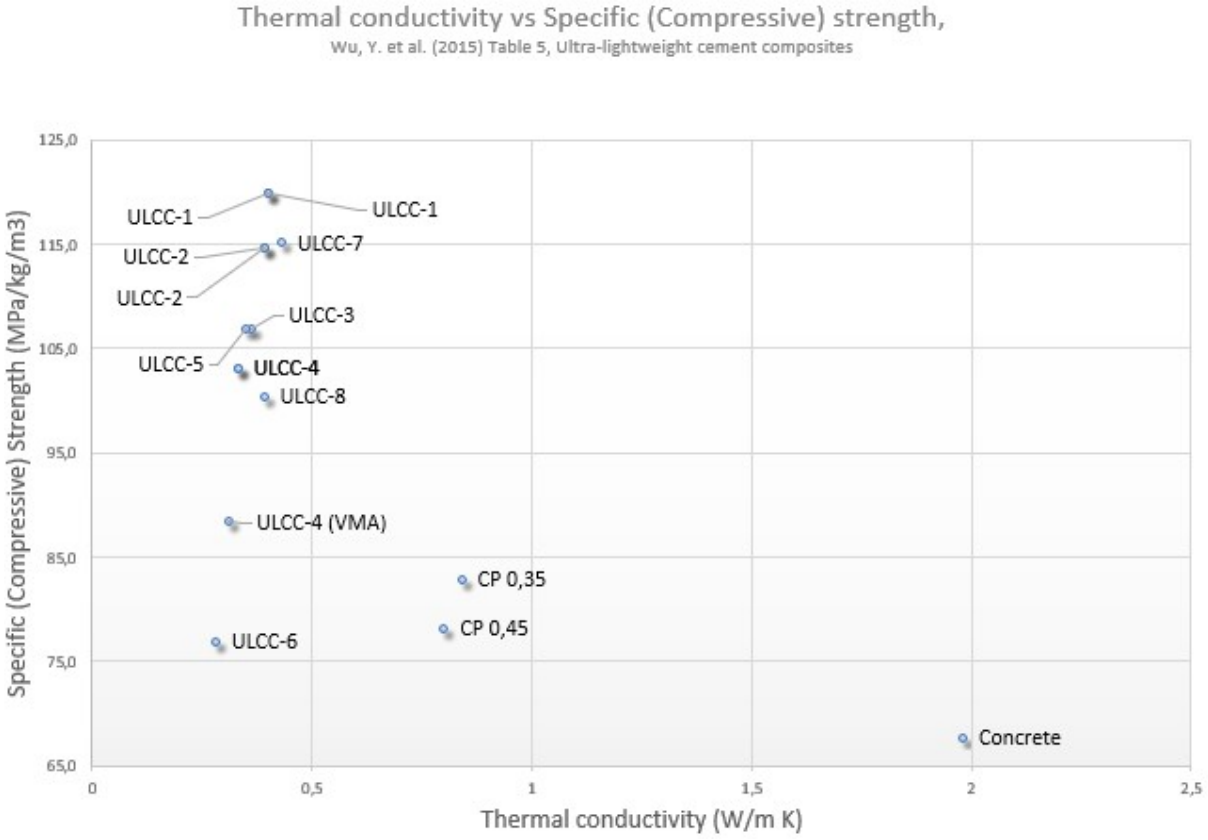

Figure 7. 1: Thermal conductivity vs Specific (Compressive) Strength . Wu, Y. et al. (2015) Table 5, Ultra-lightweight cement composites

Bibliography

Ali, M. R. et al. (2018) Thermal-resistant lightweight concrete with polyethylene beads as coarse aggregates, Construction and Building Materials, 164, pp. 739-749. doi: 10.1016/j.conbuildmat.2018.01.012.

Cuce, E. et al. (2014) Toward aerogel based thermal superinsulation in buildings: A comprehensive review, Renewable and Sustainable Energy Reviews, 34, pp. 273-299. doi: 10.1016/j.rser.2014.03.017.

Fernando, P. L. N., Jayasinghe, M. T. R. and Jayasinghe, C. (2017) Structural feasibility of Expanded Polystyrene (EPS) based lightweight concrete sandwich wall panels, Construction and Building Materials, 139, pp. 45-51. doi: 10.1016/j.conbuildmat.2017.02.027.

Gangassaeter, H. F. et al. (2017) Air-Filled Nanopore Based High-Performance Thermal Insulation Materials, 11th Nordic Symposium on Building Physics, NSB 2017, June 11, 2017 - June 14, 2017, Trondheim, Norway. Elsevier Ltd, pp. 231-236.

Hajmohammadian Baghban, Kioumarsi and Grammatikos (2018) Prediction Models for Thermal Conductivity of Cement-based Composites

Hasan, M. A. et al. (2017) Prospect of Thermal Insulation by Silica Aerogel: A Brief Review, Journal of The Institution of Engineers (India): Series D, 98(2), pp. 297-304. doi: 10.1007/s40033-017-0136-1.

Iswar, S. et al. (2018) Reinforced and superinsulating silica aerogel through in situ cross-linking with silane terminated prepolymers, Acta Materialia, 147, pp. 322-328. doi: 10.1016/j.actamat.2018.01.031.

Joly, M. et al. (2017) Competitive high performance Aerogel-Based Composite material for the European insulation market, Energy Procedia, 122, pp. 859-864. doi: 10.1016/j.egypro.2017.07.450.

Khavanov, P., Fomina, E. and Kozhukhova, N. (2018) The improvement of thermal characteristics of autoclave aerated concrete for energy efficient high-rise buildings application, 2017 International Scientific Conference on High-Rise Construction, HRC 2017, September 4, 2017 - September 8, 2017, Samara, Russia. EDP Sciences.

Koebel, M. M. et al. (2016) Breakthroughs in cost-effective, scalable production of superinsulating, ambient-dried silica aerogel and silica-biopolymer hybrid aerogels: from laboratory to pilot scale, Journal of Sol-Gel Science and Technology, 79(2), pp. 308-318. doi: 10.1007/s10971-016-4012-5.

Lu, Z. et al. (2018) Thermal, mechanical, and surface properties of poly(vinyl alcohol) (PVA) polymer modified cementitious composites for sustainable development, Journal of Applied Polymer Science, 135(15). doi: 10.1002/app.46177.

Mohamed, G. and Djamila, B. (2018) Physical, mechanical and thermal properties of Crushed Sand Concrete containing Rubber Waste, 2nd International Congress on Materials and Structural Stability, CMSS 2017, November 22, 2017 - November 25, 2017, Rabat, Morocco. EDP Sciences.

Ng, S. et al. (2015) Experimental investigations of aerogel-incorporated ultra-high performance concrete, Construction and Building Materials, 77, pp. 307-316. doi: 10.1016/j.conbuildmat.2014.12.064.

Parale, V. G., Lee, K.-Y. and Park, H.-H. (2017) Flexible and transparent silica aerogels: An overview, Journal of the Korean Ceramic Society, 54(3), pp. 184-199. doi: 10.4191/kcers.2017.54.3.12.

Qun, X., Shuai, W. and Chun, L. (2018) Axial Compression Behavior of a New Type of Prefabricated Concrete Sandwich Wall Panel, 2017 4th International Conference on Advanced Engineering and Technology, ICAET 2017, December 15, 2017 - December 17, 2017, Incheon, Korea, Republic of. Institute of Physics Publishing, pp. Incheon Disaster Prevention Research Center (IDPRC); Incheon National University (INU).

Samson, G., Phelipot-Mardele, A. and Lanos, C. (2017) A review of thermomechanical properties of lightweight concrete, Magazine of Concrete Research, 69(4), pp. 201-216. doi: 10.1680/jmacr.16.00324.

Schnellenbach-Held, M. et al. (2016) Development of high performance aerogel concrete Entwicklung von Hochleistungsaerogelbeton, Beton- und Stahlbetonbau, 111(9), pp. 555-563. doi: 10.1002/best.201600017.

Shahedan, N. F. et al. (2017) Review on thermal insulation performance in various type of concrete, Advanced Materials Engineering and Technology V: International Conference on Advanced Material Engineering and Technology 2016, 8-9 Dec. 2016, USA. AIP - American Institute of Physics, pp. 020046 (020046 pp.).

Simek, B. and Uygunolu, T. (2018) Thermal, electrical, mechanical and fluidity properties of polyester-reinforced concrete composites, Sadhana - Academy Proceedings in Engineering Sciences, 43(4). doi: 10.1007/s12046-018-0847-5.

Strzalkowski, J. and Garbaliska, H. (2016) Thermal and strength properties of lightweight concretes with the addition of aerogel particles, Advances in Cement Research, 28(9), pp. 567-575. doi: 10.1680/jadcr.16.00032.

Tasdemir, C., Sengul, O. and Tasdemir, M. A. (2017) A comparative study on the thermal conductivities and mechanical properties of lightweight concretes, Energy and Buildings, 151, pp. 469-475. doi: 10.1016/j.enbuild.2017.07.013.

Tsioulou, O., Ayegbusi, J. and Lampropoulos, A. (2017) Experimental investigation on thermal conductivity and mechanical properties of a novel Aerogel Concrete, 2017 fib Symposium - High Tech Concrete: Where Technology and Engineering Meet, June 12, 2017 - June 14, 2017, Maastricht, Netherlands. Springer International Publishing, pp. 125-131.

Wang, C.-q. et al. (2018) Utilization of oil-based drilling cuttings pyrolysis residues of shale gas for the preparation of non-autoclaved aerated concrete, Construction and Building Materials, 162, pp. 359-368. doi: 10.1016/j.conbuildmat.2017.11.151.

Welsch, T. and Schnellenbach-Held, M. (2017) High performance aerogel concrete, 2017 fib Symposium - High Tech Concrete: Where Technology and Engineering Meet, June 12, 2017 - June 14, 2017, Maastricht, Netherlands. Springer International Publishing, pp. 117-124.

Westgate, P., Paine, K. and Ball, R. J. (2018) Physical and mechanical properties of plasters incorporating aerogel granules and polypropylene monofilament fibres, Construction and Building Materials, 158, pp. 472-480. doi: 10.1016/j.conbuildmat.2017.09.177.

Wu, Y. et al. (2015) Development of ultra-lightweight cement composites with low thermal conductivity and high specific strength for energy efficient buildings, Construction and Building Materials, 87, pp. 100-112. doi: 10.1016/j.conbuildmat.2015.04.004.

Xu, B., Ma, H. and Li, Z. (2015) Influence of magnesia-to-phosphate molar ratio on microstructures, mechanical properties and thermal conductivity of magnesium potassium phosphate cement paste with large water-to-solid ratio, Cement and Concrete Research, 68, pp. 1-9. doi: 10.1016/j.cemconres.2014.10.019.

Appendix

Appendix 1, Table of results.

Appendix 2, Table of references.

Appendix 3A, Thermal insulating concrete, A state of the art review, The condensed version.

Appendix 3B, Thermal insulating concrete, A state of the art review, The short version.

Ali, M. R. *et al.* (2018) Thermal-resistant lightweight concrete with polyethylene beads as coarse aggregates, *Construction and Building Materials*, 164, pp. 739-749. doi: 10.1016/j.conbuildmat.2018.01.012.

Cuce, E. *et al.* (2014) Toward aerogel based thermal superinsulation in buildings: A comprehensive review, *Renewable and Sustainable Energy Reviews*, 34, pp. 273-299. doi: 10.1016/j.rser.2014.03.017.

Fernando, P. L. N., Jayasinghe, M. T. R. and Jayasinghe, C. (2017) Structural feasibility of Expanded Polystyrene (EPS) based lightweight concrete sandwich wall panels, *Construction and Building Materials*, 139, pp. 45-51. doi: 10.1016/j.conbuildmat.2017.02.027.

Gangassaeter, H. F. *et al.* (2017) Air-Filled Nanopore Based High-Performance Thermal Insulation Materials, *11th Nordic Symposium on Building Physics, NSB 2017, June 11, 2017 - June 14, 2017*, *Trondheim, Norway*. Elsevier Ltd, pp. 231-236.

Hasan, M. A. *et al.* (2017) Prospect of Thermal Insulation by Silica Aerogel: A Brief Review, *Journal of The Institution of Engineers (India): Series D*, 98(2), pp. 297-304. doi: 10.1007/s40033-017-0136-1.

Iswar, S. *et al.* (2018) Reinforced and superinsulating silica aerogel through in situ cross-linking with silane terminated prepolymers, *Acta Materialia*, 147, pp. 322-328. doi: 10.1016/j.actamat.2018.01.031.

Joly, M. *et al.* (2017) Competitive high performance Aerogel-Based Composite material for the European insulation market, *Energy Procedia*, 122, pp. 859-864. doi: 10.1016/j.egypro.2017.07.450.

Khavanov, P., Fomina, E. and Kozhukhova, N. (2018) The improvement of thermal characteristics of autoclave aerated concrete for energy efficient high-rise buildings application, *2017 International Scientific Conference on High-Rise Construction, HRC 2017, September 4, 2017 - September 8, 2017*, *Samara, Russia*. EDP Sciences.

Koebel, M. M. *et al.* (2016) Breakthroughs in cost-effective, scalable production of superinsulating, ambient-dried silica aerogel and silica-biopolymer hybrid aerogels: from laboratory to pilot scale, *Journal of Sol-Gel Science and Technology*, 79(2), pp. 308-318. doi: 10.1007/s10971-016-4012-5.

Lu, Z. *et al.* (2018) Thermal, mechanical, and surface properties of poly(vinyl alcohol) (PVA) polymer modified cementitious composites for sustainable development, *Journal of Applied Polymer Science*, 135(15). doi: 10.1002/app.46177.

Mohamed, G. and Djamila, B. (2018) Physical, mechanical and thermal properties of Crushed Sand Concrete containing Rubber Waste, *2nd International Congress on Materials and Structural Stability, CMSS 2017, November 22, 2017 - November 25, 2017*, *Rabat, Morocco*. EDP Sciences.

Ng, S. *et al.* (2015) Experimental investigations of aerogel-incorporated ultra-high performance concrete, *Construction and Building Materials*, 77, pp. 307-316. doi: 10.1016/j.conbuildmat.2014.12.064.

Parale, V. G., Lee, K.-Y. and Park, H.-H. (2017) Flexible and transparent silica aerogels: An overview, *Journal of the Korean Ceramic Society*, 54(3), pp. 184-199. doi: 10.4191/kcers.2017.54.3.12.

Qun, X., Shuai, W. and Chun, L. (2018) Axial Compression Behavior of a New Type of Prefabricated Concrete Sandwich Wall Panel, *2017 4th International Conference on Advanced Engineering and Technology, ICAET 2017, December 15, 2017 - December 17, 2017*, *Incheon, Korea, Republic of*. Institute of Physics Publishing, pp. Incheon Disaster Prevention Research Center (IDPRC); Incheon National University (INU).

Samson, G., Phelipot-Mardele, A. and Lanos, C. (2017) A review of thermomechanical properties of lightweight concrete, *Magazine of Concrete Research*, 69(4), pp. 201-216. doi: 10.1680/jmacr.16.00324.

Schnellenbach-Held, M. *et al.* (2016) Development of high performance aerogel concrete

Entwicklung von Hochleistungsaerogelbeton, *Beton- und Stahlbetonbau*, 111(9), pp. 555-563. doi: 10.1002/best.201600017.

Shahedan, N. F. *et al.* (2017) Review on thermal insulation performance in various type of concrete, *Advanced Materials Engineering and Technology V: International Conference on Advanced Material Engineering and Technology 2016, 8-9 Dec. 2016*, *USA*. AIP - American Institute of Physics, pp. 020046 (020046 pp.).

Simek, B. and Uygunolu, T. (2018) Thermal, electrical, mechanical and fluidity properties of polyester-reinforced concrete composites, *Sadhana - Academy Proceedings in Engineering Sciences*, 43(4). doi: 10.1007/s12046-018-0847-5.

Strzalkowski, J. and Garbaliska, H. (2016) Thermal and strength properties of lightweight concretes with the addition of aerogel particles, *Advances in Cement Research*, 28(9), pp. 567-575. doi: 10.1680/jadcr.16.00032.

Tasdemir, C., Sengul, O. and Tasdemir, M. A. (2017) A comparative study on the thermal conductivities and mechanical properties of lightweight concretes, *Energy and Buildings*, 151, pp. 469-475. doi: 10.1016/j.enbuild.2017.07.013.

Tsioulou, O., Ayegbusi, J. and Lampropoulos, A. (2017) Experimental investigation on thermal conductivity and mechanical properties of a novel Aerogel Concrete, *2017 fib Symposium - High Tech Concrete: Where Technology and Engineering Meet, June 12, 2017 - June 14, 2017*, *Maastricht, Netherlands*. Springer International Publishing, pp. 125-131.

Wang, C.-q. *et al.* (2018) Utilization of oil-based drilling cuttings pyrolysis residues of shale gas for the preparation of non-autoclaved aerated concrete, *Construction and Building Materials*, 162, pp. 359-368. doi: 10.1016/j.conbuildmat.2017.11.151.

Welsch, T. and Schnellenbach-Held, M. (2017) High performance aerogel concrete, *2017 fib Symposium - High Tech Concrete: Where Technology and Engineering Meet, June 12, 2017 - June 14, 2017*, *Maastricht, Netherlands*. Springer International Publishing, pp. 117-124.

Westgate, P., Paine, K. and Ball, R. J. (2018) Physical and mechanical properties of plasters incorporating aerogel granules and polypropylene monofilament fibres, *Construction and Building Materials*, 158, pp. 472-480. doi: 10.1016/j.conbuildmat.2017.09.177.

Wu, Y. *et al.* (2015) Development of ultra-lightweight cement composites with low thermal conductivity and high specific strength for energy efficient buildings, *Construction and Building Materials*, 87, pp. 100-112. doi: 10.1016/j.conbuildmat.2015.04.004.

Xu, B., Ma, H. and Li, Z. (2015) Influence of magnesia-to-phosphate molar ratio on microstructures, mechanical properties and thermal conductivity of magnesium potassium phosphate cement paste with large water-to-solid ratio, *Cement and Concrete Research*, 68, pp. 1-9. doi: 10.1016/j.cemconres.2014.10.019.

Hajmohammadian Baghban, Kioumarsi and Grammatikos (2018) Prediction Models for Thermal Conductivity of Cement-based Composites